Downstream strategies for VLPs as candidate universal vaccine for Influenza

Sofia Baptista de Carvalho

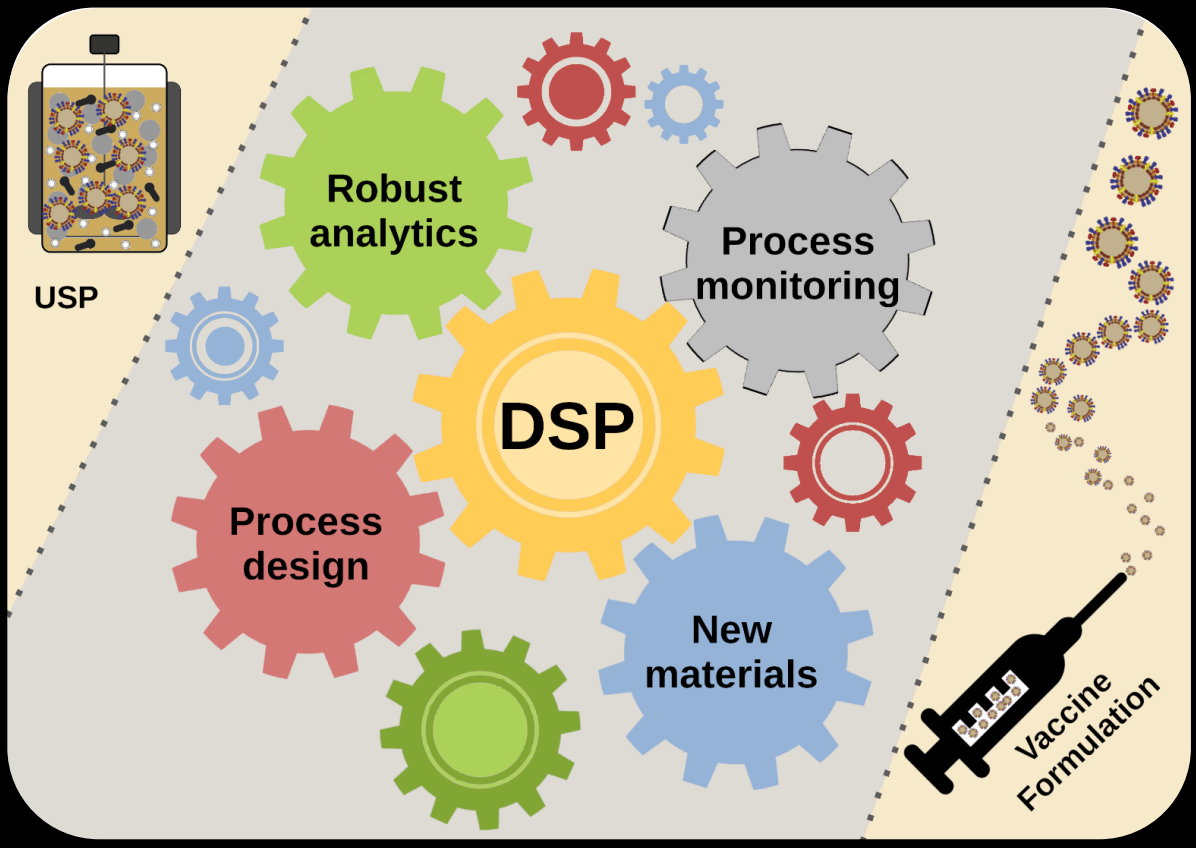

Dissertation presented to obtain the Ph.D degree in Biotechnology

Instituto de Tecnologia Química e Biológica António Xavier | Universidade Nova de Lisboa

Oeiras,
December, 2018

UNIVERSIDADE NOVA DE LISBOA

Downstream strategies for VLPs as candidate universal vaccine for Influenza

Sofia Baptista de Carvalho

Dissertation presented to obtain the Ph.D degree in Biotechnology

Instituto de Tecnologia Química e Biológica António Xavier | Universidade Nova de Lisboa

Oeiras, December, 2018

Em memória do meu pai

Para o Diogo e para a Matilde, as minhas pessoas preferidas

"Like science, emerging viruses know no country. There are no barriers to prevent their migration across international boundaries or around the 24 time zones"

Richard M. Krause

Acknowledgments

There is an old African proverb that says: *It takes a village to raise a child*

It took the work, knowledge, help and support of so many people to "raise" this child and turn it into a PhD thesis - to all of them I want to express my deepest gratitude.

To my supervisor, Professor Manuel Carrondo, it was really a privilege to be your student. Thank you for your demanding orientation (as it should), for betting in me and for always pushing me to my best. You taught me so much about science but, and more importantly, you taught me so much about life. I owe you a lot of my scientific and personal growth during the last years. I am very grateful for your open door to help me put things in perspective and move forward - "If you can keep your head when all about you are losing theirs (...) yours is the Earth and everything that's in it, and-which is more-you'll be a Man, my son!"

To my other supervisor Dr. Cristina Peixoto, I can not thank you enough for this amazing opportunity. Thank you for seeing potential in me, even when you did not know me at all. For all the challenges you proposed me and the opportunities you gave me. I know you did your best to create the work-conditions and opportunities to allow me to grow as much as possible as a scientist. It was really good to know that you

were always there to listen to my (sometimes crazy) ideas and that you tried hard to say yes to most of them. Thank you also for fighting for what was the best for me, scientifically and personally.

To Dr. Paula Alves - thank you for the confidence you had in me from the very first day. I was an "outsider" but you welcomed me to Animal Cell Technology Unit and gave me the infrastructure and possibility to perform an excellent work, with all the opportunities a PhD student may wish. Thank you also for always trying to have time to listen and help and for letting me feel that at the end of the day what matters is people.

To all the members of Animal Cell Technology Unit, in particular the DSP team that welcomed me: Ricardo, Pier, Duarte and Bárbara and the members that were arriving: Mafalda, Sofia Júnior (sorry about the nickname!), Sara, João and Tiago. To Dr. Ana Sofia Coroadinha and Dr. Ana Filipa Rodrigues for having always space at your lunch table. For all the laughs but also for all the serious conversations when the times were more difficult and I needed someone to complain.

To Mafalda Moleirinho, for embracing my ongoing projects as her own. For always have time to help me (in particular when I was so pregnant I can not reach the lab bench) and for having always a word of encouragement. You were the best first student a scientist could ask for.

To Dr. Ricardo Silva, it was a pleasure to share this journey with you. It was so much easier to be sitting on the desk next to you. Thank you for all your help, patience in explaining to me "hardcore engineering" part, for your scientific advice and for your friendship.

To Dr. Bárbara Cunha and Dr. Patrícia Gomes-Alves. For pushing me forward and for having the right words to direct me towards what really matters. For all your scientific support and friendship.

To the EDUFLUVAC upstream team, especially António Roldão, Marcos Sousa - it was a tough journey, but we did a good job.

To the Pilot plant team, in particular, João Clemente and Rute Castro. Thank you, João for your patience in teaching me how to work with a bioreactor. Thank you Rute for always have time for my "cell growth

and infection" doubts, even during Sunday morning.

To Dr. Pedro Cruz, for all the help during this final phase, for your scientific input and fresh perspective about my work.

To our collaborators at IMM, Dr. Gonçalo Bernardes, Professor Miguel Castanho, Dr. Diana Gaspar and especially Dr. João Freire. To David Wheatley and John Welsh at Pall Life Sciences. Thank you for having me in your lab. To Alex Xenopoulos from Merck Millipore, thank you for all the work we did together. To the Downstream Processing Group at Max Planck Institute, in particular Ana Raquel Fortuna and Dr. Michael Wolff. It was an amazing experience to work with you.

To my thesis committee members, Dr. Alex Xenopoulos and Dr. Michael Wolff for all the fruitful discussions about my work and for sharing your knowledge and good ideas.

Aos meus amigos. Aos de infância: Mariana, Vera, Mafalda, Ricardo e Daniela. Obrigada por todas as palavras de apoio e por me fazerem sentir que não importa quanto tempo passo sem vos ver, vocês estão lá sempre. Aos que o Grupo 23 de Queluz me trouxe, em especial ao David, à Liliana, à Sara e à Filipa. Ser escuteira moldou muito do que sou hoje e trouxe-me tantas coisas boas. Vocês foram uma delas. Aos que se cruzaram comigo pela Bioquímica. João e Pedro, mesmo longe estão perto, sempre. Joana, é tão bom ter-te na porta ao lado!

À minha família, à que era minha e à que ganhei. Aos meus pais, por todo o esforço e dedicação que puseram na minha educação. Por tentarem sempre ser o melhor pai e mãe, mesmo quando o meu mau feitio vinha ao de cima. Sei que é graças a vocês que me tornei no que queria e me sinto feliz e realizada. Ao meu pai, por me ter dito vezes sem conta enquanto eu crescia que o importante não era eu ser a melhor, mas dar o meu melhor em tudo o que fazia. Sei que este dia te deixaria feliz e orgulhoso. À minha mãe e ao meu irmão, pelo apoio constante, pela paciência infinita e ajuda mesmo quando eu não pedia. Obrigada por compreenderem a minha ausência nos últimos tempos. Aos mais recentes avó "Chinda" e avô Tó. Obrigada por dizerem sempre que sim a todos os

pedidos para tomarem conta da Matilde enquanto eu trabalhava, por me (nos) tirarem de cima todas as tarefas que conseguiam e por serem um apoio constante. Tornaram esta jornada muito mais simples, obrigada. À prima Sara, por ter sido uma ajuda preciosa para este coração de mãe de primeira viagem. Obrigada por me teres deixado descansada!

Ao Diogo. Por partilhar esta(s) aventura(s) comigo, lado a lado. Por me fazeres rir sempre, nos dias bons e naqueles em que me apeteceu mandar o PhD pela janela. Por me ajudares sempre, mesmo quando não percebias nada do que eu estava a dizer. Por acreditares sempre em mim, muito mais do que eu própria. Por me picares todos os dias e me obrigares a testar os meus limites (da paciência também)! Sou uma pessoa e uma cientista melhor por tua causa. À Matilde. Por ter revolucionado a vida como nós a conhecíamos. Para tão melhor. Por me ter ensinado o verdadeiro sentido de relativizar e me ter feito acreditar que ser mãe dela é um desafio tão maior que qualquer doutoramento. Sou muito mais feliz desde que existes. Aos dois, por tudo o que não cabe nestas linhas.

Preface

This PhD thesis is the result of a four years research conducted at the Downstream Processing Laboratory of Animal Cell Technology Unit of Instituto de Biologia Experimental e Tecnológica (iBET) and Instituto de Tecnologia Química e Biológica António Xavier (ITQB). The work was performed under the supervision of Professor Manuel Carrondo and Doctor Cristina Peixoto and was developed under the scope of European project EDUFLUVAC which stands for EDUcate inFLUenza VACcine, of which iBET is a key partner. The main goal of the collaborative project is to develop a combinatorial immunization strategy to educate the immune system towards cross-recognition and coverage against antigenic drift in seasonal influenza virus exposure. It aims to develop a novel influenza vaccine candidate that include a combination of multiple influenza haemagglutinin (HA) or neuraminidase (NA) antigens delivered on Virus-like particles (VLPs). This alternative vaccine should be capable of inducing a long-lived broad coverage against seasonal influenza. My PhD project, in particular, aims to improve the downstream processes for these VLPs candidates and to develop novel analytical tools that will allow the on-line/at-line monitoring, characterization and quality control of VLP-based human vaccines during bioprocessing.

Taking into account that some of the proposed studies required technical skills and equipment not available at that moment at iBET/ITQB,

several fruitful collaborations were established with other research groups and companies. The development of a haemagglutinin quantification method using BioLayer Interferometry with Octet platform resulted from the collaboration with Pall Life Sciences and an internship at Pall Corporation. From this work, we published the "Universal label-free In-process Quantification of Influenza Virus-like particles" manuscript. "Bioorthogonal processing of specific-site-functionalized enveloped Influenza-virus-like particles" was a joint effort with two other groups, Physical Biochemistry of Drugs & Targets Laboratory and Chemical Biology & Pharmaceutical Biotechnology Laboratory from IMM. With this work we were able to develop a valuable platform for the downstream processing and monitoring of enveloped Influenza VLP and refine the discrimination and separation between VLPs and baculovirus — the major contaminant of the process. A collaboration with Merck Millipore was set up with the purpose to develop a non-chromatographic purification process for Influenza VLPs. The manuscripts "Efficient filtration strategies for the clarification of influenza virus-like particles derived from insect cells" and "Membrane-based approach for the downstream processing of influenza virus-like particles" resulted from this project. Aiming to develop improved Downstream processing unit trains adapted for virus and Influenza VLPs a collaboration with the Downstream Processing Laboratory from Bioprocess Engineering group at Max Planck Institute was started. It resulted in an internship and in the work entitled "Purification of influenza virus-like particles using sulfated cellulose membrane adsorbers".

The PhD project was funded by The Portuguese Science Foundation (FCT-MCTES) (SFRH/BD/52302/2013), under the scope of MolBioS Program and by European Union (EDUFLUVAC project, FP7-HEALTH-2013-INNOVATION).

Sofia Carvalho
Oeiras, Portugal

Abstract

Influenza virus seasonal epidemics is a global public health concern. Annually, it affects millions of people worldwide, representing significant health and economic burdens. Moreover, sporadic pandemic outbreaks have caused devastating effects, resulting in millions of deaths. Vaccination continues to be the cornerstone to prevent the infection with Influenza viruses. However, there are several challenges and unmet limitations to overcome for a successful vaccination. Influenza constant antigenic drift and sporadic shift results in a variability of the circulating virus, requiring annual vaccines' update with high inherent costs and, in some cases, low efficiency. Therefore, efforts are being made to develop a universal influenza vaccine, that will confer a broader, better and longer lasting protection to cover virus constant evolution. It is important to note that the reported diversity of virus surface epitopes contributes to a variability in the bioprocess, which can affect manufacturability. Vaccine production and processing capacity should be achieved in a very short period and supply an adequate number of doses to cope with global demands, highly critic for pandemics. Increasing manufacturing speed, capacity, and flexibility has supported cell-based vaccine production, an alternative to conventional egg-based systems. In fact, there are new vaccines in the market produced using mammalian and insect cell lines and several platforms, including virus-like particles (VLPs), are under

development as candidates for both seasonal and pandemic Influenza virus. VLPs are promising recombinant vaccine antigens: they have the ability to stimulate an immune response to different influenza strains combined with safety since they lack the viral genetic material required for replication.

To fully exploit the potential of these novel manufacturing platforms, research efforts are being put on the development of more efficient and cost-effective downstream processes. To keep up with fast progress on downstream processing, there is a driving force toward developing new process monitoring, product quantification and robust characterization methods.

The main goals of this thesis are to improve existing downstream strategies and establish new process trains for influenza VLPs candidate for a universal vaccine, and to develop novel analytical tools that will allow the on-line/at-line monitoring, characterization and quality control of VLP-based human vaccines during bioprocessing.

An introduction in Chapters 1 and 2 reviews the current advances in the downstream bioprocessing of influenza virus and virus-like particles, with emphasis on the different state-of-the-art unit operations, from clarification to sterile filtration. Moreover, a broad overview of analytics and quality control methods for virus-based biopharmaceuticals is described. Focus is given to the currently available possibilities to process, analyze and characterize viral particles, from production bulks to highly purified samples.

One of the main bottlenecks on influenza bioprocessing is the lack of analytical tools to detect and quantify VLPs. Traditional methods, such as hemagglutination assay, Single Radial Immunodiffusion assay or NA enzymatic activity assays are designed for virus particles and are not optimized for VLPs. Moreover, the time required to process, and the inefficient quantification of in-process samples poses challenges for efficient downstream process development (DSP) and in-line monitoring. Chapter 4 reports the development of a label-free tool that uses Biolayer

interferometry technology applied on an octet platform to detect and quantify Influenza VLPs at all stages of DSP, from crude sample up to final VLP product. It is worth to note that this method does not require the use of antibodies or red blood cells. By taking advantage of hemagglutinin (HA) (Influenza's main envelope protein) binding to sialic acid receptors HA content could be quantified in several mono- and multivalent Influenza VLP strains. Moreover, it shows better detection limits than the gold standard method. This analytical method uses a high throughput technology, providing an efficient and fast tool for process control that can be applied as a PAT (process analytical technology) tool.

Chapter 5 presents a strategy for the downstream processing and monitoring of tagged enveloped VLPs. By using a click-chemistry approach that involves Azidohomoalanine incorporation and functionalization, Influenza VLPs were selectively and fluorescently tagged during in vivo production. Importantly, this labeling does not influence VLP production and allows the construction of functionalized VLPs that maintain their size, charge and biological function. The reported strategy uses the baculovirus expression vector system that results in a considerable increase in downstream processing complexity because of routine purification procedures and analytical methods are not able to strictly discriminate between VLPs and baculovirus. However, combining this technique with a fluorescence-activated cell-sorting (FACS) step it is possible to refine discrimination and separation between VLP and baculovirus, the major impurity of the process. This is a versatile and valuable tool broadly applicable to the production, online/at-line product monitoring, during DSP optimization of functionalized enveloped VLPs for vaccine design trial runs, targeted drug delivery, and molecular imaging.

Taking into account the need for faster and better processes, the work developed on Chapter 6, 7 and 8 is focused on the downstream processing strategies, detailing the improvements on the different unit operations. The first two chapters address the implementation of single-use techno-

logies on a platform process for purification of Influenza VLPs. An effort to replace chromatographic steps from the purification platform was undertaken, with the ultimate goal of an all filtration purification process. Chapter 8 describes an economically competitive chromatographic step that works for both Influenza virus and VLPs.

Chapter 6 starts with the clarification stage, a critical step, not well characterized for most of the purification processes, but with a strong impact on the downstream performance. Aiming to establish a universal influenza clarification framework, efforts were made to develop a clarification platform for the manufacturing of several influenza strains, mono and multivalent, at different production scales (up to 11 L). The applicability of different filtration methodologies, as normal and tangential flow filtration was evaluated in terms of product recovery and impurity clearance. The selected train presents a product recovery of approximately 100% and a turbidity value below 10 NTU, resulting from high impurity clearance, and consistent with an efficient clarification step. Notably, these results were independent of strain, cell viability and turbidity at harvest time. The recommended clarification strategy appears to be easily scalable to larger process volumes and can be applied to different influenza strains, contributing to a speed-up of influenza vaccine manufacturing.

Moving forward to the purification stage, a membrane-based approach is described on Chapter 7. Following the clarification train previously developed (Chapter 6), the proposed process employs a cascade of ultrafiltration and diafiltration steps using membrane cassettes, followed by a sterile filtration step. Different process parameters were assessed in terms of product recovery and impurities' removal. Membrane chemistry (PES vs Regenerated Cellulose), pore size (ranging from 1000 to 100 kDa) and mode of operation (parallel vs series), critical flux, transmembrane pressure, and permeate control strategies were evaluated. After membrane selection and parameter optimization, concentration factors and diafiltration volumes were also defined. By optimizing the filtration

mode of operation, we were able to achieve product recoveries of 80%. Overall, we speeded up the process, improved its scalability and reduced the costs due to the removal of chromatographic, cleaning and validation steps.

The study of Chapter 8 describes the optimization and establishment of a chromatography capturing technique using sulfated cellulose membrane adsorbers (SCMA) for purification of influenza VLPs. Design of experiments was used to describe and optimize the critical factors for membrane performance. For optimal conditions regarding membrane ligand density, salt concentration on loading and elution as well as the corresponding flow rates, 80% of product recovery was obtained. In terms of impurity clearance, the yields for total protein removal and DNA were higher than 89% and 80%, respectively. SCMA showed noteworthy improvements when compared to conventional ion exchanger membrane adsorbers. Moreover, it is easily scalable and reduces the number of steps required compared to conventional purification methods. Based on the reported results, SCMA can be applied as a general platform for purification of VLP-based influenza vaccines.

Overall, this thesis contributed to the field of vaccination and bioengineering of virus-based biopharmaceuticals, in particular for influenza virus. On one hand, the implementation of innovative analytical tools for in-process control, product quantification and characterization will contribute to downstream process understanding and optimization. On the other hand, the development of efficient unit operations, based on rational design and parameter optimization, created knowledge that will contribute to more efficient and cost-effective strategies, globally speeding-up influenza vaccine manufacturing.

Keywords - Analytics, Downstream Processing, Design of Experiments, Influenza, Process monitoring, Process control, Vaccines, Virus-like particles

Resumo

As epidemias de influenza sazonal são um problema global de saúde pública. Afectam anualmente milhões de pessoas representando uma sobrecarga significativa, quer ao nível da saúde, quer em termos económicos. Para além disso, os surtos esporádicos de influenza pandémica têm causado efeitos devastadores, resultando em milhões de mortes. A vacinação continua a ser a forma mais eficaz para prevenção de infeções através do vírus influenza. No entanto, existem ainda vários desafios e limitações a superar de modo a conseguir atingir uma vacinação de sucesso. O vírus de influenza apresenta uma constante deriva e uma esporádica mudança antigénica, resultando numa significativa variabilidade das estirpes em circulação, tornando necessário uma atualização anual das vacinas. Esta renovação apresenta elevados custos associados e, por vezes, uma baixa eficiência. Por esse motivo, estão a ser feitos esforços para desenvolver uma vacina universal que confira uma protecção melhor, mais ampla e mais duradoura, de modo a acompanhar a evolução constante do vírus. É importante referir que a diversidade reportada relativamente aos epitopos da superfície viral contribui para a variabilidade no bioprocesso, o que pode afectar a manufaturabilidade. A produção de vacinas e a capacidade de as processar são dois passos que devem ser atingidos num curto espaço de tempo, de forma a fornecer um número adequado de doses para as exigências globais, extremamente críticas em casos de pandemias. A

necessidade de aumentar a velocidade, a capacidade e a flexibilidade de fabrico tem suportado a produção de vacinas em linhas celulares como alternativa aos sistemas convencionais baseados em ovos. De facto, existem novas vacinas disponíveis no mercado produzidas usando linhas celulares de mamífero e insecto e estão em desenvolvimento diferentes plataformas, incluindo partículas semelhantes a vírus (VLPs), como candidatos a vacinas contra vírus de influenza sazonal e pandémico. As VLPs são antigénios recombinantes promissores para utilização em vacinas: possuem a capacidade de estimular uma resposta imune contra diferentes estirpes de influenza, garatindo uma segurança inerente ao facto de não conterem o material genético necessário à replicação viral.

De modo a explorar todo o potencial das novas plataformas de produção, estão a ser desenvolvidos processos de purificação mais eficientes e economicamente viáveis. Para acompanhar o rápido progresso nos processos de purificação, há uma força motriz para se desenvolver métodos mais robustos para monitorização de processo, quantificação e caracterização do produto.

Esta tese tem como principais objetivos melhorar as estratégias de purificação existentes e estabelecer novas unidades de operação para VLPs de influenza candidatas a uma vacina universal e desenvolver novas ferramentas analíticas que permitam a monitorização em tempo real/em linha, a caracterização e o controlo de qualidade durante o bioprocesso de vacinas humanas baseadas em VLPs.

A introdução dos Capítulos 1 e 2 descreve os últimos avanços nos processos de purificação de vírus e VLPs de influenza, dando particular ênfase às atuais unidades de operação utilizadas, desde a clarificação à filtração estéril. Para além disso, são descritos, de uma perspetiva ampla, os analíticos e métodos de controlo de qualidade para biofarmacêuticos baseados em vírus. Em particular, são focadas as possibilidades atualmente disponíveis para processar, analisar e caracterizar partículas virais, desde amostras provenientes de suspensões iniciais de material até amostras altamente purificadas.

Uma das principais dificuldades inerentes ao processo de purificação e produção de influenza é a falta de ferramentas analíticas para detetar e quantificar VLPs. Os métodos tradicionais, tais como o ensaio de reação de hemaglutinação, o teste de imunodifusão radial simples, ou o ensaio de atividade enzimática da neuraminidase, estão desenhados para particulas virais e não estão optimizados para VLPs. Para além disso, o tempo de processamento das amostras, e as dificuldades na quantificação eficiente de amostras de processo torna-se um desafio no desenvolvimento de processos de purificação (DSP) eficientes e na monitorização em linha do produto. O Capítulo 4 reporta o desenvolvimento de uma ferramenta para detectar e quantificar VLPs de influenza em todos os passos de purificação, desde a amostra inicial até ao produto final. Esta ferramenta não requer a marcação das amostras e utiliza a tecnologia de Interferometria de Biocamada (BLI) aplicada numa plataforma Octet. É importante referir que este método não necessita de anticorpos ou de eritrócitos. A ligação entre a hemaglutinina (HA) (a proteína principal do envelope do vírus) e receptores de ácido siálico permite a quantificação da HA de várias estirpes, em VLPs mono e multivalentes. Para além disso, apresenta limites de deteção menores que o método standard. Uma vez que este método analítico utiliza tecnologia high throughput, torna-se numa ferramenta de controlo de processo rápida e eficiente que pode ser aplicada como PAT (tecnologia analítica de processo).

No Capítulo 5 é apresentada uma estratégia para a purificação e monitorização de VLPs envelopadas e marcadas. Através de reações químicas de "click", que envolvem a incorporação de Azidohomoalanina e posterior funcionalização, as VLPs de influenza foram seletivamente marcadas com fluorescência durante a sua produção *in vivo*. Esta marcação não influencia a produção de VLPs e permite a construção de partículas funcionalizadas que mantêm o seu tamanho, carga e função biológica. A estratégia reportada utiliza o sistema de expressão em baculovírus, o que resulta num aumento da complexidade do processo de purificação, uma vez que os procedimentos de rotina e os métodos analíticos comuns não

são capazes de discriminar rigorosamente baculovírus e VLPS. No entanto, a combinação desta técnica com um passo de separação de células ativadas por fluorescência (FACS) torna possível refinar a discriminação e a separação entre VLPs e baculovírus, a maior impureza do processo. Esta ferramenta pode ser amplamente aplicada na produção, monitorização do produto em tempo real/em linha e durante a optimização de processos de purificação de VLPs envelopadas e funcionalizadas em corridas de teste para desenho de vacinas, entrega direccionada de fármacos e imagiologia molecular.

Tendo em consideração a necessidade de novos processos de purificação, melhores e mais rápidos, o trabalho desenvolvido nos Capítulos 6, 7 e 8 foca-se em estratégias de purificação, detalhando as melhorias em diferentes unidades de operação. Os primeiros dois capítulos visam a implementação de tecnologias de uso único numa plataforma de purificação de VLPs de influenza. Para esta plataforma fez-se o esforço de substituir os passos de cromatografia, tendo como objetivo principal desenvolver um processo de purificação baseado apenas em filtração. O Capítulo 8 descreve um passo cromatográfico, competitivo em termos económicos, que pode ser aplicado tanto em virus de influenza como em VLPs.

O Capítulo 6 inicia o trabalho de desenvolvimento de estratégias de purificação com a clarificação, um passo que embora crítico, não está ainda bem caracterizado para a maioria dos processos de purificação, tendo um grande impacto na performance do mesmo. Tendo como objetivo estabelecer um esquema universal de clarificação de influenza, desenvolveu-se uma plataforma de clarificação para a produção e purificação de diferentes estirpes do vírus, mono e multivalentes, utilizando diferentes escalas de produção (até 11 L). Avaliou-se a aplicabilidade de diferentes métodos de filtração, como a filtração normal ou de fluxo tangencial, em termos de recuperação de produto e de remoção de impurezas. A sequência de filtros seleccionada apresenta uma recuperação de produto de aproximadamente 100% e um valor de turbidez abaixo dos 10 NTU, resultante de uma grande remoção de impurezas e consistente

com o que se espera de um passo de clarificação eficiente. Notavelmente, estes resultados demonstraram ser independentes da estirpe, da viabilidade celular e valor de turbidez no tempo de recolha. A estratégia de clarificação recomendada aparenta ser facilmente escalável para processos com maiores volumes e pode ser aplicada a diferentes estirpes de influenza, o que contribui para acelerar a produção de vacinas.

O Capítulo 7 descreve uma abordagem para o passo de purificação baseada apenas no uso de membranas. Após a etapa da clarificação (Capítulo 6), no processo proposto é aplicada uma sequência de passos de ultrafiltração e diafiltração utilizando módulos de cassetes, seguida de um passo de filtração estéril. Foram avaliados diferentes parâmetros do processo, quer em termos de recuperação de produto quer em termos de remoção de impurezas. A química da membrana (PES vs celulose regenerada), o tamanho do poro (variando entre 100 e 1000 kDa) o modo de operação (paralelo vs série), o fluxo crítico, a pressão transmembranar e diferentes estratégias de controlo do fluxo do permeado foram avaliados. Após a seleção das membranas e a optimização dos parâmetros de operação, os factores de concentração e os volumes de diafiltração foram definidos. Através da optimização do modo de operação da filtração atingiu-se um rendimento de recuperação de produto de cerca de 80%. No geral, o processo de purificação foi acelerado, a sua escalabilidade foi melhorada e o custo associado foi reduzido devido à remoção dos passos de cromatografia, limpeza e validação.

O estudo reportado no Capítulo 8 descreve a optimização e implementação de uma técnica cromatográfica de captura para a purificação de VLPs de influenza utilizando adsorventes de membrana de celulose sulfatada (SCMA). A técnica do desenho de experiências (DoE) foi utilizada para descrever e optimizar os fatores críticos na performance da membrana. Em condições ótimas no que diz respeito à densidade de ligando, concentração de sal no passo de carga e na eluição, bem como os caudais correspondentes a cada um desses passos, obteve-se uma recuperação de produto de cerca de 80%. Em termos de impurezas, os rendimentos

de remoção obtidos foram acima de 89% e 80% para proteína total e DNA, respetivamente. O processo utilizando SCMA demonstrou melhorias significativas quando comparado com os tradicionais adsorventes de membrana para cromatografia de troca iónica. Para além disso, é uma estratégia facilmente escalável e reduz o número de passos necessários quando comparado com os métodos de purificação convencionais. Tendo em conta os resultados reportados, o SCMA pode ser aplicado como uma plataforma geral para purificação de VLPs para vacinas de influenza.

Globalmente esta tese contribuiu para as áreas da vacinação e da bioengenharia de biofarmacêuticos baseados em vírus, em particular no que diz respeito ao vírus de influenza. Por um lado, a implementação de métodos analíticos inovadores para o controlo do processo, quantificação e caracterização do produto permitirá um aprofundamento do conhecimento e optimização dos processos de purificação. Por outro lado, o desenvolvimento de unidades de operação eficientes, baseado num desenho racional e na optimização de parâmetros, permitiu criar conhecimento que irá contribuir para o desenvolvimento de estratégias mais eficientes e economicamente viáveis, acelerando globalmente a produção de vacinas.

Palavras-chave - Analíticos, Controlo de processo, Desenho de Experiências, Influenza, Monitorização de processo, Partículas semelhantes a vírus, Purificação, Vacinas

Thesis publications

Ana F. Rodrigues*, **Sofia B. Carvalho***, Paula M. Alves, Manuel J. T. Carrondo, Ana S. Coroadinha, and Cristina Peixoto. *Analytics and quality control for virus-based biopharmaceuticals: from the classical methods to the newest tools.* Manuscript in preparation.

*Authors contributed equally.

Sofia B. Carvalho, Ricardo Silva, Paula M. Alves, Cristina Peixoto, and Manuel J. T. Carrondo. *Downstream processing for influenza vaccines and candidates: an update.* Manuscript in preparation.

Sofia B. Carvalho, Ricardo Silva, Mafalda G. Moleirinho, Ana Sofia Moreira, Bárbara Cunha, Paula M. Alves, Manuel J. T. Carrondo, Alex Xenopoulos, and Cristina Peixoto. *Membrane-based approach for the downstream processing of influenza virus-like particles.* Manuscript submitted.

Sofia B. Carvalho, Ricardo Silva, Ana S Moreira, Bárbara Cunha, João J. Clemente, Paula M. Alves, Manuel J. T. Carrondo, Alex Xenopoulos, and Cristina Peixoto. *Efficient filtration strategies for the clarifica-*

tion of influenza virus-like particles derived from insect cells. Under revision.

Sofia B. Carvalho⋆, A Raquel Fortuna⋆, Michael W Wolff, Cristina Peixoto, Paula M. Alves, Udo Reichl, and Manuel J. T. Carrondo. *Purification of influenza virus-like particles using sulfated cellulose membrane adsorbers.* Journal of Chemical Technology and Biotechnology (2018) 93:1988.

⋆Authors contributed equally.

Sofia B. Carvalho, Mafalda G. Moleirinho, David Wheatley, John Welsh, René Gantier, Paula M. Alves, Cristina Peixoto, and Manuel J. T. Carrondo. *Universal label-free In-process Quantification of Influenza Virus-like particles.* Biotechnology Journal (2017) 12:1700031.

Sofia B. Carvalho⋆, João M. Freire⋆, Mafalda G. Moleirinho, Francisca Monteiro, Diana Gaspar, Miguel Castanho, Manuel Carrondo, Paula M. Alves, Gonçalo Bernardes, and Cristina Peixoto. *Bioorthogonal processing of specific-site-functionalized enveloped Influenza-virus-like particles.* Bioconjugate chemistry (2016) 27:2386.

⋆Authors contributed equally.

Additional publications

Sofia B. Carvalho*, Ana Sofia Moreira*, Joana Gomes, Manuel J. T. Carrondo, David J. Thornton, Paula M. Alves, Julia Costa, and Cristina Peixoto. *A detection and quantification label-free tool to speed up downstream processing of model mucins.* PloS one (2018) 13:e0190974.

*Authors contributed equally.

Bárbara Cunha, Tiago Aguiar, **Sofia B. Carvalho**, Marta M. Silva, Ricardo A. Gomes, Manuel J. T. Carrondo, Patrícia Gomes-Alves, Cristina Peixoto, Margarida Serra, and Paula M. Alves *Bioprocess integration for human mesenchymal stem cells: from up to downstream processing scale-up to cell proteome characterization.* Journal of Biotechnology (2017) 248:87.

Joana Gomes, Patrícia Gomes-Alves, **Sofia B. Carvalho**, Cristina Peixoto, Paula M. Alves, Peter Altevogt, and Júlia Costa. *Extracellular Vesicles from Ovarian Carcinoma Cells Display Specific Glycosignatures.* Biomolecules, (2015) 5:1741.

Contents

List of Figures

List of Tables

List of Abbreviations

AEX	anionic exchange chromatography
AFM	atomic force microscopy
Aha	azidohomoalanine
BEVS	baculovirus expression vector system
BLI	biolayer interferometry
BV	baculovirus
CCI	cell concentration at infection
CIP	cleaning in place
CRC	composite regenerated cellulose
DF	diafiltration
DFV	diafiltration volumes
DSP	downstream processing
DoE	design of experiments
ELISA	enzyme linked immunosorbent assay

IC	ionic capacity
IEX	ion exchanger
IIV	inactivated influenza vaccine
FACS	fluorescence-activated cell-sorting
FWHM	full width at half maximum
HA	Hemagglutinin protein
HA Assay	Hemagglutination Assay
HIC	hydrophobic interaction chromatography
HF	hollow fibers
hpi	hours post infection
HPLC	high-performance liquid chromatography
LAIV	live attenuated influenza vaccine
LD	ligand density
LMH	L m^{-2} h^{-1}
LOD	limit of detection
LOQ	limit of quantification
LRV	log reduction value
MF	microfiltration
MMC	Mixed-mode chromatography
MOI	multiplicity of infection
MW	molecular weight
MWCO	molecular weight cut off
NA	Neuraminidase protein
NFF	normal flow filtration
NTA	nanoparticle tracking analysis

NTU	nephelometric turbidity units
PAT	process analytical technology
PBS	phosphate buffered saline
PCC	periodic countercurrent chromatography
PEG	polyethylene glycol
PES	polyethersulfone
PS	polysulfone
PSF	point-spread function
PVDF	polyvinylidene fluoride
QbD	Quality by Design
qPCR	quantitative real time PCR
RBC	red blood cells
RI	refractive index
RT	room temperature
SAX	high precision streptavidin
SCMA	sulfated cellulose membrane adsorbers
SEC	size-exclusion chromatography
SRID	Single Radial Immunodiffusion
SPAAC	strain-promoted alkyne–azide [3+2] cycloaddition
SXC	steric exclusion chromatography
TagE-VLPs	tagged enveloped VLPs
TCR	T cell receptor
TFF	tangential flow filtration
TMP	transmembrane pressure
TOH	time of harvest

TP	total protein
UF	Ultrafiltrate
USP	upstream processing
VBBs	Virus-based biopharmaceuticals
VLPs	virus-like particles
vRNA	viral RNA
WVPs	whole virus particles

1

Downstream processing for influenza vaccines and candidates: an update

Influenza seasonal and pandemic outbreaks constitute a huge worldwide concern, with significant health and economic burdens associated. Moreover, the re-emergence of pandemic strains in the last decade made clear that influenza is still a global threat. Despite all the improvements on the field, there are still several limitations on influenza vaccines' global availability and effectiveness. The ultimate goal is to develop universal vaccines that could provide a broad, long-lasting protection against multiple influenza subtypes, including potential pandemic ones.

To cope with these global needs, several expression platforms and novel influenza vaccine designs are under development, in clinical trials, or in the market. Amongst multiple possible solutions, namely inactivated or live-attenuated virus, virus-like particles or recombinant antigens, it is not yet clear which one(s) will have the desired effectiveness. For all of them, there are still unmet challenges on bioprocessing. Downstream processing (DSP) of influenza viruses is always facing new challenges: it needs to deal with new influenza virus strains repeatedly, requiring continuous research efforts; in the case of pandemic outbreaks, the time required for research and development is shorter and there is a pressure increase to develop fast bioprocesses. Moreover, it often entails for the major production costs, and coupled with the advances in upstream processing and new regulatory demands on product quality and

safety, it is critical to increasing the efficiency of the existing DSP trains, and to develop new unit operations and integrated processes for novel vaccine formats.

This review focuses on the purification of influenza vaccine formats and intends to offer a comparison between the DSP reported for the different types of influenza vaccine products that are currently being developed. Insight is given on how the differences in the type of vaccine design and expression system impact DSP operations, from harvest to sterile filtration. In particular, the challenges of moving from egg-based processes to cell-based or recombinant productions are addressed. Case studies for the manufacturing of products still under research development, in clinical trials or in the market are also discussed, highlighting the current challenges on Influenza DSP.

1.1 Influenza virus

Influenza virus belongs to the *Orthomyxoviridae*, a family of enveloped viruses that are characterized by segmented genomes of single-stranded negative-sense RNA. There are four types of Influenza (A,B,C, and D), however, only Influenza A and B are the relevant responsible for the annual human infections [1]. The structure of genera A and B is very similar and despite the antigenic differences, the viral proteins of both types have similar functions [2]. Each influenza A virus is composed of three main components: a viral envelope, that contains hemagglutinin (HA), neuraminidase (NA) and M2 transmembrane proteins, an intermediate layer of M1 matrix protein and an internal viral ribonucleocapsid (vRNP) core containing a nucleoprotein (NP) and viral RNA (vRNA) (Figure 1.1) [1, 3, 4]. All of these components have an important role on virus mechanism of infection. HA is responsible for the binding to receptor containing sialic acid, commonly Neu5Ac, promoting viral entry into the cells. NA cleaves the sialic acid receptor, releasing the virus and facilitating viral spread. M1 is a structural protein that gives rigidity

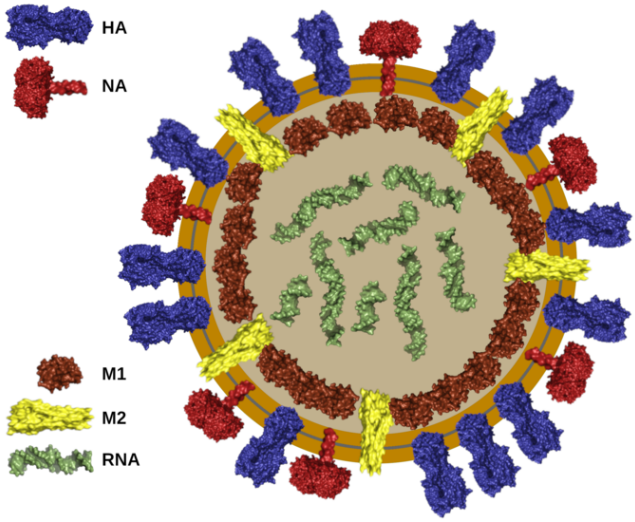

Figure 1.1: Influenza virus structure.

to the virus and helps on the regulation of viral RNA segments into the cell. M2 protein is a proton ion channel with an important role in the life cycle of the virus, namely the release of viral RNA to the cytoplasm (via pH changes) for replication by the host cell. There are also minor components such as the nonstructural protein NS1 and nuclear export protein (NEP). The virus presents a pleomorphic structure, with particle shapes ranging from spheres to long filaments [1]. The virus spherical particles have a size ranging from 80 to 120 nm [1, 3, 4].

Characterization of Influenza A viruses are based on the subtype of their two major surface glycoproteins HA and NA. Up to now there are 18 HA (H1–H18) and 11 NA (N1–N11) subtypes known. Influenza B viruses are described according to their lineage, with current circulating virus belonging to "Victoria" and "Yamagata" [1, 4]. HA plays an important role in host tropism since the viral receptors vary according to the host, it impacting infection and replication of influenza A virus amongst species. For instance, avian influenza viruses engage preferentially α-2,3-linked sialic acid (SA) moieties, whereas human-adapted ones have higher affinity to α-2,6-SA. Interestingly, swine has been indicated

as a "mixing vessel" as this animal has receptors with both α-2,3-SA and α-2,6-SA moieties, allowing the binding of both avian and human viruses and a possible reassortment [5, 6].

1.2 Preventing and treating infection

Influenza is responsible for acute respiratory infections. Annually it is estimated that influenza A and B viruses can cause about 3 to 5 million cases of severe illness, and up to 650 000 respiratory deaths, related to seasonal epidemics [7]. Moreover, the potential for sporadic pandemics outbreaks, caused by influenza A viruses, can lead to millions of deaths, as observed in the past [4].

Influenza virus undergoes constant antigenic variation in their envelope proteins, known as antigenic drift and antigenic shift. Antigenic drift is a continuous process that results from two mechanisms: the selective pressure mediated by antibodies and the accumulation of point mutations in the HA and NA genes, due to the absence of proofreading ability of the viral RNA polymerase. This process induces the variability observed each year. Antigenic shift is the result of a genetic reassortment that originates a novel virus that can potentially cause pandemics (Figure 1.2) [4].

There are four classes of antiviral drugs that have been developed for prophylaxis and therapy of influenza infection: adamantanes, neuraminidase inhibitors, membrane fusion inhibitors, and RNA-dependent RNA polymerase inhibitors [8]. Only the first two are approved for use in the European Union or the USA, and currently, due to the widespread adamantane resistance of all the circulating influenza strains, only NA inhibitors are recommended [9]. However, even NA inhibitors present limitations: they have a short therapeutic window to be used and there is also an emergence of resistance to these type of drugs [4].

Therefore, vaccination continues to be the leading strategy to prevent virus infections. Due to the antigenic drift mechanism, an annual

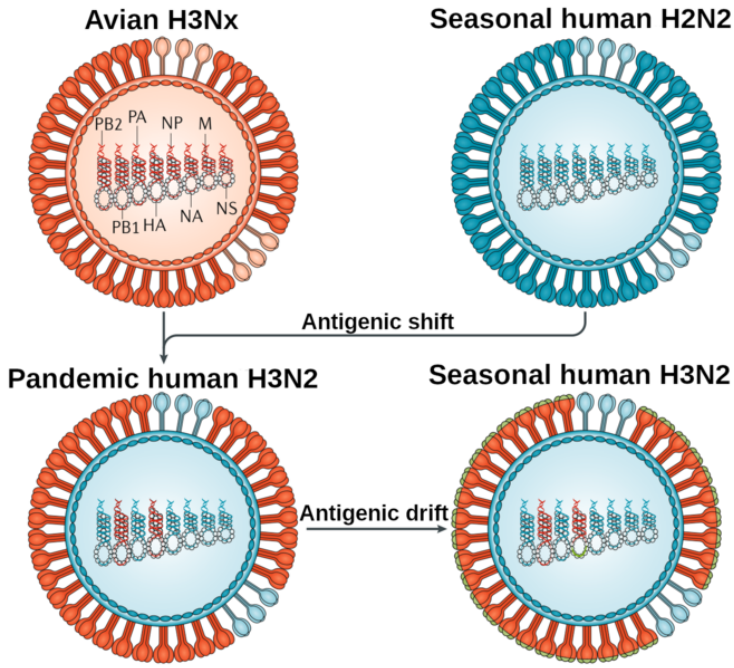

Figure 1.2: Schematic representation of influenza antigenic shift and drift processes. Example for 1968 pandemic human influenza H3N2 virus reassortment. Adapted from [4].

update on vaccine design is required. Therefore, research efforts to reduce the time needed for seasonal vaccine production time as well as the need for continuous updates are being made. The ultimate goal is to develop a universal vaccine with a longer-lasting and broader protection against multiple strains of seasonal influenza virus as well as emerging pandemic strains. There are several projects putting research efforts on the development of universal vaccines, including EDUFLUVAC [10]. The mechanism exploited in this project is based on a concept developed by Davenport and Hennessy [11] and relies on the broadening of the antibody responses by increasing the relative concentration of common epitopes, thus diluting out strain-specific epitopes. This is accomplished by selecting a plethora of antigenic variants presenting a high diversity in their sequences [10]. The timely production processes developed and approved by the authorities, will not be able to prevent the rapid spread of

a pandemic virus strain [12]. Most of the Influenza vaccines are trivalent, having in its composition two influenza A strain and one B strain. Some improvements are being implemented, such as producing quadrivalent vaccines, by adding a second B strain or using new adjuvants [13].

1.2.1 Influenza vaccines and production platforms

The conventional platform for influenza vaccine production has remained, for the last 50 years, the egg-based approach. From the several vaccines against influenza available on the global market and currently under development at the pre-clinical or clinical stage, most of them are still being manufactured using this method [14]. This strategy offers high viral titers for almost all strains, its manufacturing capacity is high and the production costs are low. Nevertheless, several drawbacks are associated with this platform. First, the need for virus adaptation to eggs leads to timely and sometimes ineffective productions which limits the flexibility of the manufacturing process. Moreover, as avian receptors differ from human (see section 1.1) it is frequent that, during egg adaptation, the HA protein from human viruses suffers mutations due to a selective pressure to adapt to the avian receptors to grow. This implies that there is a mismatch between the strain produced and the circulating one, affecting the efficacy of the vaccine. Additionally, it is a risk to rely only on egg availability, either in terms of the required numbers, a problem in case of pandemics, but also if we are not able to use the existing ones if the avian population is infected with an avian influenza disease. Therefore, the paradigm is changing and new solutions must be achieved that cope with the demand for faster and more cost-efficient vaccine productions. These needs paved the way for the development of new production platforms and new products [14, 15].

One of the major changes is the replacement of egg productions by cell-based platforms. In fact, there are already approved vaccines that are manufactured using mammalian MDCK (Flucelvax) or insect Sf9 cell lines (Flublok) [14]. The mammalian cell-based approach eliminates the

constraints related to egg-shortages and turns the process and the timeline more flexible. Moreover, the match between vaccine and circulating strains is improved, as there is a reduction of the HA mutations related to egg selective pressures. The glycosylation profile achieved also have a positive impact on the immunogenicity of the vaccine. Moreover, it eliminates the issues with egg allergies. Still, there is some adaptation needed when using this strategy and, currently, there is no global capacity to manufacture the number of doses needed worldwide. To completely replace the egg-based platforms it will take a significant investment. Moreover, up to now, the manufacturing costs are around 40% higher than the conventional platform. Flublok uses the Baculovirus Expression Vector System (BEVS) to infect Insect Cells and produce a recombinant HA vaccine. The protein produced has exactly the same amino acid sequence as the circulating strain, enhancing the efficacy of the vaccine. This is a more flexible and faster manufacturing platform. There is no need for eggs or virus growth adaptation and it avoids the need of rescuing circulating virus and selecting high producer variants. Similarly to the mammalian production strategy, the vaccine costs doubled and there is no suitable infrastructure to cope with global demands. Other influenza vaccine production platforms, like plants or bacterial cells, are being evaluated for the longer term [16, 17].

Currently, there are three types of vaccines approved: Live attenuated influenza vaccine (LAIV), Inactivated influenza vaccine (IIV) and recombinant subunit (Figure 1.3). Depending on the type of inactivation, the vaccine can be composed of whole viruses - if treated with formaldehyde of β-propilacton) or disrupted virus. Disruption can originate a split vaccine - if treated with ethyl ether or SDS - or a subunit vaccine - if treated with detergents. Besides these strategies, new influenza vaccine designs are in development or in clinical trials for both seasonal and pandemic influenza strains, such as: Virus-like particles (VLPs) [14, 16–20], nanoparticles [21, 22], nucleic acid platforms - DNA [23–26], RNA [27–29] and viral vectors [30, 31], peptide-based approaches [15, 32, 33]

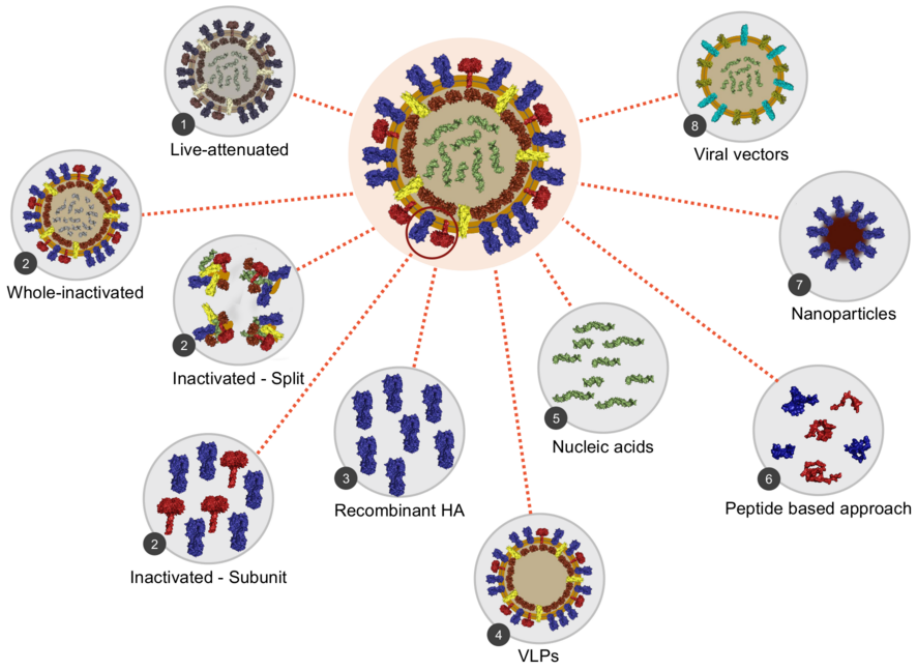

Figure 1.3: Schematic representation of different influenza vaccine approaches. 1-Live-attenuated, 2-Inactivated, 3-Recombinant HA, 4-VLPs, 5-Nucleic acid based, 6-Peptide-based approach, 7-Nanoparticles, 8-Viral vectors.

or synthetic platforms [34, 35].

All of these solutions present advantages and disadvantages and are under constant research and development. With the knowledge we have now, it is still impossible to identify which product(s) or production platform(s) will be finally selected as the most effective. There could even be implemented more than one vaccine type. This selection will be based on product effectiveness and the implementation of a scalable, fast and cost-effective manufacturing process. Here in this review, the focus will be placed on VLPs and on the development of suitable downstream processing strategies for these particles as a vaccine candidate.

Virus-like particles

VLPs display intact and active antigens that resemble the native virions, triggering a protective humoral and cellular immune response. Since these particles lack the viral genetic material, they are not infectious nor replicative, making them safer alternatives to inactivated or attenuated viruses [36]. VLPs have been long established for vaccines for hepatitis B and human papillomavirus [37, 38] and they constitute a promising platform for the development of vaccine candidates for both seasonal and pandemic Influenza viruses [14, 39–43]. Beyond vaccines, engineered VLPs can be used as nanoscale carriers in targeted drug-delivery and molecular imaging [44], as a delivery platform of active proteins to cells [45] or as drug-delivery systems for targeted delivery of cytotoxic agents to tumors [46, 47].

1.3 DSP for Influenza Vaccines and Vaccine candidates

Figure 1.4 compares the purification processes described for representative cases of vaccines formats currently available on the market produced using different strategies: an egg-based vaccine (FLUAD), a mammalian cell-based (Flucelvax) and the recombinant based approach that uses insect cells (Flublok).

After harvesting of the virus-containing bulk, either by extraction and pooling of the allantoic fluid or by the collection of the virus fraction (pellet or supernatant), cell lysis with detergent is performed. The clarification step uses a combination of centrifugation and filtration or only a depth filtration stage, depending on the production system. From this step on, the processes diverge, although they have some points in common. The recombinant vaccine produced by BEVS requires an extraction step with detergent but does not need an inactivation step, contrarily to the other vaccine examples. Split and subunit vaccines have

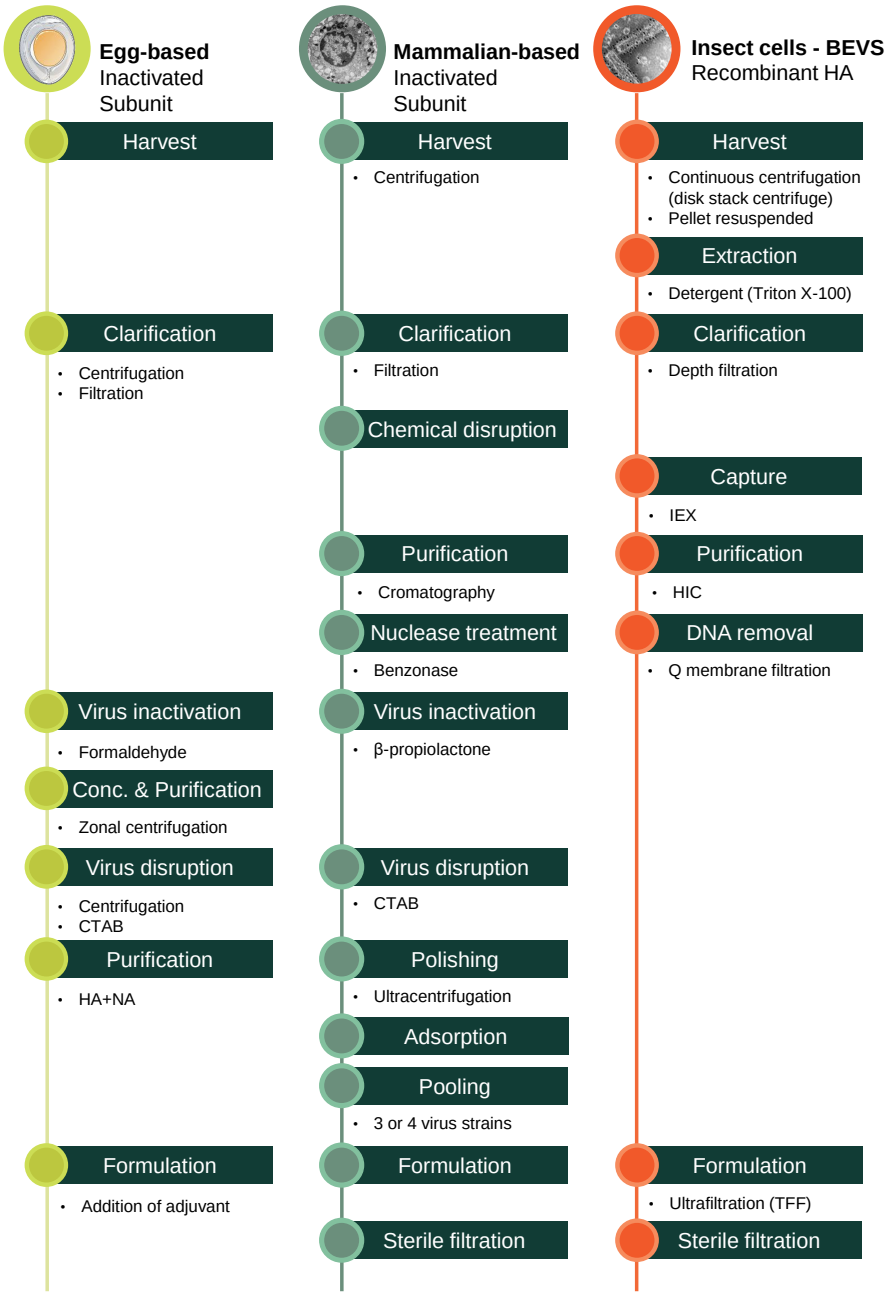

Figure 1.4: Comparison of downstream processes for licensed influenza vaccines produced using different strategies.

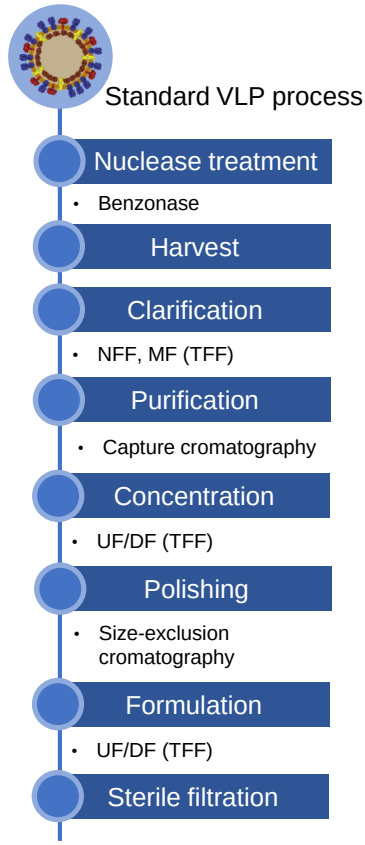

Figure 1.5: Schematic flowchart of a standard downstream processing for influenza VLPs.

an additional treatment step with detergent to dissociate the viral lipid envelope, exposing all viral proteins and subviral elements [14, 48–51].

A standard purification process for influenza VLPs can be designed based on the lessons learnt from virus purification, namely from implemented and approved methods (Figure 1.5). Although some of the steps are not required, virus inactivation for example, the similarity between VLPs and virus gives a good starting point for downstream processing development. Nevertheless, there are still several unmet challenges, either product or production platform related. There are several points to take into consideration while selecting a DSP for virus or VLPs: the ca-

pacity to process large volumes, delivering high product recovery yields and maintaining product stability, process cost-efficiency and easy scale-up as well as purity levels complaint with regulatory authorities requests [52].

1.3.1 Harvest

Virus harvest optimization is of critical importance to determine the success of the viral production and the subsequent downstream processing. The optimum point for harvest should take into consideration parameters such as product concentration and stability, cell density and viability. Pushing the time of harvest (TOH) for longer can increase the amount of product produced, although it is difficult to evaluate the impact it may have on its quality. Moreover, as time advances, cell viability decreases. As a consequence, proteins, DNA or even cellular organelles and debris are released to the supernatant changing characteristics of the bioreaction bulk, which can have a detrimental effect on later purification tasks or even degraded the quality of the product. Therefore, a balance between these parameters should be achieved as it will strongly impact the next steps. The way virus particles are harvested depends on the production platform in use and on the type of product release. Some viruses such as adenoviruses or adeno-associated viruses are present in both intra and extracellular fractions, requiring a cell lysis step to recover both. Cell lysis can be accomplished using, for example, freeze-thaw cycles, detergents, liquid homogenization or sonication. In the case of enveloped Influenza viruses or VLPs, as these particles are secreted by budding, no lysis is required. Nevertheless, even without the lysis step, cell viability decreases releasing host cell DNA and enriching the virus/VLP-containing bulk with other impurities. In the case of VLPs produced using the baculovirus-insect cell system, the optimal point of harvest is usually after 48 h post infection (hpi) when cell viability is around 50-70% [53–59]. Below these values, there is an increase in proteolytic activity and other impurities, which may lead to product degradation. To overcome this

issue, Baculoviruses with a decreased cell lysis capacity were developed [60, 61]. However, TOH can change depending on the influenza strain being produced as different strains present different viability profiles. As previously discussed, maximizing VLP production may lead to low cell viabilities, which will compromise the downstream process. Therefore, an acceptable minimum value of cell viability should be defined to decide TOH [57].

1.3.2 Nuclease treatment

Host-cell DNA is one of the major impurities that should be taken into account on this type of processes. Its removal during the DSP is critical, as to comply with regulatory authorities requirements, the DNA values should be below 10 ng per dose with a size of less than 200 base pairs [62, 63]. Moreover, as DNA increases bulk viscosity and can form complexes with the virus, its concentration and size impact the DSP performance and product recovery yields. Therefore, most of the reported processes include a nuclease treatment, usually with Benzonase although there are several other possibilities [64]. For the sake of process cost-efficiency, DNase incubation step should be performed after a concentration step, to reduce the required amount (U mL^{-1}) of nuclease. However, depending on the product and selected process, it can also be applied before or after clarification [14, 64]. In fact, for several influenza VLPs it is described that the best point for incubation with the nuclease is 12 hours before harvest, which will maximize the capacity of the primary clarification filter without compromising recovery [57].

As the use of Benzonase or other similar products still represents a significant cost on vaccine production, selective precipitation is an alternative for the removal of host cell DNA [64]. A protocol was reported, for the influenza virus, using the cationic polymers protamine sulfate and polyethyleneimine [65]. Using a Design of Experiments (DoE) approach, the authors were able to achieve an optimal condition were DNA removal was around 85%. However, they observed co-precipitation of virus

particles with these polymers, which lowered the recovery yields. The acidic isoelectric points of the virus particles may have been the cause for this. This is a drawback that would probably be observed also for VLPs. In the case of VLPs produced using the baculovirus expression system, co-precipitation of baculovirus with the product of interest can also occur. Moreover, the wide range of isoelectric points observed for influenza strains (from 4.0 to 7.0) [66] poses challenges on universal optimal conditions definition for selective precipitation, which will not occur when using the nuclease treatment. Nevertheless, the conditions for optimal nuclease activity should be balanced with product stability, as for instance, pH, temperature or ionic strength affect the enzyme performance [57]. Additionally, the removal of nuclease or precipitation agents should be confirmed later on the DSP.

1.3.3 Clarification

Clarification is considered the initial step of the purification, connecting up and downstream processes. Although it is not extensively studied, the research efforts on the improvement of this operation are increasing, as it has a critical impact on the downstream purification train, affecting product recovery and process performance. To be considered efficient, a clarification step should deliver a solution with turbidity levels below 10 NTU [61, 67], with minimal impact on product recovery, while also removing process and product-related impurities. Clarification can be divided into two different stages, defined as primary and secondary clarification steps. At a first stage, primary clarification is responsible for the removal of large particulate matter, including intact and non-viable cells. The main goal of secondary clarification is the removal of colloidal matter, suspended species, and process- or product-related insoluble and soluble impurities including large aggregates [43, 57, 61, 64]. In some cases, removal of host cell proteins, DNA or baculovirus is also possible using depth filters [57].

As described in Figure 1.4, there are several strategies that can be

applied for the clarification stage, depending on the type of product and production system. Although most of the processes are still using the conventional centrifugation methods, new membranes and filtration process technologies are attractive alternatives to replace them. If we move to an industrial scale, to keep this unit operation, the only viable option is a continuous flow centrifugation, using disc-stack centrifuges. From the point of view of influenza processes, centrifugation is strain-independent, being a robust option for a universal process [62]. However, this implies high capital investments and scale-up drawbacks, as these continuous disc-stack centrifuges only operate with volumes that are not compatible with pilot-scale optimization experiments [64].

The clarification of egg-based vaccines should be able to handle with the allantoic fluid, which is extremely challenging due to its high viscosity, high protein content, and presence of residual tissue compounds. For this cases, centrifugation continues to be a widely used method delivering product recovery yields of about 70 %. However, new filtration techniques are also being applied, such as Normal Flow Filtration (NFF), using polypropylene or cellulose-based depth filter. A second step can easily be performed with an NFF cellulose, polypropylene or glass fiber filter. Microfiltration (MF) membranes using Tangential Flow Filtration are also a viable option [14, 61].

Cell-based processes are easier to clarify as the harvested bulks are cleaner than allantoic fluid. For this cases, NFF can be applied directly after the bioreactor harvest. Filter sizing should be optimized according to cell culture conditions, to handle with different cell densities and viabilities at time of harvest. In fact, improvement of upstream productivity has led to high cell density cultures, so the clarification filters have an increased burden with high DNA content, cell debris, and large aggregates [68]. There are several reports where clarification of influenza virus was successfully achieved using depth filters or microfiltration, with HA recoveries of 85% and 93%, respectively [69]. TFF can also be applied to Influenza VLPs [14, 57]. A clarification train using a depth

filter followed by a sterile filter was successfully applied to the clarification of different influenza VLP strains, including mono and multivalent VLP strains, with recovery yields close to 100 % and turbidity values below 10 NTU. MF was also evaluated presenting high recoveries and low turbidities. This strain-independence is of extreme importance for the development of universal processes for influenza [57]. It is important to note that influenza virus, and VLPs also, are prone to form complexes with impurities present in the bulk, which may lead to adsorption losses during the clarification step [57, 61, 70]. Moreover, VLPs are a more complex system, as they are more shear sensitive than the virus and due to baculovirus presence, usually presenting a similar size [61]. Therefore, careful selection of the filters and optimization of the operation parameters requires critical handling. These membrane and filtration technologies offer process flexibility, rapid product changeover, the possibility of single-use and capital savings as well as ease of scale-up [57, 61, 71].

1.3.4 Concentration

Volume reduction will simplify the handling of the clarified material, as well as the scale selected for the next operations, accelerating the purification process. Moreover, it is often necessary to change the product buffer to one more amenable for the next purification tasks [64]. There are several options to perform concentration, such as tangential ultra and microfiltration, or gradient ultracentrifugation (sucrose cushion, iodixanol or cesium chloride gradients) [72]. Although tangential ultracentrifugation is one of the most selected methods for virus concentration and initial purification at laboratory scale, it is time and equipment intensive requiring an initial investment on scale-up. Quite often several ultracentrifugation cycles are needed to achieve the desired purity. Furthermore, the density gradient forming material should be removed after this step, either by dialysis or Size-exclusion chromatography (Figure 1.4) [14, 64, 73]. Nevertheless, this technique combines two steps into one and presents some advantages in terms of separation of different populations, such as empty

capsids and full viruses [64]. In fact, Novavax reported the discrimination between Influenza VLPs and Baculovirus using a sucrose cushion procedure [74]. However, other authors reported that VLPs produced using insect cell line Sf9 or mammalian cells HEK293 are too fragile for allowing ultracentrifugation cushions and iodixanol gradients without damaging the particles. Moreover, the resolution of Baculovirus and VLPs was challenging [59]. These different observations among literature reports may be due to differences in the influenza strains produced, as well as the structural matrix protein used, which can confer different stabilities. These contrasting results combined with the drawbacks described above, are probably the main reasons why there are few reports on the use of ultracentrifugation for large-scale manufacturing [64] although some authors still propose its applicability [74].

Ultrafiltration is one of the key methods for large-scale virus concentration and buffer exchange (diafiltration), being one of the unit operations for most of the reported virus purification processes. This filtration method is based on molecular weight differences between the product of interest, that should be rejected by the membrane, and process impurities, that should be able to permeate the membrane.

The UF modules can be presented as flat-sheet cassettes or hollow fibers (HF). The selection of the module to use depends on the stability of the product of interest and on process parameters. On the one hand, HF have wider flow paths which implies lower shear rates, critical for processing fragile components, such as viruses and cells. On the other hand, cassettes present shorter processing times at higher shear rates, as the hydrodynamics of its flow channel causes lower concentration polarization near the membrane, decreasing the propensity to gel layer formation and clogging, suitable for more viscous solutions [62, 64, 72].

Ultrafiltration uses membranes that can have different chemistries, such as regenerated cellulose (RC), polysulfone (PS), polyethersulfone (PES) and polyvinylidene fluoride (PVDF) and with a molecular weight cutoffs (MWCO) that range from 0.5 to 1000 kDa.

According to the cell producing system, influenza strain and harvest conditions the most suitable options and key operating parameters can vary. Transmembrane pressure (TMP), cross-flow, retentate and permeate fluxes, concentration factor or diafiltration volumes should be optimized in order to maximize product retention, assuring the highest separation from impurities at high permeate fluxes. Moreover, the specific goal of the ultrafiltration step as well as the DSP steps prior to the concentration (usually clarification) have an impact on the device performance [58, 75].

Kalbfuss el al [69] evaluated different PS HF with different MWCO (750 kDa, 0.1 μm, and 0.45 μm) to concentrate influenza virus produced using MDCK cells. Prior ultrafiltration, the bulk was clarified by depth filtration, followed inactivation and a microfiltration step. Distinct product recoveries were obtained: 0.45 μm device did not retain the virus, 0.1 μm HA recovery was 54 % and the 750 kDa provided 100 % recovery. Reported strategies for influenza VLPs vaccine processing also uses HF devices for concentration and diafiltration [74].

Although HF are widely used for influenza virus with high product recoveries, membrane cassettes are also an option for VLPs and virus processing. Nayak et al selected a 100 kDa PES membrane cassette to concentrate an equine influenza strain produced in MDCK cells. Prior to UF, the viruses were clarified using a depth filter followed by virus inactivation. In this case, a 95 % HA recovery was obtained [76]. Wickramasinghe et al selected a 300 kDa PES cassette and reported a yield of around 100 % using also MDCK cells and the same clarification process [77]. The differences in the selected MWCO can be strain-dependent but it is important to note that the pore size defined for a device can vary according to the manufacturer. Asanzhanova et al produce the virus in eggs and the selected cassette for concentration after depth filtration had an MWCO of also 300 kDa. The yields obtained were all above 92 % [78]. Tseng et al also selected the same MWCO for the influenza virus evaluated that was also produced in eggs. However, the clarification process

was slightly different having used a depth filter and a second filter after inactivation. The defined DSP had two ultrafiltration steps: one immediately after clarification and a final one after chromatography. For the first UF step, the virus (HA) recovery yield was 76 %. However, the second UF provided 93 % of recovery. This reveals that bulk conditions and operation parameters had an impact on the cassette performance [75]. The selection and performance of different membrane cassettes for a complete DSP of influenza VLPs(evaluation of several chemistries, MWCO, operation parameters) were reported by Carvalho et al [58] and will be addressed on Chapter 5. Membrane chemistry (PES vs RC), pore sizes (ranging from 100 to 1000 kDa), operation modes, critical flux, transmembrane pressure, and permeate control strategies were evaluated. The best performance was reported for 1000 and 300 kDa PES membrane cassettes, depending on the step of the process. Globally, the ultrafiltration process achieved product recoveries of 80 %. Taking into account that this method is independent of influenza strain, it is compliant with a universal process for influenza. Ultrafiltration PES membranes of 300 kDa were also evaluated successfully for DSP that included chromatographic unit operations [54, 55]. As mentioned previously, the Baculovirus expression system adds a layer of complexity to the DSP as it is challenging to discriminate them from influenza VLPs.

Overall, ultrafiltration can be designed as a very robust method resulting in high virus particle yields. The scale-up is relatively straightforward and both HF and membrane cassettes can be used as fully disposable. Moreover, it can be coupled with diafiltration providing a buffer exchange step [64, 73].

1.3.5 Chromatography

Due to the multitude of separation types, availability of materials and operation modes, chromatography is commonly regarded as the bedrock of DSP. It can be used at different stages with distinct purposes. A capture step intends to concentrate and isolate the product of interest.

Ideally, this should be a fast step to remove the product from conditions that may affect its stability. Its use at a second stage, intermediate purification, should remove contaminants using orthogonal approaches. Finally, a polishing step will remove trace impurities [62, 64, 72].

Chromatographic separation is based on the exploitation of the physicochemical differences between the target virus or VLPs and impurities against the substrate surface. The stationary phases can be physically structured as packed beds, membrane adsorbers or monoliths. Packed beds are composed of beads packed into a column. This arrangement is widely used in the field of biopharmaceuticals, although most of the materials are optimized for protein purification rather than for virus particles. The main disadvantages are related to limitations on the operation flow rate, due to the needed balance between pressure drop and mass transfer, and low dynamic binding capacity, as a result of reduced intraparticle diffusion. These impact process time, decreasing throughput and implies an increase on the scale needed [62, 64, 72]. The development of convective media such as membrane adsorbers and monoliths, offers improvements in processing time, capacity and recovery [64, 73, 79]. Monoliths are continuous blocks of stationary phase with interconnecting channels that offer transport via convective flux. They have a large process capacity and high-resolution [62, 64]. However, they present mechanical instability, their lack of homogeneity limits scalability [79] and there are reports claiming that they are prone to clog in the presence of high levels of DNA, due to DNA-virus complex formation [64, 80]. Membrane adsorbers are able to process large volumes offering high operational flow rates, low-pressure drops, and neglectable compression or channeling. However, their short diffusion times limits binding capacity [81]. Moreover, as these membranes present larger void volumes than monoliths, their resolution is also lower [73]. Membrane adsorbers' low production costs make them a cost-effective strategy for single-use unit operations. Recent developments on monoliths should allow them to follow the same trend somewhere in the future.

Ion exchange chromatography (IEX) exploits the reversible interaction between a charged viral surface and an oppositely charged matrix to give high-resolution elution gradients with high sample loading capacity. It can be operated in positive (bind-elute) or negative (flow through) mode. Most of the DSP reported in the literature use bind-elute mode. Depending on the isoelectric point of the virus, and the desired operation mode, one can select anionic or cationic exchangers. Elution of the product of interest is accomplished by increasing ionic strength or by a pH change. It is important to note that these elution strategies can affect virus stability. Influenza viruses stability shows a pH-dependent behavior, in particular for acidic conditions. However, high salt concentrations do not affect significantly the virus [72]. Nevertheless, as influenza is an enveloped virus, high salt concentrations should be used for short periods of time. This is also true for VLPs, that usually are more sensitive than the virus [59]. There are several reported examples of DSP for influenza virus using anion exchangers, such as Sartobind Q [54, 82, 83], Q monolith or DEAE monolith [84] or sulfonic acid cationic exchanger [84]. More recently, Tseng et al reported a purification train that uses the anion exchanger Capto Q in a flow-through mode for influenza purification [75].

Influenza purification using affinity chromatography (AC) is widely reported in the literature [85]. It is highly specific as it is based on the affinity of a ligand to a specific component of the virus envelope. There are examples exploiting the affinity of influenza to lectins [86], metal ions [87], sulfated carbohydrate matrices [62, 72, 88–94] or sulfated cellulose membrane adsorbers [56, 93–95]. Its specificity delivers high yields and simplifies the DSP however, scale-up is expensive due to ligand purification and immobilization costs. A drawback related to high specificity is the possible lack of robustness for processing different influenza strains, which limits its application as a purification platform [62, 64]. Moreover, for insect cells-based VLPs, both influenza particles and baculovirus will have an affinity to the current ligands. Budding

is responsible for common components in their envelope coming from the host cell [54, 55, 96, 97]. A ligand that targets conserved regions of influenza virus proteins, a not present in baculovirus, may deliver a strain-independent affinity unit operation. Opitz et al reported an affinity strategy that uses a lectin to efficiently capture two different influenza strains. However, this lectin presented different specificities for strains produced using different host cell lines, probably due to different product glycosylation profiles [98].

Hydrophobic interaction chromatography (HIC) is routine for protein purification procedures but is not commonly used for virus purification. Tough, there are some examples in the literature [99, 100], for influenza virus [101] and recombinant influenza proteins [14]. One of the main reasons for the lack of popularity among viral vaccine DSP is the need for high salt concentrations and, sometimes, kosmotropic salts to achieve desorption, which can impact virus integrity [64].

Mixed-mode chromatography (MMC) exploits simultaneously multimodal binding mechanisms. One example is hydroxyapatite, which use was reported for the purification of dengue virus. Additionally, research efforts are being made to apply it to influenza viruses [102]. Another recent example is GE's CaptoCore technology. This resin is composed of a ligand-activated core and an inactive shell. It operates under a multimodal strategy, due to octylamine ligand dual functionality. The size exclusion properties allow virus particles to be excluded from the core, and ligands on inside the core capture efficiently contaminants. Several strains of cell-derived influenza A and B viruses were purified combining Capto Q and Capto Core 700 resins [103]. The results obtained are in agreement with the requirements of European Pharmacopeia [104]. A flow-through purification process for H7N9 and H5N1 influenza viruses was reported employing this combination [75].

Size exclusion chromatography (SEC) separates virus particles and impurities by differences in size. Viruses are excluded from the matrix, eluting in the void volume. The process conditions are gentle, which

is critical for stability and infectivity of fragile viruses. SEC has been widely used for viral particles purification [64], including influenza virus [76, 83] and VLPs [53–55], using several production platforms and usually delivering high recovery yields [62]. In most of the cases, SEC is used at the end of the DSP as a polishing step, but it can be applied also in early stages [83]. As viral particles do not bind to the resin, buffer composition does not directly affect resolution, meaning that conditions can vary to suit different product or process requirements. It is a main advantage for the development of universal processes for viruses that are constantly changing, such as influenza. In fact, Carvalho et al reported a charge-independent purification process for several influenza VLPs strains produced in insect cells [54, 55]. One challenge related to this producing system is the discrimination between VLPs and baculovirus. Using this strategy most of the baculovirus co-eluted with VLPs. There are other drawbacks related to SEC low capacity, product dilution, matrix limited pressure resistance and scale up challenges related with column packing, poor flow distribution, and time-consuming cleaning in place (CIP) procedures [64].

The increasing demand for better and more cost-efficient purification processes impose continuous research developments. New concepts and strategies are being proposed to virus bioprocesses, including influenza viral particles. Steric exclusion chromatography (SXC) is based on the capture of a target product at a non-reactive hydrophilic surface by the mutual steric exclusion of polyethylene glycol (PEG) from both the target species and the stationary phase. No direct chemical interactions between ligand and target product are required and lower molecular weight (MW) impurities are washed away. The product can be eluted by reducing the PEG concentration in the mobile phase. This strategy was recently applied for influenza virus purification, yielding a product recovery above 95% and host cell DNA and total protein clearance of 99.7% and 92.4%, respectively [105]. Continuous chromatography has been recently exploited for recombinant proteins or antibody products due to its

higher productivity and consistency (versus batch) and the possibility for process automation [106]. Recent examples of the use of this technique for influenza virus purification using SMB size-exclusion [65] or anion exchange approaches [107] are reported in the literature. From the different continuous systems currently being employed in the biopharmaceutical industry, countercurrent simulated moving bed (SMB) [65, 106, 108] or periodic countercurrent chromatography (PCC) [109] are the most advanced. Despite the increased process design complexity, these strategies are able to reduce buffer consumption, increase productivity and product recovery while improving clearance of impurities [64].

1.3.6 Process Design and optimization

Optimization of bioprocesses requires a fundamental understanding of the process and characterization of product recovery and impurity clearance across the different steps. Beyond an initial design of process decision, DSP optimization for viruses, including the selection of unit operations and process conditions often relies on trial and error approach, as little is known about the physicochemical properties of these complex biomolecules. In order to reduce time and resources to optimize conditions, new tools for process understanding are being implemented. In this context, and as part of the Quality by Design (QbD) concept [110], Design of Experiments (DoE) is a valuable tool allowing a rational, fast screening and optimization of factors' levels impacting product yield and impurity levels even more so if scaled down tools are needed [111]. The advantages of its application in the production of biopharmaceuticals, using different chromatographic matrices were reported [64, 111–116]. A DoE experiment should have a goal, definition of critical parameters (factors) and boundary conditions for the defined factors that cover the intended experimental space. The multivariate data acquired is fitted into a mathematical model that describes the system. The evaluation of the model obtained allows the understanding of the relevant factors and their impact on the process responses. DoE strategies were recently

employed to investigate the influence of both matrix and process-related critical factors on the purification of influenza virus derived from mammalian cell cultures [95] and influenza VLPs derived from insect cells [56].

2

Analytics and quality control for virus-based biopharmaceuticals: from the classical methods to the newest tools

Since the very first visualization of a virus by electron microscopy in the late 30's of the 20th century until the most recent Nanopore-based technologies, a myriad of tools have been developed for processing, analyzing and characterization of virus and virus-based particles. With the expansion of the therapeutic potential of these particles - vaccines, gene therapy and oncolytic therapy - such methods assume critical relevance to assure the highest standards of quality and safety.

Herein, an overview of the methods and techniques for the analysis and quality control of virus-based particles is provided. Many of them are reinventions or combinations of very classical methodologies originally developed for other applications, typically, proteins. Others are new approaches using state-of-the-art equipment specifically targeting the monitoring and characterization of nanoparticles. The methods are presented based on their operation principle - spectroscopy, microscopy, chromatography, microfluidics, etc. - and output - viral particles isolation, fractionation, modification, and characterization. They are additionally discussed as tools for monitoring upstream and downstream process and in the context of assessing important manufacturing quality control parameters such as identity, potency, toxicity, and purity.

This review offers an overview of currently available possibilities to

process, analyze and characterize viral particles preparations, from production bulks to highly purified samples. It intends to aid and speed-up the selection of the appropriate methods through user-friendly decision-trees and structured tables guiding readers into the several options and relevant literature.

2.1 A growing market of very complex products

Virus-based biopharmaceuticals (VBBs) comprise a multitude of products derived from viral particles, namely viral vectors, inactivated or attenuated viruses or VLPs, targeting important therapeutic applications [117]. The interest in these products has experienced substantial growth in the past decades mainly driven by (viral) Gene Therapy and modern Vaccinology. Significant research efforts are being made on new designs, production platforms, and cell line development as well as downstream process development for these products [64, 117, 118]. After initial bumps and setbacks, Gene Therapy has established as a 21st century medicine to target orphan diseases derived from monogenetic defects [119]. Outside of monogenic disorders, Gene Therapy is also growing due to the success of T-cells-based cancer immunotherapy, which typically use viral vectors to modify T cells either by altering the specificity of the T cell receptor (TCR) or by introducing antibody-like recognition in chimeric antigen receptors (CARs) [120]. Classical vaccines have long secured a safe position in the biopharmaceuticals market for a number of reasons, including i) growing demand worldwide especially in emerging markets, ii) low exposure to revenue declines from the expiry of patents and iii) reduced competition due to complex manufacturing process [121, 122]. Apart from the classical vaccines - educators of the immune system, typically prophylactic, and directed at microbial targets - a new wave of therapeutic vaccines is growing. Virus-based particles are harnessed as protein and/or nucleic acids delivery vehicles to target infectious diseases such as influenza [123], hepatitis B or human papillomavirus [37, 38],

cancer [46, 47] or neurodegenerative disorders [124, 125]. The complexity of VBBs is incomparably higher than that of small molecules or even proteins. While this has sheltered the manufacturing industry from competitors, it is also a main challenge for analytics and quality control. In fact, proper characterization and robust product quantification are critical for bioprocess development and successful clinical trials of vaccine candidates [96]. There are strict guidelines from regulatory authorities on what type of quality and potency tests should be performed (Table 2.1) but also which are the approved methods that can be used [126–128].

The methods and analytical tools available for virus particles detection, visualization and quantification is vast and continue evolving, increasing the toolbox available for vaccine development (Figure 2.1).

Table 2.1: Standard specifications for biopharmaceuticals (Adapted from Refs. [64, 129]).

Attribute	Specification
Appearance and description	Color
	Physical state
	Clarity/turbidity
Identity	Several tests may be required:
	Physicochemical
	Biological
	Immunochemical e.g. ELISA
Purity: Product-related impurities	Enzymatic degradation products
	Truncated forms
	Molecular variants
	Dimers, multimers, aggregates
	Misfolded product and/or product with random disulphide bridge forms
	Deamidated product variants
	Product with oxidation of methionine
	Product with heterogeneity of post-translational modifications such as glycosylation, phosphorylation and acylation
Purity: Process-related impurities	Host cell protein (HCP)
	Host cell DNA, other nucleic acids
	Cell-culture media components
	Enzymes/chemicals
	Proteolytic enzymes, other enzymatic activity
	Endotoxins
	Virus
	Cell debris, lipids
	Antifoams, antibiotics
	Leakage, e.g., from affinity columns
	Extractables, e.g., from plastic surfaces
	Water, buffers
Potency	Cell- or Animal-based tests
Quantity	Protein mass or
	Potency (if applicable)
	Virus titers or virus particles
Safety	Sterility
	Adventitious viruses
	Endotoxins/Pyrogens
	Mycoplasma
General	pH
	Osmolarity

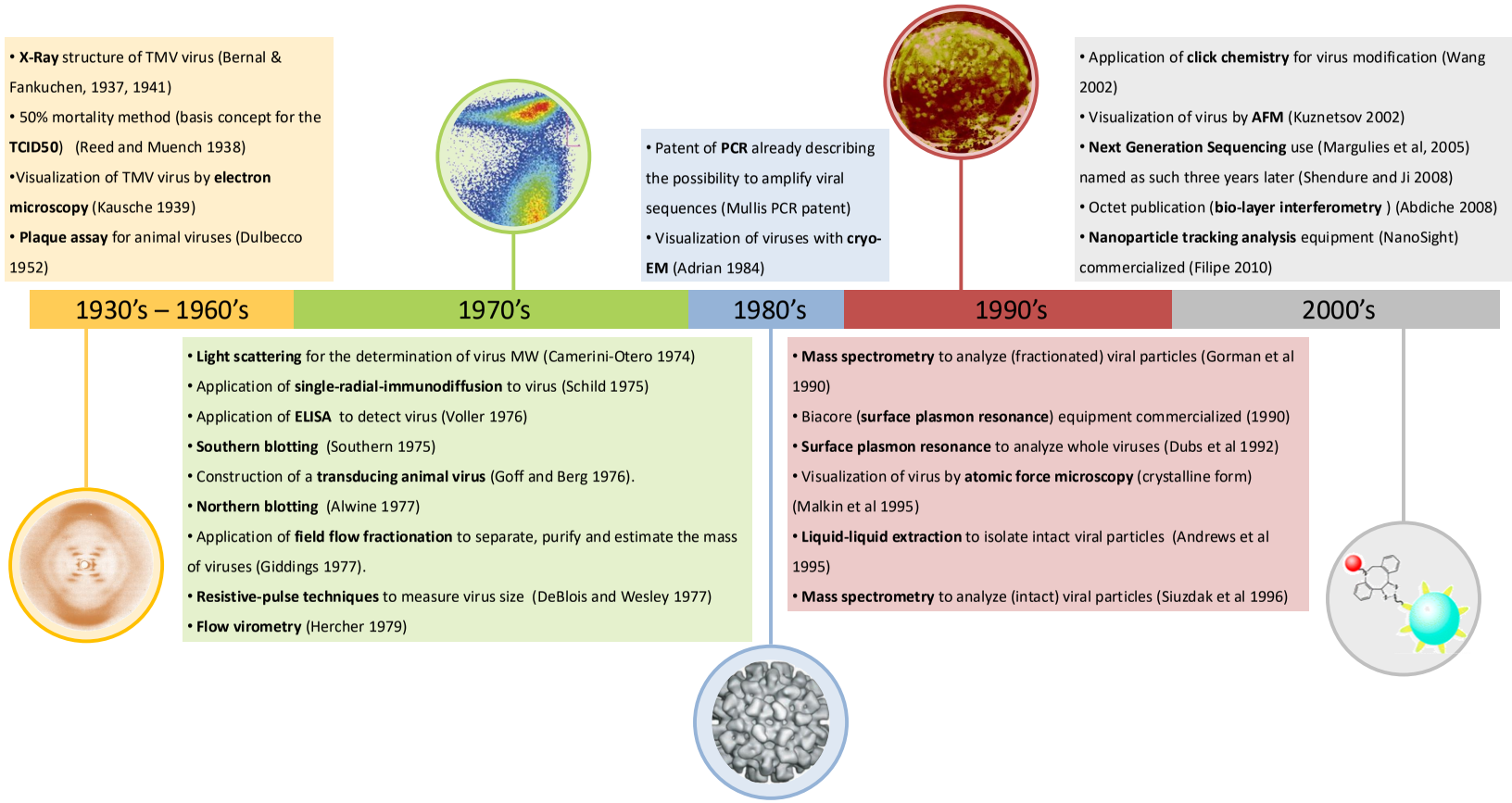

Figure 2.1: Main landmarks in the development of methods and techniques for virus detection, visualization and quantification.

However, there are still unmet needs requiring research investment to cope with regulatory entities demands for improved vaccine safety. Figure 2.2 highlights, in the form of a decision tree, currently available analytics and quality control methods for virus-based biopharmaceuticals, grouped by type of analysis or output needed.

2.2 Analytical tools for Influenza candidate vaccines

The increasing interest in VLPs as vaccine candidates is raising the demand for new process monitoring and product characterization tools. The improved methods should be fast, reliable, easy to set up, and applicable for in-process samples, from upstream harvesting bulk to downstream purified product. VLPs are also becoming established as vaccine candidates for influenza. Despite the innovations observed in the bioprocessing methods, VLPs are still being characterized by the standard influenza virus analytical tools: Single Radial Immunodiffusion (SRID) and Hemagglutination assays [96, 130]. These methodologies present several drawbacks: they are time-consuming, cumbersome, and not supportive of efficient downstream process development and monitoring, as will be discussed in the following sections. Furthermore, they are not optimized for VLPs. Therefore, research efforts are being made to develop new tools, namely alternative influenza potency assays, ideally strain-independent, as recommended by the regulatory authorities [131]. It is important to have tools available that enable process monitoring, allowing viral particles' detection and enabling discrimination of process impurities, in particular baculovirus, for Influenza VLPs produced using insect cells.

This chapter will be focused on analytical tools for influenza Virus-like particles' quantification, since a new method was developed. A multitude of analytical tools and biophysical methods were used throughout this thesis, whose details are described in the corresponding chapters.

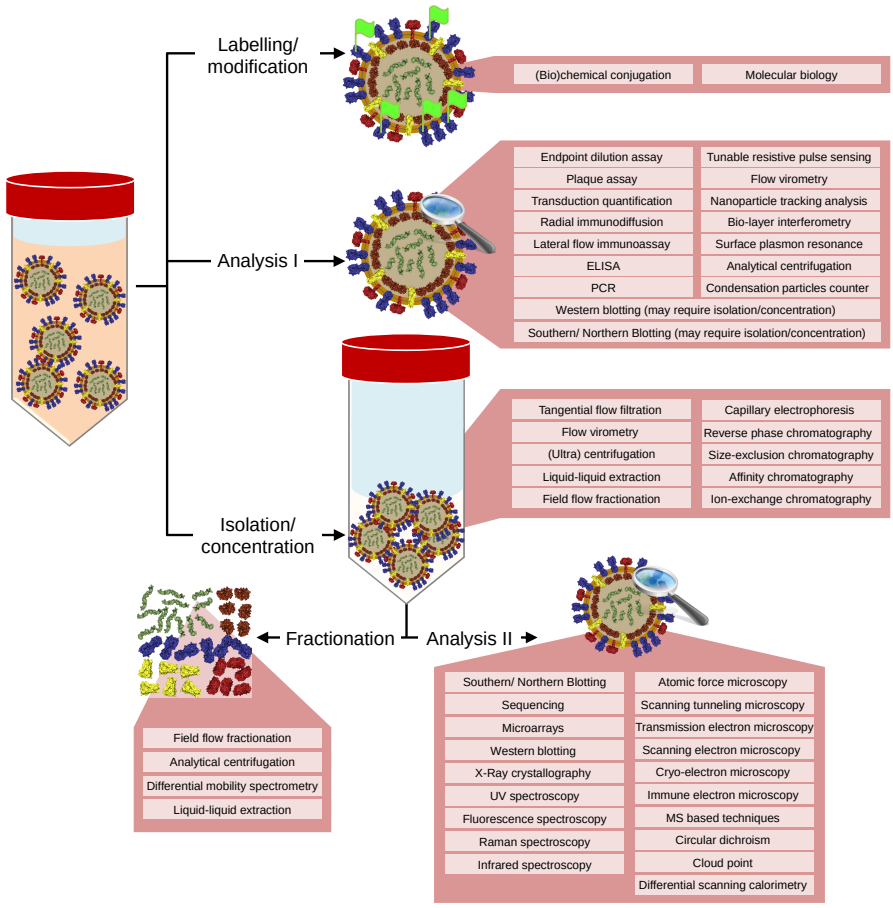

Figure 2.2: Decision tree: analytics and quality control methods for virus-based biopharmaceuticals.

2.2.1 Influenza VLP quantification

SRID

Single Radial Immunodiffusion (SRID) was established and validated in the 1970s [132] and remains the only FDA and WHO approved method to measure influenza vaccines' potency and determine dose [133, 134]. This method requires two types of reagents: an antibody reactive to the influenza strain to be assayed and a reference antigen with a known concentration (and homologous to the assayed strain). In this assay, the

polyclonal anti-HA antibody is incorporated uniformly in an agarose gel that is then punched to form wells. These wells are then loaded with several dilutions of the standard reference antigen and the samples with unknown concentration. Antibody-antigen complex formation creates a precipitation ring, that is stained with Coomassie blue, allowing antigen (HA) concentration measurement by measuring rings' diameter [96, 130]. Although it is the current gold standard, it presents several drawbacks posing the need for better alternatives. Briefly, it is a simple assay that does not require complex and expensive equipment. However, its implementation is not straightforward, requiring specific HA antigen references and antibodies that need to be constantly updated, delaying the release of new vaccines, critical in the case of pandemics. It is time-consuming, taking up to 3 days to perform, which is impractical for process development. Moreover, its low sensitivity (3-5 μg mL^{-1}) and interference with the presence of HA aggregates and non-aqueous components encumber measurement of in-process unpurified samples [96, 130]. Not all the strains can be digested to be analyzed by SRID, namely the pandemic H1N1 pdm009 [135] and the method is not optimized for VLPs or viral particles produced using insect cell systems [134].

Hemagglutination assay

Hemagglutination assay (HA assay) is an antibody-free method for quantification of influenza virus. It takes advantage of the HA protein binding capacity for sialic acid receptors present in red blood cells (RBC) and its agglutination properties. In the absence of viral particles, RBC will fall at the bottom of the 96-well plate and form a button. When combined, if the influenza particles are present in high enough concentration, there is an agglutination reaction and the RBC link together to form a diffuse lattice [96, 130, 136]. Serial dilutions of a known concentration reference and of process samples are applied on a 96-well plate containing RBC and visually inspected. The result is positive until the dilution at which there is a button on the bottom of the well. Although it is not con-

sidered a standard method by the regulatory entities, and no standard protocol exists, this assay has been used for evaluation of production and purification yields of both Influenza virus and VLPs. It is relatively fast compared to SRID, but it presents other critical drawbacks. It requires fresh RBC to obtain reproducible results. Due to the differences in cell supply (type and donor), an external standard is required to be used for each assay. This is critical for VLPs that lack this standard. The principle of the method assumes that one viral particle binds to one cell. Since VLPs are more heterogeneous than the influenza virus, its agglutination abilities differ and the ratio of red blood cells to VLPs can differ from one. Changing this ratio can lead to an erroneous estimate of total particles. It presents also problems with in-process samples as free protein and process impurities can also react with RBC [96, 130]. Moreover, quantification of VLPs produced using insect cells present an additional challenge as Baculovirus also have HA protein in their envelope [137].

NA enzymatic assay

Currently, no standardized assay is available to quantify viral glycoprotein neuraminidase in influenza vaccines. However, enzymatic NA assay can be applied to confirm the presence of NA activity. There are several commercially available kits for NA activity measurement that have been used for both virus and VLPs: a colorimetric method (TBA), a chemiluminescence-based assay (NA-star system), and two fluorometric methods (Amplex Red and FL-MU-NANA) [96]. NA-star is reported to yield higher sensitivity but is not suitable for non-purified samples [138]. FL-MU-NANA seems more robust for in-process samples analysis [139]. However, NA enzymatic assays are unacceptable for accurate quantification. Therefore, Influenza vaccines that are on the market do not have controlled NA concentration [140].

Emerging analytical tools

Due to the increasing need to replace the current quantification methods, there are several emerging tools attempting to overcome the drawbacks described above. ELISA (enzyme-linked immunosorbent assay) is the most common alternative to SRID, namely using monoclonal antibodies [141]. There is also receptor-based ELISA that uses synthetic sialic acid receptors to HA quantification [131]. Flu-Toc, an immunoassay that uses subtype specific but broadly reactive monoclonal antibodies, was reported as a time-saving approach for HA quantification [142]. There are several reports of methods based on reversed-phase HPLC (high-performance liquid chromatography) to quantify HA, from different strains and produced by different cell lines [143–147]. qPCR (quantitative real-time PCR) and $TCID_{50}$ for infectious particles can also be performed for influenza viruses quantification but not for VLPs [96, 130]. Several authors also report surface plasmon resonance (SPR) assays using antibodies or sialic acid receptors [148–150]. Mass spectrometry methods are also being evaluated [151, 152]. These new methods have to become simple, cost and time effective, therefore the need for antibody or antigen updates, the lack of proper standards and the capacity to quantify in-process samples and from different strains at the same time have to be taken into consideration.

Biolayer interferometry

Biolayer interferometry (BLI), the technology used by the Octet platform, is based on the principles of optical interferometry. Briefly, when two propagating waves are perfectly in phase, there is a constructive interference and the resulting wave has an amplitude equal to the sum of the two waves. When the two propagating waves are completely out of phase, the destructive interference results in a wave with zero amplitude. On the Octet platform, the interference pattern of white light reflected from two surfaces, a layer of immobilized protein on a biosensor tip,

and an internal reference layer is analyzed. When molecules bind to the biosensor tip, there is a shift in the interference pattern. The binding between a ligand immobilized on the biosensor surface and a molecule in solution produces an increase in optical thickness at the biosensor tip, which results in a wavelength shift. These interactions are measured in real time, providing the ability to monitor binding specificity, rates of association and dissociation, or concentration, with precision and accuracy.

This thesis reports the development of a VLP Influenza label-free quantification tool based on biolayer interferometry applied on an Octet platform (Chapter 4). The method takes advantage of HA interaction with human (α2,6-linked sialic acid) and avian (α2,3-linked sialic acid) receptors, eliminating the need for antibodies or RBC. It can quantify Influenza VLPs at all stages of bioprocess, from crude bulk to final purified product, mono and multivalent strains. It allows for real-time results, critical for in-line monitoring of downstream processing, improving process development, control, and optimization.

3

Aims and Scope

The production of influenza viral particles towards vaccine applications still faces major challenges. Amongst them are: i) the need for constant updates due to antigenic drift, annually requiring new vaccines; ii) the development of improved analytical tools for new vaccine formats, not only to speed up the process of vaccine delivery, but also to properly monitor the process and the target products; iii) development and optimization of downstream process (DSP) unit trains enabling high product titers and minimal presence of residuals, to cope with regulatory requirements.

The main goals of this PhD project, schematically represented in Figure 3.1 were:

1. **DSP improvement**

    - Design a universal, efficient and scalable DSP, adaptable to several influenza VLPs, from different strains, subtypes, and groups. A basic DSP backbone and operation conditions were improved to obtain such process. This was accomplished by optimizing all the unit operations and by combining orthogonal methods (filtration and chromatography) to obtain a hybrid bioseparation process. New materials such as sulfated cellulose membrane adsorbers were assessed.

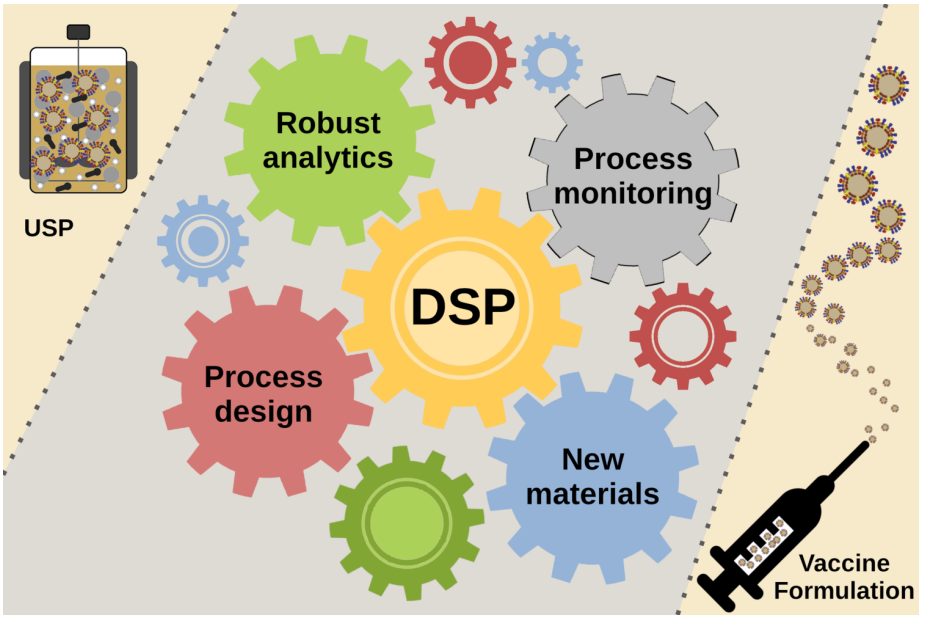

Figure 3.1: Schematic representation of the main goals of this thesis.

2. **VLP characterization and development of analytical tools**

   - Characterize the physical properties and structural features of VLPs using several biophysical techniques. Develop and implement new quantification methods, suitable for in-process sample analysis at all stages of the bioprocess, as well as process monitoring tools. A label-free tool, that uses BLI technology, was developed to quantify VLPs by exploring the interaction between sialic acid receptors and HA protein. A "tag and modify" strategy through site-selective protein modification was used to fluorescently label VLPs and monitor the bioprocess.

4

Universal label-free In-process Quantification of Influenza Virus-like particles

Sofia B. Carvalho, Mafalda G. Moleirinho, David Wheatley, John Welsh, René Gantier, Paula M. Alves, Cristina Peixoto, and Manuel J. T. Carrondo

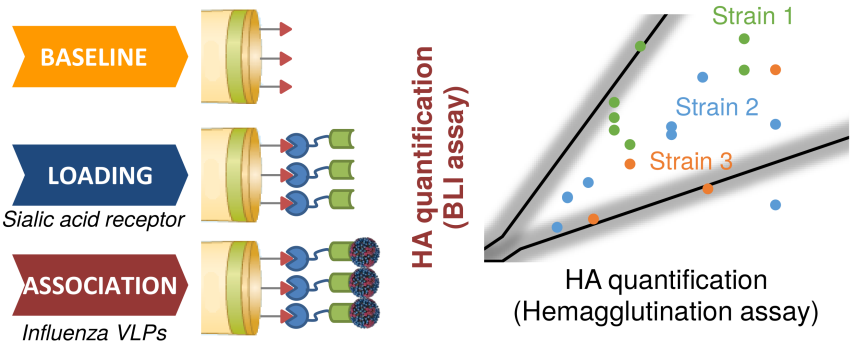

Contents

4.1 Context

One of the main goals of this thesis was to develop a universal downstream process for influenza VLPs as vaccine candidates. Such process should be independent of virus group and strain and capable of processing both mono and multivalent particles. However, at the beginning of the work it was evident that we lack a robust quantification tool for this type of VLPs, since most methods in the literature are optimized for viruses and not for VLPs. Moreover, they are dependent of antibodies or erythrocytes and the read-out varies with the operator. In this chapter it is described the development of an Octet HA quantification tool, based on the needs described above. This approach enabled us to analyse in-process samples, from crude bulk to final purified bioprocessing product, allowing the monitor and optimization of the downstream process. It was exploited the HA interaction with sialic acid receptors, eliminating the need of antibodies or red blood cells.

I was involved in the conception of the study and I performed, together with a colleague, the cell culture and VLPs' productions as well as the downstream processing steps. Moreover, I worked with the collaborators to design the biolayer interferometry experiments and all of them were performed by me. I wrote the manuscript with contributions from all authors.

This work was published in Biotechnology Journal (2017,12:1700031. DOI: 10.1002/biot.201700031) and it is available at `https://onlinelibrary.wiley.com/doi/full/10.1002/biot.201700031`.

4.2 Abstract

Virus-like particles (VLPs) are becoming established as vaccines, in particular for influenza pandemics, increasing the interest in the development of VLPs manufacturing bioprocess. However, for complex VLPs, the analytical tools used for quantification are not yet able to keep up with the bioprocess progress. Currently, quantification for Influenza relies on traditional methods: hemagglutination assay or Single Radial Immunodiffusion. These analytical technologies are time-consuming, cumbersome, and not supportive of efficient downstream process development and monitoring. Hereby we report a label-free tool that uses Biolayer interferometry (BLI) technology applied on an Octet platform to quantify Influenza VLPs at all stages of bioprocess. Human (α2,6-linked sialic acid) and avian (α2,3-linked sialic acid) biotinylated receptors associated with streptavidin biosensors were used, to quantify hemagglutinin content in several mono- and multivalent Influenza VLPs. The applied method was able to quantify hemagglutinin from crude samples up to final bioprocessing VLP product. BLI technology confirmed its value as a high throughput analytical tool with high sensitivity and improved detection limits compared to traditional methods. This simple and fast method allowed for real-time results, which are crucial for in-line monitoring of downstream processing, improving process development, control and optimization.

4.3 Introduction

Influenza virus infections in humans remain a worldwide concern, resulting in significant health and economic burdens [6]. During seasonal epidemics, 5% to 10% of the adult population and 20% to 30% of children are affected, resulting in 3 to 5 million cases of severe illness and up to 500 000 deaths annually worldwide [153]. Pandemic strains are also a significant global threat and can lead to millions of deaths [6].

Hemagglutinin (HA) and neuraminidase (NA) are the two influenza glycoproteins on which virus subtype classification is based. HA, the major envelope protein, contains the epitopes for neutralizing antibodies and is responsible for virus binding to host cell receptors, glycans that contain sialic acids. NA is a sialidase that removes the sialic acid receptor from the host cell surface playing an important role in the release of the virus progeny [3, 5, 154].

Host cell receptors contain α-2,6-linked or α-2,3-linked sialic acids moieties. Depending on the HA proteins present on the virus surface, the binding specificity for the two linkages is different. Human influenza virus engages preferentially to α-2,6-linked sialic acids whereas avian virus primarily binds to α-2,3-linked sialic acid receptors [5]. Binding preferences of different strains are an important determinant for species barrier, restraining human infections with avian influenza virus. However, virus ligand preferences change: some mutations in avian HA proteins can lead to the emergence of new pandemic strains with different binding preferences, acquiring human receptors' specificity. The same can happen for mutations in human HA proteins leading to changes in binding specificity to avian receptors [5, 155, 156].

Vaccination is a key strategy for prevention of influenza infections for both seasonal and pandemic virus. Due to the genetic processes of antigenic drift and shift, the content of the influenza vaccine needs to be reviewed annually [157]; furthermore seasonal vaccines do not provide protection against novel pandemic strains [39]. Most current licensed in-

fluenza vaccines are still produced using egg-based manufacturing, limiting vaccine supply, critical in the case of pandemics. This is driving a need for faster vaccine development and more effective vaccines against influenza. New vaccines have recently reached the market using both mammalian and insect cell lines [14].

Virus like particles (VLPs) display native virus proteins, triggering a protective immune response. Since they lack genetic material, VLPs are not infectious nor replicative, making them safer alternatives to killed or attenuated virus [36] and have been long established for Hepatitis B and human Papillomavirus viruses [37, 38]. Several platforms, including VLPs, are under development as candidates for both seasonal and pandemic Influenza virus [14, 39–43].

These trends increase the need for improved characterization and quantification tools: fast, reliable and easy to set up, applicable for use with in-process samples, from upstream crude extract to downstream purified product. Single radial immune diffusion (SRID), the approved method by regulatory authorities for potency determination, and hemagglutination assay (HA assay) are the main methods to quantify HA protein. HA assay has been used for evaluation of production and purification yields of Influenza-VLPs. However, there are several disadvantages associated with these assays. SRID is a time consuming assay, taking 2-3 days to perform, which is impractical for process development. It has a low sensitivity (3-5 μg mL^{-1}) and there are several limitations regarding presence of aggregates and non-aqueous components that interfere with HA diffusion in the gel. Importantly, it requires HA antigen references and specific monoclonal antibodies that need to be constantly updated, delaying the release of new vaccines. The HA assay, although it is relatively fast compared to SRID, requires fresh red blood cells to obtain reproducible results. Due to the different cell origin and different cell types, an external standard is necessary to use for each assay. Since VLPs are more heterogeneous than the influenza virus particles, the ratio of red blood cells to VLPs can differ from 1. Usually, for normal

Influenza virus, this ratio is approximately 1. Changing this ratio, which happens for VLPs, can lead to an erroneous estimate of total particles [96, 130].

The regulatory authorities recommend using alternative influenza vaccine potency assays [131]. There are several emerging methods that attempt overcome the issues described above: receptor-based ELISA (enzyme linked immunosorbent assay) that uses synthetic sialic acid receptors to HA quantification [131], Flu-Toc immunoassay for HA quantification using subtype specific but broadly reactive monoclonal antibodies [142], reversed-phase HPLC (high-performance liquid chromatography) [145–147], NA activity assays, qPCR (quantitative real time PCR) [96, 130], surface plasmon resonance assays using antibodies or sialic acid receptors [148–150]. These new methods have to become simple, cost and time effective, therefore the need for antibody or antigen update, the lack of proper standards and the capacity to quantify in process samples and from different strains at the same time have to be evaluated.

Here we report a VLP Influenza label-free quantification tool based on biolayer interferometry applied on an Octet platform that constitutes a step forward to the related methods already reported because it takes advantage of HA interaction with human (α2,6-linked sialic acid) and avian (α2,3-linked sialic acid) receptors it eliminates the need for antibodies. The method is able to analyse in-process samples from crude bulk to final purified bioprocessing product with improved detection and quantification limits, compared to the approved method. This simpler and faster tool facilitated the measurement of results in real-time, which is crucial for the monitoring and optimization of the bioprocess. It is universal in the sense that it is suitable for different influenza groups and strains; it is not just for monovalent but also for multivalent vaccine candidates.

4.4 Materials and Methods

4.4.1 Cell culture

High Five cells (Trichoplusia ni derived BTI-Tn-5B1-4 cell line) (B855-02, Invitrogen Corporation, Paisley, UK) were routinely cultured in Insect-XPRESS medium (Lonza, Basel, Switzerland) and kept in a humidified incubator at 27 °C and 110 rpm. Cells reach a concentration of 2-3$\times 10^6$ cells mL^{-1} every 2-3 days and were re-inoculated at 3×10^5 cells mL^{-1}. Cell concentration and viability were determined by using haemocytometer cell counts (Brandt, Wertheinmain, Germany) and trypan blue exclusion dye method (Merck, Darmstadt, Germany).

4.4.2 VLP production and harvest

For VLP production, High Five cells were infected with recombinant baculovirus (kindly provided by Redbiotec AG) encoding different strains of Influenza HA and M1 proteins (described in Samples section). Cell concentration at infection (CCI) was 2×10^6 cells mL^{-1}, and the multiplicity of infection (MOI) was 1 IP $cell^{-1}$(infectious particles per cell). Baculovirus titers were determined using the MTT assay [158, 159].

High Five infected cells were harvested at a viability of 50-60%, corresponding to approximately 48 hpi, by centrifugation at 200 g for 10 min (JA10 rotor, Avanti J25I centrifuge, Beckman Coulter, USA). The pellet was discarded and Benzonase (101654, Merck Millipore, Germany) was added to the supernatant at a final concentration of 50 U mL^{-1} and incubated at room temperature (RT) (22 °C) for at least 15 min.

4.4.3 VLP Downstream processing

The clarification of VLP-containing bulk was carried out by dead-end filtration using a Sartopore filter with 0.45+0.2 μm pore size (SART5445307H7-SS-A, Sartorius, Germany). The filtration module was previously conditioned with 50 mM HEPES, pH 7.4, 300 mM NaCl (working buffer). The

clarification was performed at a constant flow rate of 100 mL min^{-1} using a Tandem 1081 Pump (Sartorius Stedim Biotech,Germany) and the pressure was monitored by an in-line pressure transducer (080-699PSX-5, SciLog, USA) to control possible overpressure.

Clarified bulk was concentrated using tangential flow filtration (TFF). For ultrafiltration flat sheet Pellicon 2 Mini Ultrafiltration Module Biomax 300 kDa 0.1 m^2 (P2C300C01, Merck Millipore, USA) was used. The membrane module was set up accordingly with the manufacturer's instructions. A fixed feed flow rate of 500 mL min^{-1} was set up. Transmembrane pressure (TMP) was controlled by adjusting the retentate flow rate using a flow restriction valve. The pressure was monitored at feed inlet, retentate outlet and permeate outlet by in-line pressure transducers. The feed/retentate and the permeate volumes were monitored using a technical scale (TE4101, Sartorius Stedim Biotech, Germany). At a proper feed volume, three diafiltration volumes with working buffer were performed. After achieving the desired concentration factor, the TFF loop was completely drained and the VLP retentate was recovered.

Concentrated VLPs were loaded into a size exclusion chromatography column HiLoad 26/600 Superdex 200 pg column (GE Healthcare, USA) coupled to an ÄKTA Avant liquid chromatography system (GE Healthcare, USA.) equipped with UV and conductivity/pH monitors. System operation and data gathering/analysis was done using the UNICORN 6.3 software (GE Healthcare, U.K.). The column was loaded with 13 mL of concentrated VLPs, using a 13 mL capillary loop, at a constant flow rate of 3 mL min^{-1}. Working buffer was used as eluent and the eluted fractions were collected for further analyses.

VLPs' corresponding fractions were further concentrated and diafiltrated with working buffer using a flat sheet Pellicon XL Ultrafiltration Module Biomax 300 kDa 0.005 m^2 (PXC300C50, Merck Millipore, USA) at a constant flow rate of 40 mL min^{-1}. Final product was sterile filtered using a 0.2 μm syringe filter unit (10462960, Whatman - GE Healthcare, USA).

4.4.4 Samples

All Influenza VLP samples were produced and purified as described above. Influenza vaccine Influvac (Abbott, USA) was used as positive control. Different Influenza strains from distinct subtypes and groups were selected (H1, B, and Group2 - H3, H4, H7, H10, H14, and H15) to replicate genetic diversity. VLPs produced contained HA and M1 Influenza proteins. Multivalent particles are composed of a combination of multiple HA proteins.

4.4.5 Nanoparticle tracking analysis

Particles presence, concentration and size distribution were measured using the NanoSight NS500 (Nanosight Ltd, UK). The samples were diluted in D-PBS (14190-169, Gibco, UK) so that virus-like particles concentration would be in the 10^8-10^9 particles mL^{-1} - the instrument's linear range. All measurements were performed at 22 °C. Sample videos were analysed with the Nanoparticle Tracking Analysis (NTA) 2.3 Analytical software - release version build 0025. Capture settings (shutter and gain) were adjusted manually. For each sample 60-seconds videos were acquired and particles between 70 and 150 nm were considered.

4.4.6 Hemagglutination assay

Hemagglutinin protein detection and quantification was performed by hemagglutination assay for all the samples and for all stages of bioprocess evaluated. The assay was carried out according to the procedure described in the literature [54]. The predictive range of concentrations calculated for the Hemagglutination assay was determined based on the error associated with the 1:2 serial dilution used between plate wells. For VLPs' hemagglutination assay, the concentrations are typically in μg mL^{-1}, which does not happen for virus hemagglutination, where a measure of activity is obtained, typically in HAU (hemagglutination units).

4.4.7 Biolayer interferometry quantification assay

Influenza VLPs' binding to sialic acid receptors was measured by biolayer interferometry (BLI) using Octet RED96 and Octet RED384 systems (fortéBIO, Pall Corp., USA). Data was acquired (kinetics mode) and analysed using the Data acquisition software v9.0 (fortéBIO, Pall Corp., USA) or Data Analysis software v9.0 (fortéBIO, Pall Corp., USA). When necessary, data was exported as a Microsoft Excel file for further analysis in other software packages. Binding was calculated from the response amplitude (wavelength shift in nm) obtained in the first 100 s of each step. Avian 3'-SLN (3'SiaLacNAc-PAA-biot, 0036-BP) and human 6'-SLN (6'SiaLacNAc-PAA-biot, 0997-BP) receptors (Lectinity, Moscow, Russia) containing 20 mol% receptor analogue and 5 mol% biotin on a 30-kDa polyacrylamide backbone were resuspended in 50 mM HEPES, pH 7.4, 300 mM NaCl (working buffer) with 3 mM EDTA and 0.005% Tween-20. High Precision Streptavidin (SAX) Biosensors (18-0037, fortéBIO, Pall Corp., USA) were hydrated and blocked with Sample diluent (18-5028, fortéBIO, Pall Corp., USA). Unless otherwise stated all the samples were diluted with working buffer. To prevent cleavage of the receptors by influenza neuraminidase, Influvac vaccine samples were incubated for 1 hour at RT with 100 μM Oseltamivir phosphate (CAS number 204255-11-8, Sigma-Aldrich) and 100 μM Zanamivir (CAS number 139110-80-8, Sigma-Aldrich) inhibitors.

The quantification assay was set up by diluting biotinylated receptors with sample diluent and loaded into SAX Biosensors. Influenza VLP samples were then associated to the biosensors and association and dissociation profiles were measured. The method was defined with five steps: Baseline, Loading, Baseline, Association and Dissociation. Experiments were performed at 25 °C and sample plates (microplate 96 well, F-bottom, black, 655209, from Greiner bio-one and microplate 96 well half-area, F-bottom, black, 3694, from Corning Costar) were agitated at 1000 rpm.

Limit of detection (LOD) and limit of quantitation (LOQ) were cal-

culated based on the FDA Guidelines (FDA, ICH Guidance for Industry, Q2B Validation of Analytical Procedures: Methodology, 1996). The approach used for determining both limits was based on the standard deviation of the response and the slope of the calibration curve:

$$\mathrm{LOD} = \frac{3.3\sigma}{S} \tag{4.1}$$

$$\mathrm{LOQ} = \frac{10\sigma}{S} \tag{4.2}$$

where σ is the standard deviation of the response and S the slope of the calibration curve. Quantifications were made taking into consideration the initial values (0 to 100 s) of the binding responses.

4.5 Results

4.5.1 Design of a quantification assay for Influenza VLPs

The Influenza VLPs quantification assay is based on biolayer interferometry analysis and performed on an Octet RED system. The approach takes advantage of the binding of Influenza virus hemagglutinin to sialic acid receptors present in host cells. The method uses high precision functionalized streptavidin (SAX) biosensors and biotinylated α-2,3 and α-2,6-linked sialic acid receptors. Figure 4.1 schematizes the quantification assay. Briefly, biosensors are hydrated and blocked for non-specific binding with sample diluent at the initial baseline step. Then, the loading of the biotinylated sialic acid receptors is performed; a new baseline step with working buffer guarantees that the receptors that are not correctly linked are removed. Influenza VLPs are then associated to the receptors. Depending on the sample stage of purification, there are impurities that can be removed during the dissociation step. For the cases studied, the dissociation was negligible when compared to association (data not shown). Non-specific binding was evaluated by VLP association to naked biosensors, i.e, without loading of sialic acid receptors.

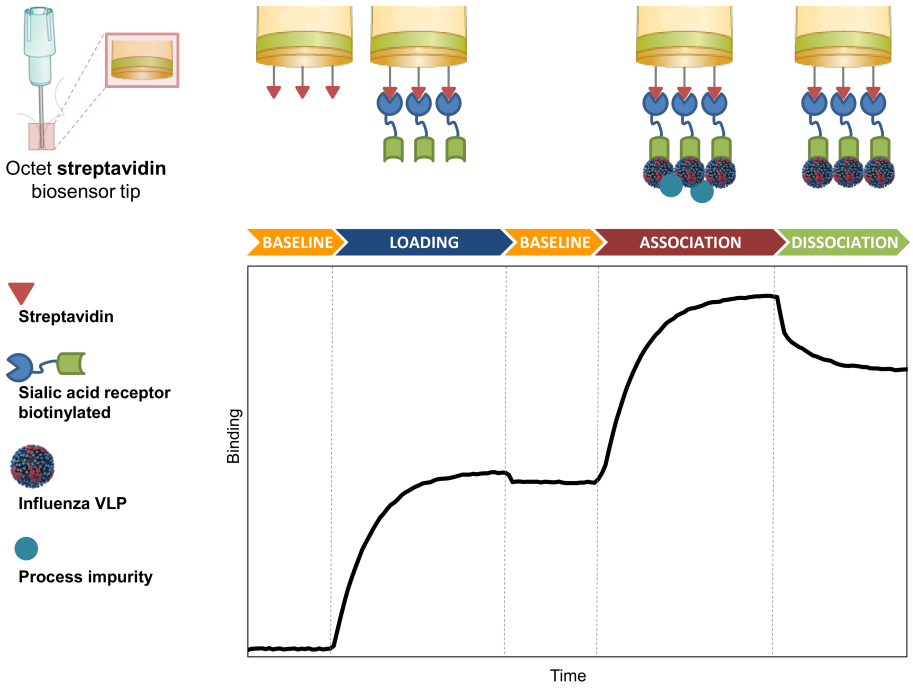

Figure 4.1: Schematic representation of Influenza quantification assay. Biotinylated α-2,3 and α-2,6-linked sialic acid receptors, hydrated and blocked (baseline), are loaded into high precision streptavidin biosensors (loading). After a second baseline step, HA protein from Influenza VLPs bind to the receptors, giving a response (association). Possible process impurities or non-bound VLPs are removed in the dissociation step.

Having the biosensors blocked, the binding magnitude to naked biosensors is significantly lower than the one observed for the receptor, which was confirmed by subtracting both binding curves (Figure A.1).

4.5.2 Criteria definition and optimization for the assay implementation

Human Influenza VLP strains were quantified using BLI technology. As the results obtained with BLI analysis were compared with chicken erythrocyte agglutination assay, it was necessary to evaluate influenza strains' binding to α-2,3, α-2,6 or a mixture of both receptors. It is expected that strains with higher affinity for α-2,6 present a higher binding response for that receptor. The same should occur for α-2,3 strains.

The binding to the different sialic acid receptors of different influenza strains (mono- or multivalent VLPs from different groups) was measured (Figure 4.2a-e). Both receptors, alone or in a 1:1 ratio mixture, were loaded. It was expected that different strains would present different binding responses, according to their specificity for the receptors [160]. The binding profiles were different for all analysed strains. As predicted, depending on the strain type higher binding responses for α-2,6 receptor or for the mixture of both receptors were observed. The mixture of both receptors gives more reliable results to compare the binding responses calculated with BLI and HA assays. Thus, the quantification assay was implemented using a mixture of both receptors in a 1:1 ratio.

Receptor concentrations ranging from 0.5 μg mL^{-1} to 4 μg mL^{-1} were evaluated to define the optimal loading. At concentrations above 2 μg mL^{-1} biosensor saturation occurred (data not shown) thus those values were not considered. Figure 4.2f presents the fine tuning optimization for α-2,6, α-2,3 and mixture receptor loading. Optimal receptor concentration was chosen at 1.2 μg mL^{-1}, just before the saturation plateau for α-2,6 receptor and the mixture, although not for the α-2,3 receptor to avoid overcrowding of the biosensor and consequently VLP binding interference (fortéBIO, PALL Life Sciences, Biomolecular Binding Kinetics Assays on the Octet Platform, Application Note 14, 2013). Commercial influenza vaccine Influvac was used as HA assay positive control. This vaccine has both HA and NA influenza proteins. As described in the literature [5] NA catalyses the cleavage of sialic acid so the binding of Influvac vaccine to the receptors is affected by sample incubation with NA inhibitors (Zanamivir, Oseltamivir) [161]. In the absence of NA inhibitors α-2,6 receptor binding curve suffers a significant decrease due to enzyme activity (Figure 4.3a). However, even with NA inhibitors incubation, vaccine binding behaviour is quite different from VLP samples, presenting two binding transitions (Figure 4.2a-e and 4.3a). Moreover, the vaccine does not significantly bind α-2,3 sialic acid receptor (with and without NA inhibitors), as compared with α-2,6 receptor binding curves;

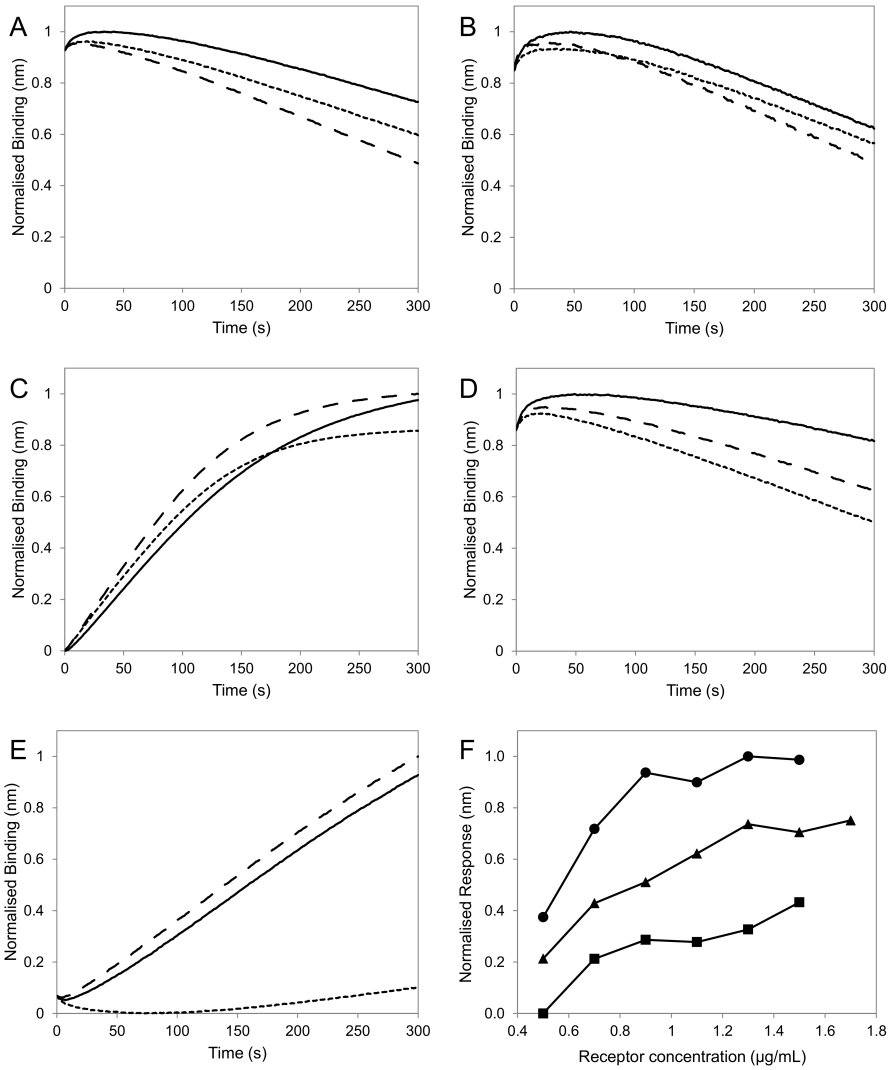

Figure 4.2: Binding of Influenza strains to sialic acid receptors and receptor loading optimization. Both α-2,3 and α-2,6-linked receptors were loaded into high precision streptavidin biosensors, alone or mixed in a 1:1 ratio. Solid line corresponds to α-2,3, long-dash-dot line to α-2,6 and square-dot stands for the mixture of both receptors. Binding curves for B monovalent strain (A), B trivalent strain (B), H1 monovalent strain (C), H3 monovalent strain (D), and Group 2 monovalent strain (E). Representative example of the fine tuning optimization (n=2) for α-2,6, α-2,3 and mixture receptor loading (F). Circle marker corresponds to α-2,6 receptor, square marker to α-2,3 and triangle marker to the mixture of both receptors.

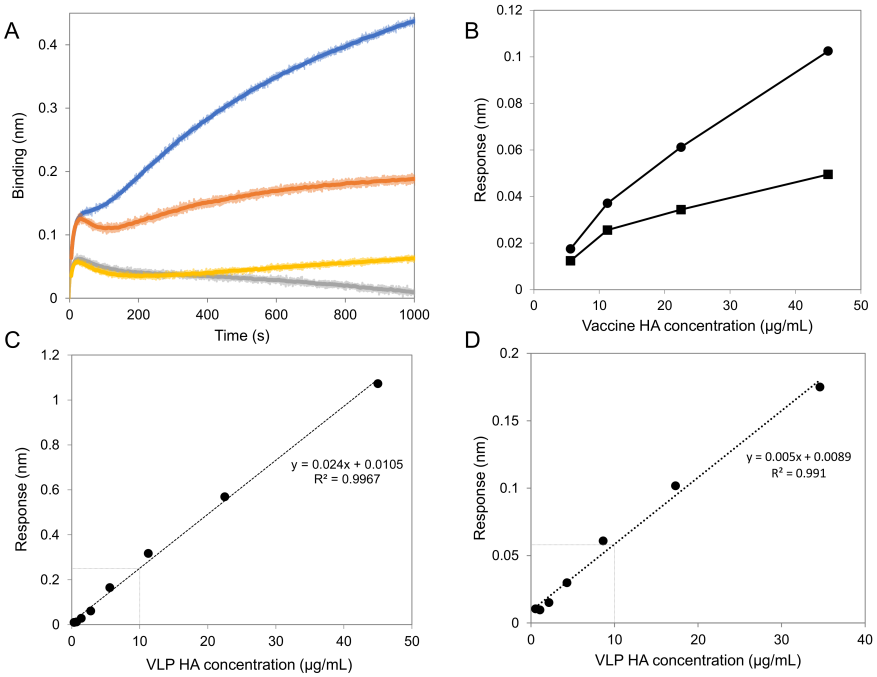

Figure 4.3: Calibration curves for Influenza VLPs and Influvac vaccine. Representative binding curves (n=3) of Influvac vaccine at a HA concentration of 45 μg mL^{-1} to α-2,3 and α-2,6 sialic acid receptors. Incubation with NA inhibitors was evaluated. Blue line corresponds to α-2,6 receptor incubated with NA inhibitors and orange line to α-2,6 receptor without inhibitors. Grey line corresponds to α-2,3 receptor with inhibitors and yellow line to α-2,3 receptor without inhibitors (A). Representative calibration curves (n=3) of Influvac vaccine binding to α-2,3 and α-2,6 sialic acid receptors. Circle marker corresponds to α-2,6 and square marker to α-2,3 (B). Representative calibration curves of H1 strain Influenza VLP binding to α-2,3 and α-2,6 receptor mixture. Ultrafiltration retentate sample without trehalose (C) and with trehalose (D). The standard error of the estimation associated with the linear regression is 0.02 nm (which corresponds to 0.53 μg mL^{-1}) (C) and 0.006 nm (which corresponds to 0.26 μg mL^{-1}) (D).

this is due to different affinities for the receptors, as it is well established that human strains bind preferably to α-2,6 receptor [5]. Nevertheless, to establish a calibration curve for the assay, vaccine at different concentrations was loaded onto α-2,6 and α-2,3 receptors. As can be observed in Figure 4.3b, initial response does not present a linear behaviour, in contrast to what is observed for VLP samples (Figure 4.3c-d). These results show that Influvac vaccine is unsuitable for assay calibration. A recombinant HA protein was also evaluated, presenting extremely low binding values (below 0.03 nm), even at high concentrations (20 μg mL^{-1}) as well as non-specific binding and high levels of dissociation (Figure A.2).

Ultrafiltrate (UF) retentate samples of each VLP were used to construct the calibration curves. Figure 4.3c-d show representative calibration curves for one of the evaluated strains. The linear behaviour is identical to the other strains in the concentration range analysed (Figure A.3). Limit of detection (LOD) was estimated as 0.5 μg mL^{-1} for all the group 1 monovalent strains, 0.6 μg mL^{-1} for multivalent and 0.9 μg mL^{-1} for group 2 strains. Limit of quantitation (LOQ) was estimated as 1.6 μg mL^{-1} for the monovalent strains, 1.8 μg mL^{-1} for multivalent and 2.7 μg mL^{-1} for group 2 strains (Table A.1). The addition of trehalose to improve long-term product stability was investigated. The sugar was found to interfere with the assay, drastically changing the response values of otherwise identical samples. Even for samples measured using calibration curves that also contained trehalose, the results were inconsistent.

4.5.3 BLI quantification method enables in-process samples' quantification

To evaluate the BLI quantification method, samples of mono and multivalent strains and different steps in the purification process were analysed (Figure 4.4, Table A.2). For comparison samples were also quantified by HA assay. As an example, Figure 4.4a confirms the methodology for a B monovalent strain for the entire purification process, from bulk sam-

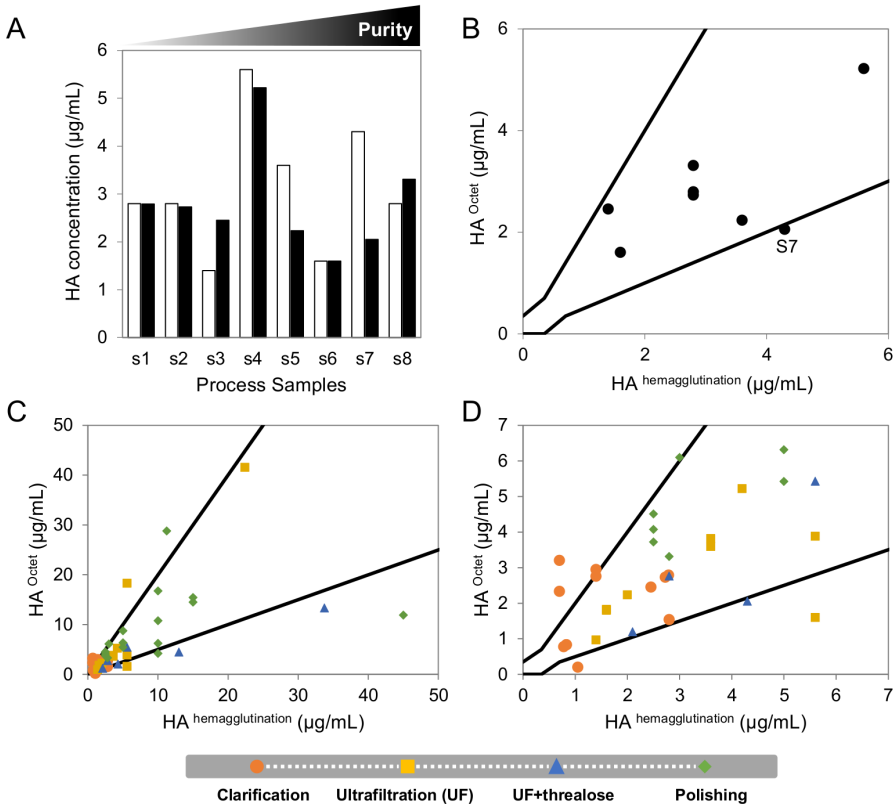

Figure 4.4: Downstream process samples' quantification using BLI method. B monovalent strain quantified by BLI method (black bars) and by hemagglutination assay (white bars) at several stages of purification. s1: before harvest, s2: before clarification, s3: after clarification, s4-s6: ultrafiltration (UF) retentate, s7: UF retentate with trehalose, s8: final product (A). Calculated HA concentration values compared with hemagglutination assay. Black lines correspond to hemagglutination assay error range, x axis to HA values calculated by hemagglutination and y axis to HA values calculated by octet assay (B). Error bars for panel A and B are omitted for clarity (see standard errors of the estimation in Figure A.3b). Overview of HA quantification of different VLP samples from several steps of the downstream process. Orange circles correspond to clarification samples, yellow squares to UF samples, blue triangles to UF samples with trehalose and green diamonds correspond to samples after the polishing step. Black lines correspond to hemagglutination assay error range, x axis to HA values calculated by hemagglutination and y axis to HA values calculated by octet assay (C). Zoom of the most populated range of HA concentrations from panel C (D).

ples to final bioprocessing product (before formulation): concentration values correlate well between methods. A reduced number of samples present differences in HA concentrations; this may be due to errors associated with the hemagglutination assay. Considering the errors associated with the hemagglutination assay, the majority of the calculated values with BLI assay fall between the predictive range of concentrations (Figure 4.4b). The same results were observed for the other evaluated strains, including multivalent ones (Figure A.4).

Samples have different purity levels, depending on the DSP (Downstream Processing) step, leading to slightly changes in binding response behaviour. Grouping all the samples per DSP step confirms that the majority of quantifications are within the predictive range of concentrations in accordance with HA assays (Figure 4.4c-d). The overview of the results shows that samples from the clarification stage contain culture media compounds, possibly interfering with the analyses, as routinely observed in laboratory HA assays; thus small differences between quantification methods for these early stage samples are to be expected. As the DSP advances, purity increases and HA concentrations calculated with BLI assay became closer to those acquired with HA assay. Samples with trehalose at the storage concentration used here (15% w/v) do not allow robust quantifications.

4.5.4 BLI quantification method is specific for subtype and group VLP strains

To evaluate specificity, several strains from the same subtype or group were analysed against the same calibration curve; experiments were performed for H1, H3 and B subtypes for several mono and multivalent strains. Strains from H1 subtype group were quantified using only one H1 strain as calibration curve; a UF retentate sample was used as calibration and three monovalent, one trivalent and one pentavalent VLP samples were quantified (Figure 4.5). Results confirm subtype and group quantification is possible, with only one sample out of the error limits.

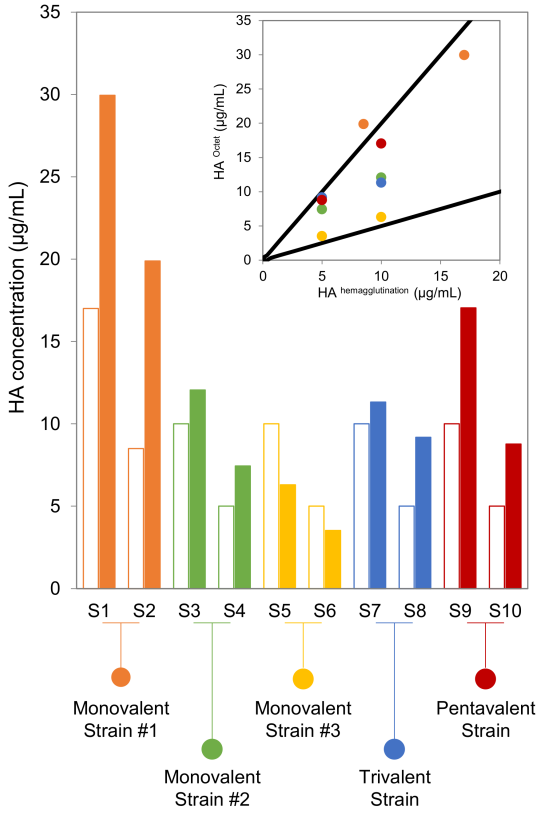

Figure 4.5: Example of subtype and group strain specificity. HA quantification of several mono and multivalent strains from H1 subtype (n=2). UF retentate samples from one monovalent strain were used as calibration. Bars without fill correspond to HA values calculated using hemagglutination assay. Bars with coloured fill correspond to HA values calculated using octet assay. For each strain, two different samples with two different concentrations are presented. Monovalent strain #1 is coloured in orange, monovalent strain #2 in green and monovalent strain #3 in yellow. Blue corresponds to trivalent strain and red to the pentavalent one. Top right panel presents calculated HA concentration values compared with hemagglutination assay. Black lines correspond to hemagglutination assay error range, x axis to HA values calculated by hemagglutination and y axis to HA values calculated by octet assay. Monovalent strain #1 is coloured in orange, monovalent strain #2 in green and monovalent strain #3 in yellow. Blue corresponds to trivalent strain and red to the pentavalent one. Error bars are omitted for clarity (see standard errors of the estimation in Figure 4.3c).

This was also observed for H3 and B group samples containing tri and pentavalent VLPs (Figure A.5).

4.6 Discussion

Constant Influenza antigenic shift and drift drives rapid development of vaccines and more efficient production and purification processes, requiring fast and reliable analytical tools to characterize final bioprocessing product but also all stages of the upstream and downstream processes. As mentioned before, the main limitations of current methodologies, SRID and hemagglutination assays were reviewed [96, 130]. These influenza quantitation methods were designed for purified virus samples and are not suitable for crude samples or for VLPs bioproduction assays.

Here we report a HA quantification assay permitting the analysis of in-process samples of influenza multivalent VLPs involving sialic acid receptors interaction with the virus.

As a proper standard was not available, a commercially available influenza vaccine (Influvac) already implemented as HA assay positive control was evaluated. However, initial responses obtained with this "standard" were not linear, precluding the design of a calibration curve. Moreover, the vaccine association to the sialic acid receptors does not present the expected behaviour, when compared to the association curves reported for the BLI technique. This is probably due to the presence of NA that catalyses the cleavage of sialic acid receptors. However, even when vaccine samples were incubated with NA inhibitors, the binding response continues to be partially affected, meaning that vaccine formulation, in particular the stabilizers, could also have a role.

Searching for a new standard with similar protein content and the same production conditions as the evaluated samples, ultrafiltrate (UF) retentate samples of each VLP were used for calibration curves. Recombinant HA protein was also evaluated as a standard but no significant binding was observed, mainly because the protein was not in the na-

tive conformational trimeric structure, required for receptor interaction [150, 162].

The HA assay was performed for comparison to BLI technology. Erythrocytes used in HA assays should be chosen depending on the receptor selectivity of the targeted virus. However, it is not feasible to use human erythrocytes for process development quantification assays. Human Influenza virus agglutinates chicken erythrocytes and, due to their characteristics they are routinely used in HA assays. These erythrocytes contain both α-2,3 and α-2,6-linked sialic acid receptors, although in different proportions [160]. Therefore, to improve the comparison of both assays a 1:1 ratio between both receptors was used. This ratio represents a broader condition to quantify different samples because different strains have different affinities for the sialic acid receptors.

The developed method was designed for in-process VLP samples and to be able to quantify HA for the entire bioprocess. As a proof of concept, several influenza VLPs from different strains, groups, stages of the process, mono and multivalent were evaluated. Most of the quantified values are within the predictive range of concentrations, stipulated based on the HA assay associated errors. However, there are several factors that can influence the binding response and, therefore, the method robustness, as reported elsewhere [148]. Our samples contained different levels of impurities such as DNA and total protein, different concentrations of cell culture medium and NaCl, and presence or absence of trehalose. Only samples with trehalose fall slightly out of the predictive range of concentrations.

The method is able to quantify different samples from the same subtype, using a single calibration curve. The binding affinities of strains from the same subtype are close enough to give concentration values that are within the predictive range.

This quantification method is an appealing tool for bioprocess development, from time of harvest control to final bioprocessing product quantification. Leading with broad spectra of samples from bulk to fi-

nal product, residual amounts of baculovirus and/or exosomes can be present. Analogously to the traditional and approved methods, our tool is not able to distinguish HA that is present on VLPs or in other particles. This issue is not completely addressed due to the lack of proper DSP processes and analytical tools. It is also worth to note that recent reports showed that residual baculovirus, present in VLP samples, can to trigger an innate immune response. This raises the question whether baculovirus presence is harmful or an advantage [59, 163]. Nevertheless, this method presents several advantages compared to the methods already settled for influenza virus. The method is an advance over the SPR-based assays that use microfluidics and is not compliant with bulk samples. Moreover, both the sialic acid receptos and the samples can be recovered, and the biosensors can be regenerated, in contrast with the SPR-methods. Being antibody- independent it eliminates the constant update, required for SRID and other methods. Moreover, the replacement of erythrocytes by sialic acid receptors solves the issue of influenza strains that do not agglutinate chicken erythrocytes and makes the assay more robust, when compared with HA assay, eliminating the use of fresh cells and decreasing the variations associated with user operation and host-origin. Importantly, it is possible to quantify a plethora of strains and multivalent influenza VLPs with an improved LOD and LOQ [96], a step further in the development of a universal quantification tool suitable for bioprocess development.

4.7 Acknowledgments

The authors acknowledge funding from the European Union (EDUFLUVAC project, FP7-HEALTH-2013-INNOVATION). S.C. was funded by the PhD fellowship SFRH / BD / 52302 / 2013 within the scope of the PhD program Molecular Biosciences PD / 00133 / 2012 funded by Fundação para a Ciência e Tecnologia. The authors acknowledge RedBiotec for kindly providing the baculovirus, António Roldão, Marcos

Sousa and Ricardo Correia for providing extra validation material and Attila Aranyos for technical support and profitable discussions.

5

Bioorthogonal Strategy for Bioprocessing of Specific-site-functionalized Enveloped Influenza-virus-like Particles

Sofia B. Carvalho[1], João M. Freire, Mafalda G. Moleirinho, Francisca Monteiro, Diana Gaspar, Miguel A. R. B. Castanho, Manuel J. T. Carrondo, Paula M. Alves, Gonçalo J. L. Bernardes, and Cristina Peixoto

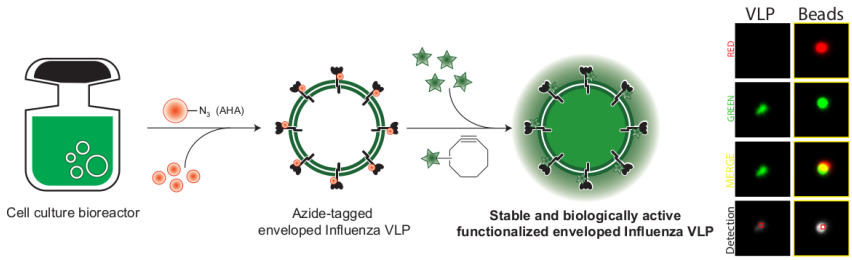

Contents

[1]The first authorship is shared between me and João M. Freire.

5.1 Context

When developing or improving bioprocesses it is critical to have analytical tools to monitor the product across the production and purification steps. For the downstream processing development, this will be of extreme importance to control where the product is being lost and to optimize the yields. The typical way is to tag the product of interest, usually with fluorescent labels, such as GFP. However, to directly apply the knowledge obtained with the trial runs with purification process for unlabelled VLPs, the labelling method should not affect the size and the charge of the particles. Tagged enveloped VLPs is a bioorthogonal strategy that we developed to overcome this issue. By using a click chemistry approach, we were able to functionalize VLPs and add a fluorescent tag during *in vivo* production. This tool allows the monitoring and control of the process from the production stage until the end of the purification. Using this method coupled with FACS, we were also capable to discriminate and separate VLPs from Baculoviruses, the main impurity of the process.

This study and all the required experiments were conceived by me and J.M.F.. Cell culture and VLP production as well as metabolic labelling were performed by me. I also performed the Downstream processing steps and most of the analytical tools to characterize VLPs and impurity sample content. Me and J.M.F. wrote the manuscript with contributions from all authors.

This work was published in Bioconjugate Chemistry (2016,27:2386–2399. DOI: 10.1021/acs.bioconjchem.6b00372) and it is available at `https://pubs.acs.org/doi/abs/10.1021/acs.bioconjchem.6b00372`.

5.2 Abstract

Virus-like particles (VLPs) constitute a promising platform in vaccine development and targeted drug delivery. To date, most applications use simple non-enveloped VLPs as human papillomavirus or hepatitis B vaccines even though the envelope is known to be critical to retain the native protein folding and biological function. Here we present tagged enveloped VLPs (TagE-VLPs) as a valuable strategy for the downstream processing and monitoring of the in vivo production of specific-site-functionalized enveloped Influenza VLPs. This two-step procedure allows bioorthogonal functionalization of azide-tagged nascent influenza type A hemagglutinin proteins in the envelope of VLPs through strain-promoted [3+2] alkyne-azide cycloadditioneaction. Importantly, labelling does not influence VLP production and allows for construction of functionalized VLPs without deleterious effects on their biological function. Refined discrimination and separation between VLP and baculovirus – the major impurity of the process – is achieved when this technique is combined with flow cytometry analysis as demonstrated by atomic force microscopy. TagE-VLPs is a versatile tool broadly applicable to the production, monitoring and purification of functionalized enveloped VLPs for vaccine design trial runs, targeted drug-delivery, and molecular imaging.

5.3 Introduction

Virus-like particles (VLPs) hold great promise as a platform for the development of long-lasting vaccine candidates, i.e., more effective vaccines that do not require constant updates [37]. Vaccines with improved clinical activities that use recombinant VLPs as their antigens have been developed [36, 164, 165], namely against Hepatitis B as well as human Papillomavirus viruses [37, 38]. Moreover, engineered VLPs carry additional promise for the generation of a wide range of nanoscale carriers in targeted drug-delivery and molecular imaging [44]. Previous studies have also shown VLPs to be a safe and efficient platform to deliver active proteins to cells [45]. Additionally, genetically engineered VLPs have been exploited as drug-delivery systems for targeted delivery of cytotoxic agents to tumors [46, 47].

The versatility of VLP platforms has prompted development of strategies to functionalize them. In contrast with genetic methods, chemical-based approaches for the production of modified VLPs are experimentally simpler, more efficient, less time-consuming, and more cost-effective. In one report, surface modification of adenovirus vectors was achieved by metabolic incorporation of azidohomoalanine (Aha) followed by a copper(I)-catalyzed alkyne-azide cycloaddition reaction [166]. Alternatively, Francis and co-workers produced synthetic MS2 viral capsids functionalized with antibodies by using a oxidative coupling strategy [167]. However, to date, the production of synthetically modified VLPs has been limited to simple non-enveloped VLPs. Complex enveloped VLPs show potential as platforms for the presentation of membrane proteins. The envelope is thus essential to maintain the proteins in their folded and biologically functional state, which is critical to vaccine efficacy [168]. There are clinical trials that report efficacy and safety improvements only after the incorporation of membrane proteins on the VLP surface, which induces a more specific antibody response [169]. Enveloped VLPs have the potential to generate antibodies of high diagnostic and therapeutic

relevance to target transporters, ion channels, and membrane proteins present in the human genome that lack inhibitory antibodies because of current technical limitations [170]. The potential of enveloped VLP platforms as vaccine candidates and drug carriers together with the strict constraints of regulatory agencies for higher quality and safety control of biopharmaceuticals highlights the need for new downstream processing methods for the production of functionalized enveloped VLPs.

Herein we present a bioorthogonal labelling strategy that enables us to successfully functionalize complex enveloped Influenza VLPs within live cells. The approach reported here, termed as tagged enveloped VLPs (TagE-VLPs) comprises four key components: (i) residue-specific replacement of methionine (Met) by Aha [171, 172] to access azide-tagged precursor enveloped Influenza VLPs, (ii) Aha-specific modification by strain-promoted alkyne-azide [3+2] cycloaddition (SPAAC) reaction [173], (iii) downstream processes monitoring and optimization, and (iv) discrimination between VLPs and baculovirus. The TagE-VLP strategy uses the baculovirus expression vector system that results in a considerable increase in downstream processing complexity because routine purification procedures and analytical methods are not able to strictly discriminate between VLPs and baculovirus [170, 174]. The goal is to have a minimal size tag that does not disrupt particle size, charge and biological function. This is critical to develop and improve a purification process that can be applied also for untagged particles. With Aha incorporation we can label our VLPs with other molecules of interest, not only fluorescence tags, in order to address unmet medical needs. The versatility and flexibility of TagE-VLP offers potential to develop functionalized enveloped VLPs for applications in vaccine design and targeted drug-delivery systems.

5.4 Results and Discussion

5.4.1 Design criteria and implementation of the TagE-VLP platform

The ability to achieve fully functional chemically modified enveloped VLPs relies on efficient incorporation of a tagged non-canonical amino acid at specific residues followed by bioorthogonal modification. This strategy, if performed in live cells, enables the monitoring, characterization, and VLP quantification from the beginning of the production process. This is a valuable tool to improve upstream and downstream processes. To achieve site-specific in vivo VLP modification and labelling we designed a two-step approach (Figure 5.1). The first step involves metabolic incorporati on of non-canonical amino acid Aha, a Met analogue that contains an azide tag, into the hemagglutinin (HA) protein of Influenza VLPs. We chose triplet codon for Met to code our chemical tag because of the low incidence of Met in the gene of HA. In addition, Met replacement by Aha has been shown to be a powerful tool to introduce azide tags at specific residues on recombinant proteins or newly synthesized proteins on a cell without affecting the physico-chemical properties or biological functions [171, 172, 175, 176]. The second step consists of bioorthogonal labelling with a cyclooctyne derivative, in this case Click-iT Alexa Fluor 488 DIBO alkyne, through strain-promoted alkyne-azide [3+2] cycloaddition (SPAAC) that enables precise placement of a modification into the nascent enveloped VLPs in vivo. Labelling may be performed at the desired purification step to achieve optimal yields and purified VLPs. Briefly, to produce in vivo labelled enveloped VLPs, cells were grown in culture and fed with Aha during protein synthesis. Met was added to a parallel cell culture, which was used as a control. During protein synthesis, Aha is incorporated as a surrogate for Met throughout the gene sequence of HA.

HA is a protein from the envelope, thus the VLPs carry the azide-tagged amino acid after budding from the host cells. At this stage, a

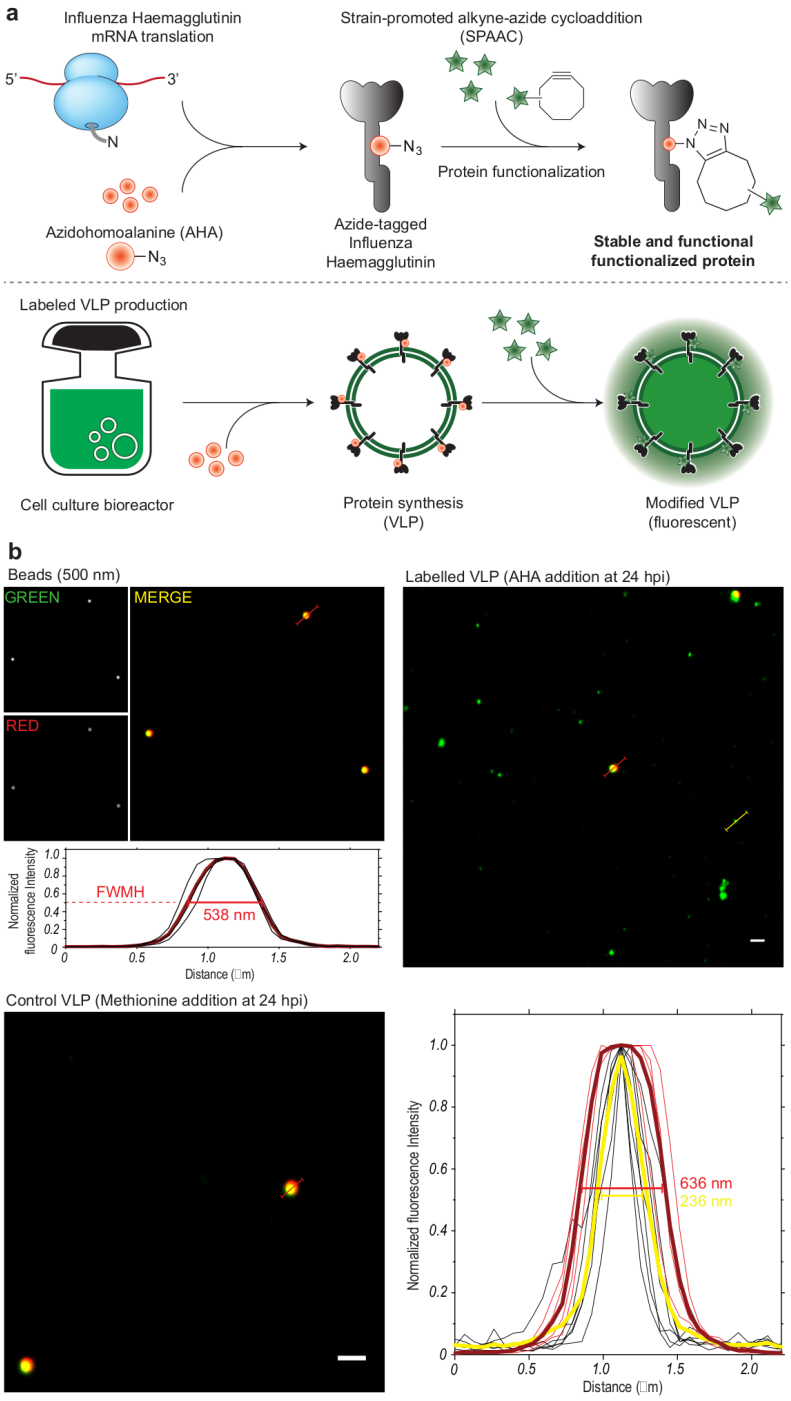

(Caption next page.)

Figure 5.1: Site-specific in vivo labelling of enveloped Influenza VLPs. **a.** Schematic representation of the procedure to metabolically introduce an azide-tagged non-canonical amino acid Aha for subsequent strain-promoted alkyne–azide [3+2] cycloaddition (SPAAC) labelling. During cellular protein synthesis the Aha added to the culture medium is incorporated into nascent HA proteins. Addition of the Alexa 488-cyclooctyne reagent allows site-specific modification of HA (fluorescent tag in our case), which is reflected in VLP production. The modified HAs are incorporated into the vesicles' envelope that is secreted from the cells that carry the chemical modification with it. **b.** Confocal microscopy analysis of chemically modified VLP with the fluorescent probe Alexa 488. 100-fold dilution of bulk VLPS (10^7 particles mL^{-1}) were deposited onto IbiTreat 8 μ-well slides. 500 nm multi-colour fluorescent beads were used as size and green signal reference (converted to grey scale). Red signal was also acquired (converted to grey scale) and from green–red merge images 500 nm beads can be discriminated from VLPs (yellow and green dots, respectively). In addition to colour discrimination, for each particle detected the full width at half maximum (FWHM) was determined to evaluate the approx. 500 nm size of the control beads (Yellow) and the sub-diffraction limit VLP size (see Experimental Section for more detail). The control VLP sample shows no green signal (no labelling with Alexa 488), specific of SPAAC ligation in the experiment samples. Scale bars (white) indicate 2 μm in all images. Additional information regarding particle detection and RAW confocal images can be found in Figure B.1.

complex particle is obtained that displays Aha-tagged HA in the envelope and that is ideally suited for post-expression bioorthogonal labelling with a cyclooctyne fluorescent probe (Figure 5.1a). The time of addition of amino acids was optimized through small-scale (50 mL) batch production. The incorporation of Aha into HA protein was performed 12, 24, 36, and 48 hours post infection (hpi) of cells with baculovirus and assessed by confocal microscopy and flow cytometry analysis (Figure 5.1b, B.1 and B.2). The time of addition that resulted in a higher concentration of fluorescent VLPs was found to be 24 hpi (Figure 5.1b). Further scale-up (500 mL) of Influenza VLP production was performed with this time reference. The versatility of our TagE-VLP strategy allows for bioorthogonal labelling at different stages of the production process of Influenza enveloped VLPs. We chose to perform the SPAAC labelling after the VLPs were harvested because downstream processing (DSP) is the major bottleneck of bioprocess design. Fluorescent beads (500 nm) were used in confocal microscopy analysis as fiducial markers of size and green fluorescence signal as visual reference of successful VLP labelling

and detection. As a result of its multi-colour fluorescence profile, red signal was also acquired. Green–red merged images allowed discrimination between VLPs (green) and beads (yellow) dots, not only by particle size, but also by colour. With this methodology one can perform quantitative analysis on the detected VLPs. The number per μm^2 and mean fluorescence intensity (I_f) of labelled-VLPs determined by imaging processing of confocal images indicates the optimal conditions to perform the bioorthogonal functionalization step.

Particles with sizes below the diffraction limit of the microscope will appear as the point-spread function (PSF) of the instrument. VLPs are sub-diffraction limit particles, therefore their signal is the PSF of the microscope (approximately 240 nm). Particle size analysis was performed and the full width at half maximum (FWHM) was determined, a parameter that is a better approximation to particle size. Control fluorescent beads (size approx. 500 nm) alone present a FWHM value of approximately 540 nm. The mixture between VLPs and beads showed a bimodal size distribution, which indicates the presence of both particles (Figure 5.1b and B.1). As mentioned, with sizes below the resolution limit of the microscope, the signal is limited by the PSF and the value observed for the VLPs has an average size distribution of 240 nm, which is the microscope's PSF. The control VLP sample with added Met showed no green fluorescence signal, even after incubation with Alexa probe. This means that incorporation of Aha is necessary to observe fluorescence and that azide ligation between the non-canonical amino acid and the fluorophore is site-specific. The best time to incorporate Aha into HA protein was 24 hpi (time-dependent baculovirus infection was performed and is described in the SI, Figures B.2a and B.2b) (one reached approx. 3722 labelled-VLP per cm^2 with an I_f of 670.5±167 a.u. (arbitrary units) (mean ± SD), 40% and 100% higher than 12 hpi or 36/48 hpi, respectively).

5.4.2 TagE-VLPs platform improves downstream processing of Influenza VLPs

By optimizing the amino acid incorporation, the system becomes suitable for scale-up production and purification of labelled VLPs, detailed in Figure B.3a. During production, to label mainly the HA protein, addition of Aha amino acid to the cell culture was only performed after the late onset of gene expression (hpi=24).

DSP proceeded with a standard protocol for Influenza VLP purification already established in IBET's laboratory. Analysis of all DSP steps to monitor the presence and concentration of modified VLP across the process was performed by confocal microscopy (Figures B.3 and B.4) and by flow cytometry (Figures B.6 and B.7) for both labelled and control VLPs. Alexa probe was added to the samples before analysis. Clarification of the supernatant, to remove any remaining cells and cell debris, was performed by means of depth filter technology [68]. Intermediate purification involved an anionic exchange chromatography (AEX) and a concentration/diafiltration step by using ultrafiltration technology. AEX was operated in negative (flow through) mode, which means that the working volume is still high. To make the process cost effective, labelling with Alexa during purification was only performed after concentration of the flow through bulk. Size exclusion chromatography (SEC) was used in this case as a model of polishing step to remove a significant part of the remaining impurities such as baculovirus, DNA, or host cell proteins (Figure 5.2, B.4 and B.8). Elution of Influenza VLPs was monitored by detecting the absorption of the eluted solution at 234 and 494 nm (Maximum absorption wavelength of Alexa Fluor 488). Absorption at 234 reports roughly, all biomolecules that pass through the detector, whether the absorption at 494 is specific for the fluorescent VLPs that incorporated the Alexa-488 probe. This dual detection allows better discrimination between the particles of interest VLP and all other contaminants such as baculovirus. Although SEC removed some baculovirus, the product still contained impurities. A fluorescence-activated cell-sorting

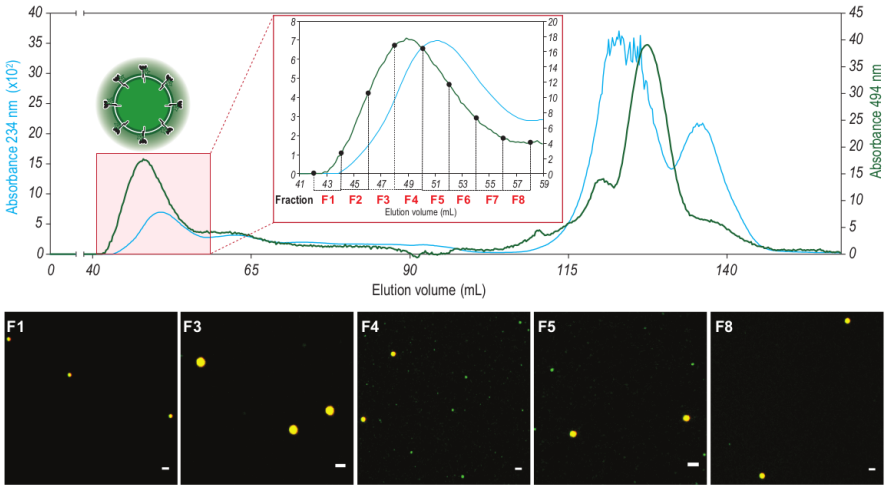

Figure 5.2: Detailed interpretation of VLP polishing step by means of size exclusion chromatography (SEC) for the Alexa-488 labelled VLP. Two detection signals were used to monitor SEC. The elution profile was monitored by detecting the absorption of the eluted solution at both 234 nm (blue curve) and 494 nm (green curve) (emission wavelength of Alexa probe). The absorption at 234 where roughly, all biomolecules that pass through the detector contribute to the signal obtained either by absorption or light scattering (DNA, proteins, lipids). The detection of the absorption at 494 is specific for the fluorescent VLPs that incorporated the Alexa-488 probe. This dual detection allows better discrimination between the particles of interest VLP and all other contaminants such as baculovirus. VLPs are contained in the column void volume. For each SEC fraction, confocal microscopy images were taken to monitor the presence of modified VLP (green fluorescent VLP). Scale bars (white) indicate 2 μm in all images. Images are ROI from larger independent images to better visualize the sub-diffraction green dots. Merge (green-red) images are shown for clarity. According to the scheme highlighted in Figure 5.1, red signal was also acquired and from green:red merge images 500 nm beads can be discriminated from VLPs (yellow and green dots, respectively). At the end of the SEC, between 115-130 mL of elution volume, concerning the elution of small molecules, there is evidence of detector signal saturation due to the elution of a high concentration of free Alexa-488 in the solution used in the labelling of VLPs.

(FACS) step was added at the end to overcome this issue and separate VLPs from baculovirus by taking advantage of their distinct particle sizes (150–200 nm and 300–400 nm, respectively) (Figure B.5). Additional information regarding particle detection, individual Green and Red channels and RAW confocal images can be found in the SI, Figures B.4a and B.4b for the control and Aha addition experiments. In order to validate the approach, each sample of the DSP process was also studied by flow cytometry. SSC–green fluorescence and Red–Green fluorescence 2D correlograms are depicted in the SI, Figures B.8a and B.8b, respectively. Detailed procedures for confocal microscopy and flow cytometry acquisition and apparatus are available in the Experimental Section.

Recent reports have described the ability to detect and sort lipid-based particles, exosomes and enveloped viruses, with flow cytometry [177, 178]. HA concentration and number of particles measurement was performed to assess VLP production yields using the TagE-VLPs strategy. HA concentration at harvest time was 1.4 μ ml^{-1} for both Met control and Aha experiments. Nanoparticle tracking analysis revealed that both cultures, control and experiment, produced VLPs in the same order of magnitude: 1.56×10^9 particles ml^{-1} and 1.39×10^9 particles ml^{-1}, respectively, meaning that the VLP production yields were not affected.

Further analysis of total protein, DNA concentration and baculovirus content were also performed during upstream and downstream processing. These analytical methods are essential to characterize the bioprocess and to make sure that control and labelled VLPs' data are comparable (data not shown). The polishing step (SEC; Figures 5.2 and B.4) and FACS (Figures 5.3, B.6, B.7, and B.8) are discussed later. It is consistently observed (Figure 5.1b) that the control VLP, with Met, does not exhibit significant green fluorescence signal, as seen in the flow cytometry 2D correlograms from Figures B.6, B.7, and B.8 (VLP gate for every DSP step of the control reveals no increase in positive Alexa 488 population, whether for the Aha experiment a positive Alexa 488 signal is observed). Moreover, the concentrated Aha-labelled VLP sample showed

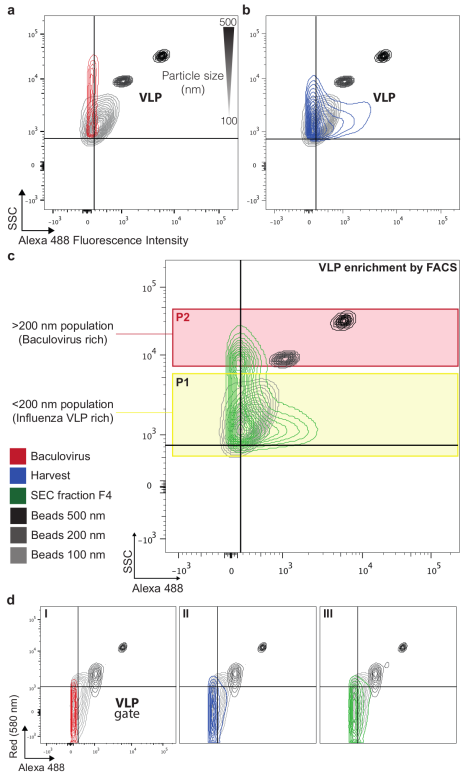

Figure 5.3: Discrimination between VLPs and baculovirus by FACS analysis. **a.** Flow cytometry of a baculovirus sample (used for infection and VLP production). 2D correlogram of side scatter and green fluorescence signals are shown with 5% contour plots of each population. Size scatter size ruler was made with 100, 200 and 500 nm size fluorescent beads (greyscale). Gate thresholds for negative and positive populations were performed using 100 nm beads signal – Top-right quadrant indicates green fluorescent positive >100 nm particles – VLP. In each chart, the [100-200] nm per Alexa 488 positive population gate – VLP – was built to quantify and sort the presence of labelled-VLP. This analysis monitors the scatter profile of the 200-400 nm rods (Red) of baculovirus that have no green fluorescence. **b.** Flow cytometry of a VLP sample before the DSP steps (Blue) shows that there are clearly two particle populations, one green positive population at $\sim$ 200 nm and one with lower/inexistent green fluorescence that has a wider size distribution. **c.** Flow cytometry of F4 from the VLP SEC purification step. Analysis of the green fluorescent signal shows that the >200 nm fraction is reduced relative to A as a result of the VLP specific green fluorescence signal. This sample was sorted with populations P1 (<200 nm population VLP-rich) and P2 (>200 nm population baculovirus-rich). **d.** 2D correlogram of Red and green fluorescence signals are shown for each population depicted in I (baculovirus), II (before DSP) and III (SEC F4). Gate thresholds for negative and positive populations were performed using 100 nm beads signal: Bottom-right quadrant is the VLP positive quadrant (green positive:Red negative particles. Significant green signal and none red correlate with modified VLP samples. SI Figures B.6a, B.6b, B.7a, B.7b, B.8a and B.8b depict additional flow cytometry performed in the study for all steps of the DSP process.

an I_f of 670.5±167 a.u. in the confocal images, whereas only background fluorescence intensity levels were detected in the control VLP samples. The residual green signal detected at the control concentration step is mainly a result of unspecific binding of the probe (incorporation onto hydrophobic moieties of lipid membranes) to process impurities that are more easily observed at higher concentrations. Furthermore, the concentration detected was residual relative to the labelled VLPs (Figures B.6, B.7, and B.8). The data confirmed the presence of labelled VLPs across DSP, with levels of concentration and purity consistent with the evaluated step. Ultrafiltration permeates and column-wash fractions from both AEX and SEC were analysed and no loss of labelled VLP was detected. These results demonstrate that this methodology is a powerful tool to monitor, on-line or at-line, each of the steps during manufacture of the product of interest, which can play an important role in DSP optimization [179]. On-line and at-line process analysers are inserted in one of the major categories of Process Analytical Technology (PAT) tools, having important applications in the biopharmaceutical industry.

The purification process flowchart was chosen as a proof of concept for the applied methodology, which means that other schemes and types of chromatography can also be exploited. As already discussed, labelling was performed prior to the SEC step to decrease the process cost. Because the previous chromatographic step was performed in a negative mode, the SEC step allowed the optimization process to be fine-tuned. Each fraction of this polishing step was interpreted in detail by confocal microscopy (Figure 5.2 and B.4) and confirmed by flow cytometry analysis (Figure B.8). One of the drawbacks of the baculovirus expression system is that it is difficult to remove baculovirus from the purified complex enveloped product [97, 180]. The rod-shape form of baculovirus makes it difficult to diffrentiate them from VLPs because, even with different detection methods, there are angles at which their sizes appear similar. Like VLPs, baculovirus also bud out of the cell to give an envelope content that is similar in the two species [97]. Control VLPs

were injected onto a SEC column and the elution profile was followed at 234 nm (280 and 260 nm were also tested but showed lower absorbance intensity and signal-to-noise ratio) (data not shown). The elution profiles of both the labelled VLP and control samples are very similar, with the VLP sample eluting at the void volume of the SEC column as expected (Figure 5.2). For modified VLP bulk, the absorbance intensity at 494 nm was also evaluated (emission wavelength of Alexa probe). Usually, VLP samples are contained in the void volume peak of the chromatogram as a result of their high Stoke radius. However, analysis of the two wavelengths shows that the two peaks are not superimposable. Fraction F4 presented a higher fluorescence (494 nm) value, which does not correspond to the peak maximum at 234 nm. Confocal microscopy images also revealed that F4 contains a higher concentration of labelled VLPs, which is in agreement with results from SEC chromatogram and flow cytometry analyses (Figures 5.4a, 5.4b and B.8). This means that a mixture of VLPs and other components elute in the void volume. Due to its rod-shape, baculovirus elutes in different volumes of the chromatogram [180]. Notably, this labelling methodology enables better discrimination between VLPs and other process impurities, in particular baculovirus, which is the major contaminant in this process. The on-line detection of VLPs leads to a more informed decision as to which fractions should be selected to continue in the purification process; an important step to obtain a higher recovery yield with improved VLP purity. The peak at the end of the chromatogram corresponds to free probe (494 nm) or DNA and low molecular weight contaminants (234 nm).

5.4.3 TagE-VLPs maintain integrity and functionality

Modified VLP integrity and HA biological function were assessed by means of a hemagglutination assay (Figures 5.4c and 5.4d). The correlation of their biological integrity with the number of fluorescent particles is also demonstrated by the quantification of the acquired images and particle counting (Figures 5.4a and 5.4b). Control and modified VLP

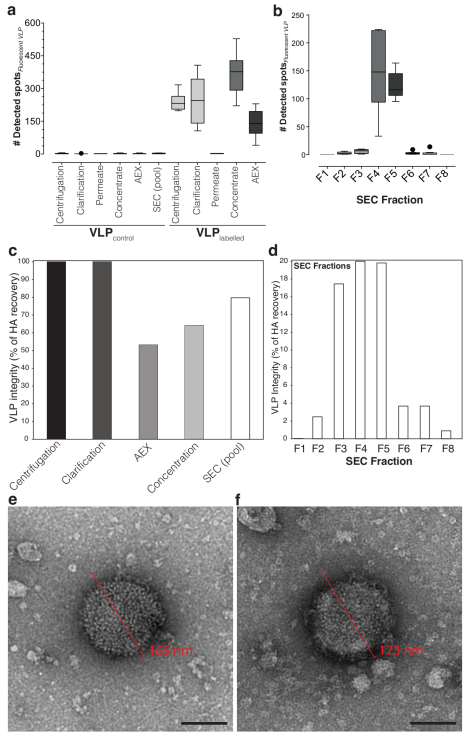

Figure 5.4: Integrity and functionality of modified VLPs. **a.** Quantification of the number of fluorescent particles detected in each DSP step in the control, unlabelled VLP and in the labelled VLP (steps from Figure B.3a). **b.** Quantification of the number of fluorescent particles detected in each SEC fraction in the labelled VLP purification (SEC from Figure 5.2). **c.** Hemagglutination assay for each step of the modified VLP purification process to assess preservation of HA biological function. **d.** Hemagglutination assay for each fraction of the SEC step. **e.** TEM analysis of control VLPs from the concentration step of the purification process. Scale bar indicates 100 nm. **f.** TEM analysis of modified VLPs from the concentration step of the purification process. Scale bar indicates 100 nm. Uncropped and additional TEM images are available in Figure B.10. The determination of the concentration of the labeled VLP solution based on the particle detection in **c.** and **d.** was also performed using equation 5.2 from the Experimental Section and is available in Figure B.4b.

HA concentration values are comparable for each step of the production and purification processes. This assay evaluates the biological interaction between sialic acid receptors present in erythrocytes and HA protein [5, 181, 182]. The same interactions happen under our conditions, which proves that the HA biological function is preserved even after chemical functionalization and labelling. The ability of these enveloped VLPs to maintain their characteristics may indicate that this methodology could be used to functionalize these particles with distinct targets. HA content increases as fluorescence intensity increases (Figures 5.2 and 5.4d), which means that the labelling is specific for Aha-containing Influenza VLPs. SEC fractions F4 and F5 give a higher percentage of HA recovery, which is in agreement with confocal microscopy results and number of fluorescent VLP detected (Figures 5.2, 5.4a and 5.4b) and flow cytometry data (Figure B.8).

As mentioned above, modified VLPs can be fluorescently labelled using Alexa Fluor488 probe. By taking advantage of this labelling, both control and TagE-VLPs were incubated with Alexa, separated in a SDS-PAGE gel and revealed using a fluorescent image analyser (Figure 5.5c and B.11). No fluorescent bands were detected for control VLPs, meaning that no labelling occurs without the noncanonical aminoacid incorporation, as previously described. However, in VLP samples with Aha modification, it was possible to detect three fluorescent bands. These bands were excised from the gel and identified by NanoLC-MS (Table B.1). Bands identified with (2) and (3) were confirmed by mass spectrometry as Hemagglutinin of Influenza A virus. Band (3) is probably a result of protein degradation during time. Band (4) was identified by mass spectrometry as Telokin-like protein of *Autographa californica* nuclear polyhedrosis virus, i.e., a protein from the baculovirus. As this virus replicate during infection and VLP production, it is possible to obtain some residual baculovirus Aha incorporation. However, Aha addition to the cell culture was only performed after the late onset of gene expression to minimize this possibility. Gel fluorescent data supports the

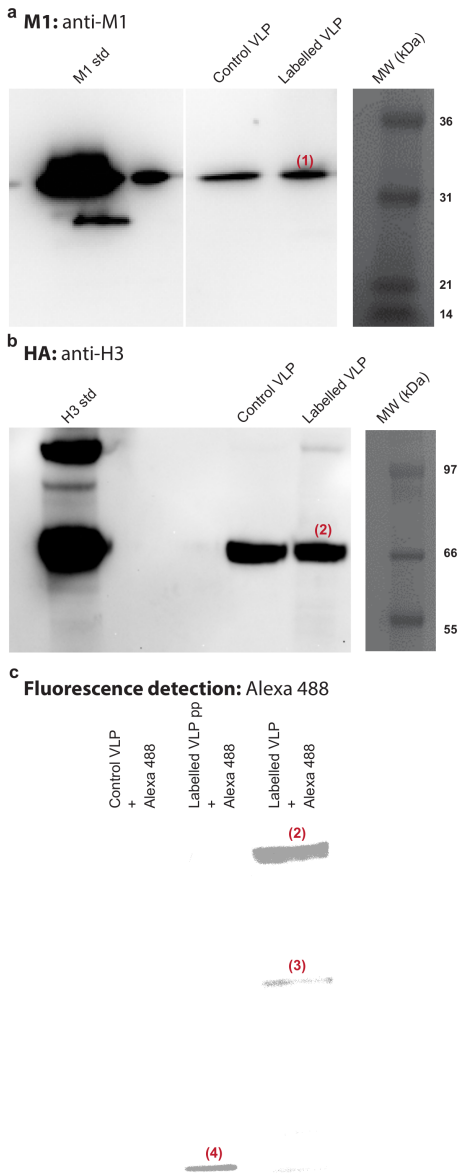

Figure 5.5: Identification of HA and M1 proteins by western blot analysis and fluorescent band detection of labelled Influenza VLPs' proteins. **a.** M1 Influenza protein detection on control and labelled VLPs by western blot analysis. M1 protein from Influenza A H1N1 strain was used as positive control (M1 std). Band (1) was excised and identified as M1 by mass spectrometry. **b.** HA Influenza protein detection on control and labelled VLPs by western blot analysis. H3 VLP from Influenza A H3 strain was used as positive control (H3 std). Band (2) was excised and identified as HA by mass spectrometry. **c.** SDS-PAGE gel fluorescence detection of control and labelled VLPs incubated with Alexa 488 probe. Bands (2) and (3) were excised and detected as HA by mass spectrometry. Band (4) was detected as a Telokin-like protein of baculovirus. "pp" means precipitated sample.

specificity of Aha incorporation into HA. Fluorescence intensity of baculovirus (band (4)) is clearly lower than HA corresponding ones and only appears when samples were precipitated resulting in VLP degradation. Mass spectrometry also detected Met-Aha modification in several peptides of the fluorescent bands, observed by a shift in the spectra (Table B.1). Therefore, Aha incorporation is preferentially made into HA proteins, a result of amino acid time of addition optimization. TEM analysis was performed to assess presence, integrity, and morphology of both control (Figure 5.4e) and modified VLP samples (Figure 5.4f). The morphology is maintained: their size ($\sim$ 170 nm) and spherical shape are similar. Furthermore, ultrastructural details of both VLP envelopes revealed characteristic Influenza HA spikes [183, 184]. Moreover, western blot analysis for HA and M1 specific detection was performed (Figure 5.5a, 5.5b and B.11) revealing that both control and modified VLPs have the two Influenza proteins. Protein identity was confirmed by mass spectrometry (Band ID 1 and 2 from Table B.1). This result further confirms the intact composition of modified VLPs.

5.4.4 FACS analysis enables VLP and baculovirus discrimination

Flow cytometry analysis allowed the detection and characterization of labelled VLPs and size discrimination between these particles (100-200 nm spheres) and baculovirus (200-400 nm rods). Fluorescent beads of 100, 200, and 500 nm were used as a particle size ruler in flow cytometry with the side-scatter signal [177, 178], which was then used to evaluate the VLP samples size distribution. It is possible to do a direct correlation between bead size and VLP samples because their refractive indexes are similar.

2D correlogram of side scatter and green fluorescence signals was acquired for each bead (100, 200, and 500 nm) for the VLP and control samples to detect the presence of baculovirus and evaluate further particle separation by cell sorting. A baculovirus sample (used for cell in-

fection and VLP production) was analysed to monitor the scatter profile of these 200-400 nm length rod-shape particles. Sizes that ranged $\sim$ 200-500 nm were observed, which indicates that these rods are polydisperse (Figure 5.3a). A sample from the harvest step showed that at this stage there are clearly two particle populations, one green positive population at $\sim$ 200 nm and one with lower green fluorescence that has a wider size distribution (Figures 5.3b and B.7). The size heterogeneity comes from a VLP/baculovirus mixture because the sample is from an early purification step still rich in baculovirus contaminants. A fraction from the SEC step (Figures5.3c and B.8) shows that the green fluorescent signal of the >200 nm fraction is reduced relative to baculovirus and harvest panels (Figures 5.3a and 5.3b). The presence of baculovirus is reduced relative to VLP in the SEC sample that is from a final purification step. However, the SEC fraction still contains some baculovirus because the baculovirus has a broad elution profile as a result of their rod-like shape. VLP sorting of the SEC F4 fraction sample was performed to separate the VLPs from baculovirus. Fluorescent beads (200 nm) were used to define two sorting populations: P2 (>200 nm particles) is a baculovirus-rich population and P1 (<200 nm particles) is VLP rich (Figure 5.3c). This strategy increased the yield on VLP production and minimized the presence of baculovirus in the final DSP product.

TEM analysis of baculovirus control (used to infect cells) and modified VLP (after concentration) was used to evaluate the size and heterogeneity of samples (Figure 5.6a). Baculovirus samples are characteristically rod-shaped with an average size of approximately 250 nm. As expected, the concentrated VLP sample contained both small and large particles, which corresponds to VLPs or baculovirus and process impurities, respectively. The size of the VLPs is different from the one presented previously (Figure 5.4e and 5.4f), which confirms the heterogeneity of the system [59]. It is clear that there are unwanted larger particles at this stage of the process that are not VLPs, or at least not complete ones, because of the lack of HA spikes. This result provides an indication of

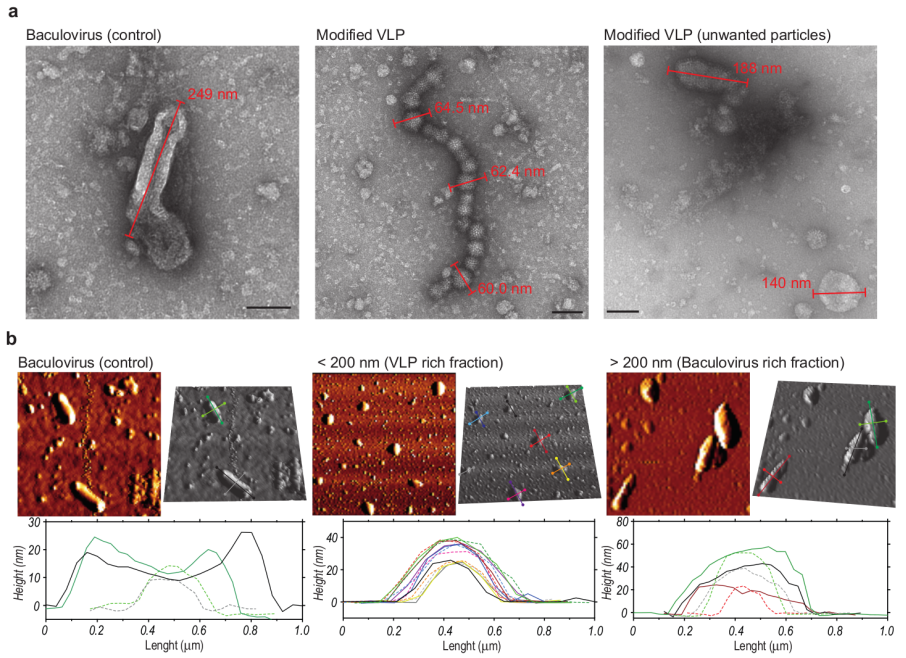

Figure 5.6: Modified VLP detailed analysis. **a.** TEM images of the major impurity in VLP production, baculovirus and a VLP sample before sorting revealing optimal VLP and large undesirable particles. Scale bars indicate 100 nm in all images. Uncropped and additional TEM images are available in Figure B.10. **b.** AFM images (error and 3D images) of a baculovirus control sample, which shows rod-like morphology of this virus. Samples from each DSP step were sorted into P1 and P2 as described in Figure 5.3c. AFM images of P2 and P1 samples clearly show <200 nm spherical particles, consistent with VLP and on the opposite side the >200 nm show rod-shaped, non-spherical particles, more akin to baculovirus morphology as shown in the left AFM panels. The longitudinal (fill line) and transversal (dashed lines) cross sections were performed to better illustrate the spherical and rod shapes of each particle visualized in each sample.

what to expect from both sorting populations. The presence of VLP and baculovirus was performed for baculovirus control, P1 and P2 sorting populations by atomic force microscopy (AFM; Figure 5.6b). AFM images of the baculovirus control samples revealed the well-known rod-like structure. Images of the P1 sorting population (<200 nm, VLP rich fraction) revealed only the presence of spherical particles. However, the P2 sorting population (>200 nm, baculovirus rich fraction) presented only large particles, which mainly consisted of baculovirus rod-shaped particles and other large process impurities. The baculovirus size in the P2 sorting population is similar to that calculated from the control sample. This data confirms that our system is suitable as a FACS purification step, and represents important progress to meet the increasing demand for VLP-baculovirus separation and DSP quality control requirements.

5.5 Conclusions

Herein we report a straightforward two-step strategy to chemically functionalize and label complex enveloped VLPs in vivo by using SPAAC. Unlike previous reports, this methodology is designed for VLPs that are able to display membrane proteins in their lipid bilayer and potentiate the plethora of antigens that can be presented to cells in vaccine design. The functionalization of these particles, in particular of membrane proteins, is not straightforward with current methods. The technical challenges and antigen choice limitations can be overcome by using the TagE-VLPs strategy described here. This flexible and site-specific system does not have an impact on biological function of the VLPs studied and can be potentially used in several virus or VLPs. The reported strategy can be used to functionalize these particles and expand their utility in exciting applications, such as vaccine design, drug delivery or molecular-imaging agents for diagnostics.

Importantly, the use of flow cytometry to analyze polydisperse lipid suspensions that contain VLPs has greatly enhanced our knowledge on

their heterogeneity. Techniques that characterize, discriminate, and accurately separate each individual population with particle counting and concentration determination are scarce for nano-sized particles. By extended use of FACS to characterize VLPs provides a better description and understanding of purified VLPs produced under different methods and systems, and enables proper identification/separation of contaminants and desired particles. This easy-to-use and fast methodology only requires fluorescent beads for size calibration, which lends this technique to be used as an at-line, high-throughput, non-disruptive method to monitor all stages of VLP production in addition to current techniques, which are time consuming and typically do not allow analysis of the VLPs in their native form. Both fluorescent labelling and FACS methods described in this manuscript are powerful tools for DSP monitoring and optimization that allow the improvement of product recovery yields and increase VLP purity levels.

It is worth to note that this method is not exclusively dependent on two-dimension particle discrimination. The new bioorthogonal labelling method here reported allows to engineer biologically functional VLPs, for instance, by conjugation of synthetic epitopes that are non-fluorescent, as the size signal enables one-dimension functionalized VLP:Baculovirus separation. We have sorted VLPs from baculovirus using their distinctive size and green colour discrimination (Figure B.9). Having both differentiating parameters only increased the accuracy of the method but restricting to one variable does not obviates its application and multifunctionalize the Aha moiety with other bioactive molecules.

5.6 Experimental Section

5.6.1 Cell culture

High Five cell line (Trichoplusia ni derived BTI-Tn-5B1-4) was obtained from Invitrogen (B855-02, Invitrogen Corporation, Paisley, UK). Cells were routinely cultured in ESF921 protein-free medium (96-001-01, Ex-

pression Systems, USA) in 125 mL Erlenmeyer flasks (430421, Corning, USA) with a working volume of 10 mL. High Five cells were kept in a humidified incubator at 27 °C and 110 rpm. Every 3-4 days, after reaching a cell concentration of 2-3$\times 10^6$ cells mL^{-1} they were re-inoculated at 3×10^5 cells mL^{-1}. Cell concentration and viability were determined by haemocytometer cell counts (Brandt, Wertheinmain, Germany) and trypan blue exclusion dye method (Merck, Darmstadt, Germany). High Five cells were chosen as producer cell line due to the higher productivity achieved for the proof-of-concept of the method described. However, when considering late stage biopharmaceutical production, it is crucial to evaluate the safety of this host cell line, since it was reported the presence of latent alphanodavirus in the High Five genome [185, 186]. By itself, the virus may not constitute a burden, however if it assumes the replicative form may contaminate final product preparations requiring extra downstream processing efforts [187]. Nevertheless, it has been described that there is no contamination present in Invitrogen master High Five cells bank [188], the cell source used, and additionally there are not any reports indicating the infection of human hosts by the alphanodavirus. In fact, both High Five and Sf9 cell lines have regulatory acceptance for manufacturing of biologicals, such as Cervarix, GSK HPV vaccine, or Flublock, Protein Sciences Influenza vaccine [185].

5.6.2 VLP production and metabolic labelling optimization

For production studies, cells were cultured in 500 mL Erlenmeyer flasks (431145, Corning, USA) with a working volume of 50 mL or in 2000 mL Erlenmeyer flasks (431255, Corning, USA) with a working volume of 250 mL. High Five cells infection with recombinant baculovirus (kindly provided by Redbiotec AG) encoding the H3 subtype Influenza A/Johannesburg/33/94 and M1 A/California/06/2009 Influenza virus strains was performed at a cell concentration at infection (CCI) of 2×10^6 cells mL^{-1}, with a multiplicity of infection (MOI) of 15 IP cell^{-1}. After 12 hours

post-infection (hpi) the culture medium was removed by centrifugation at 200 g for 10 min and the cells were washed with D-PBS (14190-169, Gibco, UK). ESF921 methionine deficient and protein-free medium (96-200-01, Expression Systems, USA) was then added to the infected cells. Noncanonical amino acid incorporation was tested at several hpi values (18, 24, 36 and 42 hpi) in order to identify the best condition for VLP production. The culture medium was supplemented with 4 mM Aha (AS-63669, AnaSpec, USA). To generate appropriate controls, this study also carried out with 4 mM L-Methionine (M2893, Sigma-Aldrich, Switzerland) at the same conditions.

5.6.3 Harvest and Clarification

High Five infected cells were harvested at 48 hpi by centrifugation at 200 g for 10 min (JA10 rotor, Avanti J25I centrifuge, Beckman Coulter, USA). Harvest was set to 48 hpi, at which time productivity was highest, a parameter that was screened and optimized previously (data not shown). The pellet was discarded and Benzonase (101654, Merck Millipore, Germany) was added to the supernatant at a final concentration of 50 U mL^{-1} and incubated at room temperature (22 °C) for 15 min. The clarification of supernatant was performed by dead-end filtration using a Sartopore filter with 0.45 + 0.2 μm pore size (SART5445307H7-SS-A, Sartorius, Germany). The clarification of VLP-containing bulk was performed at a constant flow rate of 100 $mL.min^{-1}$ using a Tandem 1081 Pump (Sartorius Stedim Biotech, Germany). The pressure was monitored by an in-line pressure transducer (080-699PSX-5, SciLog, USA) to control possible overpressure. The filtration module was previously conditioned with three capsule volumes of buffer 50 mM HEPES, pH 7.4, 300 mM NaCl (working buffer).

5.6.4 Anion exchange chromatography

Sartobind Q MA 75 (93IEXQ42DB-12V, Sartorius, Germany) membrane adsorber was used as a first purification step, operated in negative mode

(flow through (FT)). The membrane adsorber was equilibrated with 50mM HEPES, pH 7.4, 400 mM of NaCl equilibration buffer. The VLP clarified suspension was diluted with concentrated NaCl buffer to match the conductivity of equilibration buffer. The flow rate was set to 4.76 MV min^{-1} and the VLPs were collected in the FT pool. A final elution step was performed with 50 mM HEPES, pH 7.4, 1.0 M NaCl elution buffer in order to guarantee that all particles were removed from the membrane adsorber. VLP concentration along these fractions was determined by hemagglutination assay and nanoparticle tracking analysis. All chromatographic steps were performed at room temperature (RT) (22 °C).

5.6.5 Ultrafiltration and Diafiltration

Sartobind Q FT pool containing VLPs were concentrated using tangential flow filtration (TFF). Ultrafiltration experiments were conducted using flat sheet Pellicon XL Ultrafiltration Module Biomax 300 kDa 0.005 m^2 (PXB300C50, Merck Millipore, USA). The membrane module was set up accordingly with the manufacturer's instructions. The ultrafiltration module was preconditioned with deionized water, to eliminate trace preservatives and equilibrated with working buffer before the concentration step. To ensure sterility, the TFF system was sanitized with 0.1 M NaOH and incubated with this solution for 60 min. A Tandem 1081 Pump (Sartorius Stedim Biotech,Germany) was used on the feed side set up to a fixed flow rate of 40 mL min^{-1}. Transmembrane pressure (TMP) was controlled by adjusting the retentate flow rate using a flow restriction valve. The pressure was monitored at feed inlet, retentate outlet and permeate outlet by in-line pressure transducers (080-699PSX-5, SciLog, USA). The feed-retentate and the permeate volumes were monitored using a technical scale (TE4101, Sartorius Stedim Biotech, Germany). At a proper feed volume, three diafiltration volumes with working buffer were performed. After achieving the desired concentration factor, the TFF loop was completely drained and the VLP retentate was recovered.

Samples of the final retentate and permeate were taken to assess process yield.

5.6.6 Size-exclusion chromatography

Concentrated VLPs were labelled with 20 μM of Alexa Fluor 488 (C-10405, Life Technologies, USA) for 60 min, according to manufacturers' instructions and prior to the polishing step. Size exclusion chromatography was performed using a HiLoad 16/600 Superdex 200 pg column (GE Healthcare, USA) coupled to an ÄKTA explorer 10 liquid chromatography system (GE Healthcare, U.K.) equipped with UV and conductivity-pH monitors. System operation and data gathering and analysis was done using the UNICORN 5.0 software (GE Healthcare, U.K.).

The column was loaded with 5 mL of concentrated VLPs, using a 5 mL capillary loop, at a constant flow rate of 0.5 mL min^{-1}. Working buffer was used as eluent and the eluted fractions were collected for further analyses. Elution of Influenza VLPs was monitored by detecting the absorption of the eluted solution at 234 and 494 nm (maximum absorption wavelength of Alexa Fluor 488). Absorption at 234 reports roughly, all biomolecules that pass through the detector either by absorption or light scattering (DNA, Proteins, lipids). The detection of the absorption at 494 is specific for the fluorescent VLP that incorporated the Alexa-488 probe. This dual detection allows better discrimination between the particles of interest VLP and all other contaminants such as baculovirus.

5.6.7 Hemagglutination assay

Hemagglutinin protein was quantified using a hemagglutination assay. The assay was carried out based on the protocol described elsewhere [189] with some modifications. Briefly, 25 μL of D-PBS (14190-169, Gibco, UK) were added in each well of a clear, V bottom 96-well microtiter plate (611V96, Sterilin, USA). In the first well (upper left), 25 μL of each sample were added and then two fold serial dilutions (25 μL of sample in an equal volume of PBS) were performed. The excess 25 μL

from the final dilution were discarded. After this step, 25 μL of 1% chicken erythrocytes (LOHMANN TIERZUCHT GmbH, Germany) was added to each well of each serial dilution series. The plate was incubated at 4 °C for 30 min without disturbance. As a positive control, Influenza vaccine (Influvac, Abbott, USA) was used. The level of hemagglutination was inspected visually for all the wells and the highest dilution capable of agglutinating chicken erythrocytes was determined.

We have plotted the hemagglutination assay according to the percentage (%) of HA recovery in each analysed sample. This percentage is determined according to equation 5.1:

$$\%\text{HA recovery} = \frac{[\text{HA}]_{\text{DSP step}} \times V_{\text{DSP step}}}{[\text{HA}]_{\text{initial step}} \times V_{\text{initial step}}} \times 100 \tag{5.1}$$

5.6.8 Total Protein Quantification

Total protein was quantified using the BCA Protein Assay Kit (23225, Thermo Fisher Scientific, USA) according to the manufacture's protocol. Bovine serum albumin (BSA) was used for the calibration curve (23209, Thermo Fisher Scientific, USA). In order to avoid matrix interference, the samples were diluted between 2-256 fold. The assay took place in a clear 96-well microplate (260895, Nunc,USA) and the absorbance at 562 nm was measured on Infinite 200 PRO NanoQuant (Tecan, Switzerland) microplate multimode reader.

5.6.9 Total dsDNA Quantification

Total DNA was quantified using the fluorescent-based Quant-iT Picogreen dsDNA assay kit (P7589, InvitrogenTM, UK) according to the manufacturer's instructions. In order to avoid matrix interference, the samples were diluted between 2-256 fold with the provided reaction buffer. The assay took place in a black 96-well microplate, flat transparent (3603, Corning, USA) and the fluorescence was measured on Infinite 200 PRO NanoQuant (Tecan, Switzerland) microplate multimode reader.

5.6.10 Nanoparticle tracking analysis

Total virus-like particles concentration and size distribution were measured using the NanoSight NS500 (Nanosight Ltd, UK). The samples were diluted in D-PBS (14190-169, Gibco, UK) so that virus-like particles concentration would be in the 10^8-10^9 particles mL^{-1} - the instrument's linear range. All measurements were performed at 22 °C. Sample videos were analysed with the Nanoparticle Tracking Analysis (NTA) 2.3 analytical software - release version build 0025. Capture settings (shutter and gain) were adjusted manually. For each sample 60 s videos were acquired and particles between 70 and 130 nm were considered.

5.6.11 Confocal Microscopy

Using Life Technologies (Carlsbad, CA, USA) TetraspeckTM beads one can use as visual reference of successful VLP labelling and detection. Due to its four-colour fluorescence using green (which also detects labelled VLP) and orange (specific for beads) one can perform quantitative analysis on the detected VLP. An inverted confocal point-scanning Zeiss LSM 710 microscope equipped with 405, 458, 488, 561 and 633 nm lasers was used. Due to the diffraction limit associated with microscopy techniques, no particle below that threshold can be visualized with high resolution. Thus it would appear the point-spread function (PSF) of the instrument. VLP are sub-diffraction limit particles, thus their signal in the microscope would be the PSF of the microscope (approx. 240 nm). By using 500 nm size fluorescent beads as a control, together with their dual-fluorescence emission spectra, one can perform an accurate detection of sub-diffraction limit particles - VLP. This methodology was used to evaluate the best time for amino acid (Aha or Met) addition after baculovirus infection: 12, 24, 36 and 48 hpi were evaluated. 100-fold dilutions of each condition supernatant were deposited into IbiTreat 8 μ-well slides (Ibidi, Martinsried, Germany) and allowed to attach for 1 h. Each preparation was then labelled with 20 μM of Alexa Fluor 488 (C-10405,

Life Technologies, USA) for 30 min, according to manufacturers' instructions. The sample was washed 3 times with PBS and 500-fold dilution of 500 nm fluorescent beads were added to each sample for 30 min. Medium was changed for fresh PBS. In all steps, the PBS used for dilution preparation, wash steps and sample acquisition, was filtered with a 0.1 μM nylon filter. Control VLP (methionine amino acid added during VLP production, M2893, Sigma-Aldrich, Switzerland), modified VLP (with the Click-it noncanonical amino acid, Aha, AS-63669, AnaSpec, USA), and 500 nm beads were imaged using a 63×-oil objective and green and orange channels were acquired. From each independent experiment at least 3 images at different viewfields in the μ-slide were taken for all samples. ImageJ software was used to perform merge images as well as to perform particle count/detection and size analysis in each preparation from which the full width at half maximum was determined (reflects particle size). From the number of particles detected we estimated the concentration of fluorescent VLP [$\mathrm{VLP_{fluo}}$] in each DSP step and SEC fraction according to the relationship in equation 5.2:

$$[\mathrm{VLP_{fluo}}] = N \times (a_{\mathrm{coverslip}}/a_{\mathrm{image}}) \times dil \times \frac{1}{V} \tag{5.2}$$

where N is the number of fluorescent VLP detected in the microscopy image, $a_{\mathrm{coverslip}}$ and a_{image} are, respectively the area of the microscope coverslip (9.4×10.7 mm for each μ-well) and the area of the acquired image (44.5×44.5 μm), dil is the dilution factor of the added VLP (100-fold in our case) and V is the sample volume.

5.6.12 Flow Cytometry

Detection and characterization of labeled VLP and size discrimination between VLP (spheres of 100-200 nm) and Baculovirus (rods of 200-400 nm) with flow cytometry were performed using a BD LSR Fortessa (BD Biosciences, San Jose, CA, USA). It is equipped with 3 lasers (violet, 405 nm; blue, 488-nm; red, 640 nm), forward and side scatter detectors

and 9 fluorescence emission detectors (530/30 - green channel was used for VLP-A488 and 100, 200 and 500 nm Tetraspeck fluorescent beads). Side scatter detector was used to define the detection threshold. Using 100, 200 and 500 nm beads one can build a particle size ruler in flow cytometry with the scatter signal [178] which can then be used to evaluate the VLP samples size distribution. The refractive index (RI) depends on the material of the scattered solution, thus direct correlation of bead size and VLP can only be achieved if each sample has approximately the same RI. The RI for PBS, UF Retentate, SEC fractions (100-fold dilution), Baculovirus (100-fold dilution), 100 nm (2000-fold dilution), 200 nm (1000-fold dilution) and 500 nm beads (500-fold dilution) are respectively, 1.334, 1.335, 1.335, 1.336, 1.334, 1.334, and 1.334, measured using a digital refractometer (13950000, AR 200 Digital Refractometer, Leica, USA). The side-scatter–alexa-488 correlograms were acquired for each bead and VLP sample, at the dilutions previously stated, to detect baculovirus presence and evaluate further particle separation by sorting. In all steps, the PBS used for dilution preparation, wash steps and sample acquisition, was filtered with a 0.1 μM nylon filter.

5.6.13 VLP sorting

Sorting of the SEC F4 sample from the downstream processing was performed to separate VLPs from the baculovirus-rich fraction ($>$ 200 nm). Fluorescence activated sorting was performed in a BD FACS Aria III equipped with 3 lasers (blue, 488 nm; yellow-green, 561 nm; and red, 633 nm). The 200 nm fluorescent beads were used to define two sorting populations: P2 corresponding to the $>$ 200 particles detected, which is a baculovirus-rich population and P1 which is the $<$ 200 nm particles that, in contrast to P2 is VLP-rich. Each population was acquired in vials filled with PBS and the presence for VLP and baculovirus was performed by atomic force microscopy.

5.6.14 Atomic force microscopy

AFM images of VLPs and baculovirus were acquired using a JPK Nano Wizard II (Berlin, Germany) mounted on a Zeiss Axiovert 200 inverted microscope (Göttingen, Germany). The AFM head is equipped with a 15 μm z-range linearized piezoelectric scanner and an infrared laser. All samples were prepared in freshly cleaved mica. For scanning in liquid environment the mica was pretreated with poly-D-lysine for 20 min and rinsed with miliQ water. A 50 μL drop of each sample was added to the mica and rinsed with PBS buffer at least 4 times. The sample was then allowed to air-dry or maintained in buffer for subsequent imaging. Scanning was performed using uncoated silicon ACL cantilevers from Applied NanoStructure for air-dried samples and uncoated silicon cantilevers HQ:CSC38–No Al from MikroMasch for samples in liquid medium. ACL cantilevers had typical resonance frequencies between 145 and 230 kHz and an average spring constant of 45 N/m. HQ:CSC38 cantilevers had typical resonance frequencies between 5 and 17 kHz and an average spring constant of 0.03 N/m. All measurements were carried out in contact mode. All images were obtained with the same or similar AFM parameters (setpoint, gain and scan rate) values. Setpoint and gain were continuously adjusted during scanning to maintain the lowest possible value and reduce sample damage.

5.6.15 Transmission Electron Microscopy

To analyze the presence, integrity and morphology (shape, size) of the VLPs, electron microscopy was performed as follows: a drop (5 μl) of sample was adsorbed onto a formvar coated 150 mesh copper grid from Veco (Science Services, Germany) for 2 min. The grid was washed 5 times with sterile filtered dH2O. Then it was soaked in 2% uranyl acetate for 2 minutes and dried in air at room temperature (22 °C). The samples were examined with a Hitachi H-7650 120 Kv electron microscope (Hitachi High-Technologies Corporation, Japan).

5.6.16 PCR

Baculovirus viral DNA was extracted and purified using the High Pure Viral Nucleic Acid Kit (Roche Diagnostics, Germany) using the manufacturer's instructions. The number of genome containing particles were monitored by real time quantitative PCR (q-PCR) following the protocol described elsewhere [190].

5.6.17 Western Blot analysis

Western blot analysis was performed for control and modified Influenza VLPs, with both precipitated and not precipitated samples. As a control M1 protein from Influenza A H1N1 strain (SinoBiological) and H3 Influenza VLP (produced and purified at iBET) were used. Protein precipitation was performed with 20% (v/v) ethanol overnight. Loading buffer (LDS sample buffer and reducing agent (Invitrogen)) was added and protein samples were incubated at 70 °C for 10 min. Influenza VLPs were separated in a 4-12% (w/v) polyacrylamide NuPAGE gradient precast gel (Invitrogen). Samples were resolved for 60 min at a constant voltage of 200 V and transferred into a PVDF membrane using iBlot Dry Blotting System (Invitrogen). Membranes were blocked with 5% (w/v) of dry milk (Merck Millipore) in Tris-buffered saline with 0.1% (w/v) of Tween 20 (T-TBS buffer) for 1 h. After blocking, membranes were incubated overnight with the respective primary antibody: Anti-Influenza A Virus M1 goat antibody (dilution 1:2000) (Abcam ab20910) or a 1:1 mixture of Anti-A–Johannesburg/33/94 sheep serum (dilution 1:1000) and anti-A–Nanchang/933/95 (H3N2) HA sheep serum (dilution 1:1000) (both provided by NIBSC). Western blot detection was performed with the corresponding anti-goat or anti-sheep secondary antibody (dilution 1:2000, 1 h incubation) conjugated to Horseradish peroxidase and developed using the ECL Detection Reagent protocol (GE Healthcare).

5.6.18 Fluorescence imaging

Control and labelled VLP samples were incubated with 20 μM of Click-iT Alexa Fluor 488 fluorescent probe for 30 min prior to SDS-PAGE gel running. FLA-5100 fluorescent imaging system (FLA-5100 fluorescent imaging system, Fujifilm Life Sciences, USA) was used to reveal the gel and analyse the presence of fluorescent bands. The 473 nm laser was used and images were acquired with 25 μ of resolution and at a voltage of 600 V.

5.6.19 Mass Spectrometry

HA and M1 protein bands, detected by western blot, and fluorescent bands were destained, reduced, alkylated and digested with trypsin (Promega, 6.7 ng/μL) overnight at 37 °C. The tryptic peptides were desalted using POROS R2 (Applied Biosystems) and analysed by NanoLC-MS using TripleTOF 6600 (ABSciex). External calibration was performed using β-galactosidase digest (ABSciex). The 40 most intense precursor ions from the MS spectra were selected for MS/MS analysis. Data were acquired with the Analyst software TF 1.7 (ABSciex). The raw MS and MS/MS data were analysed using Protein Pilot Software version 5.0 (ABSciex) for protein identification. The search was performed against the HA and M1 protein sequences and against Swissprot Viruses database plus the protein sequences of Influenza VLP proteins' HA and M1. Protein identification was considered with an unused score greater than 1.3 (95% confidence). In order to detect modified peptides, data were also analysed using the BioPharmaView software version 1.0 (ABSciex) considering a Met-Aha modification (mass shift of -4.986 Da) with m/z tolerance of $\pm$10 ppm.

5.7 Acknowledgments

The authors acknowledge funding from the European Union (EDUFLUVAC project, FP7-HEALTH-2013-INNOVATION), the Fundação para

a Ciência e Tecnologia (FCT, Portugal; project HIVERA/0002/2013 and FCT Investigator to G. J. L. B.), the European Commission, Marie Skłodowska-Curie Actions (MSCA), and RISE project grant 644167. S. B. C., J. M. F., F. M., and D. G. acknowledge FCT for fellowships SFRH / BD / 52302 / 2013, SFRH / BD / 70423 / 2010, SFRH / BD / 70139 / 2010, and SFRH / BPD / 73500 / 2010, respectively. The authors acknowledge Ricardo Silva for all his help in fluorescence analysis implementation and fruitful discussions. The authors also acknowledge Patrícia Gomes-Alves for her help for mass spectrometry analysis. Mass spectrometry data was obtained by the Mass Spectrometry Unit (UniMS), ITQB/iBET, Oeiras, Portugal. G. J. L. B. is a Royal Society University Research Fellow and the recipient of a European Research Council Starting Grant (*TagIt*).

6

Efficient filtration strategies for the clarification of influenza virus-like particles derived from insect cells

Sofia B. Carvalho, Ricardo Silva, Ana Sofia Moreira, Bárbara Cunha, João J. Clemente, Paula M. Alves, Manuel J. T. Carrondo, Alex Xenopoulos, Cristina Peixoto

Contents

6.1 Context

As described in the preface, this PhD thesis was developed under the scope of the European Project EDUFLUVAC. As a key partner, iBET was responsible for the production and purification of more than thirty different influenza VLPs, from different groups, strains and some of them multivalent. With this variability, the downstream process applied should be as much as possible independent on the product charge, meaning strain-independent. The first issue we faced on the development of this process was to have a clarification step capable of handling with the variability on the upstream, not only in terms of strain differences but also in what it implies on cell viability, product concentration and process impurities obtained for each one of them. This chapter reports the study performed to implement a universal clarification strategy for influenza VLPs. We were able to obtain a scalable train that decreases the turbidity to values below 10 NTU without compromising product recovery yield.

I was involved in the conception of the study, on the design and upstream production of VLPs. I was the main responsible for the clarifications studies, analytics for quality control as well as writing of the manuscript.

This work was submitted to an international peer reviewed journal and is currently under revision.

6.2 Abstract

Vaccination remains the most effective available tool for preventing influenza infection, which affects millions of people annually. The virus is constantly mutating, requiring annual immunization. Vaccine production should be achieved in a very short period to cope with global requirements for seasonal treatment. Moreover, pandemic outbreaks require quick production of large amounts of vaccines. Virus-like particles (VLP) have become a promising alternative for influenza vaccines due to their versatility, immunogenicity and safety profile. However, the diversity of virus surface epitopes contributes to a variability in downstream purification, that could ultimately affect manufacturability and necessitate yearly redevelopment of processes. Therefore, there is a demand for development of better and faster influenza vaccine bioprocesses. Clarification is a critical step, not well characterized for most of the purification processes, but with a strong impact on the downstream performance. For that purpose, we have undertaken an effort to develop a clarification platform for the manufacturing of several influenza strains, mono and multivalent, at different production scales (1–11 L). Both normal and tangential flow filtration approaches were evaluated in terms of product recovery and removal of impurities. The selected clarification train results in essentially 100% product recovery with a turbidity value below 10 NTU, as well as high impurity clearance. Most importantly, these results are independent of strain, cell viability and turbidity at harvest time. The developed clarification framework may be applied to different influenza strains, contributing to a speed-up of vaccine manufacturing.

6.3 Introduction

Due to antigenic shift and drift, the influenza virus still affects 5 million people worldwide leading to 250k-500k deaths annually [191]. Limitations in production processing time and capacity are the main bottlenecks preventing global immunization. Furthermore, seasonal vaccines are not suitable for pandemic outbreaks, which require fast availability of doses to cope with global demand [39]. Therefore, new manufacturing strategies are being evaluated to enable a fast response and to improve product yield and consistency. New options are moving away from egg-based platforms to new expression systems such as mammalian, insect or plant cells, bacteria or yeast [14].

Virus-like particles (VLP) have been recently used for vaccine development given their strong immunogenicity as they mimic the virus from which they were derived. Furthermore, due to their lack of genetic material they are not infectious nor replicative. VLP-based vaccines are already commercially available for human papilloma virus, hepatitis B and E viruses and VLP-based vaccine candidates are being produced, for both seasonal and pandemic Influenza virus [14, 39–43].

Influenza VLP can be expressed in different cell systems, such as mammalian, plant or insect cell cultures, implying different purification strategies [96]. Advantages for the use of insect cell-baculovirus expression systems include short production times, high productivities and a straightforward scale-up, maintaining efficiency [53]. There are also drawbacks related to product stability and baculovirus removal due to size and charge similarity with VLPs [54, 61]. Initial purification strategies relying on centrifugation and ultracentrifugation using CsCl, sucrose or iodixanol gradients [14, 43, 62] are difficult to scale up, expensive and result in low recovery yield. Improvements in purification methodologies are clearly needed.

Clarification, the first stage in the purification of VLP-based vaccines, connects upstream and downstream processes, affecting yield, product

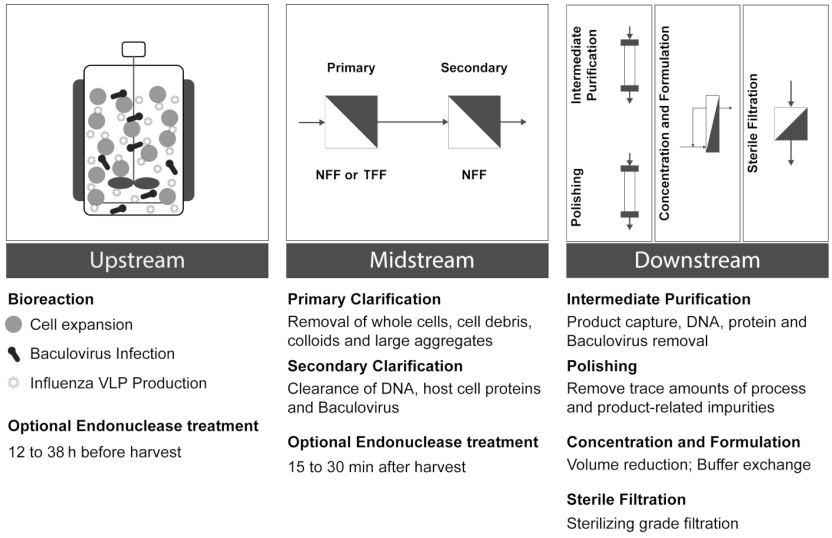

Figure 6.1: Influenza VLP bioprocess. Schematic representation of insect-cell produced influenza VLP bioprocessing workflow. Description of upstream, midstream and downstream steps.

consistency and reproducibility (Figure 6.1) [43]. An efficient clarification step should deliver a low turbidity solution with minimal impact on product recovery, while also removing process and product-related impurities. Clarification can be conceptually divided into primary and secondary steps, according to their roles (Figure 6.1). Primary clarification is used for the removal of large particulate matter, including intact and non-viable cells, whereas secondary clarification has been used for the removal of colloidal matter, suspended species, and process- or product-related insoluble and soluble impurities including large aggregates [43, 61, 64]. On top of this, the removal of host cell proteins and DNA may in some cases, be accomplished by depth filtration.

Improvement of upstream productivity has led to cultures with higher titters and consequently higher cell densities and impurity content, resulting in a burden on clarification processes and subsequent purification steps [68]. To address these challenges, conventional methods are being replaced by new membranes and filtration processes technologies. Both tangential flow microfiltration and dead-end depth filtration have been

reported for clarification of cell feedstocks [180, 192–194]. These technologies offer process flexibility, rapid product changeover, possibility of single-use and capital savings [61, 71].

The aim of the present work was to develop a platform to speed up VLP vaccine production and purification, addressing vaccine availability. Towards this goal, we established a clarification train for influenza VLPs that can replace traditional techniques, such as centrifugation. This was accomplished through the use of a rational approach for each clarification stage. Because of the characteristics and properties of the cell culture process used in VLP vaccine production, a preferred clarification step should be able to cope with upstream variability and diversity (annual vaccine update using different strains and pandemics), high DNA and protein content and, if possible, remove baculovirus [61]. To select a suitable clarification train, several influenza strains, mono and multivalent VLP, at different scales were evaluated.

6.4 Materials and Methods

6.4.1 Influenza VLP production

Influenza VLPs evaluated in the screening experiments were produced as described by Carvalho et al [55] or by Sequeira et al [53] in a disposable stirred-tank bioreactor Mobius 3L (Cat# CR0003L200, EMD Millipore, Billerica, MA) (Figure 6.1). Cells were cultured at 27 °C, pO2 was maintained above 30% adding O2 in the gas mixture at an aeration rate of 20 mL min^{-1} (0.01 vvm and agitation of 170 rpm). For 10 L scale up experiments a disposable 10 L Wave bioreactor (GE Healthcare, Uppsala, Sweden) was used. The pO2 was set to 30% of air saturation and controlled by varying the agitation rate and sequentially the percentage of N2 and O2 in the gas mixture. The gas flow rate was set to 0.03 vvm. Cell concentration and viability were determined by using haemocytometer cell counts (Brandt, Wertheinmain, Germany) and trypan blue exclusion dye method (Merck, Darmstadt, Germany). High Five (Hi5) cells were

infected with recombinant baculovirus (kindly provided by Redbiotec AG) encoding different mono and pentavalent strains from subtype H1, H3, and B with M1 core protein. Infection was performed at a cell concentration at infection (CCI) of 1×10^6 or 2×10^6 cells mL^{-1}, with a multiplicity of infection (MOI) of 0.01 or 1 IP $cell^{-1}$, respectively. Addition of antiproteases was performed 12 hours before harvest (cOmplete, EDTA-free protease inhibitor cocktail tables, Cat #05056489001, Roche Diagnostics, IN, USA).

6.4.2 Harvest and DNA digestion

Hi5 infected cells were harvested at a viability of 50-60%, corresponding to approximately 72 hours post infection (hpi) (CCI = 1×10^6) or 48 hpi (CCI = 2×10^6). Depending on the case, Benzonase (101654, Merck Millipore, Germany) was added to the bulk at a final concentration of 50 U mL^{-1}, either 12 hours before harvest, 38 hours before harvest or 15-30 min at room temperature (RT) (22 °C) after harvest.

6.4.3 Clarification

The primary clarification of VLP-containing bulk was carried out by dead-end filtration or tangential flow filtration using the devices described in Table 6.1.

Table 6.1: Specifications of the clarification devices used in the screening experiments. NFF: Normal Flow Filtration; TFF: Tangential Flow Filtration; CL: cellulose; PP: polypropylene; PVDF: polyvinylidene Fluoride; BGF: borosilicate glass fiber; MCE: mixed cellulose esters; PES: hydrophilic polyethersulfone.

	Device		Target Step	Chemistry	Manufacturer recommendations	Screening surface area (cm^2)	Nominal pore size (μm)
1.1	Millistak+ D0HC	NFF	Primary clarification	CL fibers with inorganic filter aid	Primary clarification directly out of the bioreactor	23	10 - 0.55
1.2	Millistak+ CE30	NFF		CL	Clarification of serum, plasma, vaccines, cell culture or other fluids	23	6 - 3
1.3	Polygard CN 5.0 μm	NFF		PP	Liquid and gas filtration applications, for fining operations and bioburden reduction	17.7	5
1.4	Durapore 0.65 μm	TFF		PVDF	Harvest, washing and clarification of cell cultures, lysates and fermentation broths	50	0.65
2.1	Polysep II 1/1.2 μm	NFF	Secondary clarification	BGF and MCE	Clarification and Prefiltration	17.7	1/1.2
2.2	Millistak+ CE50	NFF		CL	Clarification of serum, plasma, vaccines, cell culture or other fluids	23	1 - 0.4
2.3	Polygard CN 0.3 μm	NFF		PP	Liquid and gas filtration applications, for fining operations and bioburden reduction	17.7	0.3
2.4	Durapore 0.45 μm	TFF		PVDF	Harvest, washing and clarification of cell cultures, lysates and fermentation broths	50	0.45
2.5	Polysep II 1/0.5 μm	NFF		BGF and MCE	Clarification and Prefiltration	17.7	1.0/0.5
2.6	Miiligard 1.2/0.5 μm	NFF		MCE	Clarification and Prefiltration	17.7	1.2/0.5
2.7	Polysep II 2/1.2 μm	NFF		BGF and MCE	Clarification and Prefiltration	17.7	2/1.2
2.8	Millipore Express SHC 0.5/0.2	NFF		PES	Cell harvest (post clarification)	140	0.5/0.2

All filtration modules were previously flushed and conditioned according to manufacturer's recommendation with WFI and working buffer (50 mM HEPES, pH 7.4, and 300 mM NaCl), respectively. Both primary and secondary filters were evaluated at a constant flux. NFF filters and MF-TFF cassettes were operated at a flux and at a cross flow flux of 200 LMH, respectively and according to manufacturer's instructions. Load capacity (L m^{-2}) of primary and secondary filters in the screening experiments was evaluated until feed pressure reached a maximum of 1 bar. After selection of the primary clarification filter, clarified bulk was used as secondary clarification feed. The turbidity of the clarification samples was measured using a Turbidimeter (2100 Qis Portable HACH, Colorado, USA).

6.4.4 Nanoparticle tracking analysis

The presence and size distribution of virus-like particles and other remaining bulk particles was measured using the NanoSight NS500 (Nanosight Ltd, UK). Samples were diluted in D-PBS (14190-169, Gibco, UK) to a particle concentration between 10^8-10^9 particles mL^{-1} - the instrument's linear range. All measurements were performed at 22 °C. Sample videos were analysed with the Nanoparticle Tracking Analysis (NTA) 2.3 Analytical software - release version build 0025. Capture settings (shutter and gain) were adjusted manually for each analysis. For each sample 60-seconds videos were acquired and particles between 70 and 150 nm were considered.

6.4.5 Hemagglutination assay

Hemagglutinin protein detection and quantification was performed by hemagglutination assay. The assay was carried out according to the procedure previously described [55]. Influenza vaccine Influvac (Abbott, USA) was used as positive control.

6.4.6 Total Protein Quantification

BCA Protein Assay Kit (23225, Thermo Fisher Scientific) was used, according to the manufacturer's instructions, to quantify total protein. Bovine serum albumin was used for the calibration curve (23209, Thermo Fisher Scientific). Samples before clarification were previously diluted 8-fold to avoid interferences with the kit. After clarification, samples were diluted between 2- and 256-fold as recommended. A 96 well clear microplate (260895, Nunc) was used to perform the assay and the absorbance at 562 nm was measured on Infinite 200 PRO NanoQuant (Tecan) microplate multimode reader.

6.4.7 Total dsDNA Quantification

Total dsDNA was quantified using the Quant-iT Picogreen dsDNA assay kit (P7589, Invitrogen) according to the manufacturer's protocol. Samples before clarification were previously diluted 8-fold to avoid interferences with the kit. After clarification samples were diluted between 2- and 256-fold as recommended. A 96 well black microplate, flat transparent (3603, Corning) was used to perform the assay and the fluorescence was measured on Infinite 200 PRO NanoQuant (Tecan) microplate multimode reader.

6.4.8 Baculovirus Quantification

Baculovirus DNA was extracted and purified using the High Pure Viral Nucleic Acid Kit (Roche Diagnostics) following manufacturer's instructions. The number of genome copies was quantified by real time quantitative PCR (q-PCR) following the protocol described elsewhere [190] with some modifications. Briefly, DNA samples were diluted 1:100 in water PCR grade (03315932001, Roche Diagnostics) and diluted again 1:4 with master mix. Master mix is prepared by diluting 1:2 the Light Cycler 480 SYBR Green I Master (04707516001, Roche Diagnostics, Germany) and 0,5 μM of each primer. q-PCR reaction took place in capillaries

or in a 96-well white plate (04729692001, Roche Diagnostics) using a LightCycler 1.5 or 480 Instrument II (Roche Molecular Systems, Inc.), respectively.

6.5 Results and Discussion

6.5.1 Screening of primary and secondary filters for the clarification of Influenza VLPs

The first task in purification after bioreactor harvesting is to perform a solid/liquid separation of the product of interest from the suspended solids. In the present work, this was accomplished by a series of filters, which will play different roles. The main goal of the primary clarification step is to remove cells, cell debris, and other particulate impurities. Therefore, the optimal filter should provide efficient turbidity reduction combined with maximum load capacity and high product recovery. Figure 6.2A reports the filter load capacity (L m^{-2}) and the final turbidity (NTU) obtained for this stage. At this stage of the purification process it is difficult to evaluate the correct amount of HA due to its low concentration and the presence of several impurities that interfere with quantification. All evaluated devices resulted in complete HA recovery (within the considerable experimental error of the assay), therefore the selection criteria, was based on load capacity and turbidity. Filters 1.1 (Normal Flow Filtration) and 1.4 (Tangential Flow Filtration) presented the lowest turbidity values (20 and 26 NTU, respectively) with an associated load of 150 and 170 L m^{-2}, thus being suitable for the primary clarification step. It is noteworthy that the capacity comparison for NFF and TFF filters should not be done in a straightforward manner. Although TFF will enable higher throughput and can be reused, its operation is more complex, requiring the use of different skids. As reported in Table 6.1, Filter 1.1 is designed for primary clarification, directly out of the bioreactor. The main differences between Filter 1.1 and 1.2 and 1.3 are the materials of construction of the filter media, the num-

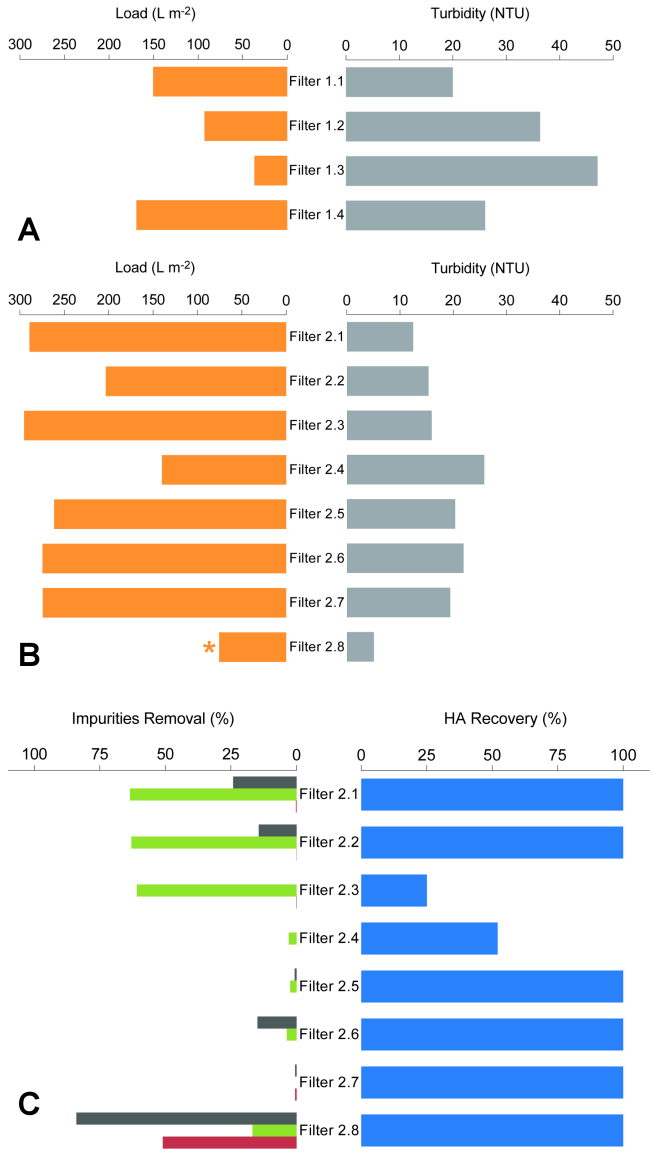

Figure 6.2: Performance screening of clarification filters. The specifications of each filter device are described on Table 6.1. (A) Load (L m^{-2}) (orange bars) and turbidity (NTU) (grey bars) values for primary clarification filters; (B) Load (L m^{-2}) (orange bars) and turbidity (NTU) (grey bars) values for secondary clarification filters. *The reported load does not correspond to the maximum capacity of the filter; (C) Product (HA) recovery (%) (blue bars) and impurity removal (%) after secondary clarification. Red bars refer to baculovirus removal, green bars refer to total protein removal and grey bars to DNA removal.

ber of layers, and the range of pore sizes. Filter 1.1 is a multilayer depth filter that incorporates an open, cellulose-based, first filtration layer followed by a tighter, diatomaceous-earth containing, second filtration layer. The combination of the open cellulose-containing layer and the tighter diatomaceous-earth containing layer allows the filter to remove more turbidity while still allowing a high filter capacity. Particles to be removed during the clarification step are attracted to the filter material and are adsorbed by a combination of electrostatic and hydrophobic interactions. This adsorption is not as efficient for filter 1.2, which contains only a single layer of cellulose filter media, or for filter 1.3, which is composed of a layer of polypropylene filter media. Moreover, both filters 1.2 and 1.3 are less retentive than filter 1.1, as shown by the higher filtrate pool turbidity values for these filters in Figure 6.2A. Filter 1.4 has a pore size of 0.65 μm which is much lower than Filter 1.1, 1.2 and 1.3. Nevertheless, it also showed a good performance which is related to the mode of operation (TFF). As mentioned previously, nonspecific adsorption for a TFF filter where the fouling layer is cleaned with cross flow cannot be directly compared to dead end filtration of filters with completely different material. The evaluated NFF (Filter 1.1) and TFF microfiltration devices (Filter 1.4) proved to be successful for the clarification of influenza VLPs. The selected filter was Filter 1.1. Filter 1.4 was not selected since the operation of a TFF-based filtration system presents some disadvantages when compared to NFF-based filtration methods. TFF membrane modules are normally much more expensive and their use requires specialized pumping equipment, and an increased set-up complexity and longer processing time.

The inlet bulk material for the secondary clarification stage contains colloidal material and cellular debris that were not retained in the preceding primary clarification stage. In addition to the filter capacity and retention requirements described above, the filters used at this stage should also provide an increased impurity clearance, reducing DNA and total protein content, as well as the presence of baculovirus. The goal

of this clarification step is to obtain a final turbidity below 10 NTU, so that the clarified material can be sterile filtered [61, 67]. Moreover, the sterilizing grade filter offers a convenient process holding point. Figures 6.2B and 6.2C depict the screening results for this stage. Filters 2.1, 2.5 and 2.7 have the same membrane chemistry: borosilicate glass fiber and mixed cellulose esters (Table 6.1). These filters combine the dirt-holding capacity similar to a depth filter with a high retention efficiency of a membrane filter. HA recovery is around 100% for all three filters, suggesting that these materials do not adsorb the product of interest. However, the pore sizes of these depth filters vary, strongly impacting the profile of impurity removal (Figure 6.2C). Clearance of total protein and DNA from filters 2.5 and 2.7, when compared to filter 2.1, is negligible. Filter 2.6 contains only a layer of mixed cellulose esters and is also inefficient in terms of its final impurity profile. Filter 2.2 was also evaluated. This filter has a similar chemistry to filter 1.2 but presents a tighter pore structure. This single layer cellulose filter did not achieve the performance of filters 2.1 or 2.8 in terms of loading capacity (200 L/m2) or the final impurity profile. Filters 2.3 and 2.4 were not selected due to low HA recovery yields (25% and 50%, respectively). Filters 2.1 and 2.8 provided the best performance in terms of final turbidity (12.5 and 5 NTU, respectively), DNA removal (24% and 84%, respectively) and Baculovirus removal (0.2% and 51%, respectively), and provided a high HA recovery. Furthermore, the reported load capacity for filter 2.8 (140 cm^2, see Table 6.1) may significantly understate the maximum capacity achievable, since due to feed volume limitations, the terminal pressure of 1.0 bar was not achieved during the filtration test. Taking this into account, filters 2.1 and 2.8 were selected for an investigation of secondary clarification performance at a larger scale.

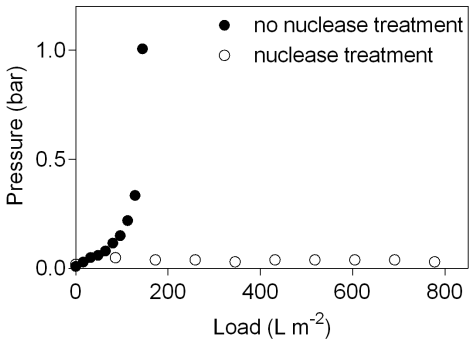

Figure 6.3: Endonuclease impact on clarification performance. Effect of benzonase treatment on Filter 1.1 load capacity (L m^{-2}). Full circles correspond to a harvested bulk clarified without benzonase incubation; empty circles correspond to harvested bulk clarified with benzonase incubation.

6.5.2 Impact of endonuclease treatment on the primary stage of clarification

The use of endonuclease is a common procedure in vaccine manufacturing [43], with a combined effect of reducing both DNA content and the viscosity of the harvested material. This strategy, however, not only increases the cost but also requires the demonstration of endonuclease removal at the end of the purification process. During bioprocess development it is important to evaluate the real need for endonuclease treatment, balancing advantages found for each individual case with inherent costs. The effect of Benzonase endonuclease addition on the load capacity was evaluated for the primary clarification filters with the best performance (1.1 and 1.4). The filter load capacity was determined at a terminal pressure of 1 bar. Without endonuclease treatment, a load capacity of 150 L m^{-2} and 170 L m^{-2} was achieved for Filter 1.1 and 1.4, respectively (Figure 6.2A and 6.3). A clear difference was observed after endonuclease addition. For depth Filter 1.1, the pressure did not reach 1 bar and was stable at low values until at least 800 L m^{-2} (Figure 6.3). Similar results were observed for the filter 1.4 (load capacity of 170 L m^{-2} without en-

donuclease treatment and at least 400 L m^{-2}, without pressure reaching 1 bar after the endonuclease treatment, data not shown). These differences in filter capacity upon endonuclease treatment may be explained by the digestion of the nucleic acids in suspension, which can reduce the viscosity of the bulk, as well as by competitive binding of nucleic acids to the filter. Critical parameters that influence Benzonase performance are: concentration, incubation temperature, incubation time, and time of addition (before or after harvest). The first two parameters were previously optimized for the studied system (see materials and methods section). The incubation time was evaluated at the following timepoints: 30 minutes after harvest, 12 hours before harvest, and 38 hours before harvest. Several experiments, with different cell viabilities at the time of harvest, were performed to evaluate the timepoints described above for filter 1.1, using only one influenza strain (Table 6.2).

Table 6.2: Impact of Benzonase endonuclease treatment on turbidity removal.

Strain	**Experiment**	**Treatment**	**Turbidity removal (%)**	**Cells viability at harvest (%)**	$\mathbf{p_{max}}$ **(bar)**
H1 Mono	1	without benzonase	97.6	62.5	1.00
	2	with benzonase incubation: for 15–30 min after harvest	97.0	67.0	0.60
	3	with benzonase incubation: starting 12 h before harvest	97.7	70.0	0.38
	4	with benzonase incubation: starting 12 h before harvest	98.9	77.2	0.30
	5	with benzonase incubation: starting 38 hours before harvest	97.6	60.6	0.13

In spite of the range of viabilities (60–77%) assessed or time of incubation, turbidity removal was above 97% for all the experiments; furthermore, pressure did not reach 1 bar for the samples treated with Benzonase. In fact, the higher the time of incubation, the lower the maximum pressure achieved for the same volume loaded, which is in accordance with the results reported in Figure 6.3. Based on these results, further clarification studies were performed with Benzonase treatment starting 12 hours before harvesting (Table 6.2). This is the point when viability starts to decrease and there is a higher amount of free DNA to digest.

6.5.3 Clarification process Scale-up

The scalability of the filters selected for each stage, filter 1.1 for primary clarification and filters 2.1 or 2.8 for secondary clarification stage was assessed (Table 6.3).

Table 6.3: Clarification scale-up data (product recovery and impurities removal) on different influenza strains, trains and working volumes. ⋆After stage I; HA: hemagglutinin protein; TP: total protein; BV: baculovirus; N/A: not available

	Clarification filters						Impurities removal after train			
Strain	Stage I	Surface area (m^2)	Stage II	Surface area (m^2)	Volume Processed (L)	HA recovery (%)	TP removal (%)	DNA removal (%)	BV removal (%)	Turbidity (NTU)
H1 Mono	D0HC	0.0023	Millipore Express SHC 0.5/0.2	0.0140	1	75	58.69	99.21	99.99	3
H1 Mono	D0HC	0.0023	Millipore Express SHC 0.5/0.2	0.0140	1	100	46.00	96.56	99.70	9
H1 Mono	D0HC	0.0023	Millipore Express SHC 0.5/0.2	0.0140	1.25	100	53.47	98.61	99.35	5
H1 Mono	D0HC	0.0023	Millipore Express SHC 0.5/0.2	0.0140	1.25	95	55.98	93.62	97.60	8
H1 Mono	D0HC	0.0023	N/A	N/A	1.29	100	30.95	93.36	N/A	40⋆
H3_1 Mono	D0HC	0.027	Millipore Express SHC 0.5/0.2	0.048	2.5	100	55.10	92.99	92.28	9
H3 Penta	D0HC	0.054	Polysep II 1/1.2 μm	0.06	10	100	59.30	97.89	98.18	16
H1 Mono	D0HC	0.054	Polysep II 1/1.2 μm	0.06	10.5	100	53.74	97.85	91.02	4
H3_2 Mono	D0HC	0.054	Polysep II 1/1.2 μm	0.06	11	100	48.77	93.12	89.51	17
H1 Penta	D0HC	0.054	Polysep II 1/1.2 μm	0.06	11	100	50.58	94.88	94.33	20

The scale-up criteria were filter throughput (L m^{-2}) at a constant Flux (200 L m^{-2} h^{-1}).

Filter train A

The stage I filter (1.1) performance was verified at an intermediate scale (approx. 1.3L) as reported in Table 6.3 with complete HA recovery and a significant total protein and DNA removal, 31% and 93.4%, respectively. Clarification scale-up studies proceeded with the train comprising filters 1.1 and 2.1 up to 10 - 11 L scale. Different VLP strains, mono and multivalent, were studied. For all of the evaluated strains, HA recovery yields were 100%, and the total protein clearance varied from 49% to 59%. The filter capacity for DNA removal was between 93% - 98% and the baculovirus reduction ranged from 89.5% to 98.2%. Despite the results on total protein clearance, DNA and baculovirus removal, turbidity values were higher than 10 NTU for most of the cases. As mentioned above, for a clarification step to be considered efficient, the filtrate turbidity should be below 10 NTU [61, 67]. An efficient clarification step should remove whole cells, cell debris as well as a large part of the soluble process impurities. Given the need to reduce turbidity, a second train, comprising filter 1.1. and 2.8, was then considered.

Filter train B

Filter 2.8 is a two-layer microporous filter with a final pore size of 0.2 μm and is often used as a sterilizing grade filter that is installed at the end of the clarification step. This filter allows for a process holding point, helps to protect further downstream processing steps and should improve turbidity reduction. Process volumes ranged from 1 L to 2.5 L and different VLP strains were also studied. HA recovery yield was 100% in most of the cases, with only two experiments having lower, but still acceptable, values (75% and 95%). Nearly the same removal was obtained for total protein (46% to 59%) and DNA (93% to 99%) as for the Train A alone. Turbidity reduction was improved with values

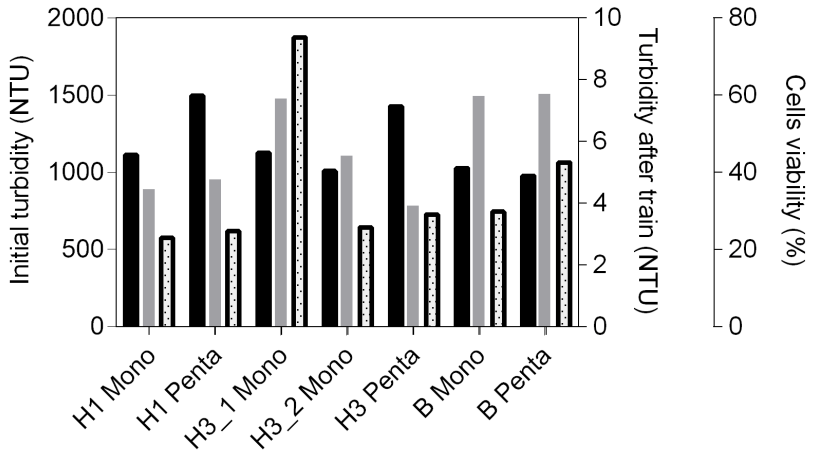

Figure 6.4: Initial turbidity and cell viability effect on after clarification turbidity. Several mono and pentavalent influenza strains, from different subtypes were evaluated. H1 Mono: H1 subtype monovalent strain; H1 Penta: H1 subtype pentavalent strain; H3_1 Mono: H3 subtype monovalent strain 1; H3_2 Mono: H3 subtype monovalent strain 2; H3 Penta: H3 subtype pentavalent strain; B Mono: B subtype monovalent strain; B Penta: B subtype pentavalent strain. Initial turbidity (NTU), at time of harvest, grey bars; Cells viability (%), at time of harvest, black bars; turbidity after clarification train (NTU), pattern bars.

below 10 NTU reported for all the experiments. Moreover, as observed for the previous clarification train, baculovirus removal was also high (from 92.3% to approximately 100%). These results confirm that filter train B, comprising filter 1.1 and 2.8 is the most suitable for a successful clarification of the studied influenza VLPs.

6.5.4 Robustness of the clarification train for different mono and multivalent strains

The robustness of the proposed clarification train was verified across different influenza VLP strains, including mono and multivalent strains (Figure 6.4). Depending on the strain complexity, in particular for the pentavalent strains, cell viability at time of harvest and the specific productivities obtained may vary. Contrary to what was expected, there is no significant correlation between viability (measured by cell membrane permeability to trypan blue) and initial turbidity, for the eval-

uated strains. As reported in Figure 6.4, turbidity after the selected clarification train (Filter train B) was always below the 10 NTU limit, independent of the strain, cell viability and turbidity at harvest. Results suggest that this two-stage filter train, a clarification stage followed by an aseptic filtration, is "universal" in the sense that is suitable for different influenza VLPs strains, mono and multivalent, produced using the baculovirus expression vector system. Importantly, the developed filter train could be extended to the purification of vaccines, particularly using multiple influenza VLPs.

6.6 Concluding Remarks

Clarification is a critical step in the purification of biologicals, having a strong impact in product recovery yields, product consistency and process reproducibility [61]. Therefore, for a candidate vaccine, it is important to select a clarification train that ensures the highest level of product recovery and impurity removal. In this work, the main goal was to develop a robust clarification process for different influenza VLPs produced using insect cells / baculovirus expression vector system.

Scale down trials were performed for screening primary and secondary clarification filters. For primary clarification, filter load capacity and turbidity level reduction were evaluated as selection criteria. In the second stage of the process, impurity clearance in terms of total protein, DNA and baculovirus content was also assessed. Millistak+ D0HC (Filter 1.1) and Durapore 0.65 μm (Filter 1.4) were the primary clarification filters that presented the best performance. Millistak+ D0HC was selected over Durapore 0.65 μm due to the ease of implementation of NFF-based depth filtration process. The selected secondary filters were Polysep II 1/1.2 μm (Filter 2.1) and Millipore Express SHC 0.5/0.2 (Filter 2.8). Millipore Express SHC 0.5/0.2 gave an improved turbidity reduction and, having a final 0.2 μm pore size, was selected for the secondary filtration step.

The impact of endonuclease treatment before and after time of har-

vest was also evaluated. Despite the efforts to eliminate its use, the load capacity of the filter was drastically reduced without nuclease treatment. Therefore, a user would need to balance a desire for a smaller footprint (favored by a higher load capacity of the filter) and a lower process cost (not favoured by the use of endonuclease).

The selected train comprising Millistak+ D0HC and Millipore Express SHC 0.5/0.2) offers a robust approach for the clarification of different influenza VLP strains, including mono and multivalent VLP strains. The resulting clarified filtrate presents a turbidity value below 10 NTU and the test results were independent of strain, viability, and turbidity at harvest time. The recommended clarification strategy appears to be easily scalable to larger process volumes.

6.7 Acknowledgments

This work was funded by Fundação para a Ciência e Tecnologia (FCT, Portugal) PhD fellowship SFRH / BD / 52302 / 2013, MolBioS Program (S.C) and SFRH / BD / 51940 / 2012, MIT-Portugal Program). The authors acknowledge funding from the European Union (EDUFLUVAC project, FP7-HEALTH-2013-INNOVATION). The authors acknowledge RedBiotec for kindly providing the baculovirus. The authors also thank Rute Castro for all the technical support and fruitful discussions and Hugo Ferreira for the help in some analytics. António Roldão, Marcos Sousa, Ricardo Correia and Daniela Sequeira are acknowledged for the upstream production of some of the VLP strains evaluated.

The authors acknowledge John Amara and Michael Dullen for providing depth filters, including small-scale prototypes used to evaluate filter capacity.

7

Membrane-based approach for the downstream processing of influenza virus-like particles

Sofia B. Carvalho, Ricardo Silva, Mafalda G. Moleirinho, Bárbara Cunha, Ana Sofia Moreira, Alex Xenopoulos, Paula M. Alves, Manuel J. T. Carrondo, and Cristina Peixoto

Contents

7.1 Context

Having the clarification step established, we moved to the downstream process itself. At this point the goal was to purify several different VLPs for toxicology animal studies. Although the regulations are less restrictive for this type of studies, there are still guidelines that need to be followed. Hence, it was important to define a balanced process in terms of product recovery, impurities' profile and cost-efficiency. As we are dealing with different products, that we need to deliver in an endotoxin-free way, we need to consider the economic and time burdens associated with cleaning and validation steps of the process. This chapter proposes a membrane-based process, eliminating the use of chromatographic steps. The strategy described here employs a cascade of ultrafiltration and diafiltration steps, followed by a sterile filtration step. We were able to maximize the yield to nearly 80% with acceptable impurity levels, while improving process time and costs.

I was involved in the conception of the study, on production of VLPs and the chromatographic downstream process used for comparison. I was the main responsible for the ultrafiltration and diafiltration studies, analytics for quality control as well as writing of the manuscript.

This work was submitted to an international peer reviewed journal and is currently under revision.

7.2 Abstract

Currently marketed influenza vaccines are only efficient against homologous viruses, thus requiring a seasonal update based on circulating subtypes. This constant reformulation adds several challenges to manufacturing, particularly in purification due to the variation of the physicochemical properties of the vaccine product. A universal platform approach capable of handling such variation is therefore of upmost importance. In this work, a filtration-based approach is explored to purify influenza virus-like particles. Switching from an adsorptive separation method to a size-based purification allows overcoming the differences in retention observed for different influenza strains. The proposed process employs a two-stage clarification step, followed by a cascade of ultrafiltration and diafiltration steps, and a sterile filtration step. Different process parameters were assessed in terms of product recovery and impurities' removal. Membrane chemistry, pore size, operation modes, critical flux, transmembrane pressure, and permeate control strategies were evaluated. After membrane selection and parameter optimization, concentration factors and diafiltration volumes were also defined. By optimizing the filtration mode of operation, product recoveries of approximately 80% were achieved. Overall, process time was decreased by 30%, improved its scalability and reduced the costs due to the removal of chromatography and associated buffer consumptions, cleaning and its validation steps.

7.3 Introduction

Influenza epidemics remains a global public health concern, affecting annually millions of people and leading to significant economic burden. Vaccination continues to be the cornerstone for influenza prevention. However, actual vaccines present several drawbacks that need to be addressed. Apart from the annual update required to cope with virus constant mutations, there is also an increasing concern regarding world readiness for

new potential pandemic outbreaks that possibly will have severe consequences. Therefore, significant research efforts are being put in the development of a universal vaccine with an efficient broad coverage against different seasonal and pandemic influenza strains. Another concern is related with relying on egg-based vaccines. Although this platform was established decades ago and represents the current standard for influenza vaccines manufacturing, it presents several drawbacks: the need for virus adaptation or the mismatch between the produced virus and the circulating one, are examples why there is an increasing need to move to cell-based technologies.

Virus-like particles (VLPs) are considered as a promising egg-independent platform for vaccine design. By displaying native virus proteins, VLPs can stimulate a high and protective immune response presenting an effective and safer alternative compared to killed or attenuated virus, due to the lack of viral genetic material [36]. In fact, there are already VLP vaccines in the market for hepatitis B virus, hepatitis E virus and human papillomavirus [37, 38]. Influenza VLPs can be produced using the Insect Cells/Baculovirus Expression Vector system as efficiently as egg or mammalian cell-based technologies [59]. Moreover, VLPs' structural flexibility allows the display of multiple hemagglutinin (HA) and/or neuraminidase (NA) proteins in their surface from different strains. Several multivalent VLPs-based vaccines are under development or in the preclinical stage presenting protective effects against both seasonal and pandemic influenza [123, 195–197].

The evolution of vaccine production technologies from egg to cell-based culture systems, and the higher product safety demands from regulatory agencies shifted the bioprocesses' bottlenecks to downstream processing (DSP) that often accounts for the majority of the production costs. (Downstream processing of viral vectors and vaccines [52, 62, 64]. Virus classical purification procedures at laboratory scale have been exploring density differences using methods such as sucrose, caesium chloride or iodixanol gradient ultracentrifugation. However, despite the pu-

rity achieved, they present several drawbacks: they are labor intensive, time-consuming, present variability in the purity profile, low yields, high cost of goods related to equipment and maintenance and limited scalability [52, 75, 198]. Therefore, there is an emergent trend to replace these traditional methods by scalable and more efficient unit operations (Downstream processing of viral vectors and vaccines [43, 52, 199].

Continuous flow ultracentrifugation is the industry's current gold standard for influenza purification, however this technique is often associated with high investment costs. Chromatography and membrane filtration techniques are widely used for virus purification [62]. Chromatographic separation is often looked as the most versatile and powerful method for large-scale production. Recent developments in materials used for virus purification have been providing improved capacities and scalability from laboratorial to commercial scale. Nonetheless, unique characteristics of virions, including physico-chemical properties, stability and variability must be considered alongside the choice of the purification strategy for maximum efficiency. Konz and coworkers [200] reported a serotype dependence on chromatographic retention for adenovirus. A similar behavior was illustrated for several other viruses and in particular for influenza by Michen and coworkers [66], where the reported isoeletric points were found to be strain dependent. This observation implies that retention in ion exchange adsorbers will also vary with different virus strains. The development of a platform approach for influenza purification should therefore be supported by techniques that make use of properties that are common to all strains. Filtration techniques are commonly used in several steps of downstream processing of virus, namely in clarification, concentration, buffer exchange or sterile filtration. The exploitation of particle size, combined with the different modes of operation - tangential flow and normal flow, and the different membrane materials available make this technique attractive for a platform approach.

The strategy proposed in this work, and illustrated in Figure 7.1, consists in a filtration-based purification process for influenza VLPs pro-

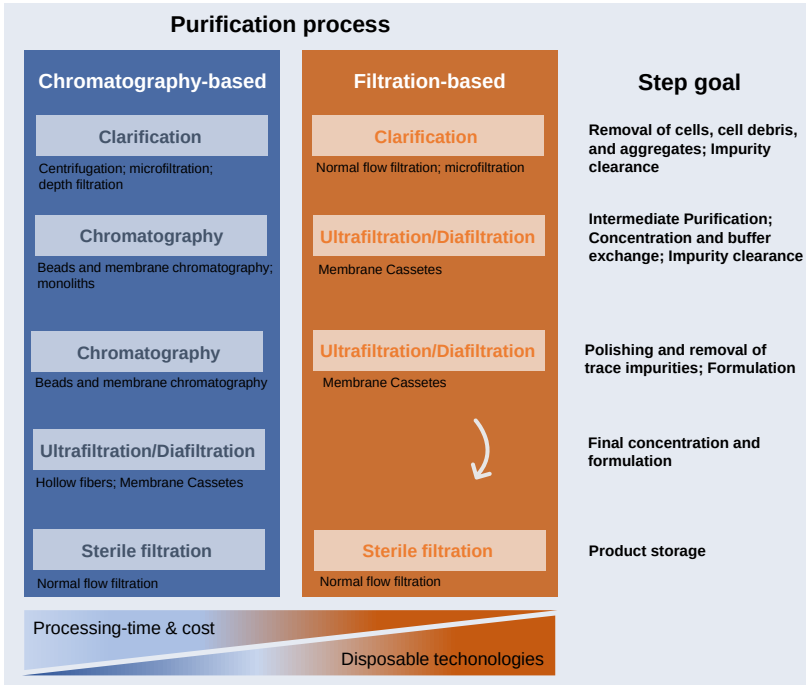

Figure 7.1: Comparison between a standard chromatographic-based DSP (left) and the proposed filtration-based DSP (right).

duced using insect cells and baculovirus expression system. Contrarily to a chromatography-based purification, in particular ion exchange, purification is carried out due to size differences between the virus particles and associated impurities. Even though it is possible to exploit this in size exclusion chromatography, its low productivity, product dilution and limited sample volume makes the use of this technique challenging for large-scale applications. Although a purification scheme, such as the one described in the left side of Figure 7.1, supported by two orthogonal chromatography steps (such as ion exchange and size exclusion) has the potential to deliver a product with a higher purity level, this has to be balanced against the final use of the product. The proposed process (Figure 7.1, right-hand side) aims to deliver product for pre-clinical studies, thus its main goal is to obtain a high product concentration, with less restrictive purity specifications. Another advantage associated with the

use of filtration devices is the availability of scalable single-use materials, contributing for a higher turnover of purification processes and reduced preparation steps.

7.4 Materials and methods

7.4.1 Production of Influenza VLPs

Influenza VLPs were produced as described by Carvalho et al [55]. Cell concentration and viability were determined using haemocytometer cell counts (Brandt, Wertheinmain, Germany) and trypan blue exclusion dye method (Merck, Darmstadt, Germany). High Five (Hi5) cells (B855-02, Invitrogen Corporation, Paisley, UK) were infected with recombinant baculovirus (kindly provided by Redbiotec AG, Switzerland) encoding a monovalent strain from subtype H1. Infection was performed at a cell concentration at infection (CCI) of 2×10^6 cells mL^{-1}, with a multiplicity of infection (MOI) of 1 IP $cell^{-1}$. Addition of antiproteases, 20 tablets per liter of cell culture (cOmplete, EDTA-free protease inhibitor cocktail tables, Cat #05056489001, Roche Diagnostics, IN, USA) and nuclease (Benzonase endonuclease, 101654, Merck Millipore, Germany), at a final concentration of 50 U mL^{-1}, was performed 12 hours before harvest.

7.4.2 Harvest and Clarification

Hi5 infected cells were harvested at a viability of 50-60%, corresponding to approximately 48 hpi. Clarification was carried out by two filters: Millistak+ D0HC (Cat #MD0HC23CL3, Merck Millipore, Germany) followed by Opticap XL 150 Capsule (Millipore Express SHC 0.5/0.2 μm, Cat #KHGES015FF3, Merck Millipore, Germany) [57]. All the filtration modules were previously conditioned with three capsule volumes of working buffer (50 mM HEPES, pH 7.4, and 300 mM NaCl). The turbidity of the clarified samples was measured using a Turbidimeter (2100 Qis Portable HACH, Colorado, USA).

7.4.3 Tangential flow filtration (TFF)

Ultrafiltration

Clarified VLPs were further processed by tangential flow filtration (TFF) and using the set-up described in Figure 7.4. The ultrafiltration screening experiments were conducted using Pellicon XL ultrafiltration modules with an area of 0.005 m^2. Different molecular weight cut off (MWCO) and membrane chemistries were evaluated (Table C.1). MWCO of 100 (Cat#: PXB100C50), 300 kDa (Cat#: PXB300C50), 500 kDa (Cat#: PXB500C50), and 1000 kDa (Cat#: PXB01MC50) were evaluated for Polyethersulfone (PES) and 300 kDa (Cat#: PXC300C50) and 1000 kDa (Cat#: PXC01MC50) for regenerated cellulose (CRC) material (Merck Millipore, USA). The membrane modules were set up according to the manufacturer's instructions. The devices were preconditioned with deionized water to eliminate trace preservatives and equilibrated with working buffer (50 mM Hepes, 300 mM NaCl, pH 7.4) before the concentration step.

Process parameters were determined by evaluating the best TMP for operation and the permeate flux decay. TMP was set from 0 to 1 bar to evaluate the permeate flux (Figure C.1). The permeate flux decay was also determined during the concentration of VLPs and the stable value was used as set point for the permeate pump (Watson Marlow Model 120S/DV 200 rpm pump, Watson-Marlow Pumps Group, Massachusetts, USA) (Figure 7.2). A Tandem 1081 Pump (Sartorius Stedim Biotech, Germany) was used on the feed side set up to a fixed flux of 480 LMH, according to the recommended flow rate. The pressure was monitored at the feed inlet, retentate outlet and permeate outlet by in-line pressure transducers (080-699PSX-5, SciLog, USA). Retentate pressure was adjusted with a valve to avoid vacuum in the permeate. The feed/retentate and the permeate volumes were monitored using a technical scale (TE4101, Sartorius Stedim Biotech, Germany).

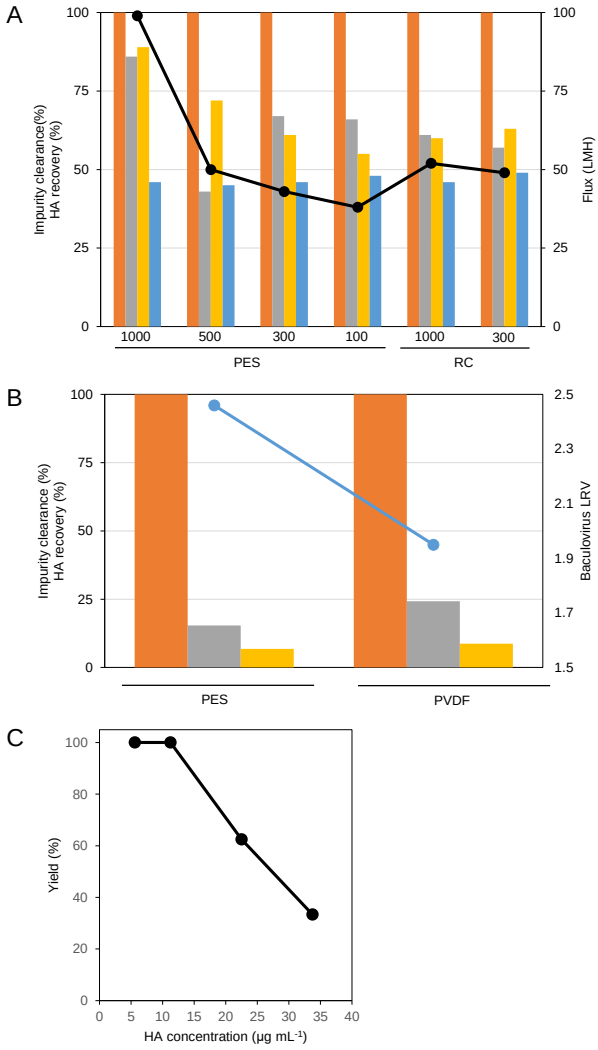

Figure 7.2: Screening experiments. Performance evaluation of different membrane cassettes with several MWCO and different chemistries (PES vs RC) (A). Permeate flux (black line), HA recovery (orange bars) and impurity clearance - DNA (gray bars), total protein (yellow bars), baculovirus (blue bars); Screening of sterile filters with different chemistries (B). HA recovery (orange bars) and impurity clearance - DNA (gray bars), total protein (yellow bars), baculovirus (blue line); Effect of product concentration on sterile filtration recovery yield (C).

Diafiltration

Diafiltration with working buffer was performed. Evaluation of the number of diafiltrations was performed for the selected ultrafiltration membrane devices, PES material with 1000 and 300 kDa. For both membranes, six diafiltration volumes were evaluated. After achieving the desired diafiltration volume, the TFF loop was completely drained and the VLPs in the retentate were recovered. Samples of the final retentate and permeate were taken to assess process yield as well as clearance of process impurities.

7.4.4 Sterile filtration

Sterile filtration screening experiments were performed using Polyethersulfone (Cat# SLGP033RS, Merck Millipore, USA) and Polyvinyl Difluoride (Cat#SLGV033RS, Merck Millipore, USA) syringe filters (Table C.2). Each filter was pre-equilibrated with working buffer prior filtration. After filtration the syringe filters were emptied with air to recover all the product.

7.4.5 Hemagglutination assay

Hemagglutinin protein detection and quantification was performed by hemagglutination assay. The assay was carried out according to the procedure previously described elsewhere [55]. Influenza vaccine Influvac (Abbott, USA) was used as positive control and as a standard for the quantification of hemagglutinin concentration.

7.4.6 Total Protein Quantification

BCA Protein Assay Kit (23225, Thermo Fisher Scientific) was used according to the manufacturer's instructions to quantify the total protein content. Bovine serum albumin was used for the calibration curve (23209, Thermo Fisher Scientific). Samples before clarification were previously

diluted 8-fold with D-PBS to avoid interferences with the kit. After clarification, samples were diluted between 2- and 256-fold, as recommended. A 96 well clear microplate (260895, Nunc) was used to perform the assay and the absorbance at 562 nm was measured on Infinite 200 PRO NanoQuant (Tecan) microplate multimode reader.

7.4.7 Total dsDNA Quantification

Total dsDNA was quantified using the Quant-iT Picogreen dsDNA assay kit (P7589, Invitrogen) according to the manufacturer's protocol. Samples before clarification were previously diluted 8-fold with D-PBS to avoid interferences with the kit. After clarification samples were diluted between 2- and 256-fold as recommended. A 96 well black microplate, flat transparent (3603, Corning) was used to perform the assay and the fluorescence was measured on Infinite 200 PRO NanoQuant (Tecan) microplate multimode reader.

7.4.8 Baculovirus Quantification

Baculovirus DNA was extracted and purified using the High Pure Viral Nucleic Acid Kit (Roche Diagnostics) following manufacturer's instructions. The number of genome copies was quantified by real time quantitative PCR (qPCR). Master mix was prepared using the Light Cycler 480 SYBR Green I Master (04707516001, Roche Diagnostics, Germany), a final concentration of 0.5 μM of each primer, for ie-1 baculovirus gene region, and PCR grade water [190]. qPCR reaction took place in 96-well white plates (04729692001, Roche Diagnostics) using a LightCycler 480 Instrument II (Roche Molecular Systems, Inc.).

7.4.9 SDS-PAGE electrophoresis

Samples' protein profiles for the diafiltration studies were analysed for both membrane devices selected through an SDS-PAGE gel. Precast SDS-PAGE gels (4-12% polyacrylamide NuPAGE (Invitrogen, USA) were

used. Loading buffer (LDS sample buffer and reducing agent (Invitrogen, USA) was added to the samples that were incubated at 95 °C for 5 min. Precision Plus Protein Dual Color Standards (Bio-Rad, USA) molecular weight markers were used. Samples were resolved for 60 min at a constant voltage (200 Volts). InstantBlue (Expedeon, San Diego, USA) was used for staining.

7.4.10 TEM analysis

TEM analysis was performed to analyse the presence, integrity and morphology of influenza VLPs across the entire purification step. Sample preparation was performed as follows: a drop (5 μL) of each sample was adhered to cooper 100 mesh grids coated with 1% (w/v) formvar (Agar Scientific) in chloroform (VWR) and carbon. The samples were washed five times with sterile filtered H2O and stained with 2% (w/v) uranyl acetate for 2 min. Grids were blotted with No. 1 Whatman filter paper and images were taken using a Hitachi H-7650 transmission electron microscope (Hitachi High-Technologies) operating at 100 keV.

7.4.11 Nanoparticle tracking analysis

Presence and size distribution of virus-like particles was measured using the NanoSight NS500 (Nanosight Ltd, UK). Samples were diluted in D-PBS (14190-169, Gibco, UK) to a particle concentration between 10^8-10^9 particles mL^{-1}, to work at the instrument's linear range. All measurements were performed at RT (22 °C). Sample videos were analysed with the Nanoparticle Tracking Analysis (NTA) 2.3 Analytical software - release version build 0025. Capture settings (shutter and gain) were adjusted manually for each analysis. For each sample 60-seconds videos were acquired and particles between 60 and 200 nm were considered.

7.5 Results and Discussion

7.5.1 Screening of ultrafiltration membrane cassettes

Ultrafiltration membrane materials of regenerated cellulose (CRC) and Polyethersulfone (PES) with different pore sizes were screened (Table C.1). An initial membrane load of approximately 10 L m^{-2} was applied to each device. This initial assessment of the devices focused on product (HA) recovery, impurity clearance (DNA, total protein, baculovirus) and permeate flux profile (Figure 7.2A). Results obtained show that no significant losses of VLPs were observed for all the assessed membranes. Although HA recovery is one undeniable factor to take in consideration for the selection of the devices, other parameters such as permeate flux and impurity clearance should also be considered.

In the chromatography-based process depicted in the left side of Figure 7.1, the intermediate purification or capture step serves a dual objective. First, due to the bind and elute operation, VLPs will be eluted at a higher concentration, and secondly due to the modulation of the ionic strength in different elution steps it is possible to deplete impurities with charges different from the VLPs. Considering the filtration process reported in the current work and described in right side of Figure 7.1, the first tangential flow filtration step should not only be able to cope with the fast processing of the clarified bulk but also be designed in such way that a similar volume reduction and impurity clearance occur, while maintaining a good product recovery yield. Moreover, at this stage the volume to process is high, thus a device with a high permeate flux should be considered in order to reduce processing time. On top of that, process time can also be reduced at the expense of increasing the membrane area. It is expected that with larger pore sizes higher permeate fluxes are achieved. This was verified in the initial material screening (Figure 7.2A). Both 1000 kDa cassettes presented the highest fluxes when compared with small pore sizes of the same material (100 – 500 kDa). However, PES showed better performance than CRC, not

only in terms of permeate flux (99 LMH vs 52 LMH) but also regarding DNA (86% vs 61%) and total protein clearance (89% vs 60%). Baculovirus' removal was similar for both materials. For the first step of ultrafiltration/diafiltration, 1000 kDa PES membrane was therefore selected. However, due to the open pore structure, increasing the volume reduction factor (data not shown) as well as the number of diafiltration volumes lead to product loss (as seen in Figure 7.3E). The goal of a second ultrafiltration/diafiltration stage was to further concentrate the product to the desired final concentration, formulate the VLP in the final buffer while refining the purity level (polishing). To identify the most suitable membrane for this step, the 500 kDa membrane (PES) and the two 300 kDa (PES and CRC) were compared (Figure 7.2A). It was observed that the permeate fluxes were similar, varying between 50 LMH (500 kDa PES), 49 LMH (300 kDa CRC) and 43 LMH (300 kDa PES). Despite the slight higher value for the permeate flux of the 500 kDa membrane, the lowest percentage of DNA removal achieved with this membrane is not satisfactory. Total protein clearance was similar for both membrane chemistries. However, the 300 kDa membrane was selected due to the highest DNA removal. It is also worth noting that during this initial screening, membranes with lower pore sizes (100 kDa) were also evaluated. Their potential to be used in the second UF/DF step (instead of 300 kDa) or as an additional step was assessed. Nevertheless, it was observed a severe permeate flux decay (approx 95%) and a loss on membrane permeability, indicating that that this pore size is too tight to concentrate these VLP suspensions.

7.5.2 Screening of sterile filters chemistries

Usually, the last step of a typical downstream process is a sterile filtration (Figure 7.1), critical to ensure sterility of the final product, and therefore patient safety. Filters with a nominal pore size of 0.22 μm and two different chemistries (PES and PVDF) were evaluated for HA recovery and for impurity removal (DNA, total protein and Baculovirus) (TableC.2,

Figure 7.2B). Both materials presented high recoveries (approximately 100%). Moreover, in terms of total protein and DNA clearance, both filters showed comparable results, with PVDF presenting slightly higher removals for DNA (15.4% vs 24.3%) and total protein (6.8% vs 8.7%). Since both filters presented a moderate baculovirus LRV (Log reduction value) equal or higher than 2 [201], the same chemistry (PES) was maintained on the process.

Figure 7.2C depicts the impact of lnfluenza VLPs' concentration on the sterile filtration process. For product (HA) concentrations lower than 11.25 μgmL^{-1}, recovery yield corresponds to 100%. However, as HA concentration increases, the recovery yield obtained for this step decreases achieving values as low as 33% for a HA concentration of 33.75 μg mL^{-1}. In fact, higher concentration leads to membrane fouling, observed by the decrease of the flux and the pressure increase during filtration. Polarization of product concentration near the membrane resulted in cake formation, which prevented VLP to pass through the filter. The effect of membrane fouling in filtration is extensively reported in the literature, in particular the critical impact protein or DNA concentration on filtration processes (ref 32 BA, Zydney2000, ALLMENDINGER 2015, Watson 2006). Based on the results obtained, and considering the target dose, an optimal load of 12.5 μg cm^{-2} was hypothesized.

7.5.3 Evaluation of process parameters and operating configurations

Device arrangement and scalability

The surface area required for purification at each stage is closely related with the volume to be processed, process time, final product concentration and purity requirements. Moreover, one should also take into consideration the surface area of the commercially available membrane devices. In order to keep the process time for increasing bioreaction volumes, the available permeation area should be increased. This can be

performed either by placing several devices in parallel or in series as depicted by Figure 7.3A and 7.3B respectively. As a proof of concept, both configurations were evaluated for the 1000 kDa membranes using two 50 cm^2 cassettes with a TMP setpoint of 0.8±0.1 bar until a volume reduction factor of 2 was achieved. The final retentate of each experiment was then collected and HA recovery was determined by hemagglutination assay. Total particle recovery for VLP size range (70-200 nm) was also evaluated by Nanoparticle tracking analysis. The parallel configuration enabled a complete VLPs recovery where only approximately 50% was recovered in the series configuration (TableC.3).

One possible explanation to the different recoveries obtained might reside in the fact that higher pressure in the feed inlet prevents the use of the entire area of the membrane, meaning that the bulk is not able to recirculate properly. This can lead to product losses in the area that is not being used. Moreover, as influenza VLPs are enveloped particles, high pressure can disrupt or destabilize them, decreasing also product recovery yield. Process time is longer for series configuration (39 min vs 18 min for parallel configuration), which can also impact on VLPs recovery as they are subjected to shear stress for longer periods.

Moreover, the pressure drop associated to the series configuration of membranes makes impractical its use since to overcome the increase on the differential pressure across the devices and to keep it within the manufacturers recommendation one must operate at lower cross flow velocities, thus reducing the permeate flux. On the contrary, a parallel configuration is easily scaled just by connecting extra devices by means of splitting the flow or by adding extra pumps to the system.

7.5.4 TMP and permeate flux control

The optimization of process parameters was developed in two stages: by evaluating different TMP values to optimize the permeate flux (Supporting Figure 1A and 1B) and by analyzing the permeate flux decay (Figure 7.3C and 7.3D). During screening experiments, a TMP excur-

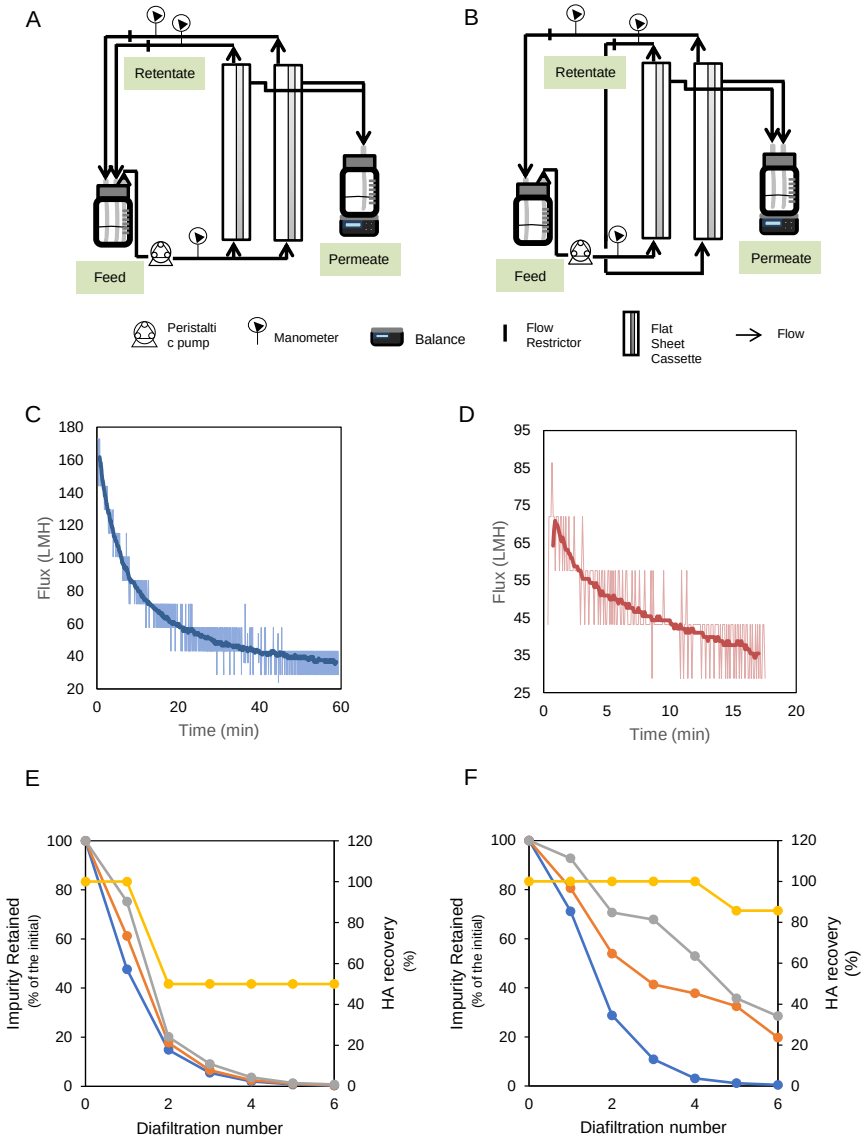

Figure 7.3: Process parameters evaluation. Configuration design, Parallel design (A) and series design (B); Permeate flux decay for PES, 1000 kDa (C), 300 kDa (D); Diafiltration studies for the 1000 kDa (E) and 300 kDa (F) membranes. HA recovery (yellow line) and percentage of impurities retained according to diafiltration number DNA (orange line), total protein (blue line), and baculovirus (gray line).

sion was carried for the 300 and 1000 kDa membranes of both PES and CRC materials (Figure C.1). Results indicate that both cassettes share the same dependence of flux on TMP for the same cutoff independently of the material. Ideally, the ultrafiltration process should be performed where the highest flux is achieved for the lowest TMP. The appropriate combination of these two parameters will minimize processing time and membrane area. On top of that, flux decay should also be considered. This is of particular importance when using ultrafiltration membranes with open pores, typically above 100 kDa, where permeability is high. The high fluxes obtained at low TMP cause a high polarization of the membranes, which might be translated in membrane fouling [202]. In order to assess the flux decay profile of each cassette, 300 and 1000 kDa (PES), an experiment was carried out with constant cross flow rate (30 mL min^{-1}) and without TMP control. The permeate flux variation was recorded and reported in Figures 7.3C and 7.3D. Both cutoffs presented an initial region where high permeate fluxes are achieved followed by a transition to a low flux region. As expected, the 1000 kDa membrane achieved higher fluxes indicative of the high permeability of the membrane. It should also be noted that the 300 kDa experiment was carried with a pre-concentrated bulk (2x) to simulate its later use in the process. In order to reduce the initial fouling of the membranes during startup, and to ensure a longer and robust operation of the UF process, permeate control at 40 LMH by means of an additional pump was introduced for both UF steps.

Diafiltration studies

The goal of a diafiltration step is usually to exchange the buffer to one that suits the next DSP step or for a formulation solution capable of promoting long-term stability to the product of interest. In addition to this, if the product is completely rejected by the membrane, as in the present case for the chosen influenza VLPs and membrane, diafiltration can also be used to permeate species smaller than the chosen cutoff.

One key point of a diafiltration operation is the definition of where it should be considered in the UF/DF process. Run a diafiltration before concentration will in principle lead to higher permeate fluxes, due to the lower protein concentration, but will have the detrimental effect of high buffer consumption and longer processing times. On the other hand, if diafiltration is considered after a concentration step, buffer savings will be evident, but lower permeate fluxes will be achieved due to higher product concentration. On top of these aspects, one most also take in consideration product stability and losses due to product aggregation and/or unspecific adsorption on the membrane. In Figure 7.3E and 7.3F, a diafiltration study was carried for the chosen 1000 kDa and 300 kDa PES membranes. From the analysis of these figures it is evident that the 1000 kDa membrane allows for a greater depletion of impurities when comparing with the 300 kDa device for the same number of diafiltration volumes. SDS-Page profile was also analyzed for retentate and permeate samples of both 300 kDa and 1000 kDa membranes confirming these results (Figure C.2). Moreover, another interesting point to observe is that in the 300 kDa membrane the impurities are depleted at different rates. Contrarily, there is not a clear differentiation of these species in the 1000 kDa membrane. This suggest that the wider pores found in this device can provide a higher increase in purity if diafiltration is considered. However, when looking at VLPs recovery, suggested by HA recovery, after the first diafiltration there is a clear drop in HA recovery, which can compromise the delivery of pure material. When looking at the same feature, HA recovery, for the 300 kDa membrane the recovery drop is less pronounced and happens only after the fifth diafiltration volume.

From the results obtained with this study and having in mind the objective of deliver enough material for pre-clinical studies and with a high process turnover, the workflow decision should be based on a holistic perspective of the DSP. Figure 7.4 depicts the current process proposal, considering only filtrations operations. The DSP starts at the clarifica-

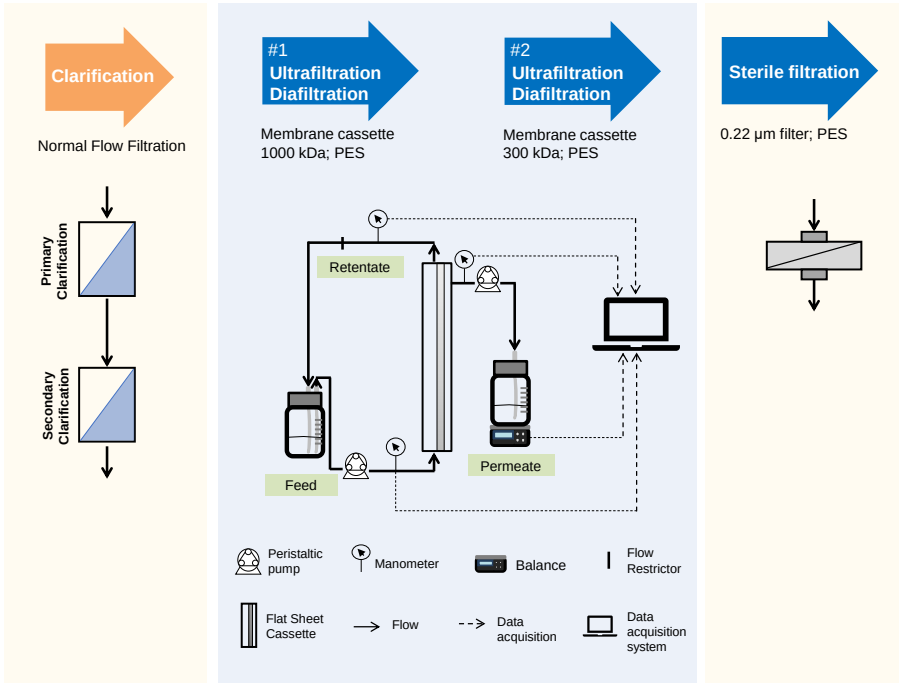

Figure 7.4: DSP for influenza VLPs using membrane-based process proposal.

tion step, where a combination of microfiltration and depth filters are used, and as previously described by our group [57]. Afterwards, two steps of UF/DF are used with different membranes cutoffs, followed by a sterilizing grade filtration. The global VRF should be able to deliver a HA concentration compatible with the dose required, while ensuring a reasonable depletion of impurities needed for pre-clinical studies.

7.5.5 Proof of concept

Influenza pre-clinical studies using mice require a dose of 1.5 μg HA and a maximum volume of injection of 100 μL [203]. Therefore, the target concentration that should be achieved is 15 μg mL^{-1}. Having this in mind, and assuming the lowest productivity obtained for this system (1 μg HA mL^{-1} bulk), VRF for both UF operations can be defined assuming the following: i) 350 mL bulk per 50 cm^2 of membrane can be processed in

a reasonable time window (considering a controlled permeate flux - 40 LMH), ii) the minimum volume that could be obtained for these devices is approximately 10 mL due to limitations of system hold-up volume, iii) global yield for this process is approx 70 – 80%. These criteria restrict the possible options of VRF combinations for both UF membranes that could be performed to achieve the target dose (Figure C.3). Having settled all the process parameters and conditions to operate, a first proof of concept run was performed. At a determined point of both UF/DF processes, permeate pressure decreased to values below zero, meaning that clogging of the membrane occurred and the permeate control using the pump cannot be maintained. Although this happened nearly the end of the operation it suggests that the operation TMP was not high enough, leading to a global HA yield of 41% (Figure 7.5A). Therefore, a second run was performed. In order to increase the TMP and since the operation was being performed at the cross-flow range recommended by the manufacturer, a restriction valve was placed on the retentate of the 300 kDa cassette since this was the step with lower recovery. It was observed an increase of 28% in the yield of this step, shifting the global yield to 64%. Given this data, a final run using restriction valves in retentates of both cassettes was performed in order to evaluate if the recovery yield could be further improved. As expected, the yield of the 1000 kDa UF/DF step increased 11% allowing a global yield of 76%. One possible explanation could be that higher recoveries with higher TMPs might be related with effective flux throughout the membrane and the set point for the permeate pump. Permeate flux is proportional to the difference between hydraulic and osmotic pressure driving forces [129]. Thus, by increasing TMP the hydraulic pressure is also increasing, leading to a higher permeate flux. Interestingly, total protein removal for all the runs (n=3) was similar (ranging from 98.4 to 98.8%). The first run (no restriction valves) presented the highest value (86.3%) for DNA removal. Adding one or two restriction valves (runs 2 and 3) showed not to impact DNA removal - 75.8% and 78.1%, respectively. These results

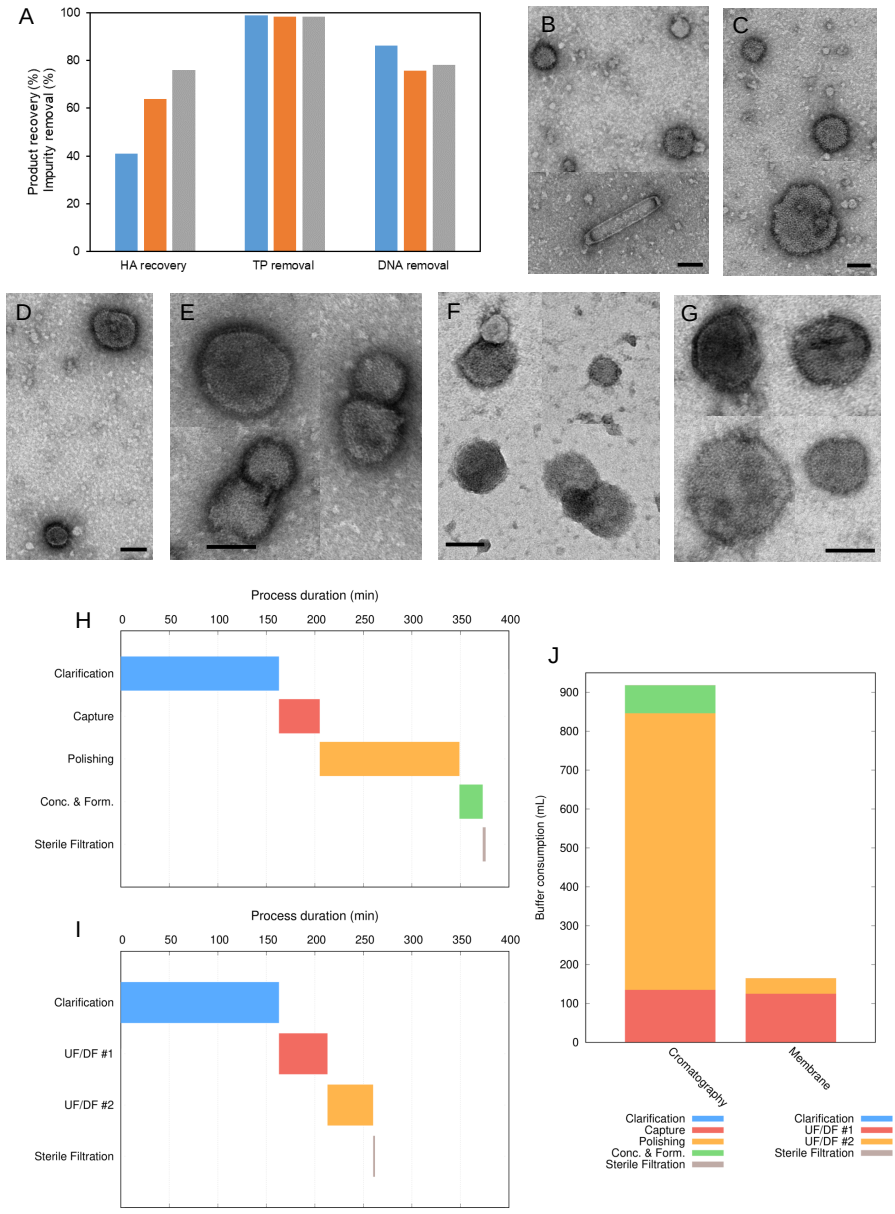

Figure 7.5: Proof of concept. Product recovery (HA), total protein and DNA removal for the three runs (A). Run 1 (blue) - Retentate flux was not restricted, Run 2 (orange) - Retentate flux 300 kDa device restricted with a valve. Run 3 (gray) - Retentate flux 1000 and 300 kDa device restricted with a valve; TEM images of the DSP steps: B - initial sample. C- 1000 kDa retentate (concentration). D - 1000 kDa (diafiltration). E - 300 kDa retentate (concentration). F - 300 kDa retentate (diafiltration). G - Sterile filtration. Scale bar corresponds to 100 nm. Gantt charts for standard chromatographic process (H) and membrane based process (I). Capture chromatography is performed with a IEX membrane. Polishing is performed with size exclusion chromatography. Concentration and formulation using Tangential flow filtration. Considered harvested volume of 0.5 L; Comparison on buffer consumption for chromatographic and membrane processes (J).

indicate that TMP value is critical for VLP recovery, allowing higher yields for highest TMP values.

TEM analysis was performed to detect VLP presence and morphology across the entire downstream process. Moreover, it was also a quality control tool for the detection of process impurities, including baculovirus. As it can be observed, VLPs maintain their shape and HA characteristic spikes across all DSP steps (Figure 7.5B - 7.5G). TEM images also revealed the heterogeneity of the particles in terms of size (ranging from 60 to 250 nm), which poses challenges for the purification process.

As previously mentioned, it is important to balance the process requirements in terms of HA recovery and impurity removal as well as process economics. The requirements for pre-clinical studies screening of efficacy are not as restricted as for human applications. Therefore, the efforts should be balanced in terms of process cost-efficiency and purity. Chromatography is often used as unit operation in DSP for vaccines. Although it can deliver product with higher purity, process time is strongly impacted. Figure 7.5H and 7.5I compare processing times for a standard chromatography-based process and the proposed membrane-based process. Globally, the chromatography process requires more steps and is time intensive (376 min vs 262 min for membrane based process). Moreover, the unit operations are more laborious, the equipment required is more expensive as well as the materials, which is not compatible with a single use process, critical to achieve high turnovers. In terms of buffer consumption, which impacts process cost, a decrease from 918 mL to 165 mL can be achieved by using the membrane process (Figure 7.5J).

7.6 Concluding Remarks

Here, a completely membrane-based DSP for influenza VLPs vaccine candidates was proposed, starting at clarification step until sterile filtration. Screening of different ultrafiltration membranes, with different chemistries (PES vs CR) and MWCO (ranging from 100 to 1000 kDa)

was performed. Membrane performance was evaluated in terms of product recovery, impurity removal and permeate flux profile. PES membranes of 1000 and 300 kDa were selected for an initial purification and polishing step, respectively. The chosen sterile filter (PES) revealed a recovery yield dependence on HA concentration, with yields decreasing abruptly for HA concentrations higher than 20 μg mL^{-1}. However, for the target dose, the filter enabled a total product recovery. Scale-up designs were also assessed using membranes in parallel and in series. The parallel strategy revealed to be the best option in terms of HA recovery and process time. Process parameters were optimized by means of TMP and permeate flux decay analysis. Permeate flux control using a pump was the best option, coupled with a restriction valve in retentates of both membranes. Moreover, the maximum number of diafiltration volumes (DFV) was defined to maximize product recovery. The 1000 kDa membrane was only able to accommodate one DFV without losing HA. In the case of the 300 kDa membrane it was possible to achieve four DFV. Importantly, analysis of the VLPs by TEM revealed that particles maintain their shape and morphology across the entire process, presenting the characteristic HA influenza spikes.

The proposed membrane-based process intends to be a scalable and robust platform for influenza VLPs expressed using insect cells - baculovirus expression system. All unit operations exploit characteristics that are strain and subtype-independent, their size and not charge, paving the way for a universal process train. Process was optimized with the ultimate goal of deliver product for pre-clinical studies, thus balancing manufacturing economics and delivery speed with product recovery and impurity clearance. In fact, when compared with a chromatographic standard process (Figure 7.1), the proposed one decreased significantly both process time and buffer consumption, using only single use materials. Nevertheless, the goal of each ultrafiltration/diafiltration unit operations can be shifted to achieve higher impurity clearance, in line with regulatory authorities' guidelines. DSP of vaccine candidates can

be sped up, which is important for annual vaccine delivery and critical for pandemics.

7.7 Acknowledgments

This work was funded by Fundação para a Ciência e Tecnologia (FCT, Portugal) PhD fellowships SFRH / BD / 52302 / 2013 MolBioS Program (S.C.), PD / BD / 114034 / 2015 MIT-Portugal Program (M.G.M.) and SFRH / BD / 51940 / 2012, MIT-Portugal Program) and Post-Doctoral fellowship SFRH / BPD / 121558 / 2016 (R.S.). The authors acknowledge funding from the European Union (EDUFLUVAC project, FP7-HEALTH-2013-INNOVATION). The authors acknowledge RedBiotec for kindly providing the baculovirus. The authors also thank João Clemente and Rute Castro for all the technical support and fruitful discussions and Hugo Ferreira for the help in some analytics. TEM data was acquired in the IGC Electron Microscopy facility. Erin M Tranfield and Ana Laura Sousa are acknowledged for analysis support, and for revising the manuscript sections where TEM is included.

8

Purification of influenza virus-like particles using sulfated cellulose membrane adsorbers

Sofia B. Carvalho[1], A. Raquel Fortuna, Michael W. Wolff, Cristina Peixoto, Paula M. Alves, Udo Reichl, and Manuel J. T. Carrondo

Contents

[1]The first authorship is shared between me and Ana Raquel Fortuna

8.1 Context

The purification step was far from being fully optimized for manufacturing of vaccines for human use as we need to cope with the acceptable impurity levels defined by the regulatory authorities. As the selection of strains narrows, it is important to further improve the process in a scalable way. To improve the process, a chromatographic capture step was established using sulfated cellulose membrane adsorbers. This strategy proved to be better than the conventional methods and worked efficiently for both VLPs and influenza virus. Therefore, it can be applied as a unit operation platform for the purification of influenza particles.

I participated actively in the design of the study and it was conceived as an internship project at Max Planck, under the scope of my PhD and funded by FCT. I performed the VLP production and together with A.R.F. did the VLP and virus purification process and also the manuscript writing.

This work was published in Journal of Chemical Technology and Biotechnology (2018,93:1988–1996. DOI: 10.1002/jctb.5474) and it is available at `https://onlinelibrary.wiley.com/doi/full/10.1002/jctb.5474`.

8.2 Abstract

Background: Vaccines based on virus-like particles (VLPs) are an alternative to inactivated viral vaccines that combine good safety profiles with strong immunogenicity. In order to be economically competitive, efficient manufacturing is required, in particular downstream processing, which often accounts for major production costs. This study describes the optimization and establishment of a chromatography capturing technique using sulfated cellulose membrane adsorbers (SCMA) for purification of influenza VLPs.

Results: Using a design of experiments approach, the critical factors for SCMA performance were described and optimized. For optimal conditions (membrane ligand density: 15.4 μmol cm^{-2}, salt concentration of the loading buffer: 24 mM NaCl, and elution buffer: 920 mM NaCl, as well as the corresponding flow rates: 0.24 and 1.4 mL mL^{-1}), a yield of 80% in the product fraction was obtained. No loss of VLPs was detected in the flow through fraction. Removal of total protein and DNA impurities were higher than 89% and 80%, respectively.

Conclusion: Use of SCMA represents a significant improvement compared to with conventional ion exchangers membrane adsorbers. As the method proposed is easily scalable and reduces the number of steps required compared to conventional purification methods, SCMA could qualify as a generic platform for purification of VLP-based vaccines.

8.3 Introduction

Every season, influenza epidemic outbreaks raise serious health concerns and lead to substantial economic burdens [6]. In fact, seasonal epidemics are responsible for 3 to 5 million cases of severe illness and up to 500 000 deaths annually worldwide [191]. Moreover, the virus potential to cause pandemic outbreaks makes it a continuous public health threat that can result in millions of deaths [6]. Vaccination remains the most effective and economical way to prevent and control infection for both seasonal and pandemic strains. However, due to antigenic drift and shift, seasonal vaccines need to be annually reviewed. Another concern relates to the poor efficacy of seasonal vaccines in case of pandemics [39]. The need to increase manufacturing capacity and flexibility, as well as decrease vaccine's time to deliver, critical specially in case of pandemics, has supported cell-based vaccine production, in alternative to conventional egg-based systems [14, 92].

New vaccines produced using mammalian and insect cell lines that have been recently licensed [14] and several platforms, including virus-like particles (VLPs), are under development as candidates for both seasonal and pandemic Influenza virus [14, 39–43]. In fact, VLPs hold great promise as vaccine candidates and have been long established for hepatitis B and human papillomavirus vaccines [37, 38]. The potential of these platforms, together with the increasing demands on safety and quality control in vaccine manufacturing stresses the need for new downstream processing (DSP) methods for their purification [72]. Influenza VLPs are being produced using different expression systems (mammalian, plant or insect cell cultures), which implies different purification strategies [96]. Insect cell-baculovirus expression system is a promising strategy to replace traditional egg and cell-based systems. Advantages are related with short production times, high production yields and a straightforward scale-up, maintaining efficiency [53]. There are several reports describing different approaches to produce and purify influenza VLPs us-

ing insect cells. Most of the downstream strategies rely on traditional methods such as centrifugation, sucrose or iodixanol gradient ultracentrifugation [96, 204, 205]. These methods are cumbersome and not easily scalable and most of the described purification strategies are not complete processes or do not cope with the purity specifications for human application. Novavax's influenza VLP vaccine manufacturing process combines these unit operations with ion exchange chromatography, ultrafiltration or diafiltration [74]. In fact, there are several separation technologies available for DSP of biopharmaceuticals, which often include bead-based chromatography [64, 206]. However, this technique presents several drawbacks, including high pressure drop across the packed bed, slow intraparticle diffusion, high process times and difficulties in scale-up [207]. Membrane-based chromatography processes overcome some of the limitations associated with packed beds and have been increasingly applied for bioprocessing of large biomolecules, such as viruses and VLPs [206]. Mass transfer constraints are improved through fully convective transport, which is possible due to the large pore size of membranes, and direct availability of the specific ligands on the membrane surface. These factors decrease process time and, together with low void volumes, reduce process and equipment costs. Moreover, membrane adsorbers can be used as disposable units, eliminating column packing, cleaning, regeneration and validation efforts [105, 206, 207]. Several chromatographic membranes have been applied for the purification of biopharmaceuticals, including whole virus particles (WVPs) and VLPs [206]. For influenza WVPs purification, the use of traditional cation and anion exchange membranes has been tested [82, 87]. However, using only this approach, protein and DNA contamination levels exceeded acceptable limits for manufacturing of vaccines for human use. As an alternative, the use of pseudo-affinity sulfated cellulose membrane adsorbers (SCMA) has been reported for DSP of influenza A WVPs. In particular, SCMA considerably improve DNA and total protein removal, show better strain robustness and productivity [62, 87, 92, 93].

VLPs resemble native viruses by displaying the membrane proteins on their envelope [36]. The similarity between both allows to transfer processes established for DSP of WVPs to VLPs' purification. However, there are several factors that increase the complexity of VLPs' purification processes: lack of proper analytical tools, high heterogeneity and low stability compared to native viruses, and presence of baculovirus particles as process impurity. Baculovirus' rod-shape makes the discrimination between them and VLPs difficult to achieve. Moreover, VLPs and baculovirus have a similar envelope, as both bud from the cell. These increases the challenges faced in the downstream processing, as most of the baculovirus can be co-eluting with the VLPs [54, 55, 96] Accordingly, process conditions have to be optimized. In this context, the use of a design of experiments (DoE) approach allows a rational and fast screening and optimization of factors impacting yield and contamination levels. Similar approaches have been successfully applied to investigate the separation of other biopharmaceutical products, using different chromatographic matrices [64, 112–116]. For instance, Fortuna et al [95], employed a DoE strategy to investigate the influence of both matrix and process-related factors on the purification of influenza WVPs derived from mammalian cell cultures.

This work presents the establishment of a pseudo-affinity chromatography method to successfully purify influenza VLPs using SCMA. The use of SCMA resulted in a superior performance in terms of product recovery and impurity removal compared to other conventional membrane adsorbers. The approach reported is therefore a step towards establishment of a generic platform for VLP purification.

8.4 Materials and Methods

8.4.1 Membrane production, characterization and assembly

Unmodified reinforced cellulose discs with a pore size of 3-5 μm (provided by Sartorius Stedim Biotech GmbH, Germany) were sulfated according to Wolff et al [87, 93, 99] adapting the reaction time and temperature to achieve ligand densities of 7.9, 11.8, and 15.5 μmol O-SO_3^- cm^{-2}. Briefly, for 3 reactions chlorsulfonic acid (1.2 mL; Sigma Adrich, Germany) was added dropwise to pyridine (30 mL, Sigma Aldrich, Germany) on ice. Subsequently, the solution was heated to 65 °C until all precipitated compounds were completely dissolved. To obtain the different ligand densities, the respective reactions were cooled to 42 °C (7.9 μmol cm^{-2}), 45 °C (11.8 μmol cm^{-2}), 55 °C (15.5 μmol cm^{-2}), cellulose discs (diameter: 13 mm) were added to the reaction mixture and incubated for 16 h, 3 h, and 3 h, respectively. Next, the discs were washed with water and stored in 20% ethanol until further usage. For all chromatography runs and the determination of the ligand density (LD) 5 discs (total membrane area and volume of 5.65 cm^2 and 0.14 mL) were mounted in a 13 mm diameter stainless steel Swinney Filter Holder (Pall Life Sciences, Germany).

Ligand density of the studied membrane adsorbers was determined via ionic capacity (IC) measurement. IC was calculated by exchanging hydrogen ion (H^+), previously bound to the membrane, for sodium ion (Na^+). Briefly, the membrane was conditioned with 1 M HCl for 35 column volumes (CV) and then washed with ultrapure water until conductivity is below 0.05 mS cm^{-1} or for a maximum of 250 CV. H^+ is then titrated with 10 mM NaOH until conductivity reaches the maximum or for 300 CV. The IC determination was made using 100% of Na^+ breakthrough, given in terms of conductivity, as the area below the chromatogram curve and considering the void volume of the membrane

adsorber device (equation 8.1):

$$ionic\ capacity = \frac{[(V_{load} - V_{void})NaOH_{conductivity} - NaOH_{peakarea}]NaOH_{molarity}/NaOH_{conductivity}}{V_{membrane}} \tag{8.1}$$

8.4.2 Virus-like particles production and clarification

Cell culture and VLP production were performed as described by Carvalho et al [55]. Briefly, High Five Cells were cultured in Insect-EXPRESS medium (Lonza, Basel, Switzerland) and infected with recombinant baculovirus (kindly provided by Redbiotec AG) encoding for hemagglutinin subtype H1 from Influenza A/Brisbane/59/2007 and M1 protein from A/California/06/2009 virus strains. Infection was performed at a cell concentration (CCI) of 2×10^6 cells mL^{-1}, with a multiplicity of infection (MOI) of 1 IP/cell. Baculovirus titers were determined by MTT cell viability assay [158, 159]. One tablet/50 mL of cell culture of EDTA-free Protease Inhibitor Cocktail (05056489001, Roche Diagnostics, Germany) and 50 U mL^{-1} of Benzonase (101654, Merck Millipore, Germany) were added to the cell culture approximately 12 hours before harvest. Cells were harvested at a viability of 50-60%, which corresponds to approximately 48 hours post infection. Clarification was performed by sequential depth filtration using a D0HC filter (MD0HC23CL3, Merck Millipore, Germany) and a Opticap XL150 Capsule with 0.5/0.2 μm pore size (KHGES015FF3, Merck Millipore, Germany). Clarified material was aliquoted and stored at -80 °C.

8.4.3 Virus production and primary processing

Influenza virus A/PuertoRico/8/34 (H1N1) whole particles were produced in suspension MDCK.SUS2 cells cultivated in chemically defined medium (Smif8, Gibco, by contact through K. Scharfenberg, FH Oldenburg/Ostfriesland/Wilhelmshaven, Germany) [208] and pre-processed as described by Fortuna et al [95].

8.4.4 Desalting and sterile filtration

Sample preparation prior to the purification step was required for both VLPs and WVPs. Buffer exchange to phosphate buffered saline (PBS) with the required NaCl concentration for the loading buffer (more details in the chromatography section) was performed with a HiPrep 26/10 desalting column (17-5087-01, GE Healthcare LifeSciences, Uppsala, Sweden). A Minisart filter unit (0.2 μm) was used for sterile filtration (16534, Sartorius Stedim Biotech, Göttingen).

8.4.5 Experimental design

A set of experiments was generated using a 3-level optimization Rechtschaffner design supported by the software MODDE Pro 11 (Sartorius Stedim Data Analytics AB, Sweden). The factors investigated (Table 8.1) were: ligand density (LD, μmol cm^{-2}), salt concentration for loading and elution (respectively $NaCl_{load}$ and $NaCl_{elution}$, mM) and flow rate in the load and elution steps (respectively Q_{load} and $Q_{elution}$, mL min^{-1}); and the responses considered: loss in the flow through and product yield in the elution fraction (both given as relative amount of the total of HA loaded). Overall, 24 chromatographic runs were carried out, including three replicates of the center point. The data was fitted using partial least squares regression (PLS) according to a general second order polynomial equation (equation D.1) [209, 210].

Based on the results of the experimental design (Table D.1) and using MODDE's *Optimizer*, a combination of factors (set point) that minimizes HA loss during the loading step and maximizes the yield of the elution step was chosen.

8.4.6 Chromatography experiments

All chromatography experiments were carried out on an ÄKTA Pure 25 system (UNICORN 6.3 software, GE Healthcare Bio-Sciences AB, Uppsala, Sweden) and monitored inline using UV absorbance (at 280 nm

Table 8.1: Factors investigated, and respective levels, for the optimization of influenza virus-like particles (VLPs) using sulfated cellulose membrane adsorbers (SCMA).

		Level		
Factors	**Abbreviation**	**Low**	**center**	**high**
Ligand density (μmol cm^{-2})	LD	7.9	11.8	15.4
Salt concentration for load (mM)	$[NaCl]_{load}$	20	40	60
Salt concentration for elution (mM)	$[NaCl]_{elution}$	200	600	1000
Flow rate for load (mL min^{-1})	Q_{load}	0.2	0.4	0.6
Flow rate for elution (mL min^{-1})	$Q_{elution}$	0.5	1.0	1.5

wavelength) and dynamic light scattering (DLS, NICOMP 380 at 633 nm wavelength, Particle Sizing Systems, Santa Barbara, CA, USA). Briefly, the SCMA were equilibrated with loading buffer and then loaded. After a wash step with the loading buffer, the membranes were eluted in a single step with elution buffer, sanitized with 0.5 M sodium hydroxide (for 15 min) and re-equilibrated. Each set of membranes was used for a maximum of 5 times. PBS was used as basis buffer system for all chromatographic runs. The concentration of NaCl in the loading and elution buffer was adjusted according to the design matrix (Table D.1) or to the predicted set-point. The total void volume of the system (1 mL considering system and membrane device) is considerably bigger than the total membrane volume, therefore every chromatography step lasted as long as required to have a correct buffer exchange to the required buffer (minimum 4 mL). For the experiments in the design matrix, the membranes were loaded with 5 mL of the desalted and filtered VLP material. Dynamic binding capacity at 20% breakthrough ($DBC_{20\%}$) was determined with the conditions of $NaCl_{load}$, $NaCl_{elution}$, Q_{load} and $Q_{elution}$ predicted for the set point. Sample loading (10 mL) was monitored

by absorbance and light scattering signal. Additionally, the amount of hemagglutinin protein in the flow through fractions was quantified offline as described in hemagglutination assay section. The $DCB_{20\%}$ and the chosen set point were experimentally verified with technical replicates (n=3). For the set point, a loading challenge of 70% of the $DBC_{20\%}$ was used. Chromatographic purification performance with SCMA was compared to Sartobind pico S and Sartobind pico Q (both 0.08 mL bed-volume) using the operation parameters described for the set point and technical replicates (n=3). The flow rates were scaled down, keeping the residence time for the loading and elution step constant. The elution of the Sartobind Q included 3 steps with elution buffers containing 600 mM, 920 mM and 2 M NaCl. For Sartobind S only the two last steps were performed.

Finally, as positive control, the SCMA performance with influenza WVPs was evaluated (n=3) under the same set-point operation conditions, loading 4 mL.

8.4.7 Total protein quantification

To quantify the total protein present in each sample, the BCA Protein Assay Kit (23225, Thermo Fisher Scientific, USA) was used, following manufacturer's instructions. Bovine serum albumin (BSA) was used for the calibration curve (23209, Thermo Fisher Scientific, USA). Samples were diluted between 2-256-fold to avoid interferences with the method. A clear flat bottom 96-well microplate (655101, Greiner Bio-One GmbH, Germany) was utilized and the absorbance at 562 nm was measured on Infinite M200 PRO NanoQuant (Tecan, Switzerland) microplate multimode reader.

8.4.8 Total dsDNA quantification

Total dsDNA was determined according to the fluorescence method described by Opitz et al [86] and using the Quant-iT Picogreen dsDNA reagent (P7581, Molecular Probes, USA). The standard curve was pre-

pared with λ-DNA (#D1501, Promega GmbH, Germany). The assay was carried out in a black 96-well microplate, flat transparent (3915, Corning, USA) and the fluorescence ($\lambda_{\text{excitation}} = 485$ nm, $\lambda_{\text{emission}} = 535$ nm) was measured on the Infinite M200 PRO NanoQuant (Tecan, Switzerland) microplate multimode reader.

8.4.9 Hemagglutination assay

Hemagglutinin (HA) protein content was evaluated using two hemagglutination assays: a quantitative assay for VLPs and an activity assay for virus, respectively. Quantitative hemagglutination assay, for HA quantification of VLPs, was carried out based on the protocol described elsewhere [54] with some modifications. Briefly, 50 μL or 66.7 μL, depending on the dilution factor, of PBS were added in each well of a clear, V bottom 96-well microtiter plate (611V96, Sterilin, USA). For each sample, two initial dilutions were performed, 1:2 and 1:3. 50 μL or 33.3 μL were added to the first well of each line and then two-fold serial dilutions (50 μL of sample in an equal volume of PBS) were performed. The final 50 μL from the last dilution were discarded. Finally, 50 μL of 1% chicken erythrocytes (LOHMANN TIERZUCHT GmbH, Germany) were added to each well. The plate was incubated at 4 °C for at least 30 minutes without disturbance. As positive control, an internal standard purified and concentrated was used. The standard HA concentration was previously evaluated by SRID assay. The level of hemagglutination was inspected visually for all the wells and the highest dilution capable of agglutinating chicken erythrocytes was determined.

Influenza WVPs were quantified according to the method described by Kalbfuss et al [211]. Briefly, each sample was prepared in two different pre-dilutions by adding PBS to 100 μl or 70.7 μl of virus sample to achieve a final volume of 200 μl. These were then diluted in series (1:2) with PBS in a U-bottom 96-well plate (650160, Greiner Bio-One, Germany). In addition, an internal standard was included and measured at least twice. 100 μl of purified chicken erythrocytes (2×10^7 cells mL^{-1}) were

added to each well and the plates were allowed to incubate for at least 2 hours, before evaluation.

8.4.10 Transmission electron microscopy

TEM analysis was performed to analyze the presence, integrity and morphology of the VLPs before and after SCMA purification step. Sample preparation was performed as follows: a drop (5 μl) of each sample was adsorbed onto a formvar coated 150 mesh copper grid from Veco (Science Services, Germany) for 2 minutes. Then, the grid was washed 5 times with sterile filtered dH2O, soaked in 2% uranyl acetate for 2 minutes and dried in air at room temperature (22 °C). A Hitachi H-7650 120 Kv electron microscope (Hitachi High-Technologies Corporation, Japan) was used to analyze the samples.

8.5 Results and Discussion

8.5.1 Experimental design and optimization

The chromatographic purification of influenza VLPs reported in this work was optimized using a design of experiments (DoE) approach considering factors already identified as critical for the purification of influenza whole virus particles (WVPs) using sulfated cellulose membrane adsorbers (SCMA) [87, 92, 93, 95]. Taking into account the similarities between WVPs and VLPs, it is also expected these factors to be important. Table 8.1 summarizes the factors investigated: ligand density (LD), load and elution conductivity were already reported; load flow rate was assessed as it was observed that residence time is important for binding and further elution; elution flow rate has also an important role on product recovery [212, 213]. The results showed that product recovery increases with the increase of the elution flow rate. This can be explained by the improvement of mechanical removal of VLPs from the membrane. Higher flow rates force the particles to detach from their binding sites

and entrapment of these large particles into membrane pores is reduced. Although product concentration is usually taken into consideration on the experimental design, in this case it was left out of investigation. Our strategy intends to use VLPs' clarified bulks (always with low HA concentrations) as loading product for the SCMA. From our knowledge, HA concentration is similar (in the same order of magnitude) amongst different influenza VLPs, and using the insect cells/baculovirus expression system. However, this factor should be evaluated in the future if one intends to use SCMA train at a different stage of the downstream process.

The initial design considered several responses: HA recovery yield (in the product fraction), loss of HA (in the flow through fraction) and contaminant removal (DNA, total protein and baculoviruses) from the product fraction. The goal was to establish a set point with the highest HA recovery and the lowest value for all the other responses. However, as a bind-elute strategy was used, total protein and DNA presented low values in the product fraction, often below limit of detection (LOD) of the quantification methods. Moreover, to minimize baculovirus content, the set point would be pushed towards higher HA losses in the flow through and lower recovery yields. The best operation set point was then adjusted to minimize the HA loss in the flow through and maximizes the product yield, excluding the impurities content from the optimization objectives. The contour plots on Figure 8.1a-b, graphically represent the mathematical fitting of the HA loss and yield to the factors that respectively describe them (equations D.2 and D.3). The regression model was significant for both responses according to the analysis of variance (Table D.2).

In the case of the HA loss in the flow through of the loading step (Figure 8.1a), the factors related to elution ($[NaCl]_{elution}$ and $Q_{elution}$) were excluded since this is only relevant in the subsequent step. Within the range of the investigated factors, the model predicts a HA loss between 15% and 45%. Lower Q_{load}, resulting in higher residences times, allows

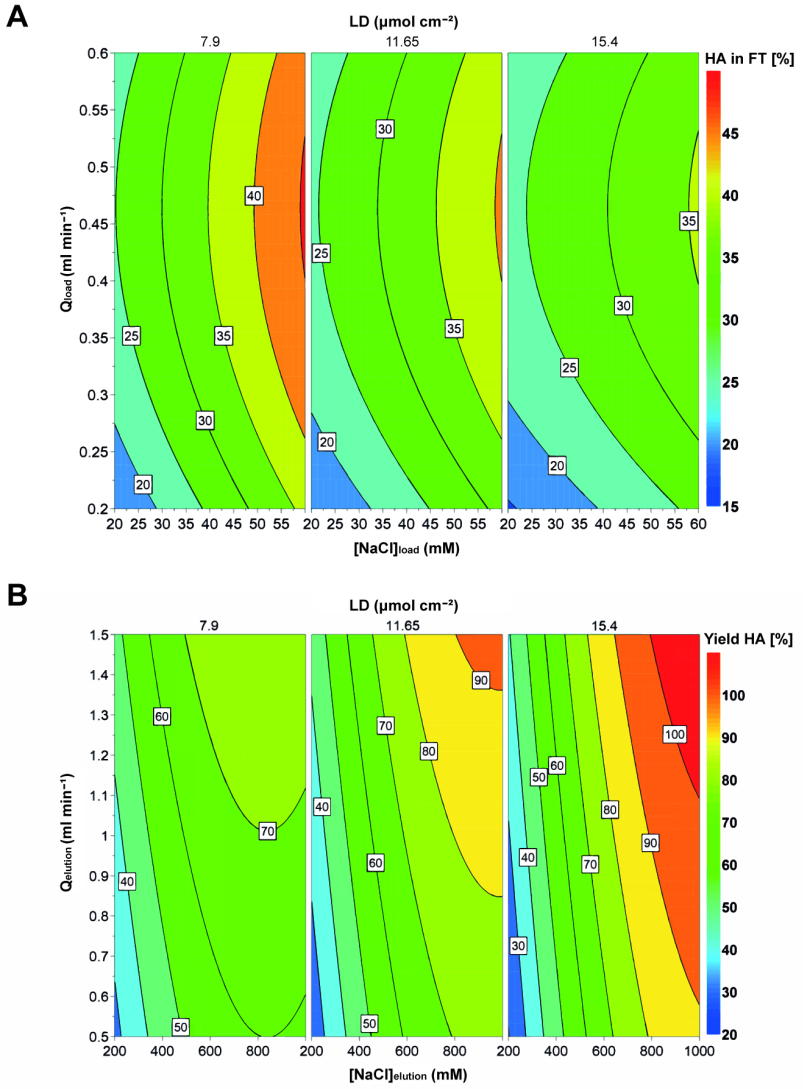

Figure 8.1: Contour plots generated with MODDE Pro 11, according to the model predicted (equations D.2 and D.3) for HA loss in the flow through (A) and yield in terms of HA (B). Membrane ligand density (LD), salt concentration for loading and elution (respectively $NaCl_{load}$ and $NaCl_{elution}$) and flow rate in the load and elution steps (respectively Q_{load} and $Q_{elution}$).

Table 8.2: Set point predicted by Monte Carlo simulation (resolution 16, 10 000 simulations per point, 95% confidence level) and experimentally implemented. The predicted values are presented as average ± standard deviation.

Factors	**Predicted**	**Experimental**
LD (μmol cm^{-2})	14.7 ± 1.2	15.4
NaCl]$_{load}$ (mM)	24 ± 16	24
NaCl]$_{elution}$ (mM)	920 ± 307	920
Q_{load} (mL min^{-1})	0.24 ± 0.15	0.24
$Q_{elution}$ (mL min^{-1})	1.4 ± 0.2	1.4

more time for the interaction between the VLPs and the chromatographic matrix to be established; while higher ligand densities increase the availability of ligands for the particles to interact with, as well as the strength of the interaction. The same trends for LD were observed by Fortuna et al [95], with influenza WVP, although they have investigated a higher range (14-25 μmol cm^{-2}). Similar to what was observed in this work, for optimal LD the salt tolerance during load is the highest and therefore the $NaCl_{elution}$ can be higher without compromising on the reduced particle losses.

Regarding the HA yield, all five factors (including linear combinations of these) describe this response. The contour plot for this response (Figure 8.1b) predicts, for a fixed Q_{load} = 0.2 mL min^{-1}, yield values from 30% up to full recovery of the HA loaded. It is possible to confirm that, as expected from the mass balances, conditions that reduce loss of HA in the flow through also benefit product yield in the elution step, i.e. higher ligand densities and lower $[NaCl]_{elution}$, in addition to a low Q_{load}. Concerning the factors directly related to the elution step, the higher range of both $[NaCl]_{elution}$ and $Q_{elution}$ results in better yield values. These conditions lead to a fast elution and concentrated fraction.

Table 8.2 summarizes the predicted set point and the conditions implemented to test the membrane performance experimentally. The only restriction to the suggested set point was in the LD, as only membranes

with a certain LD were available, the closest value was selected. The experiments were carried out with the membrane adsorbers with the highest LD (15.4 μmol cm^{-2}), which is still within the standard deviation of the predicted value.

8.5.2 Validation of the optimal set point

Using the implemented set point described in Table 8.2, SCMA dynamic binding capacity at 20% breakthrough ($DBC_{20\%}$) for the influenza VLPs was calculated. In these conditions, the $DBC_{20\%}$ was 78 $\pm$ 17 ng_{HA} mL^{-1} (n=3) with variations corresponding to the error associated with the hemagglutination assay. This value is lower than the one obtained for influenza virus (data not shown) which is expected, taking into account the differences in the strains, heterogeneity of VLPs, when compared to native virus, and also the presence of baculovirus that compete for the binding sites. Moreover, the expression system was not the same, which affects the DNA and total protein levels and, consequently, impacts DBC.

To evaluate experimental set point performance, SCMA was challenged with a load equivalent to 70% of the $DBC_{20\%}$ (0.31 μg_{HA}), the HA yield was 79.7 $\pm$ 5.8% and no losses of HA were detected in the flow through fraction. Since the loaded volume was not the same as the one used for the DoE experiments, it is not possible to directly compare the responses (HA yield and losses in the FT) with the predicted ones. However, any batch chromatography purification process, in bind and elute mode, will be carried out using a load correspondent to a reasonable challenge of the DBC, which validates the load conditions mentioned above. The representative chromatograms corresponding to these three technical replicates are represented in Figure 8.2. The UV, measured at 280 nm, and the DLS signals allow to distinguish where VLPs and baculovirus are co-eluting. In the flow through fraction UV signal is high (of the same magnitude as the elution peak), while DLS remains low. In fact, offline assays reveal that no HA is present in the flow through, so the UV signal corresponds to process impurities and

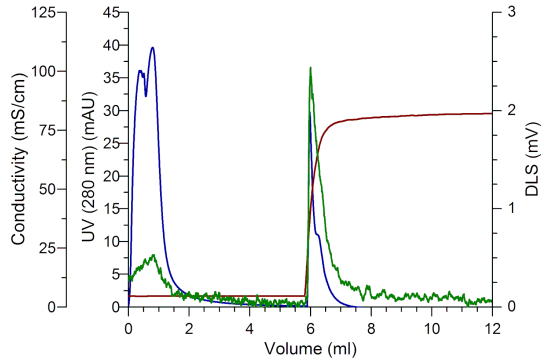

Figure 8.2: Representative chromatogram (n=3) of the purification of influenza VLPs using SCMA. Red line corresponds to conductivity, blue line to UV signal measured at 280 nm, and the green line to DLS signal.

not to influenza VLPs. UV and DLS signals are concomitant in the elution, starting to increase with the conductivity. The presence of VLPs on the elution step was confirmed not only by the higher DLS signal but also by the HA quantification. VLPs' purity was assessed by the total protein/HA and total DNA/HA ratios, before and after SCMA purification. The values for total protein were 0.39 ± 0.04 $mg_{tot.prot}$ μg_{HA}^{-1} and 0.11 ± 0.04 μg_{DNA} μg_{HA}^{-1}, before and after purification, respectively. For DNA were 0.07 ± 0.03 $mg_{tot.prot}$ μg_{HA}^{-1} and <0.02 μg_{DNA} μg_{HA}^{-1}, before and after purification, respectively. These values correspond to a total protein removal of 82.2% and a total DNA removal above 78.9% suggesting a high purity level. Moreover, to evaluate the presence, integrity and morphology of the VLPs TEM analysis was performed (Figure 8.3). Initial bulk (Figure 8.3a) and elution step of the SCMA purification process (Figure 8.3b) samples were analyzed. VLPs' morphology is maintained after the purification process; their size, although heterogeneous, and spherical shape are similar for both samples evaluated. Additionally, it is possible to observe that particles contain the ultrastructural details characteristic of influenza HA spikes [183, 184]. These results revealed that SCMA chromatography as a single unit operation does not have an impact in VLPs.

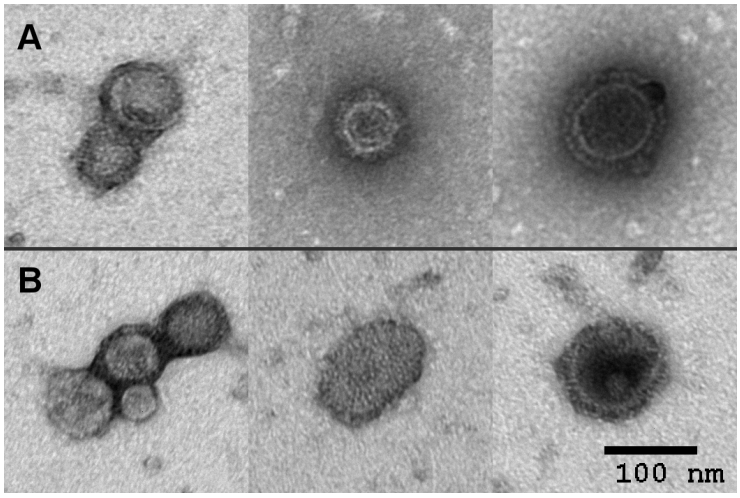

Figure 8.3: Transmission Electron Microscopy analysis of influenza VLPs from the initial bulk sample (A) and from the elution step of the SCMA purification process (B). Scale bar indicates 100 nm.

8.5.3 SCMA process performance

The potential of SCMA as chromatographic matrix for a downstream processing train for influenza VLPs was compared with the membrane adsorbers Sartobind Q and Sartobind S. HA recovery yield, losses in the flow through, DNA and total protein impurity levels were analyzed (Table 8.3).

Table 8.3: Comparison between VLPs purification with Sartobind Q and S and SCMA and between VLPs and virus purification using SCMA.

Product	**Matrix**	**HA in FT (%)**	**Yield HA (%)**	**DNA (μg_{DNA} μg_{HA}^{-1})**	**Total protein ($mg_{tot.prot}$ μg_{HA}^{-1})**
VLPs	Sartobind Q	0.0 ± 0.0 (<LOD)	47.4 ± 0.0	<LOD	0.26 ± 0.03
	Sartobind S	23.8 ± 7.8	45.9 ± 4.0	<LOD	0.18 ± 0.05
	SCMA	0.0 ± 0.0 (<LOD)	79.7 ± 5.8	<LOD	0.07 ± 0.03
Whole virus	SCMA	2.4 ± 0.1	64.0 ± 0.1	0.0038 ± 0.0003	0.013 ± 0.001

To compare these membranes, it is important to take into account several parameters: pore size, chemical properties and configuration, as well as ligand density. All membranes have similar pore sizes of >3 μm, but they present different ligand type and density. Both Sartobind membranes have a cellulose-based macro-porous structure, which is then functionalized either with quaternary ammonium ligands (Q), being a strong anion exchanger; or with sulfonic acid ligands (S), being a strong cation exchanger. SCMA have the same backbone structure and a cation exchanger character resulting from the sulfate ligands, which are directly bound to the sugar ring of the cellulose, through a covalent bond. The ligand density also distinguishes them, with SCMA presenting higher ligand densities. Since Sartobind Q and Sartobind S matrices are both ion exchangers (IEX), the mechanism of loading and elution is regulated by ionic strength. As DoE and previous reports revealed [87, 95], SCMA purification of influenza particles (virus and VLPs) requires loading with low salt containing feed streams. Also, the same conditions can promote binding to the IEX membranes. Those conditions were evaluated, avoiding unnecessary optimization efforts and material consumption. Gradient runs were performed to optimize ionic strength for elution of the IEX membranes (data not shown) . Using this information, buffer composition was determined for the performed elution steps. Interestingly, these were the same for S and Q membranes. The additional step performed for Q membrane with a higher ionic strength did not further improve virus recovery. The theoretical isoelectric point for the evaluated strain is 6.74. This value was calculated using the ExPASy ProtParam tool that assumes that all titrable aminoacid residues have the same pKa value in solution and in the protein environment. Due to product and process complexity it is very difficult to have a correct experimental value, as the overall charge of the particles can also change with the purification step. Nevertheless, considering the theoretical value, at the working pH (7.4) the VLPs have a negative charge. Therefore, as expected for the anion exchanger (Sartobind Q), like for the SCMA, no losses in the FT

were observed. HA recovery was 47.4% which is a low yield, and significantly lower (Student's two-tailed t-test for paired samples, p = 0.016) than the one obtained with SCMA (79.7%). This might indicate VLPs entrapment in the membrane, even at high conductivities. Total protein recovered in the elution fraction was more than 2.4 times higher than the level obtained with SCMA (p = 0.008). DNA value is not compared as it was below LOD. In the case of Sartobind S, HA losses in the FT were significantly bigger than zero (one sample Student's one tailed t-test, p = 0.017), around 23.8%, which can be explained by the electrostatic repulsion bet the negative charges of the virus and membrane ligands. Therefore, the recovery in the elution fraction was 45.9 %, significantly lower than SCMA (Student's two-tailed t-test for paired samples, p = 0.012). DNA level was also below LOD and the ratio total protein/HA was more than 1.7 times higher (p = 0.004). It can be discussed if changing pH will improve Sartobind S performance but these VLPs are less stable at low pH than at neutral pH. Moreover, SCMA can be used as a platform for influenza VLPs purification, applicable for several strains, which invalidates pH-dependent processes. Finally, the direct comparison of Sartobind S and SCMA also support that the interaction between the virus and the sulfate ligand in the latter case, is not solely of an electrostatic nature and rather relies on a pseudo-affinity interaction with the hemagglutinin molecules in the VLPs surface. Although both membranes have negatively charged groups, sulfated cellulose resembles Heparin, a naturally occurring glycosaminoglycan, to which several hemagglutinins are known to have affinity to [214]. The chromatography strategy presented here takes advantage of this affinity to selectively retain VLPs presenting hemagglutinin in their surface and therefore purifying them.

SCMA performance was also evaluated for influenza WVP as a positive control (Table 8.3). The recovery yield was 64% and there was around 2.4% of HA in the FT. The results were close to the ones obtained with VLPs. Differences in yield and HA losses in the FT can be

explained by different affinity for the ligand. DNA levels were measurable for virus fraction but still low (0.0038 μg_{DNA} μg_{HA}^{-1}). In the case of total protein, the value obtained for virus was 5.38 times lower than the one obtained for VLPs. The small differences can derive from the different production systems (insect vs. mammalian cells), virus strain and previous downstream treatment.

8.6 Conclusions

Herein, a downstream processing strategy using sulfated cellulose membrane adsorbers (SCMA) is reported for the first time to purify influenza VLPs.

The DoE results showed that, for an optimized process, high ligand densities, low flow rate and salt concentration for the load and high flow rate and salt concentration for elution should be used. The evaluated responses were established to define a set point with the highest HA recovery and the lowest value of HA in the FT. Using these conditions, $DBC_{20\%}$ (78 ± 17 ng_{HA} mL^{-1}) was determined and the performance of SCMA using the predicted set point was evaluated with a 70% challenge of $DBC_{20\%}$. The recovery obtained was $79.7\% \pm 5.8\%$ and no losses of HA in the FT were observed. Importantly, this system does not have an impact on the morphology of the VLPs as confirmed by TEM analysis.

SCMA were compared with conventional membrane ion exchangers, Sartobind S and Sartobind Q, and were superior not only in terms of recovery yields and losses in the FT but also concerning impurity removal. Moreover, as positive control, it was confirmed that these specific SCMA under the optimal conditions for VLPs, are also suitable for whole influenza virus particles purification.

This approach represents a step towards improvement and efficient development of purification techniques for VLPs. Moreover, this DSP unit operation is easily scalable and allows a reduced number of purification steps, overall supporting the use of SCMA as platform for purifi-

cation of influenza particles.

8.7 Acknowledgments

The authors acknowledge funding from the European Union (EDUFLUVAC project, FP7-HEALTH-2013-INNOVATION). S.C. was funded by the PhD fellowship SFRH / BD / 52302 / 2013 within the scope of the PhD program Molecular Biosciences PD / 00133 / 2012 funded by Fundação para a Ciência e Tecnologia. A.R.F. was financially supported by the Bundesministerium für Bildung und Forschung (BMBF) project grant number 0315640C. The authors acknowledge RedBiotec for kindly providing the baculovirus. The authors also thank the hospitality and openness for scientific exchange from Max-Planck Institute in Magdeburg, in particular the Bioprocess Engineering group, and the iBET, in particular the Animal Cell Technology group, which allowed the scientific stays of both PhD students.

9

Conclusions and perspectives

Virus-based vaccines have been a health care tool for more than 50 years, presenting a plethora of potential applications and a high market value [64]. For influenza virus, vaccination continues to be the most effective prophylactic strategy. However, influenza is a challenging virus to manufacture, namely due to its constant mutation. Therefore, research efforts continue to be made to develop new and more effective vaccine formats, such as VLPs, and improve current bioprocesses, both in terms of product quality attributes and process cost-effectiveness. The ultimate goal is to develop a vaccine that does not require annual updates, avoiding the constant manufacturing and annual vaccination campaigns. However, as pointed out throughout this thesis, there are still some hurdles to overcome, namely in the DSP and analytical tools. These challenges opened the path for the work developed here, aiming to establish improved analytical tools for influenza VLPs and novel purification processes. In this thesis, a novel quantification method for influenza VLPs was developed and implemented, overcoming the issues related to antibodies or fresh red blood cells requirements. Moreover, an analytical tool using a click chemistry approach enabled product monitoring throughout the bioprocess and discrimination between VLPs and baculovirus. At the DSP level, several unit operations, based on filtration and chromatographic tools, were studied and critical process parameters were optimized to maximize product recovery yield and assure the minimal presence of

impurities, consistent with the regulatory requirements. To cope with influenza virus variability challenges, research efforts were focused on process robustness and flexibility, scalability and cost-efficiency.

9.1 The EDUFLUVAC challenge

Aiming to develop a universal vaccine, EDUFLUVAC project [10] required production and purification of thirty-one different VLPs, representative of the antigenic drift within the H1, H3, and B (sub)types. Such a great diversity presented challenges for both USP and DSP. To deliver all VLP products at the target dose, the goal was to maximize productivity, recovery yield and assure the impurity clearance needed at the pre-clinical stage. Moreover, having in mind further challenge studies, the scalability of the selected process was taken into consideration. The balance of all these factors was critical, as it is not feasible to optimize USP and the DSP for each VLP, neither in terms of time, nor in terms of cost. Thus, we searched for production and purification processes that could fit all the strains. This strategy took into consideration the heterogeneity and complexity of the VLPs, requiring some flexibility during process development. Multivalent VLPs were produced using different polycistronic baculoviruses as vectors. Distinct specific productivities and vectors stability [215], as a result of influenza strains particularities, were observed. Indeed, to overcome co-infection drawbacks observed during production of one pentavalent H3 VLP, a modular strategy, combining stable and baculovirus-mediated expression was pursued [53]. As specific productivities were different, and a target dose should be achieved, parameters such as time of harvest (TOH), multiplicity of infection (MOI) or cell concentration at infection (CCI) suffered optimization during this project. Although the main focus of this thesis was on DSP development, the variability of the USP has a strong impact on VLPs' purification performance. This multitude of VLPs presenting different physicochemical properties, such as charge and viral proteins'

stability, required the adjustment of several process parameters, like pH or ionic strength. Therefore, process integration should balance USP and DSP efficiency with product quantity and quality.

9.2 An integrated DSP workflow for influenza VLPs

Manufacturing of influenza vaccine candidates is facing significant improvements, but DSP remains one of the main bottlenecks for their success. Therefore, there is an increasing interest in optimizing novel DSP strategies, to increase process efficiency, flexibility, robustness and scalability. Research efforts are also being made to speed-up the bioprocesses, enabling a faster release of vaccines, critical in the case of pandemics, and supporting worldwide demands for influenza vaccine doses [39, 40, 43, 216]. Moreover, purification processes for new vaccine formats, such as VLPs, are not yet mature, relying mostly on the processes described for virus. Additionally, implementation of proper analytical tools for product quantification and process monitoring are critical. The work reported in this thesis contributed to overcoming some of the influenza biomanufacturing limitations and can be, in the future, employed as an integrated and flexible platform for influenza VLPs, produced using IC-BEVS system.

9.3 Robust quantification tool

Current methodologies for influenza virus quantification, SRID and HA assay, present several drawbacks, namely related with the antibody or red blood cells-dependence, incapacity to analyze crude samples or for VLPs bioproduction assays [96, 130]. Chapter 4 reports a novel label-free HA quantification method, that exploits the binding capacity of the viral HA protein to sialic acid receptors present in the cells. It eliminates the use of antibodies, and their required constant updates, and

the need for fresh red blood cells, decreasing the variations associated with the user operation and host-origin. This fast tool allows the analysis of in-process samples of influenza multivalent VLPs, independently on the strain, group, and subtype. This is an advantage when considering screening experiments for pre-clinical studies, as the same tool can be applied to an entire range of products. Given its capacity to analyze in-process samples, it can also be helpful during USP optimization (Figure 9.1). This quantification method is an appealing tool for bioprocess development, being a step further in the development of a universal quantification tool.

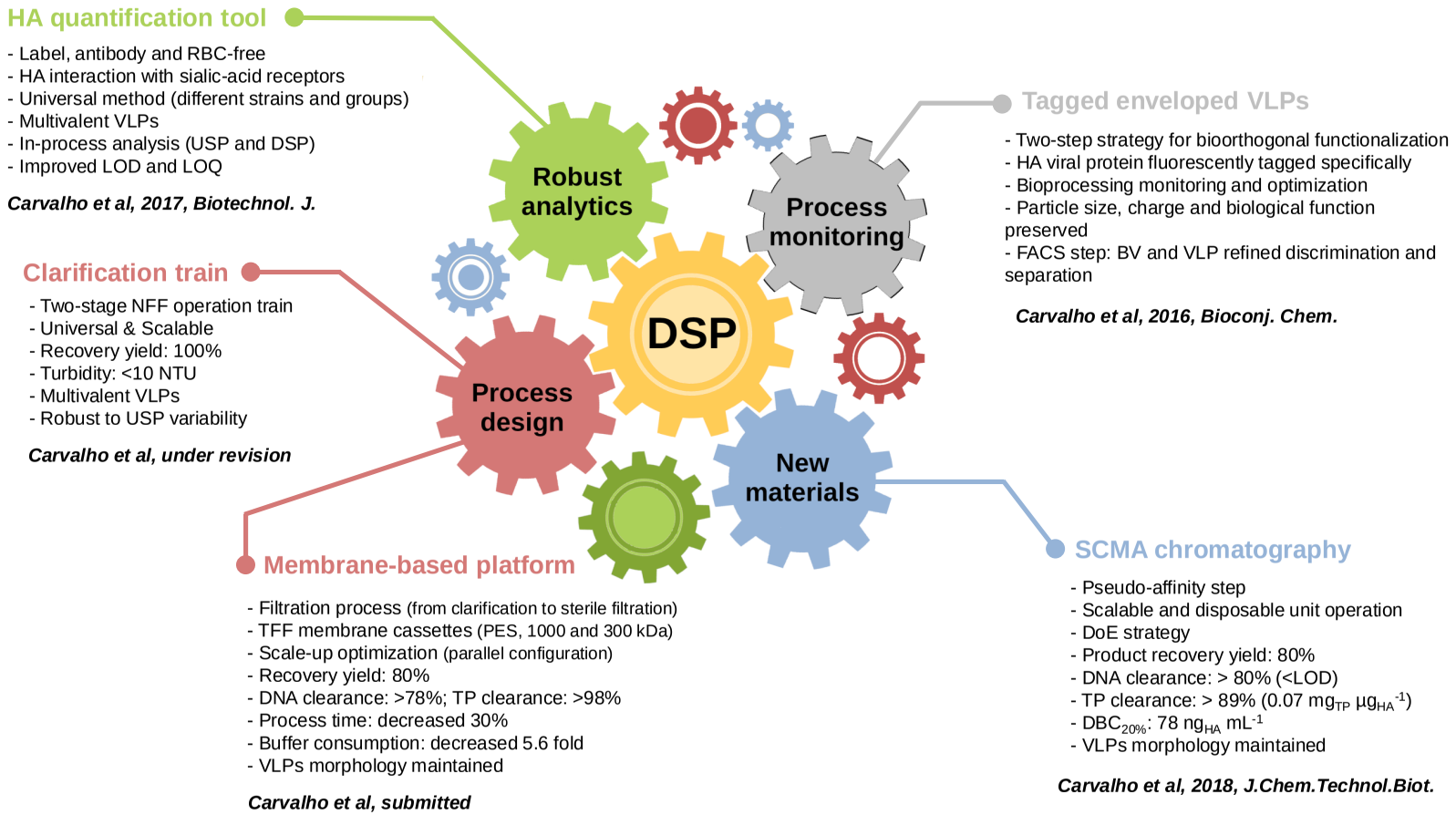

Figure 9.1: Schematic representation of the major aims of this thesis and correspondent achievements.

9.4 Establishing process monitoring tools

Monitoring is critical for process optimization, often requiring labeling of the target product to discriminate it from the remaining impurities. The ideal label does not affect product biological function, charge or size, allowing the direct comparison with the behavior of a non-labeled product. Complex systems, such as heterogeneous influenza VLPs produced here, offer an increased challenge associated with the presence of Baculoviruses, the main impurity of the process. Chapter 5 describes a straightforward two-step strategy to chemically functionalize and fluorescently label influenza VLPs, specifically, by using a click-chemistry approach. It constitutes an important support throughout the biomanufacturing process, enabling its optimization and aiding process integration, as it covers both USP and DSP. Importantly, it is not restricted to the DSP scheme reported, and labeling after particle functionalization is not reduced to fluorophores [54]. This tool coupled with a FACS step also enabled the discrimination and separation between Baculoviruses and VLPs (Figure 9.1). This strategy can be used as a powerful at-line tool for DSP monitoring and optimization leading to improved recovery yields and product purity levels. Moreover, this functionalization does not affect particle size, charge and HA biological function is preserved.

9.5 Improved downstream processing operations

When the adequate tools for process and product monitoring are implemented, the tasks of defining and optimizing a manufacturing process become easier. Nevertheless, having a process backbone already defined will speed up development. Our initial DSP strategy was based on a standard process (Figure 7.1), but as VLP complexity increased, further optimization was required. Accounting for the effects of process variability and challenges related to VLPs' variable biophysical properties, different unit operations were evaluated. The goal was to achieve a uni-

versal process, in the sense that only strain independent unit operations were applied. Moreover, a balance between product recovery, impurity clearance, processing time and costs was also considered. Starting with the clarification step, on Chapter 6, and ending with sterile filtration, a complete DSP was defined.

9.5.1 Clarification strategies

Clarification is a critical step that links USP and DSP processes, having a strong impact in product recovery yields, product consistency and process reproducibility [61]. However, it has not been well studied, representing an opportunity to improve the purification of biologicals, in particular, influenza vaccine candidates. On Chapter 6, a two-stage NFF clarification train, comprising primary and secondary filters, was selected for studied influenza VLPs. This strategy is robust to USP variability and is a scalable approach, offering a high level of product recovery and impurity clearance, presenting a final turbidity value below 10 NTU, which is desirable at this stage of the process. Importantly, it can be applied as a potential universal platform, being suitable for mono and multivalent VLPs, from different strains and groups (Figure 9.1). This clarification approach can be adapted either for screening experiments, to deliver pre-clinical material, or at a later stage, when there are only one or two selected products to develop.

9.5.2 Membrane-based process

The delivery of pre-clinical material for toxicology studies required a compromise between productivity and impurity clearance, coupled with process economics and fast turnover. Chapter 7 proposes a membrane-based DSP for influenza VLPs vaccine candidates. Selection of appropriate ultrafiltration membrane chemistries, MWCO and process operating parameters (TMP, permeate flux control, volume reduction factor, diafiltration volumes) was performed. Selection criteria were based on maximizing product recovery, critical to achieving the target dose, and

decreasing process time. Two UF/DF unit operations, using PES membrane cassettes of 1000 and 300 kDa, were optimized enabling a product yield of approximately 80%. DNA and total protein clearances were above 78% (<LOD) and >98%, respectively. All the process unit operations are scalable, single-use and strain and subtype-independent, paving the way for a universal process train for influenza VLPs. When compared with a chromatographic standard process (Figure 7.1), the proposed one decreased significantly both processing time (30%) and buffer consumption (5.6 fold), using only single-use materials (Figure 9.1). Importantly, this strategy does not impact VLPs' morphology. These unit operations can also be used for influenza viruses and for other production systems. Moreover, at clinical phases, further purification is needed to achieve impurity targets required by regulatory authorities. In these cases, TFF can also be included as a step of a wider DSP and more diafiltration volumes can be added, to improve purity.

9.5.3 Improved Chromatographic strategies

Chapter 8 offers an orthogonal chromatographic pseudo-affinity step to purify influenza VLPs and whole influenza virus particles, using sulfated cellulose membrane adsorbers (SCMA). A Design of Experiments (DoE) strategy was applied to optimize process parameters, such as ligand density, flow rate and ionic strength at load and elution steps and establish a set point with the highest HA recovery. As the selection of strains narrows, individual optimization is required to improve the process. DoE can be used to optimize the process for a selected VLP, having as a base the data reported, and achieve product and impurity specifications. A VLPs' recovery of approximately 80% was obtained with DNA and total protein clearances above 80% (<LOD) and >89%, respectively. SCMA proved to be better than the conventional chromatographic methods, are easily scalable, disposable, and can be optimized for different types of particles, supporting their potential use as a platform for purification of influenza particles vaccine candidates (Figure 9.1).

9.6 Final remarks and Future perspectives

The purification strategies developed under the scope of this thesis can provide an alternative to the conventional virus purification trains found in the literature [62, 64, 72]. Figure 9.2 depicts a possible DSP as a strategy to optimize later clinical phase processes, taking advantage of tangential flow filtration combined with an orthogonal pseudo-affinity chromatographic step. The clarification operation is compliant with upstream variability, yielding high recovery yields for the plethora of VLPs assessed, even at different scales. It is worth to note that the final pore size of the secondary clarification filter is 0.22 μm, which is ideal to store the product during a possible holding point. Depending on the clarified bulk volume, the first UF/DF step can be employed as a concentration and initial purification operation. As the chromatography proposed is a pseudo-affinity step, low flow rates are required during load, to increase residence time and enhance product capture. Therefore, a prior product concentration will impact significantly process productivity. After SCMA step, here developed as a purification stage, a new UF/DF step can be employed to further concentrate and formulate prior sterile filtration. Importantly, the developed analytical tools for product quantification and process monitoring can be applied at all stages of the process, from USP to DSP sterile filtration. Overall, the results presented in this thesis contributed to generate knowledge regarding the development of new analytical tools, for both process monitoring and product quantification, that impact undoubtedly the DSP of influenza VLPs. New processes were designed by optimizing and integrating several unit operations, including the use of new materials. Critical process parameters of filtration-based methods and chromatography were assessed. By combining membrane technology and chromatographic tools, a more efficient and robust DSP, comprised by clarification, ultrafiltration/diafiltration, pseudo-affinity chromatography, and sterile filtration unit operations, was established. Importantly, high product recovery

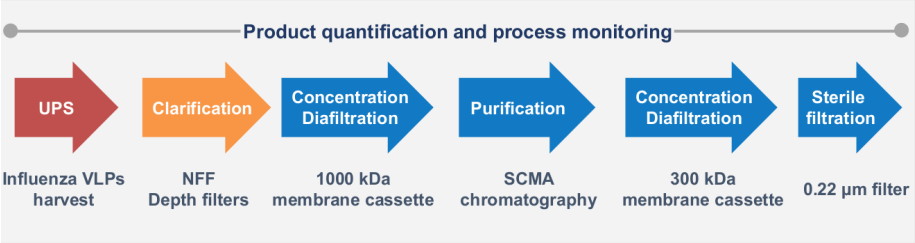

Figure 9.2: Proposed integrated process comprising the optimized unit operations: clarification, capture chromatographic (SCMA), UF/DF and sterile filtration.

was achieved, VLPs' morphology was maintained, and impurity clearance was optimized based on the stage of the clinical studies. This data can now be used as a base to develop a potential universal platform for influenza VLPs as vaccine candidates.

9.6.1 Future perspectives

There are still some hurdles to overcome and points that deserve discussion to achieve further improvements in the influenza vaccination field. The HA quantification tool (Chapter 4) lacks a proper VLP reference standard, which is true also for other methods [96, 130]. One possible solution is to use a FACS step coupled with a purification process (Chapter 5) to attain a highly pure VLP preparation, free of Baculoviruses. This will improve the specificity of the signal, by removing the contribution of the HA present on the envelope of Baculovirus. On the other hand, a gradient ultracentrifugation to purify these VLPs can also be applied [74]. However, this laborious process does not work properly for all the strains, and Baculovirus discrimination can be challenging [59]. The proper formulation should also be evaluated, to guarantee VLP stability. Research efforts are being made to develop efficient separation methods, using for instance anion exchange or hydroxyl-functionalized monoliths, that allow discrimination between baculovirus and VLPs [217, 218]. Moreover, Marek et al [219] develop a novel baculovirus-insect cell technology approach that allows the production of biopharmaceuticals with-

out contaminating baculoviruses. This strategy uses a defective baculovirus vector which lacks an essential gene for viral structure, thus disrupting virus replication. The DSP using this system is simplified, as it eliminates the need for baculoviruses removal during the purification process. Despite these achievements, that can be evaluated for influenza VLPs, the question of whether we need to remove baculoviruses from the final purified product can be raised. In fact, Baculovirus-derived VLPs are able to induce a stronger and broader immune response, when compared to VLPs derived from other expression systems, such as mammalian cells [163].

Besides Baculovirus, the presence of other extracellular vesicles on VLP preparations, such as microvesicles and exosomes, are often reported [220, 221], having a significant impact in the DSP unit operations and on product characterization. Exosome production using this insect cells and Baculovirus system is not well characterized, but these vesicles can be observed by TEM analysis, for instance. Therefore, their presence and ways to discriminate them from the product of interest should be studied in detail. This is of particular importance when dealing with this challenging system, highly heterogeneous VLPs, and Baculovirus presence. The separation of vesicles from HIV-1 gag VLPs was reported [217, 218] and can also be a starting point for influenza VLPs.

Strategies to cope with the complexity of this system and achieve better processes need to go beyond the development of robust methods for product and process monitoring. New materials and matrices should be considered for specific baculovirus and/or exosome affinity, which will greatly improve product purity. In fact, the use of affinity chromatography in influenza vaccine purification will be critical to improving yields and product purity, also enabling reduce the number of unit operations [85]. Moreover, having in mind the main goal of influenza vaccine research and manufacturing, a universal vaccine, optimization of affinity unit trains that are strain independent, targeting HA conserved regions, for instance, will be a considerable improvement on the field

[85, 222]. The design of new stationary phases is also emerging with the development of additive manufacturing ("3D printing"), which will provide a fresh perspective and opportunity to improve vaccine DSP [223]. Nevertheless, the printing technology still needs improvements regarding resolution.

To cope with global demands for seasonal vaccines and pandemic possibilities, new processes and materials should be designed taking into consideration all the new possible vaccine formats, as it is still difficult to define which one(s) will present the best efficacy and succeed as a vaccine. Furthermore, move towards single-use strategies will speed up vaccine delivery and decrease the turnover time between different products.

A

Supporting information for "Universal label-free In-process Quantification of Influenza Virus-like particles" (Chapter 4)

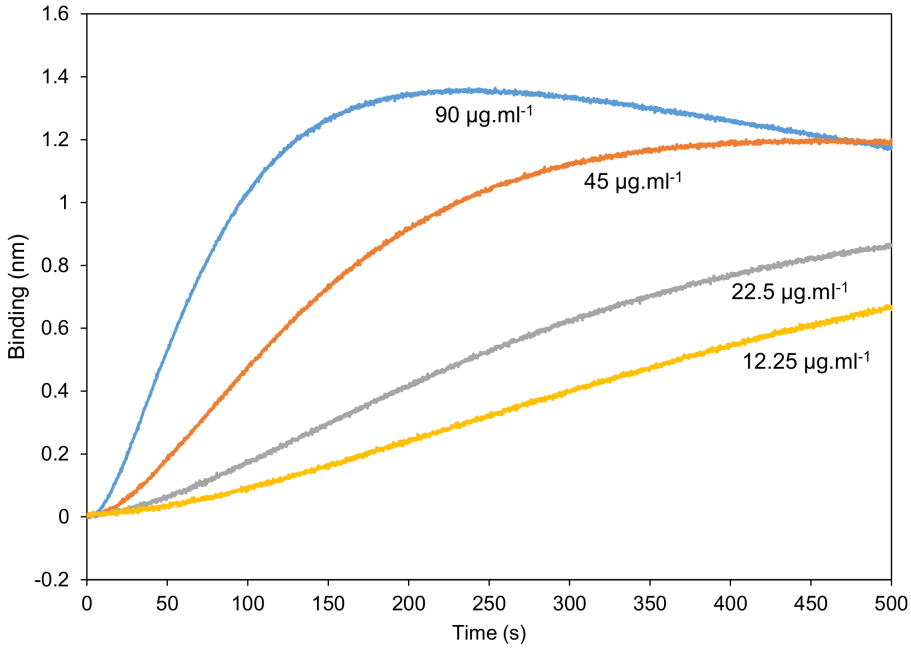

Figure A.1: Evaluation of non-specific binding for H1 VLP. Subtracted association values from VLP association to sialic acid receptors and naked biosensors, i.e, without loading of sialic acid receptors to assess non-specific binding. H1 VLP is presented as an example at different concentration values: 90 μg mL^{-1} (blue), 45 μg mL^{-1} (orange), 22.5 μg mL^{-1} (grey) and 12.25 μg mL^{-1} (yellow).

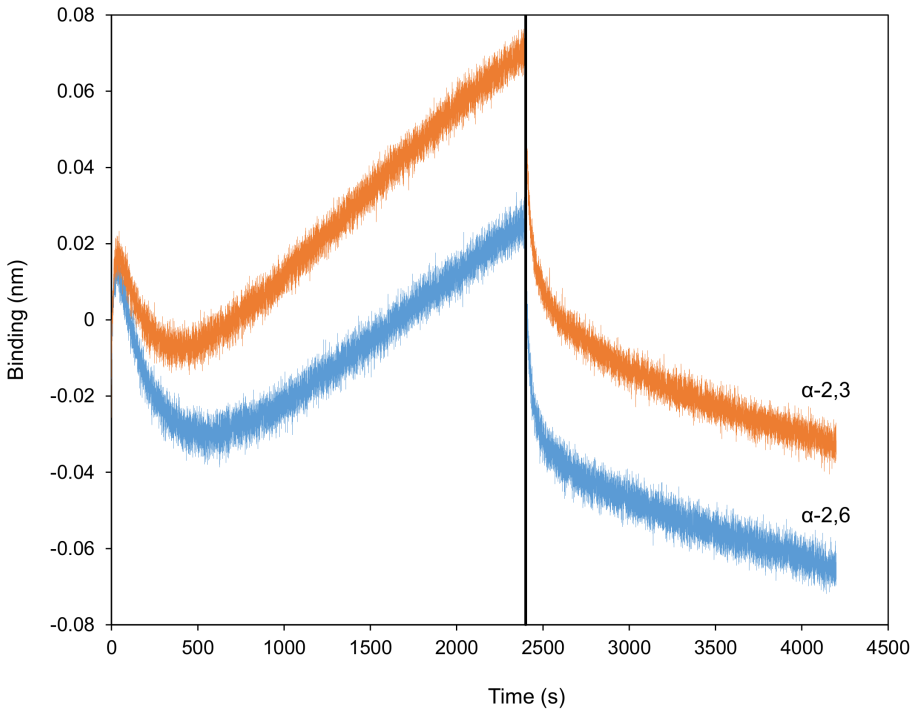

Figure A.2: rHA binding response. rHA H1N1 protein binding to sialic acid receptors α-2,3 (orange) and α-2,6 (blue). The dissociation step starts at 2400 s (black vertical line). HA protein was at a concentration of 20 μg mL^{-1}. Receptors concentration used was 0.5 μg mL^{-1}.

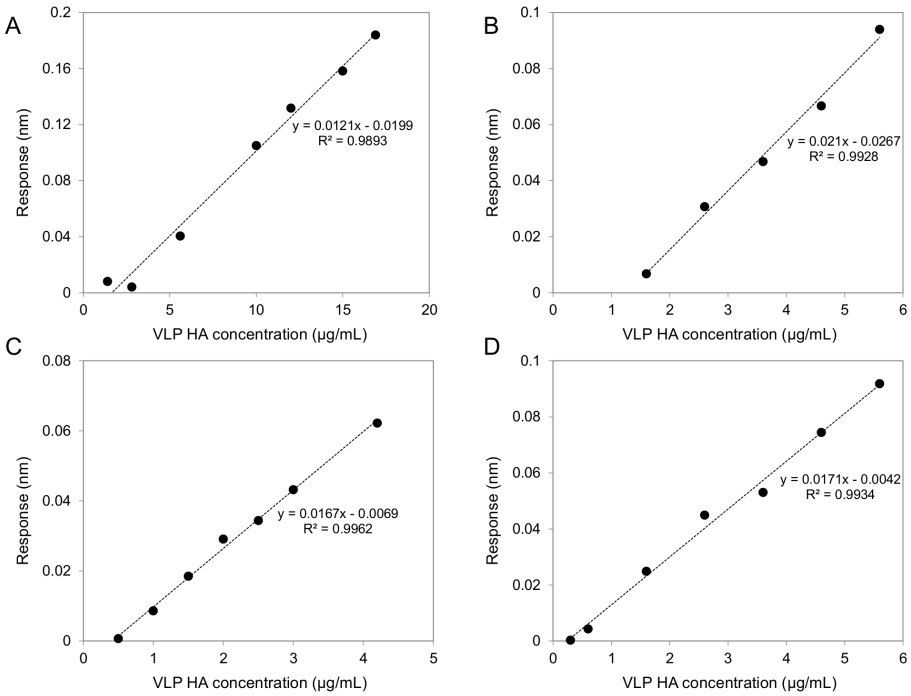

Figure A.3: Calibration curves for Influenza VLPs. Representative calibration curves of different Influenza VLP strains binding to α-2,3 and α-2,6 receptor mixture. Ultrafiltration retentate sample of H15 (A), B monovalent (B), B trivalent (C) and H3 (D) strains. The standard error of the estimation associated with the linear regression is 0.01 nm (which corresponds to $\sim$2.44 μg mL^{-1}) (A), 0.003 nm (which corresponds to $\sim$1.43 μg mL^{-1}) (B), 0.001 nm (which corresponds to $\sim$0.5 μg mL^{-1}) (C) and 0.003 nm (which corresponds to $\sim$0.43 μg mL^{-1}) (D).

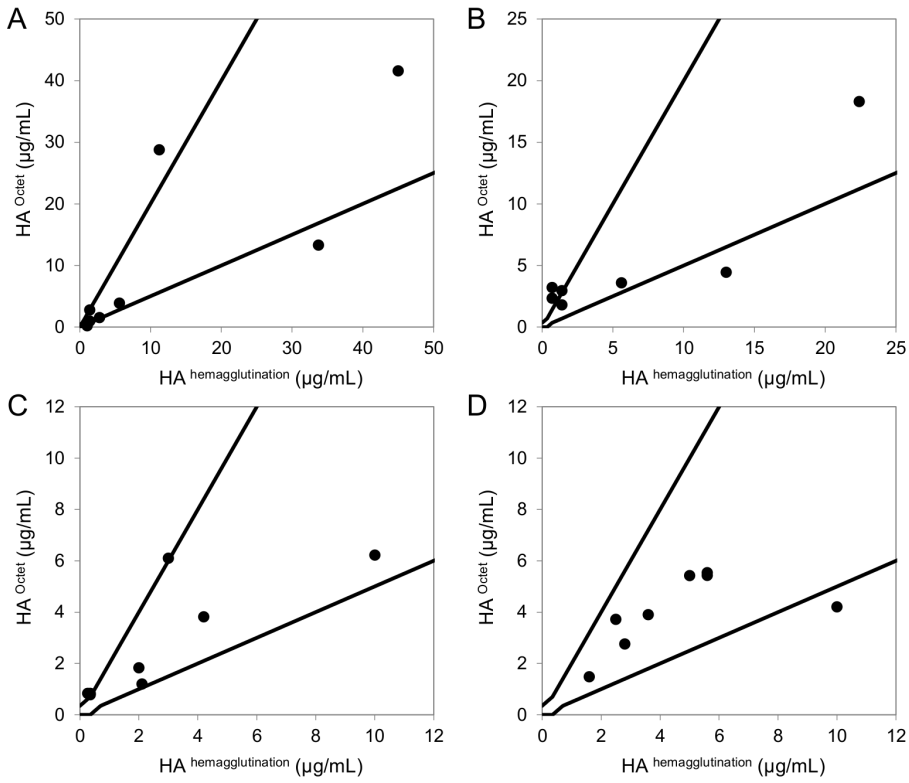

Figure A.4: Downstream process samples' quantification using BLI method. Calculated HA concentration values compared with hemagglutination assay from different Influenza strains. Black lines correspond to hemagglutination assay predictive concentration range, x axis to HA values calculated by hemagglutination and y axis to HA values calculated by octet assay. Representation for H1 (A), H15 (B), B Trivalent (C) and H3 (D) strains.

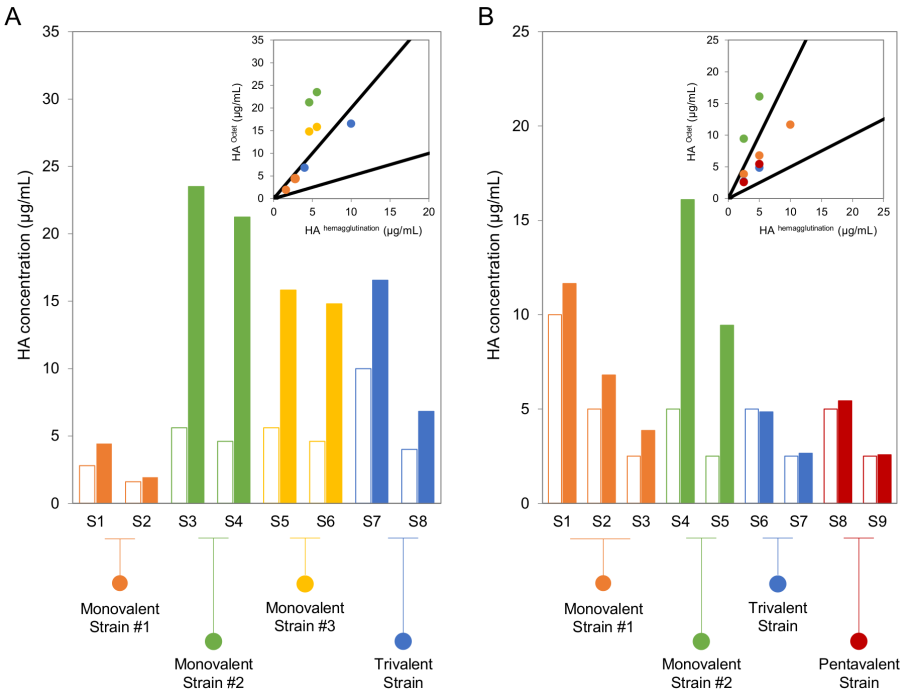

Figure A.5: Subtype and group strain specificity. HA quantification of several mono and multivalent strains from B group (A) and H3 subtype (B). UF retentate samples from one monovalent strain of each group were used as calibration. Bars without fill correspond to HA values calculated using hemagglutination assay. Bars with coloured fill correspond to HA values calculated using octet assay. For each strain, two or three different samples with different concentrations are presented. Monovalent strains #1 are coloured in orange, monovalent strains #2 in green and monovalent strain #3 in yellow. Blue corresponds to trivalent strains and red to the pentavalent one. Top right panel presents calculated HA concentration values compared with hemagglutination assay. Black lines correspond to hemagglutination assay error range, x axis to HA values calculated by hemagglutination and y axis to HA values calculated by octet assay. Monovalent strains #1 are coloured in orange, monovalent strains #2 in green and monovalent strain #3 in yellow. Blue corresponds to trivalent strains and red to the pentavalent one. Error bars are omitted for clarity (see standard errors of the estimation in Figure A.3B and A.3D).

Table A.1: LOD and LOQ for Influenza strains of different subtypes and groups.

Strain	**LOD** (μ**g mL**$^{-1}$)	**LOQ** (μ**g mL**$^{-1}$)
H1	0.43	1.30
H15	0.87	2.65
B	0.52	1.57
BTrivalent	0.61	1.85
H3	0.66	2.02

Table A.2: HA quantification by hemagglutination and Octet assay for all the samples evaluated in this study. ⋆HA concentration value obtained by the Octet was evaluated for being inside the predictive range of concentrations associated with the hemagglutination assay error.

Strain	Sample	HA^{Octet} ($\mu g\ mL^{-1}$)	$HA^{Hemagglutination}$ ($\mu g\ mL^{-1}$)	Out of Range⋆
H15	Before Harvest	3.2	0.7	Yes
	Before Clarification	2.94	1.4	Yes
	After Clarification	2.33	0.7	**No**
	UF retentate (1)	18.3	22.4	**No**
	UF retentate (2)	3.59	5.6	**No**
	UF retentate (3)	1.8	1.4	**No**
	UF retentate with trehalose	4.44	13	Yes
	Final product with trehalose	11.88	45	Yes
	Final product (1)	14.48	15	**No**
	Final product (2)	10.74	10	**No**
	Final product (3)	6.31	5	**No**
	Final product (4)	4.07	2.5	**No**
H7	Final product (1)	15.4	15	**No**
	Final product (2)	16.72	10	**No**
	Final product (3)	8.74	5	**No**
	Final product (4)	4.5	2.5	**No**

Strain	Sample	HA^{Octet} (μg mL^{-1})	$HA^{Hemagglutination}$ (μg mL^{-1})	Out of Range*
B Monovalent #1	Before Harvest	2.79	2.8	**No**
	Before Clarification	2.73	2.8	**No**
	After Clarification	2.45	1.4	**No**
	UF retentate (1)	5.21	5.6	**No**
	UF retentate (2)	2.23	3.6	**No**
	UF retentate (3)	1.6	1.6	**No**
	UF retentate with trehalose	2.05	4.3	Yes
	Final product with trehalose	3.31	2.8	**No**
	Final product (1)	4.44	2.8	**No**
	Final product (2)	1.94	1.6	**No**
B Monovalent #2	Final product (1)	23.51	5.6	Yes
	Final product (2)	21.24	4.6	Yes
B Monovalent #3	Final product (1)	15.83	5.6	Yes
	Final product (2)	14.80	4.6	Yes

Strain	Sample	HA^{Octet} (μg mL^{-1})	$HA^{Hemagglutination}$ (μg mL^{-1})	Out of Range*
B trivalent	Before Harvest	0.79	0.35	Yes
	Before Clarification	0.83	0.35	Yes
	After Clarification	0.83	0.26	Yes
	UF retentate (1)	3.81	4.2	**No**
	UF retentate (2)	1.83	2	**No**
	UF retentate with trehalose	1.19	2.1	**No**
	Final product with trehalose (1)	6.22	10	**No**
	Final product with trehalose (2)	6.10	3	Yes
	Final product (1)	16.56	10	**No**
	Final product (2)	6.82	4	**No**

Strain	Sample	HA^{Octet} (μg mL^{-1})	$HA^{Hemagglutination}$ (μg mL^{-1})	Out of Range*
H3 Monovalent #1	UF retentate (1)	5.53	5.6	**No**
	UF retentate (2)	3.89	3.6	**No**
	UF retentate (3)	1.48	1.6	**No**
	UF retentate with trehalose (1)	5.43	5.6	**No**
	UF retentate with trehalose (2)	2.76	2.8	**No**
	Final product with trehalose (1)	4.20	10	Yes
	Final product with trehalose (2)	5.42	5	**No**
	Final product with trehalose (3)	3.72	2.5	**No**
	Final product (1)	11.65	10	**No**
	Final product (2)	6.80	5	**No**
	Final product (3)	3.86	2.5	**No**
H3 Monovalent #2	Final product (1)	16.1	5	Yes
	Final product (2)	9.44	2.5	Yes

Strain	Sample	HA^{Octet} (μg mL^{-1})	$HA^{Hemagglutination}$ (μg mL^{-1})	Out of Range*
H3 Trivalent	Final product (1)	4.85	5	**No**
	Final product (2)	2.66	2.5	**No**
H3 Pentavalent	Final product (1)	5.44	5	**No**
	Final product (2)	2.58	2.5	**No**

B

Supporting information for "Bioorthogonal Strategy for Bioprocessing of Specific-site-functionalized Enveloped Influenza-virus-like Particles" (Chapter 5)

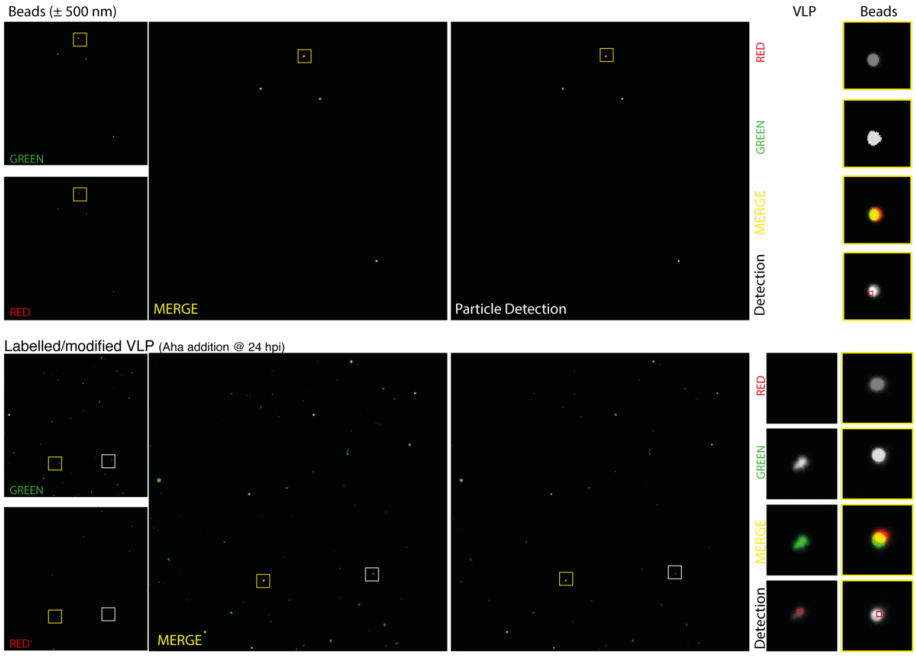

Figure B.1: Fluorescence Microscopy of VLP. Raw confocal images (2048x2048 pixels; 135x135 μm) from Figure 5.1 (Green, Red and Merge channels, and Particle detection analysis output; single channels were converted to grey scale). Right panels zoom Green/Red signal and highlight the accuracy of the Particle detection tool used throughout the study to quantify VLP production and green fluorescence emission (ImageJ Mosaic particle tracking pluggin). Observation of chemically modified VLP with a fluorescent probe (Alexa Fluor 488) that were added into IbiTreat 8 μ-well slides. 500 nm Fluorescent beads were used as size and green signal reference. Due to its multi-color fluorescence profile, red signal was also acquired. From green-red merge images one can discriminate beads from VLP (yellow and green dots, respectively) after proper total particle identification and count by Mosaic tool. Control VLP sample shows no green signal (no labeling with Alexa Fluor 488, meaning that azide ligation is specific for the non-canonical azidohomoalanine (Aha) amino acid). Observation of chemically modified VLP with the fluorescent probe Alexa Fluor 488 or control experiment was performed by depositing 100-fold dilutions of each condition supernatant into IbiTreat 8 μ-well slides and allowed to attach for 1 h. Each preparation was then labelled with 20 μM of Alexa Fluor 488 for 30 min and washed 3 times with PBS. 500-fold dilution of 500 nm stock fluorescent beads were added to each sample for 30 min and were used as size and green signal reference.

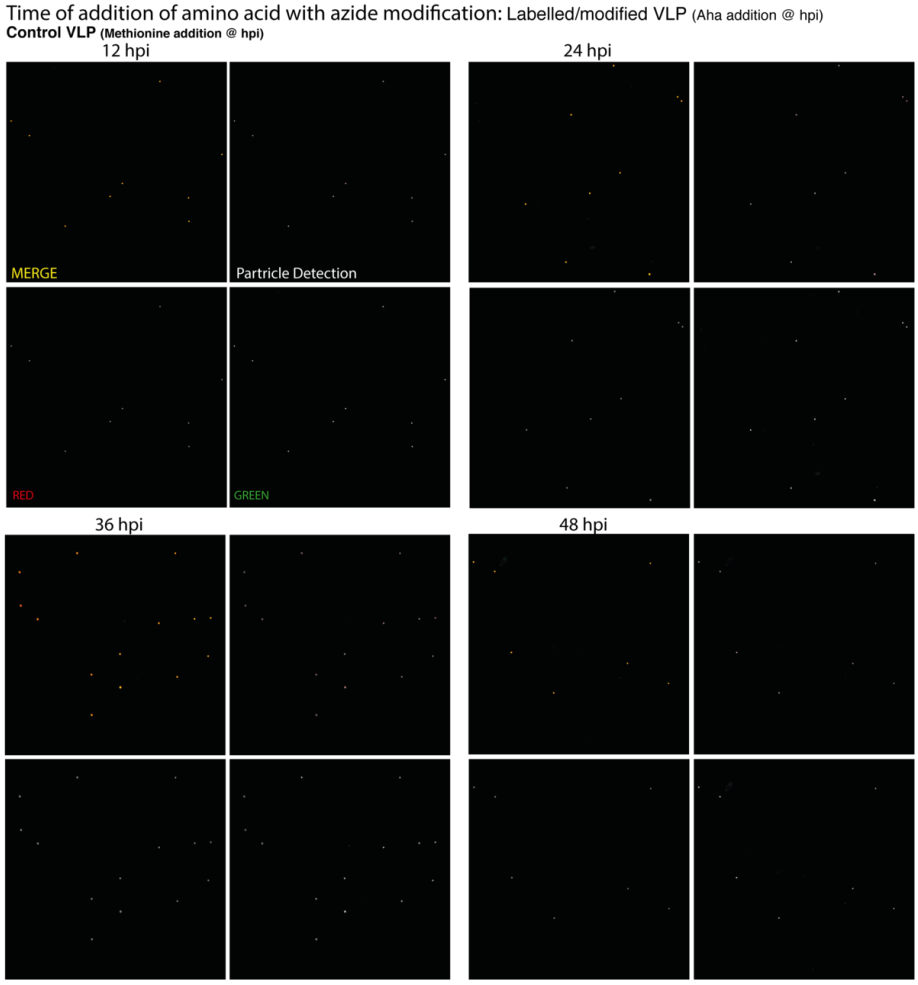

Figure B.2: **a.** Evaluation of the best time to add the non-canonical azidohomoalanine (Aha) in the experiment samples after baculovirus infection. The incorporation of Aha into HA protein was evaluated at different conditions: 12, 24, 36 and 48 h post baculovirus infection (hpi). This figure shows control experiment with the addition of methionine (Met) instead of Aha. These were performed to evaluate potential non-specific labeling with the Alexa Fluor 488 probe of Met amino acid residues from other proteins or other types of unspecific binding and confirm azide-specific ligation of our method. Observation of chemically modified VLP with the fluorescent probe Alexa Fluor 488 was performed by depositing 100-fold dilutions of each condition supernatant into IbiTreat 8 μ-well slides and allowed to attach for 1 h. Each preparation was then labelled with 20 μM of Alexa Fluor 488 for 30 min and washed 3 times with PBS. 500-fold dilution of 500 nm stock fluorescent beads were added to each sample for 30 min and were used as size and green signal reference.

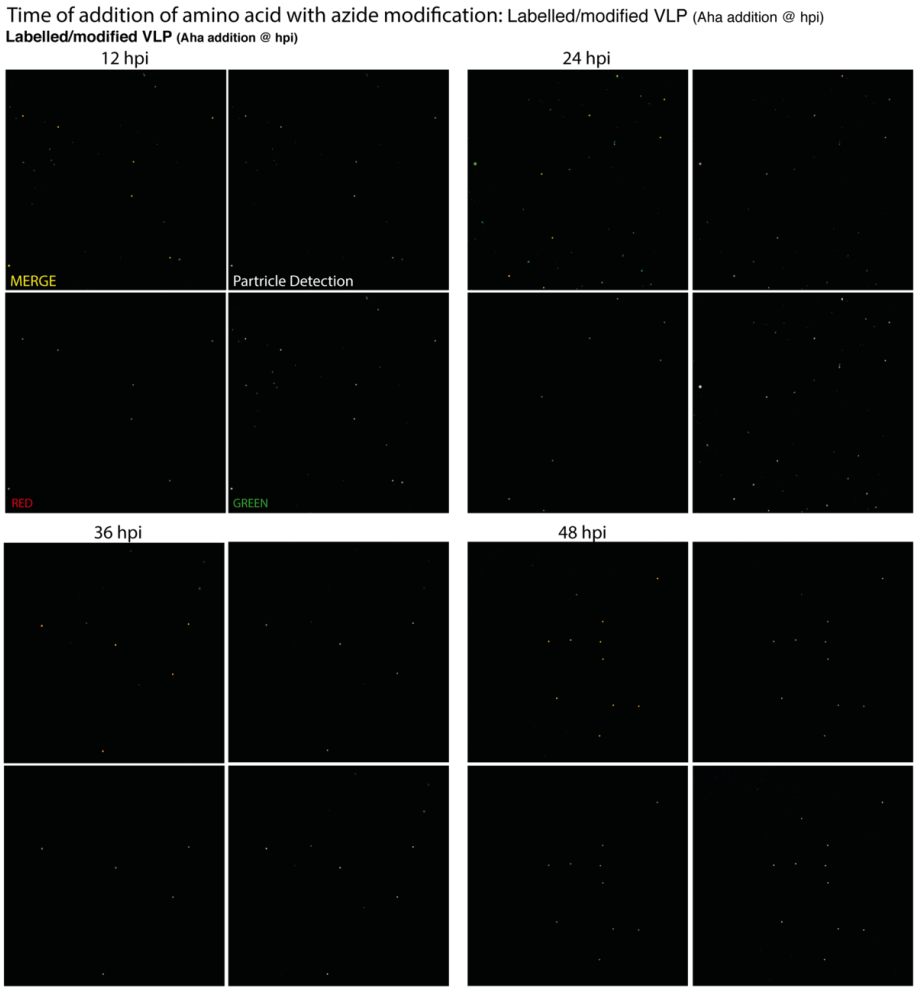

Figure B.2: **b.** Evaluation of the best time to add the non-canonical azidohomoalanine (Aha) in the experiment samples after baculovirus infection. The incorporation of Aha into HA protein was evaluated at different conditions: 12, 24, 36 and 48 h post baculovirus infection (hpi). This figure shows the existence of green labelled VLP (green dots in Merge channel) indicating site-specific azide ligation of VLP HA proteins. Observation of chemically modified VLP with the fluorescent probe Alexa Fluor 488 was performed by depositing 100-fold dilutions of each condition supernatant into IbiTreat 8 μ-well slides and allowed to attach for 1 h. Each preparation was then labelled with 20 μM of Alexa Fluor 488 for 30 min and washed 3 times with PBS. 500-fold dilution of 500 nm stock fluorescent beads were added to each sample for 30 min and were used as size and green signal reference.

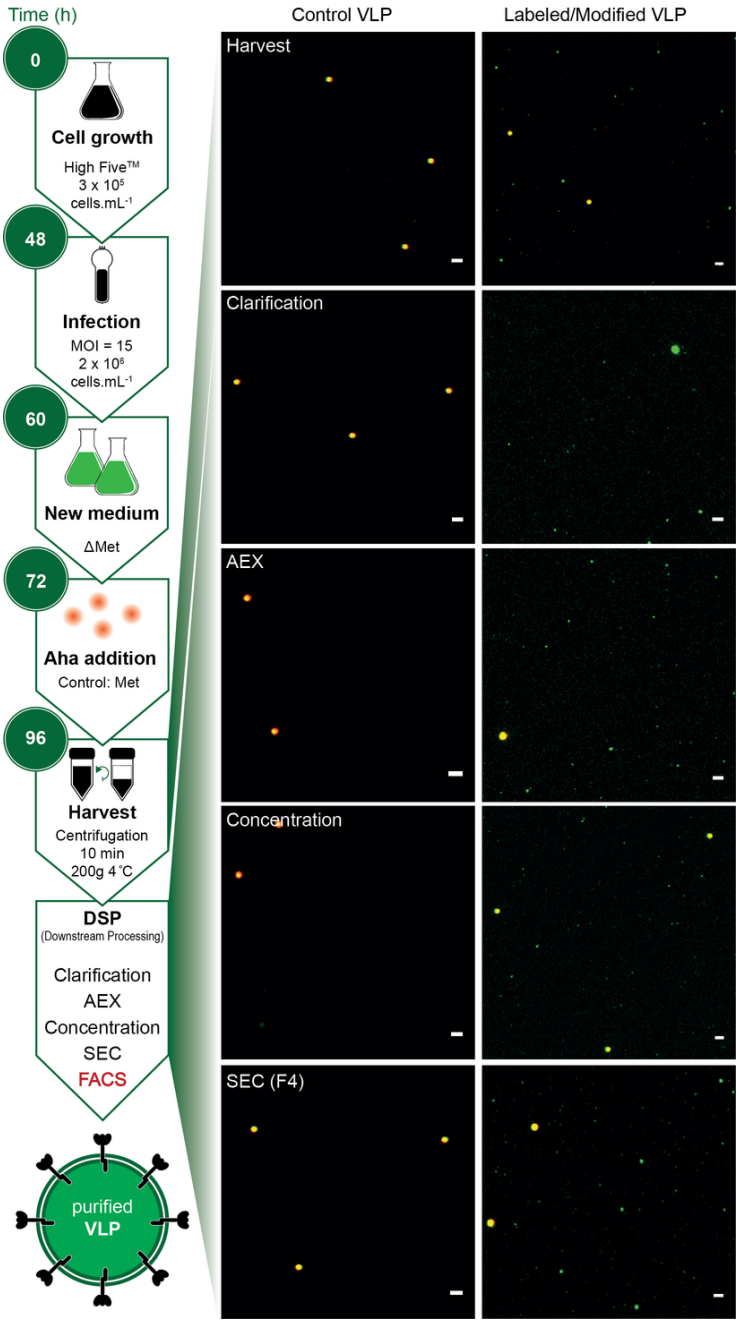

(Caption next page.)

Figure B.3: **a.** Flowchart showing specific-site-functionalized enveloped VLP production and purification steps. VLP production begins in a cell culture Erlenmeyer in which 3×105 cells mL^{-1} of High Five are added. Once 2×106 cells mL^{-1} is reached, cells are infected with baculovirus. The medium is replaced with one that does not contain Met at 12 hpi (ΔMet), and at 24 hpi the Aha non-canonical amino acid is added to the cell culture (Met is added to control cell culture). At 48 hpi, the VLP-rich supernatant is harvested and downstream processing (DSP) of VLP starts. At the end of the purification process high-purity VLPs are obtained. In each DSP step, and by including the fractions acquired in the SEC step, confocal microscopy images were recorded to monitor the presence of modified VLPs. Images for the control experiment were also acquired. Scale bars (white) indicate 2 μm in all images. Images are zoomed ROI from larger independent images to better visualize the sub-diffraction green dots (VLP signal). Merge (green-red) images are shown for clarity using the analysis described in Figure 5.1. Red signal emission was also acquired and from green:red merge images 500 nm beads can be discriminated from VLPs (yellow and green dots, respectively). Additional information regarding particle detection, individual Green and Red channels and RAW confocal images can be found in Figures B.3b and B.3c for the control and Aha addition experiments, respectively. In order to validate the approach, each sample of the DSP process was also studied by flow cytometry. SSC:green fluorescence and Red:Green fluorescence 2D correlograms are depicted in Figures B.6a, B.6, B.7a, and B.7b for the control and Aha addition experiments, respectively. Experimental procedure on confocal microscopy and flow cytometry acquisition and apparatus are available in detail in the experimental section.

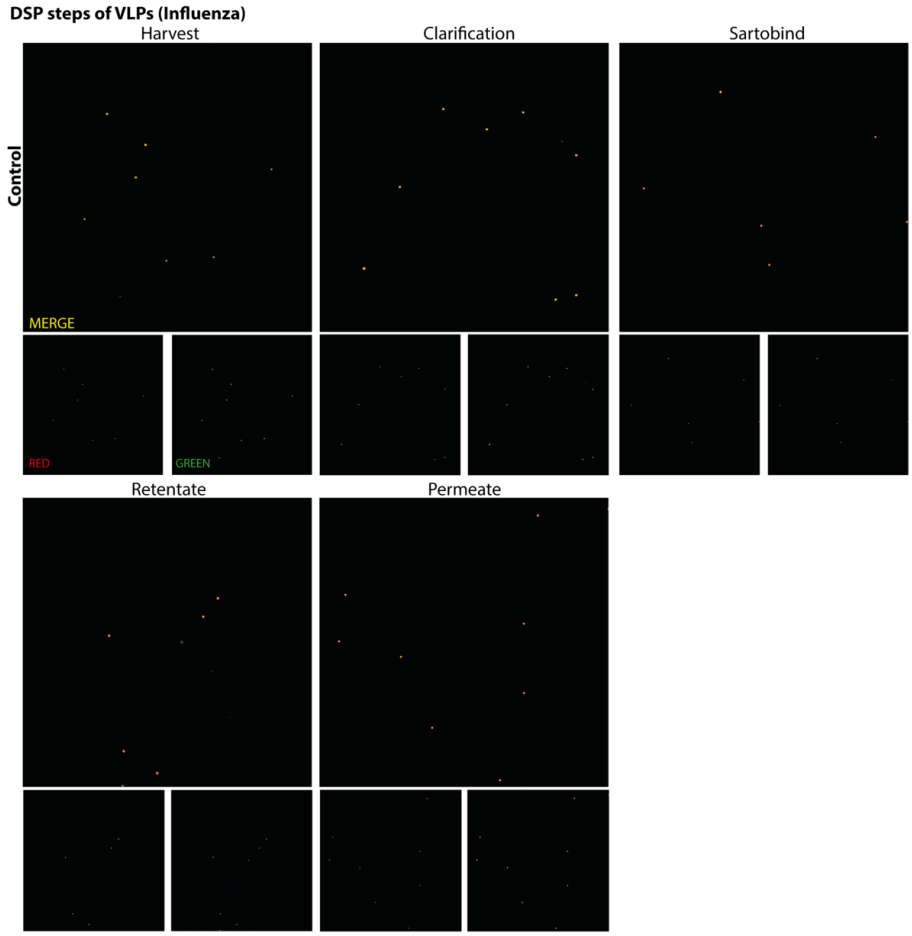

Figure B.3: **b.** Follow-up of DSP steps by confocal microscopy. Observation of the presence of green fluorescent VLP at each step of the DSP (Harvest, Clarification, Sartobind, Retentate and Permeate). Each recollected SEC fraction of the DSP step is observed in more detail in Figure B.4. RAW confocal images (2048x2048 pixels; 135x135 μm) depicted in Figure B.3a (Green, Red and Merge channels). Figure B.3b shows control experiment performed to evaluate non-specific azide-binding. Control VLP sample shows no green signal. Images were acquired from depositing 100-fold dilutions of each condition supernatant into IbiTreat 8 μ-well slides and allowed to attach for 1 h. 20 μM of Alexa Fluor 488 was then added to each preparation for 30 min and washed 3 times with PBS. 500-fold dilution of 500 nm stock fluorescent beads were added to each sample for 30 min and were used as size and green signal reference.

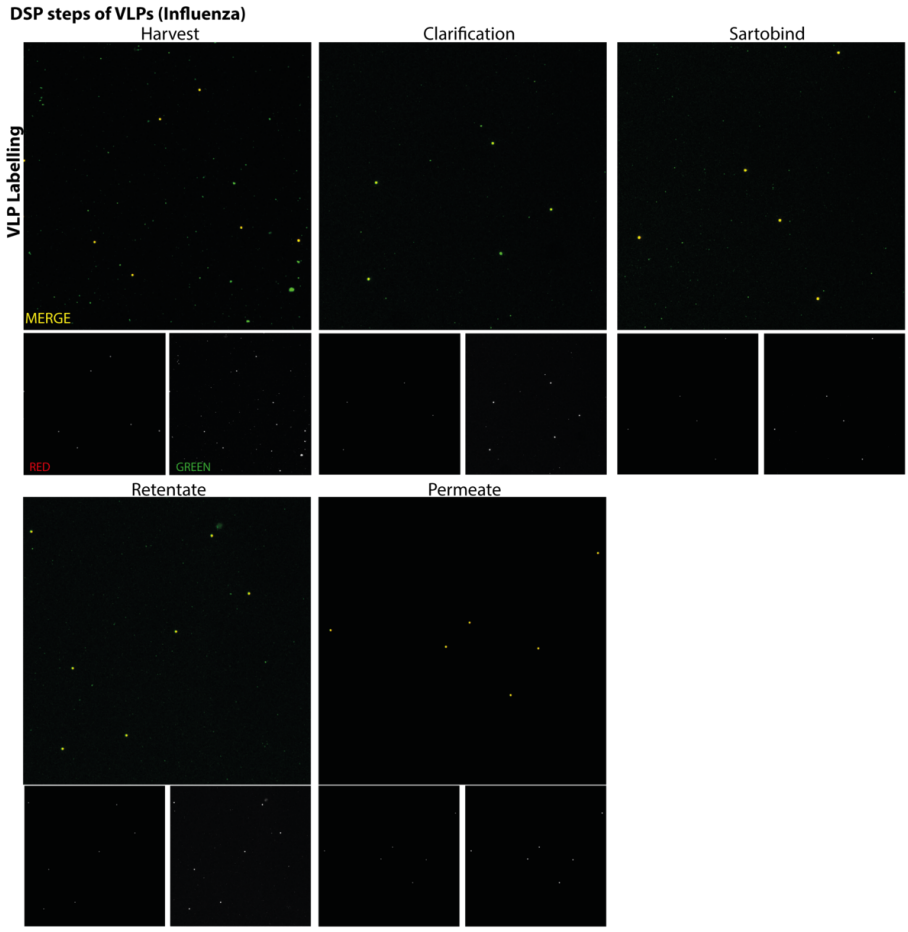

Figure B.3: **c.** Follow-up of DSP steps by confocal microscopy. Observation of the presence of green fluorescent VLP at each step of the DSP (Harvest, Clarification, Sartobind, Retentate and Permeate). Each recollected SEC fraction of the DSP step is observed in more detail in Figure B.4. RAW confocal images (2048x2048 pixels; 135x135 μm) depicted in Figure B.3a (Green, Red and Merge channels). Figure B.3c shows Aha samples to evaluate azide-binding and green fluorescence (A488 signal) from VLP HA protein. Contrary to control VLP experiment (Figure B.3b) the images reveal positive green dots specific from VLP (Merge channel). Observation of chemically modified VLP with the fluorescent probe Alexa Fluor 488 was performed by depositing 100-fold dilutions of each condition supernatant into IbiTreat 8 μ-well slides and allowed to attach for 1 h. Each preparation was then labelled with 20 μM of Alexa Fluor 488 for 30 min and washed 3 times with PBS. 500-fold dilution of 500 nm stock fluorescent beads were added to each sample for 30 min and were used as size and green signal reference.

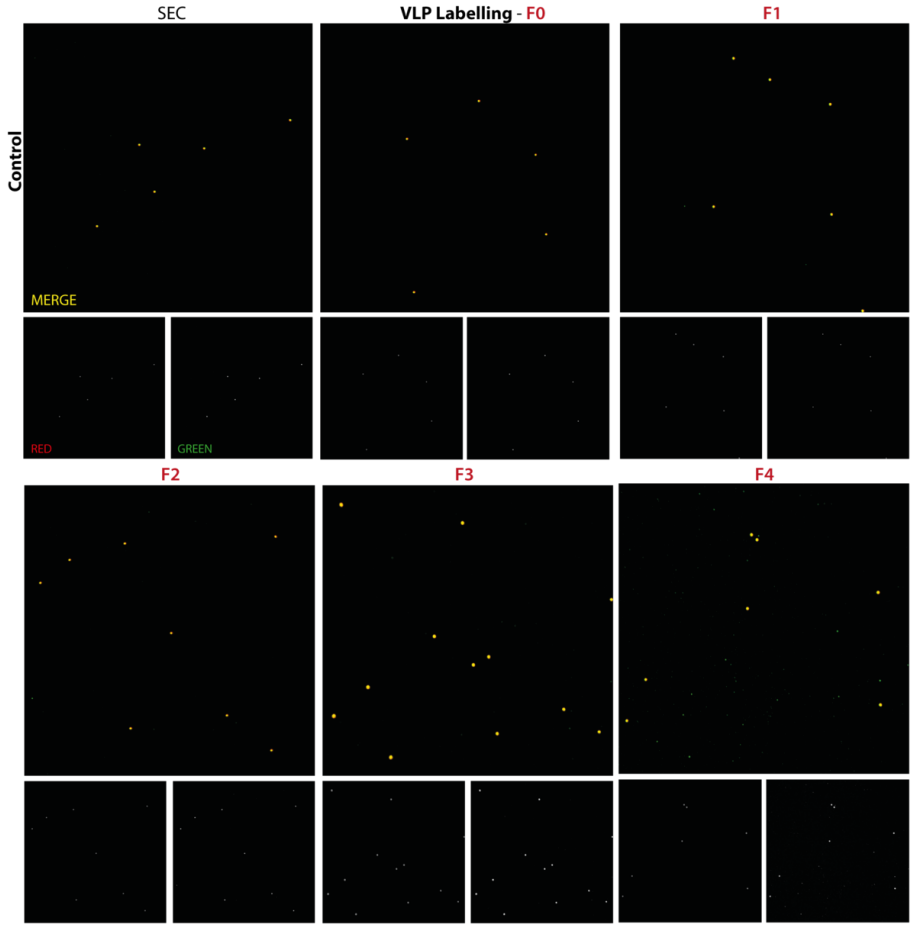

Figure B.4: **a.** Detailed follow-up of SEC DSP step by confocal microscopy. RAW confocal images (2048x2048 pixels; 135x135 μm) depicted in Figure 5.2 (Green, Red and Merge channels). This figure shows SEC from Control experiment and SEC F0 to F4 from Aha samples to evaluate azide-binding and green fluorescence (A488 signal) from VLP HA protein. Contrary to control VLP experiment the images reveal positive green dots specific from VLP in F4. Observation of chemically modified VLP with the fluorescent probe Alexa Fluor 488 was performed by depositing 100-fold dilutions of each condition supernatant into IbiTreat 8 μ-well slides and allowed to attach for 1 h. Each preparation was then labelled with 20 μM of Alexa Fluor 488 for 30 min and washed 3 times with PBS. 500-fold dilution of 500 nm stock fluorescent beads were added to each sample for 30 min and were used as size and green signal reference.

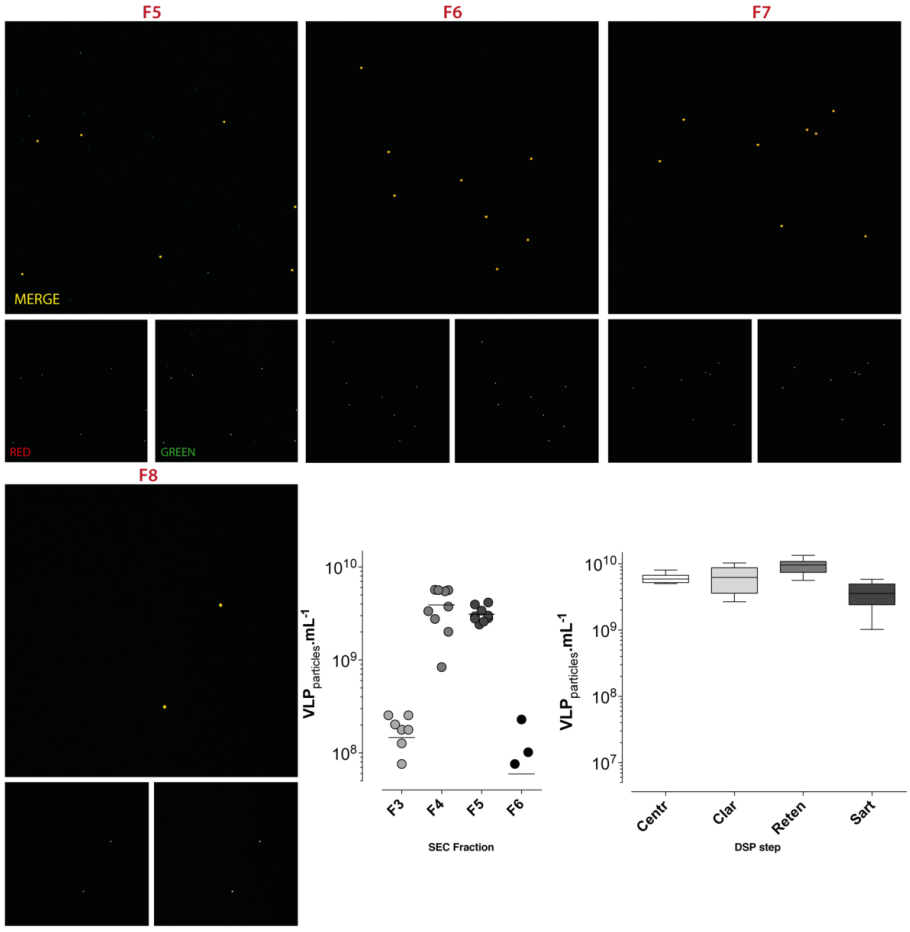

Figure B.4: **b.** Continuation of Figure B.4a. Detailed follow-up of SEC DSP step by confocal microscopy. RAW confocal images (2048x2048 pixels; 135x135 μm) depicted in Figure 5.2 (Green, Red and Merge channels). Figure B.4b shows SEC F5 to F8 from AHA samples to evaluate azide-binding and green fluorescence (A488 signal) from VLP HA protein (F5). Observation of chemically modified VLP with the fluorescent probe Alexa Fluor 488 was performed by depositing 100-fold dilutions of each condition supernatant into IbiTreat 8 μ-well slides and allowed to attach for 1 h. Each preparation was then labelled with 20 μM of Alexa Fluor 488 for 30 min and washed 3 times with PBS. 500-fold dilution of 500 nm stock fluorescent beads were added to each sample for 30 min and were used as size and green signal reference. Determination of the concentration of labelled VLP (VlP mL^{-1}) of each DSP process and SEC fraction based on the particle detection of the microscope images. Calculation was performed with equation 5.2. The number obtained is in accordance with the VLP stock solution used to perform the labelling protocol $>10^9$ particles /mL.

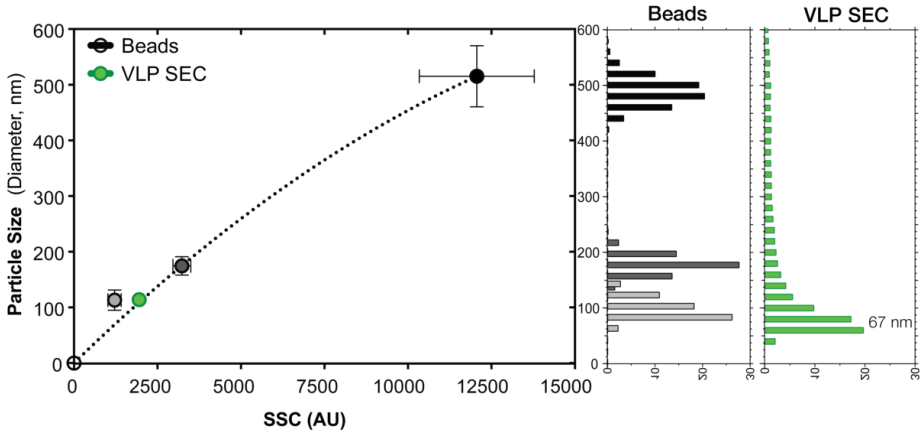

Figure B.5: **a.** Extrapolation of VLP population particle size diameter from SSC signal using standard fluorescent beads with 100, 200 and 500 nm. Size distribution of each population depicts the size heterogeneity within the VLP sample and showing the mode of the distribution at 67 nm (green histogram).

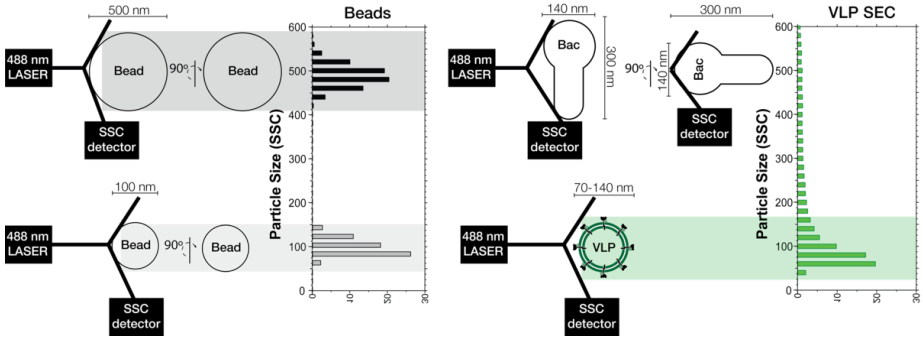

Figure B.5: **b.** Flow cytometry SSC signal and the size of polydisperse samples. For spherical particles the orientation by which the particle is detected in the flow cytometer is irrelevant, retrieving always the same SSC value, thus a monomodal size distribution around the diameter of the particle sphere (100 nm or 500 nm in the example). As for the VLP sample, apart from the spherical VLP (giving a size distribution around 70-100 nm) the presence of rod-shaped particles, baculovirus will give SSC values far from the spherical distribution. This reflects the orientation by which the rod-shaped particle was detected. So, using the beads ruler one can separate the particles that are clearly larger/longer and enrich the sample with spherical VLP.

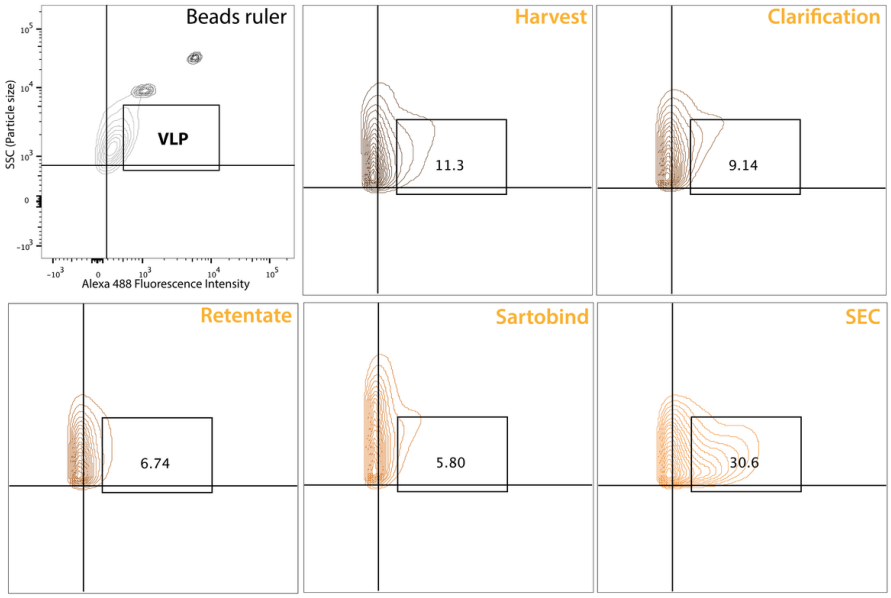

Figure B.6: **a.** Supporting data to the flow cytometry experiment shown in Figure 5.3. Observation of the presence of VLP at each step of the DSP by Flow cytometry for Control experiment: Harvest, Clarification, Retentate, Sartobind and SEC fraction F4. 2D correlogram of side scatter (SSC) and green fluorescence signals (A488) are shown with 5% contour plots of each population of each DSP step. Top left panel indicate the side scatter size ruler made with 100, 200 and 500 nm size fluorescent beads (greyscale). Gate thresholds for negative and positive populations were performed using 100 nm beads signal - Top-right quadrant indicates green fluorescent positive >100 nm particles - VLP. In each chart, the [100-200] nm/Alexa Fluor 488 positive population gate - VLP - was built to quantify the presence of HA-labelled-VLP in each stage of the DSP. Control VLP sample shows no significant green signal but rather a heterogeneous distribution in the SSC axis (presence of VLP and Baculovirus).

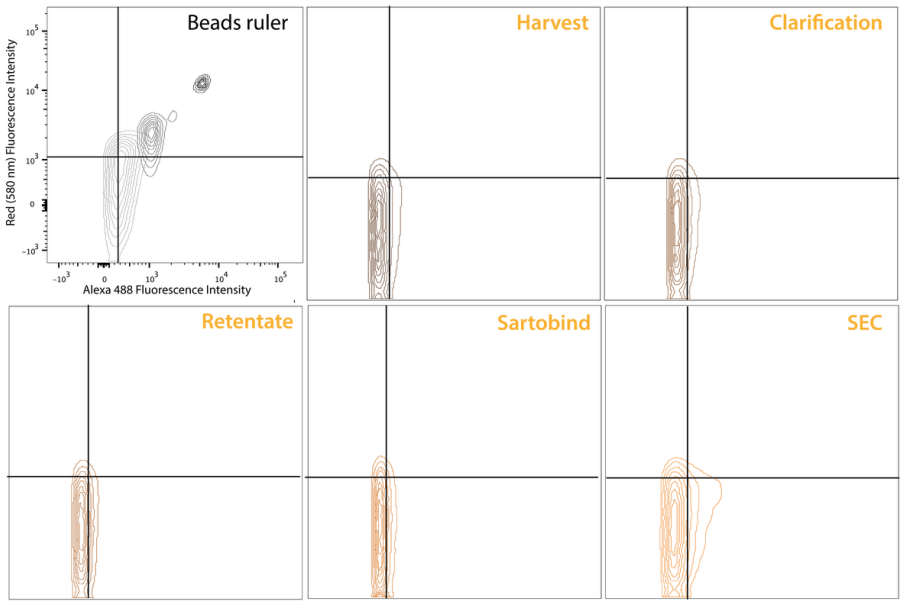

Figure B.6: **b.** Supporting data to the flow cytometry experiment shown in Figure 5.3. Observation of the presence of VLP at each step of the DSP by Flow cytometry: Harvest, Clarification, Retentate, Sartobind and SEC fraction F4. 2D correlogram of Red (580 nm) and green fluorescence signals (A488) are shown with 5% contour plots of each population of each DSP step. Top left panel indicate the signals from the 100, 200 and 500 nm size fluorescent beads (greyscale). Gate thresholds for negative and positive populations were performed using 100 nm beads signal - Top-right quadrant indicates Red:green fluorescent positive particles. Control VLP sample (Figure 5.3) shows no significant green signal but rather a heterogeneous distribution in the SSC axis (presence of VLP and Baculovirus) and residual indication of auto-fluorescence from the samples in some of the DSP steps.

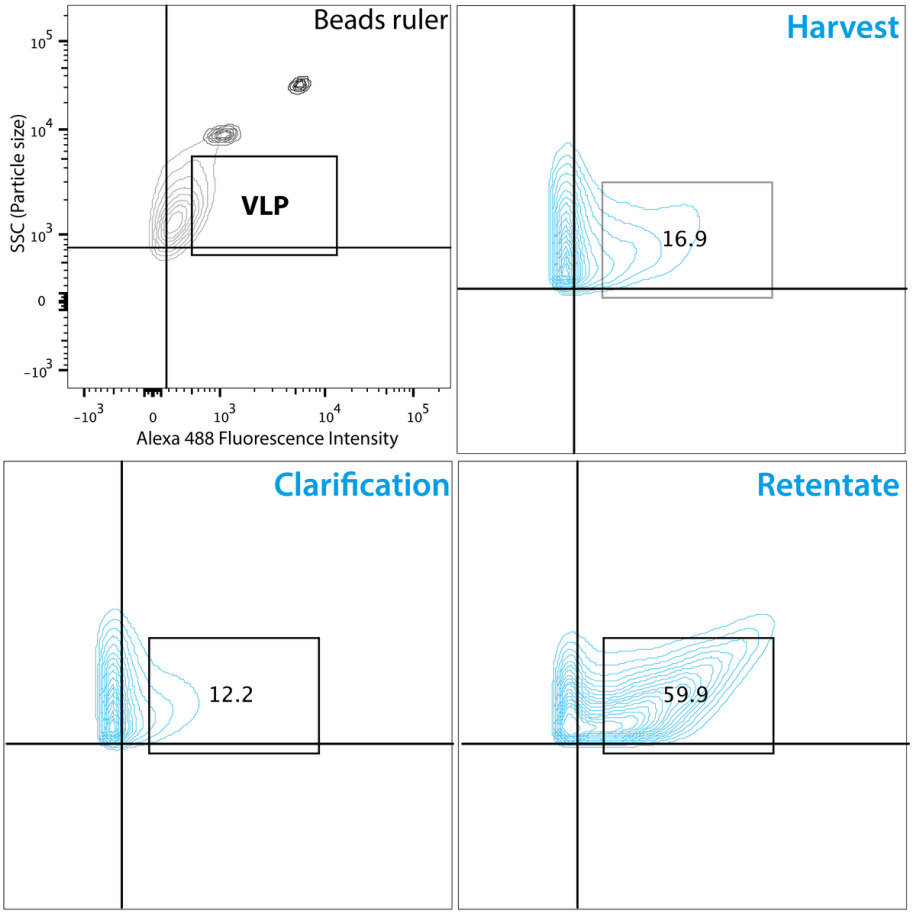

Figure B.7: **a.** Supporting data to the flow cytometry experiment shown in Figure 5.3. Flow cytometry of VLP at in each step of the DSP for the Aha VLP-labeling experiment (Harvest, Clarification, Retentate). A more detailed observation of each SEC fraction was performed (Figure B.8). 2D correlogram of side scatter and green fluorescence signals are shown with 5% contour plots of each population of each DSP step. Top left panel indicate the side scatter size ruler made with 100, 200 and 500 nm size fluorescent beads (greyscale). Gate thresholds for negative and positive populations were performed using 100 nm beads signal - Top-right quadrant indicates green fluorescent positive >100 nm particles - VLP. In each chart, the [100-200] nm/Alexa Fluor 488 positive population gate - VLP - was built to quantify the presence of labelled-VLP in each stage of the DSP. VLP sample show significant green signal of labelled VLP (59.9%), especially on the retentate sample, the concentrated sample prior to SEC DSP step.

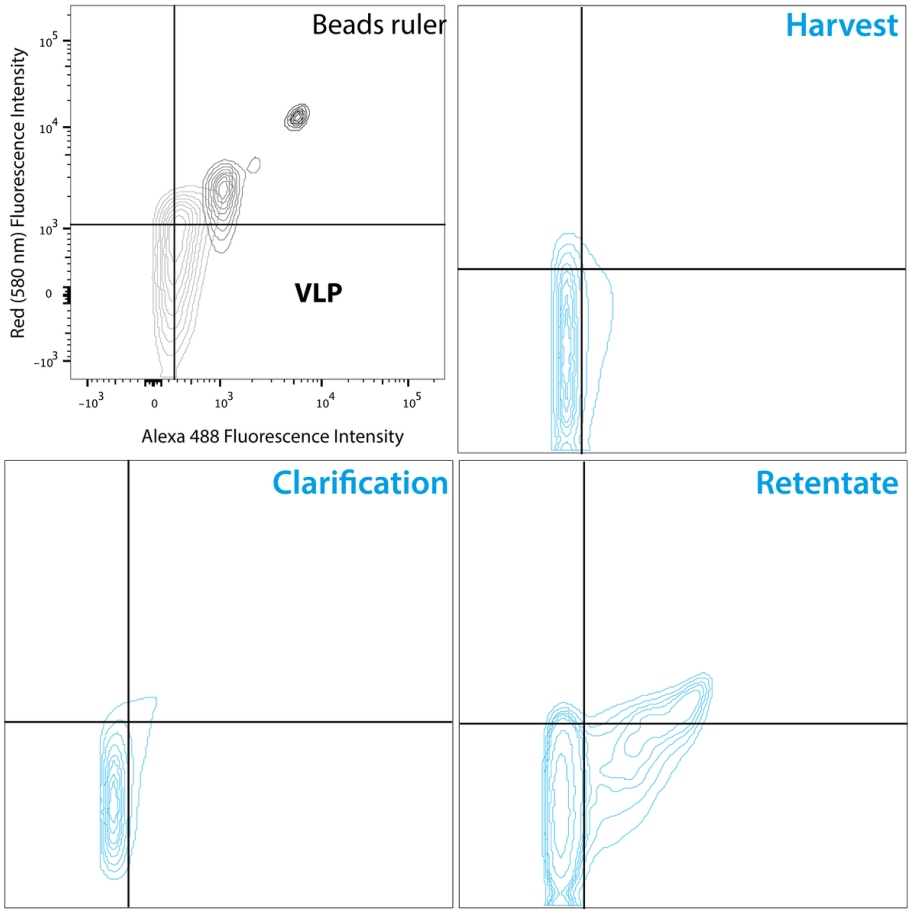

Figure B.7: **b.** Supporting data to the flow cytometry experiment shown in Figure 5.3. Flow cytometry of VLP at in each step of the DSP for the Aha VLP-labeling experiment (Harvest, Clarification, Retentate). A more detailed observation of each SEC fraction was performed (Figure B.8). 2D correlogram of Red (580 nm) and green fluorescence signals are shown with 5% contour plots of each population of each DSP step. Top left panel indicate the side scatter size ruler made with 100, 200 and 500 nm size fluorescent beads (greyscale). Gate thresholds for negative and positive populations were performed using 100 nm beads signal - Top-right quadrant indicates Red:green fluorescent positive particles. VLP sample show significant green signal of labelled VLP with no Red signal, especially on the retentate sample, the concentrated sample prior to SEC DSP step.

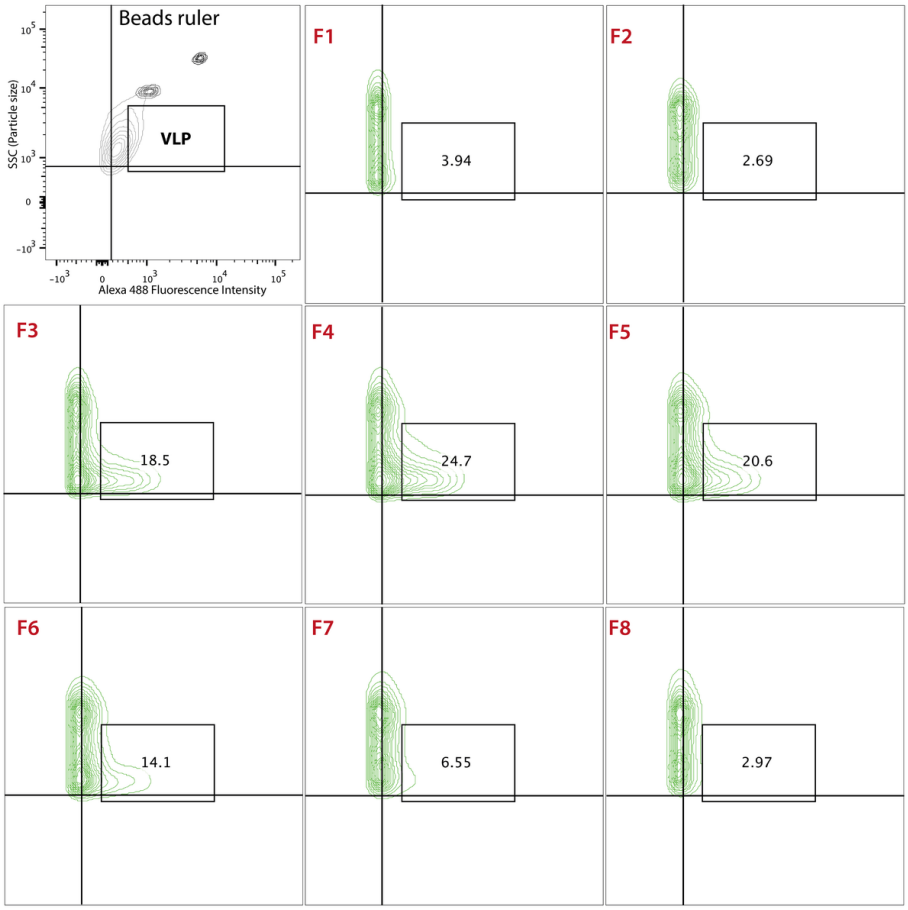

Figure B.8: **a.** Supporting data to the flow cytometry experiment shown in Figure 5.2 and Figure 5.3. Flow cytometry of each fraction collected in the SEC step of the DSP for the Aha VLP-labeling experiment. 2D correlogram of side scatter and green fluorescence signals are shown with 5% contour plots of each population of each SEC fraction. Top left panel indicate the side scatter size ruler made with 100, 200 and 500 nm size fluorescent beads (greyscale). Gate thresholds for negative and positive populations were performed using 100 nm beads signal - Top-right quadrant indicates green fluorescent positive >100 nm particles - VLP. In each chart, the [100-200] nm/Alexa Fluor 488 positive population gate - VLP - was built to quantify the presence of labelled-VLP in each stage of the DSP. The SEC fractions with major VLP concentration (F4 and F5) - significant green signal of labelled VLP - correlate with the absorbance peaks from Figure 5.2 and confocal microscopy green dots.

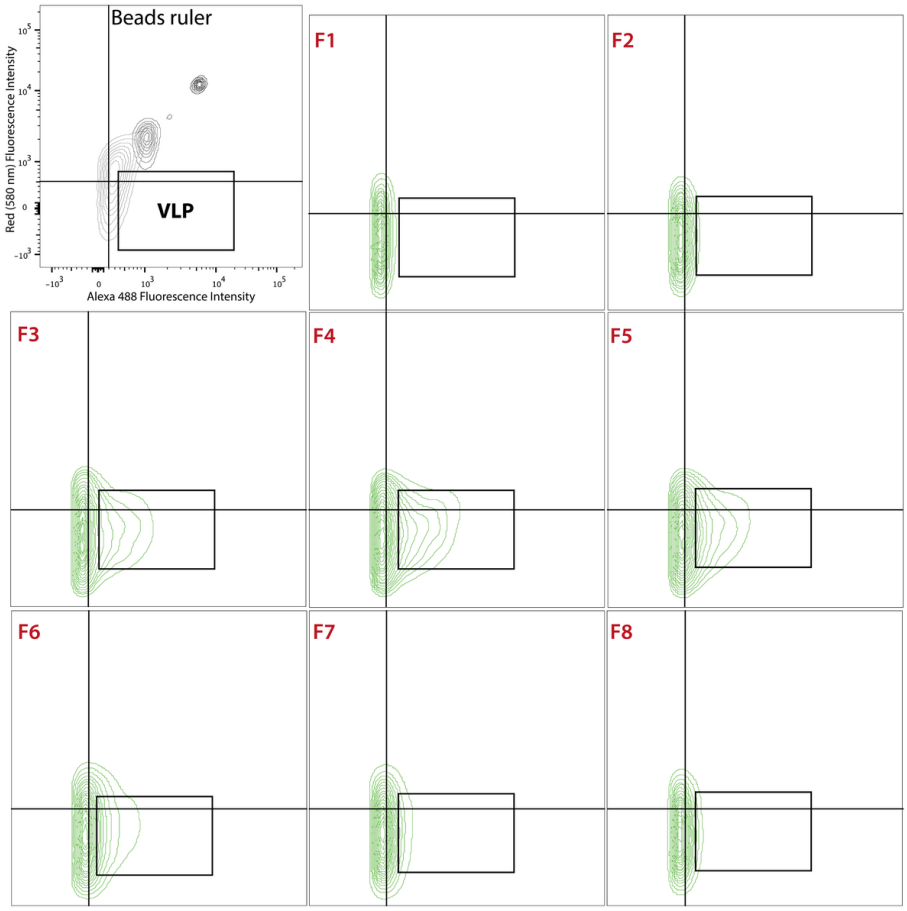

Figure B.8: **b.** upporting data to the flow cytometry experiment shown in Figure 5.2 and Figure 5.3. Flow cytometry of each fraction collected in the SEC step of the DSP for the Aha VLP-labeling experiment. 2D correlogram of Red (580 nm) and green fluorescence signals are shown with 5% contour plots of each population of each SEC fraction. Top left panel indicate the side scatter size ruler made with 100, 200 and 500 nm size fluorescent beads (greyscale). Gate thresholds for negative and positive populations were performed using 100 nm beads signal - Bottom-right quadrant indicates green fluorescent positive:Red negative particles - VLP. The SEC fractions with major VLP concentration (F4 and F5) - significant green signal and none red - correlate with the absorbance peaks from Figure 5.2 and confocal microscopy green dots.

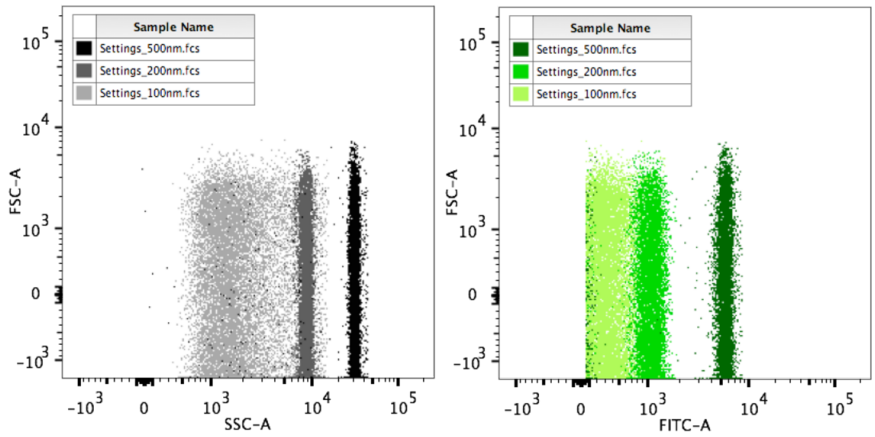

Figure B.9: Supporting data to the flow cytometry experiment shown in Figure 5.3. Flow cytometry of the nanometer sized particle controls (ruler made with 100, 200 and 500 nm size fluorescent beads) highlighting the possibility of using one-dimension discrimination features to separate VLP from Baculovirus. Left panel shows the FSC:SSC FACS plot identifying the well-defined 100-200 nm interval that enables accurate and precise VLP separation. Right panel shows the green fluorescent emission of the beads also highlighting the Green positive (VLP in the case of labeling) against the Green negative (Baculovirus in our case).

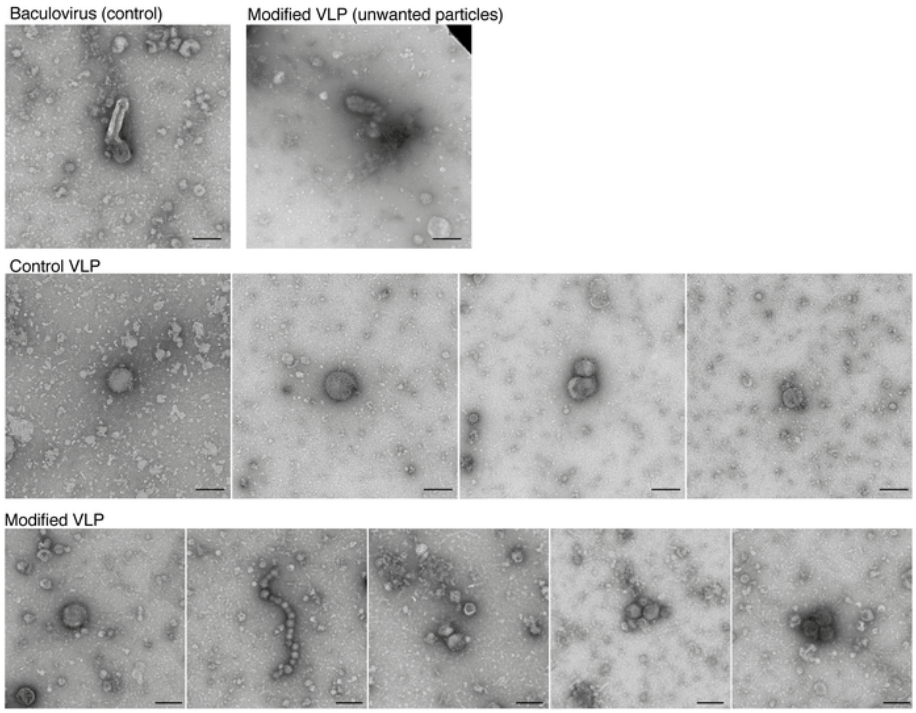

Figure B.10: Supporting data to the TEM images acquired for Baculovirus control sample, control VLPs from the concentration step of the purification process, and of modified VLPs from the concentration step of the purification process. Scale bar indicates 100 nm. Uncropped and additional TEM images from Figure 5.4 and 5.6.

Western Blot analysis and MS proteomics of HA / M1 labelled VLP

Western blot analysis was performed for control and modified Influenza VLPs, with both precipitated (pp) and non-precipitated samples. As a control, M1 protein from Influenza A H1N1 strain and H3 Influenza VLP (produced and purified at iBET) were used. SeeBlue markers were used as molecular weight (MW) control. Control and labelled VLP samples were incubated with Alexa Fluor 488 fluorescent probe prior to SDS-PAGE gel running. A fluorescent imaging system was used to reveal the gel and analyse the presence of fluorescent bands. Bands identified with numbers from 1 to 4 were excised from the corresponding gel and analysed by mass spectrometry. In order to detect modified peptides, MS data were also analysed using the BioPharmaView software version 1.0 considering a Met-Aha modification.

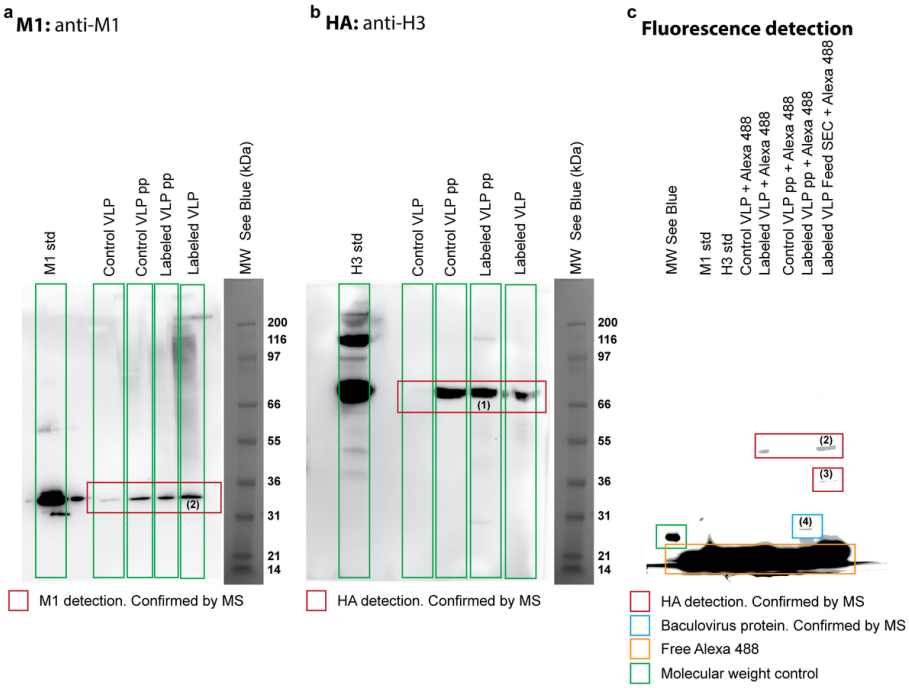

Figure B.11: Raw data of Figure 5.5 for identification of HA and M1 proteins by western blot analysis and fluorescent band detection of labelled Influenza VLPs' proteins. **a**, M1 Influenza protein detection on control and labelled VLPs by western blot analysis. M1 protein from Influenza A H1N1 strain was used as positive control (M1 std). Band (1) was excised and identified as M1 by mass spectrometry (Table B.1). pp means precipitated sample. **b**, HA Influenza protein detection on control and labelled VLPs by western blot analysis. H3 VLP from Influenza A H3 strain, produced and purified at iBET, was used as positive control (H3 std). Band (2) was excised and identified as HA by mass spectrometry (Table B.1). pp means precipitated sample. **c**, SDS-PAGE gel fluorescence detection of control and labelled VLPs incubated with Alexa Fluor 488 probe. Bands (2) and (3) (red highlight) were excised and detected as HA by mass spectrometry (Table B.1). Band (4) was detected as a Telokin-like protein of baculovirus (blue highlight). Free Alexa Fluor 488 probe was observed at the bottom of the gel (orange highlight). Fluorescent molecular weight was added as a control (green highlight). pp means precipitated sample.

Table B.1: Proteins of labelled Influenza A VLPs identified using NanoLC-MS. Bands were identified in Figure 5.6.

Band ID	**Protein Name**	**Sequence Coverage (%)**	**Queries Matched**	**Modification Met>Aha**	**Peptides Modified (Met>Aha)**
1	Matrix protein 1 of Influenza A virus (M1)	16.7	6	No	-
2	Hemagglutinin of Influenza A virus (HA_1)	7.2	3	Yes	NGKSSIMR LATGMRNVPEK
3	Hemagglutinin of Influenza A virus (HA_2)	23.7	18	Yes	LATGMR ENAEDMGNGCFK ENAEDMGNGCFKIYHK
4	Telokin-like protein of Autographa californica nuclear polyhedrosis virus	34.4	7	Yes	SSIMR

C

Supporting information for "Membrane-based approach for the downstream processing of influenza virus-like particles" (Chapter 7)

Table C.1: Technical specifications of ultrafiltration membrane cassettes evaluated. NMWL: Nominal Molecular Weight Limit; PES: Polyethersulfone; RC: Regenerated Cellulose.

Membrane type	Material	NMWL (kDa)	Screen Type	Screening surface area (cm^2)
Biomax	PES	1000	C (coarse screen)	50
		500		
		300		
		100		
Ultracel	RC	1000		
		300		

Table C.2: Technical specifications of sterile Millex filter units evaluated. PES: Polyethersulfone; PVDF: polyvinylidene fluoride.

Membrane Material	Pore size (μm)	Screening surface area (cm^2)	Filter Diameter (mm)
PES PVDF	0.22	4.5	33

Table C.3: Series and parallel device arrangement evaluation. P_F, P_R and P_P are the measured pressures at the feed, retentate and permeate ports at the experiment endpoint.

Configuration	VLPs recovery % HA assay	VLPs recovery % Nanosight	TMP bar	P_F | P_R | P_P bar
Parallel	95.4	115.0	0.74	(0.86 | 0.61 | 0.01)
Series	50.4	49.3	0.81	(1.57 | 0.05 | 0.01)

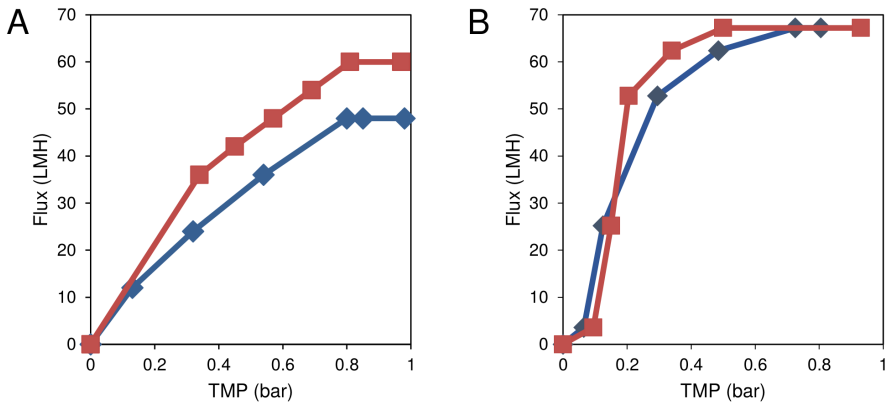

Figure C.1: TMP excursion for the 1000 and 300 kDa devices. CRC (A), PES (B). 300 kDa red series, 1000 kDa blue series.

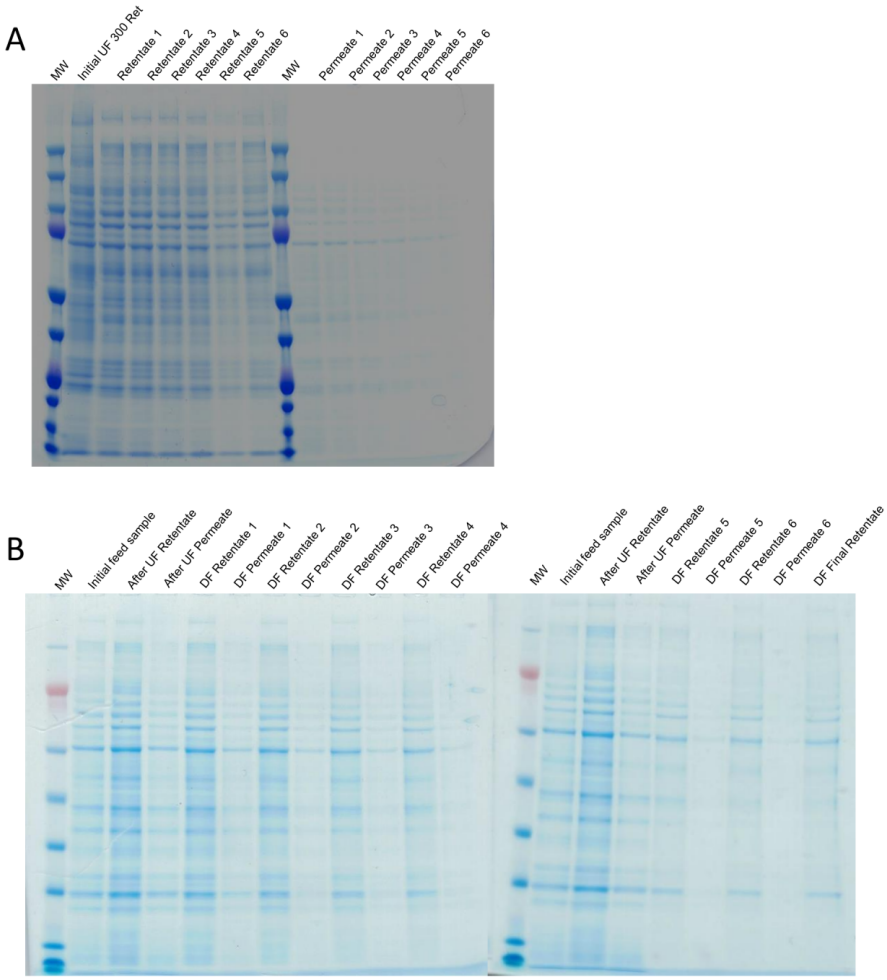

Figure C.2: SDS page analysis for the diafiltration studies. 300 kDa (A) and 1000 kDa (B).

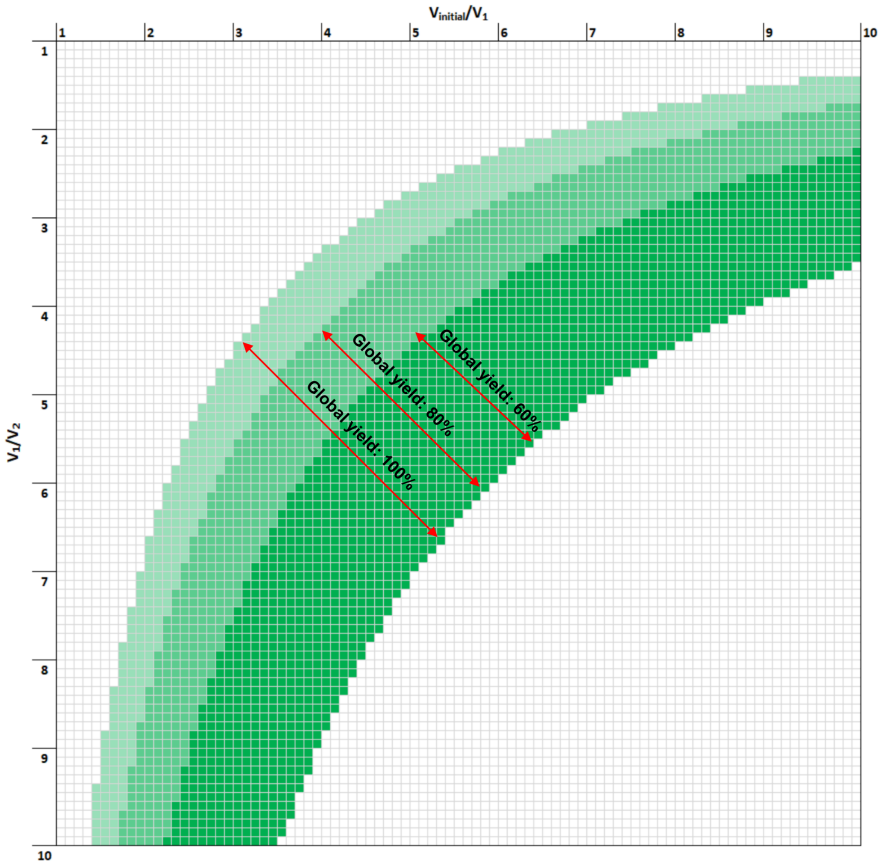

Figure C.3: Possible combination that simultaneously verify two constraints: (i) minimum operational volume for each UF step is 10 mL; (ii) The target concentration after the two UF steps, should be higher than 15 μg mL^{-1}, considering a feed concentration of 1.14 μg mL^{-1} of HA, with an initial sample volume of 350 mL. The figure depicts three process yield scenarios: 100, 80 and 60%. V_1/V_2 and $V_{initial}/V_2$ are representative of the ratio of the volumes obtained after each UF stage.

D

Supporting information for "Purification of influenza virus-like particles using sulfated cellulose membrane adsorbers" (Chapter 8)

D.1 Experimental Section

D.1.1 Baculovirus quantification

To quantify baculovirus viral copies in each sample, viral DNA was extracted and purified using the High Pure Viral Nucleic Acid Kit (11858874001, Roche Diagnostics, Germany) following manufacturer's instructions. The number of genome containing particles were monitored by real time quantitative PCR (q-PCR) following the protocol described elsewhere[190] with some modifications. Briefly, DNA samples were diluted 1:100 in water PCR grade (03315932001, Roche Diagnostics) and diluted again 1:4 with master mix. Master mix is prepared by diluting 1:2 the Light Cycler 480 SYBR Green I Master (04707516001, Roche Diagnostics, Germany) and 0.5 μM of each primer. q-PCR reaction took place in a 96-well white plate (04729692001, Roche Diagnostics) using a LightCycler 480 Instrument II (Roche Molecular Systems, Inc.).

D.1.2 Nanoparticle tracking analysis

After VLPs production and clarification, particle presence, concentration and size distribution were measured using the NanoSight NS500

(Nanosight Ltd, UK). Samples were diluted in D-PBS (14190-169, Gibco, UK) so that VLPs concentration would be in the 10^8-10^9 particles ml^{-1} - the instrument's linear range. All measurements were performed at room temperature (22 °C). Sample videos were analysed with the Nanoparticle Tracking Analysis (NTA) 2.3 Analytical software - release version build 0025. Capture settings (shutter and gain) were adjusted manually. For each sample 60-seconds videos were acquired and particles between 70 and 150 nm were considered.

D.2 Design matrix

Using MODDE 11, an experimental matrix was generated for a 3-level optimization Rechtschaffner design. Table D.1 resumes the values for each investigated factor and the resulting responses for each experiment.

D.3 Model fitting and statistical analysis

Each response Y is described as a function of each factor X and all possible factors interactions according to the general second order polynomial equation D.1:

$$Y = C_0 + \sum_{i=1}^{n} C_i X_i + \sum_{i=1}^{n} C_{ii} X_i^2 + \sum_{i,j=1}^{n} C_{i,j} X_i X_j \qquad \text{(D.1)}$$

where C_i are the calculated regression coefficients, n the total number of factors, and j all other factors except i. All coefficients were scaled, centered and normalized to the variance of each response[210].

Equations D.2 and D.3 describe respectively HA loss and HA yield,

Table D.1: Design matrix (3-level Rechtschaffner design) implemented for the optimization of the chromatographic purification of influenza VLPs using sulfated cellulose membrane adsorbers (SCMA). Five responses (ligand density (LD), salt concentration for loading and elution ($NaCl_{load}$ and $NaCl_{elution}$, respectively) and flow rate in the load and elution steps elution (Q_{load} and $Q_{elution}$, respectively)) and two responses (HA loss and HA yield) were investigated. The center points of the design are marked with a star (*) and outlier values, not considered for data fitting, appear between brackets.

Exp. no.	LD μmol cm^{-2}	$[NaCl]_{load}$ mM	$[NaCl]_{elution}$ mM	Q_{load} mL min^{-1}	$Q_{elution}$ mL min^{-1}	HA loss %	HA yield%
1	7.9	20	200	0.2	0.5	17.0	37.5
2	7.9	60	1000	0.6	1.5	41.7	97.3
3	15.4	20	1000	0.6	1.5	21.8	(155.9)
4	15.4	60	200	0.6	1.5	32.9	37.3
5	15.4	60	1000	0.2	1.5	30.9	112.9
6	15.4	60	1000	0.6	0.5	30.9	90.5
7	15.4	60	200	0.2	0.5	(0)	12.3
8	15.4	20	1000	0.2	0.5	10.9	103.9
9	15.4	20	200	0.6	0.5	23.2	19.9
10	15.4	20	200	0.2	1.5	16.7	53.4
11	7.9	60	1000	0.2	0.5	26.8	66.5
12	7.9	60	200	0.6	0.5	48.0	21.8
13	7.9	60	200	0.2	1.5	42.9	42.2
14	7.9	20	1000	0.6	0.5	21.4	21.8
15	7.9	20	1000	0.2	1.5	13.2	69.3
16	7.9	20	200	0.6	1.5	24.2	41.6
17	15.4	40	600	0.4	1.0	27.3	58.1
18	11.8	60	600	0.4	1.0	37.7	74.0
19	11.8	40	1000	0.4	1.0	36.0	102.6
20	11.8	40	600	0.6	1.0	25.9	56.7
21	11.8	40	600	0.4	1.5	28.0	80.0
22*	11.8	40	600	0.4	1.0	32.6	78.3
23*	11.8	40	600	0.4	1.0	34.9	92.3
24*	11.8	40	600	0.4	1.0	31.4	69.6

Table D.2: ANOVA for the proposed experimental design together with the predicted variation (Q^2), the validity, and the reproducibility of the model for both responses.

Response	Degrees of freedom	p-value	Lack of fit	F-value	R^2	Q^2	Validity	Reproducibility
HA loss	13	1.4e-6	0.15	20.0	0.81	0.67	0.53	0.96
HA yield	17	5.6e-5	0.52	12.1	0.82	0.55	0.84	0.85

excluding all terms found not-significant.

$$\begin{aligned} HA\ loss = {} & 32.1 \\ & - 2.3LD \\ & + 6.9[\mathrm{NaCl}]_{load} \\ & + 2.1Q_{load} \\ & + 3.9Q_{load}^2 \\ & - 1.6LD[\mathrm{NaCl}]_{load} \end{aligned} \tag{D.2}$$

$$\begin{aligned} HA\ yield = {} & 71.3 \\ & - 4.8LD \\ & + 2.8[\mathrm{NaCl}]_{load} \\ & + 22.0[\mathrm{NaCl}]_{elution} \\ & - 4.5Q_{load} \\ & + 8.3Q_{elution} \\ & - 9.3[\mathrm{NaCl}]_{elution}^2 \\ & + 7.0LD[\mathrm{NaCl}]_{elution} \\ & + 6.3[\mathrm{NaCl}]_{load}[\mathrm{NaCl}]_{elution} \\ & + 5.0[\mathrm{NaCl}]_{load}Q_{load} \end{aligned} \tag{D.3}$$

Analysis of variance (ANOVA) was used for the evaluation of the significance of the regression model of both responses (Table D.2). For both responses, the model is significant as attests the p-value (< 0.05), the F-value below the respective F_{crit} ($F_{crit} \leq 2.8$) and the lack of fit

(>0.05). Furthermore, the explained variation (R^2), predicted variation (Q^2), model validity and reproducibility are within accepted ranges[210].

Bibliography

[1] E. C. Hutchinson. Influenza virus. *Trends Microbiol.*, 2018.

[2] N. M. Bouvier and P. Palese. The biology of influenza viruses. *Vaccine*, 26:D49–D53, 2008.

[3] D. P. Nayak, R. A. B., H. Yamada, Z. H. Zhou, and S. Barman. Influenza virus morphogenesis and budding. *Virus Res.*, 143(2):147–161, 2009.

[4] F. Krammer, G. J. D. Smith, R. A. M. Fouchier, M. Peiris, K. Kedzierska, P. C. Doherty, P. Palese, M. L. Shaw, J. Treanor, R. G. Webster, and A. García-Sastre. Influenza. *Nat. Rev. Dis. Primers*, 4(3), 2018.

[5] J. E. Stencel-Baerenwald, K. Reiss, D. M. Reiter, T. Stehle, and T. S. Dermody. The sweet spot: defining virus–sialic acid interactions. *Nat. Rev. Microbiol.*, 12(11):739–749, 2014.

[6] R. A. Medina and A. García-Sastre. Influenza a viruses: new research developments. *Nat. Rev. Microbiol.*, 9(8):590–603, 2011.

[7] Influenza (seasonal). `http://www.who.int/news-room/fact-sheets/detail/influenza-(seasonal)`. Accessed: 2018-11-1.

[8] M. G. Ison. Optimizing antiviral therapy for influenza: understanding the evidence. *Expert Rev. Anti-Infe.*, 13(4):417–425, 2015.

[9] Antiviral drugs for seasonal influenza: Additional links and resources. `https://www.cdc.gov/flu/professionals/antivirals/links.htm`. Accessed: 2018-11-1.

[10] Edufluvac. http://www.edufluvac.eu/about-us/ru-test-about-page. Accessed: 2018-11-1.

[11] F. M. Davenport, A. V. Hennessy, et al. Predetermination by infection and by vaccination of antibody response to influenza virus vaccines. *J. Exp. Med.*, 106(6):835–850, 1957.

[12] V. C. Huber. Influenza vaccines: from whole virus preparations to recombinant protein technology. *Expert Rev. Vaccines*, 13(1):31–42, 2014.

[13] New influenza vaccine developments. https://ecdc.europa.eu/en/seasonal-influenza/prevention-and-control/vaccines/vaccine-developments. Accessed: 2018-11-1.

[14] E. Milián and A. A. Kamen. Current and emerging cell culture manufacturing technologies for influenza vaccines. *Biomed. Res. Int.*, 2015:504831, 2015.

[15] A. Harding and N. Heaton. Efforts to improve the seasonal influenza vaccine. *Vaccines*, 6(2):19, 2018.

[16] S. Pillet, É. Aubin, S. Trépanier, D. Bussière, M. Dargis, J.-F. Poulin, B. Yassine-Diab, B. J. Ward, and N. Landry. A plant-derived quadrivalent virus like particle influenza vaccine induces cross-reactive antibody and t cell response in healthy adults. *Clin. Immunol.*, 168:72–87, 2016.

[17] J. G. H. Low, L. S. Lee, E. E. Ooi, K. Ethirajulu, P. Yeo, A. Matter, J. E. Connolly, D. A. G. Skibinski, P. Saudan, M. Bachmann, B. J. Hanson, Q. Lu, S. Maurer-Stroh, S. Lim, and V. Novotny-Diermayr. Safety and immunogenicity of a virus-like particle pandemic influenza a (h1n1) 2009 vaccine: results from a double-blinded, randomized phase i clinical trial in healthy asian volunteers. *Vaccine*, 32(39):5041–5048, 2014.

[18] C. López-Macías, E. Ferat-Osorio, A. Tenorio-Calvo, A. Isibasi, J. Talavera, O. Arteaga-Ruiz, L. Arriaga-Pizano, S. P. Hickman, M. Allende, K. Lenhard, S. Pincus, K. Connolly, R. Raghunandan, G. Smith, and Glenn. G. Safety and immunogenicity of a virus-like particle pandemic influenza a (h1n1) 2009 vaccine in a blinded, randomized, placebo-controlled trial of adults in mexico. *Vaccine*, 29(44):7826–7834, 2011.

[19] L. F. Fries, G. E. Smith, and G. M. Glenn. A recombinant viruslike particle influenza a (h7n9) vaccine. *N. Engl. J. Med.*, 369(26):2564–2566, 2013.

[20] N. Valero-Pacheco, M. Pérez-Toledo, M. Á. Villasís-Keever, A. Núñez-Valencia, I. Boscó-Gárate, B. Lozano-Dubernard, H. Lara-Puente, C. Espitia, C. Alpuche-Aranda, L. C. Bonifaz, L. Arriaga-Pizano, R. Pastelin-Palacios, A. Isibasi, and C. López-Macías. Antibody persistence in adults two years after vaccination with an h1n1 2009 pandemic influenza virus-like particle vaccine. *PLoS One*, 11(2):e0150146, 2016.

[21] G. Smith, Y. Liu, D. Flyer, M. J. Massare, B. Zhou, N. Patel, L. Ellingsworth, M. Lewis, J. F. Cummings, and G. Glenn. Novel hemagglutinin nanoparticle influenza vaccine with matrix-m adjuvant induces hemagglutination inhibition, neutralizing, and protective responses in ferrets against homologous and drifted a (h3n2) subtypes. *Vaccine*, 35(40):5366–5372, 2017.

[22] L. Deng, T. Mohan, T. Z. Chang, G. X. Gonzalez, Y. Wang, Y.-M. Kwon, S.-M. Kang, R. W. Compans, J. A. Champion, and B.-Z. Wang. Double-layered protein nanoparticles induce broad protection against divergent influenza a viruses. *Nat. Commun.*, 9(1):359, 2018.

[23] Larry R Smith, Mary K Wloch, Ming Ye, Luane R Reyes, Souphaphone Boutsaboualoy, Casey E Dunne, Jennifer A Chaplin, Denis Rusalov, Alain P Rolland, Cindy L Fisher, M. S. Al-Ibrahim, M. L. Kabongo, R. Steigbigel, R. B. Belshe, E. R. Kitt, A. H. Chu, and R. B. Moss. Phase 1 clinical trials of the safety and immunogenicity of adjuvanted plasmid dna vaccines encoding influenza a virus h5 hemagglutinin. *Vaccine*, 28(13):2565–2572, 2010.

[24] J. E. Ledgerwood, C.-J. Wei, Z. Hu, I. J. Gordon, M. E. Enama, C. S. Hendel, P. M. McTamney, M. B. Pearce, H. M. Yassine, J. C. Boyington, R. Bailer, T. M. Tumpey, R. A. Koup, J. R. Mascola, G. J. Nabel, B. S. Graham, and VRC 306 Study Team. Dna priming and influenza vaccine immunogenicity: two phase 1 open label randomised clinical trials. *Lancet Infect. Dis.*, 11(12):916–924, 2011.

[25] A. D DeZure, E. E. Coates, Z. Hu, G. V. Yamshchikov, K. L. Zephir, M. E. Enama, S. H. Plummer, I. J. Gordon, F. Kaltovich, S. Andrews,

A. McDermott, M. C. Crank, R. A. Koup, R. M. Schwartz, R. T. Bailer, X. Sun, J. R. Mascola, T. M. Tumpey, B. S. Graham, and J. E. Ledgerwood. An avian influenza h7 dna priming vaccine is safe and immunogenic in a randomized phase i clinical trial. *npj Vaccines*, 2(1):15, 2017.

[26] A. Stachyra, A. Góra-Sochacka, and A. Sirko. Dna vaccines against influenza. *Acta Biochimica Polonica*, 61(3), 2014.

[27] M. Brazzoli, D. Magini, A. Bonci, S. Buccato, C. Giovani, R. Kratzer, V. Zurli, S. Mangiavacchi, D. Casini, L. M. Brito, E. De Gregorio, P. W. Mason, J. B. Ulmer, A. J. Geall, and S. Bertholet. Induction of broad-based immunity and protective efficacy by self-amplifying mrna vaccines encoding influenza virus hemagglutinin. *J. Virol.*, 90(1):332–344, 2016.

[28] K. Bahl, J. J. Senn, O. Yuzhakov, A. Bulychev, L. A. Brito, K. J. Hassett, M. E. Laska, M. Smith, Ö. Almarsson, J. Thompson, A. (M.) Ribeiro, M. Watson, T. Zaks, and G. Ciaramella. Preclinical and clinical demonstration of immunogenicity by mrna vaccines against h10n8 and h7n9 influenza viruses. *Mol. Ther.*, 25(6):1316–1327, 2017.

[29] D. Magini, C. Giovani, S. Mangiavacchi, S. Maccari, R. Cecchi, J. B. Ulmer, E. De Gregorio, A. J. Geall, M. Brazzoli, and S. Bertholet. Self-amplifying mrna vaccines expressing multiple conserved influenza antigens confer protection against homologous and heterosubtypic viral challenge. *PloS one*, 11(8):e0161193, 2016.

[30] R. D. de Vries and G. F. Rimmelzwaan. Viral vector-based influenza vaccines. *Hum. Vacc. Immunother.*, 12(11):2881–2901, 2016.

[31] S. Sebastian and T. Lambe. Clinical advances in viral-vectored influenza vaccines. *Vaccines*, 6(2):29, 2018.

[32] Us food and drug administration. fda approves new seasonal influenza vaccine made using novel technology. us food and drug administration (2013). `https://www.fda.gov/newsevents/publichealthfocus/ucm335635.htm`. Accessed: 2018-11-4.

[33] F. Krammer and P. Palese. Advances in the development of influenza virus vaccines. *Nat. Rev. Drug Discov.*, 14(3):167, 2015.

[34] P. R. Dormitzer, P. Suphaphiphat, D. G. Gibson, D. E. Wentworth, T. B. Stockwell, M. A. Algire, N. Alperovich, M. Barro, D. M. Brown, S. Craig, B. M. Dattilo, E. A. Denisova, I. de Souza, M. Eickmann, V. G. Dugan, A. Ferrari, R. C. Gomila, L. Han, C. Judge, S. Mane, M. Matrosovich, C. Merryman, G. Palladino, G. A. Palmer, T. Spencer, T. Strecker, H. Trusheim, J. Uhlendorff, Y. Wen, A. C. Yee, J. Zaveri, B. Zhou, S. Becker, A. Donabedian, P. W. Mason, J. I. Glass, R. Rappuoli, and J. C. Venter. Synthetic generation of influenza vaccine viruses for rapid response to pandemics. *Sci. Transl. Med.*, 5(185):185ra68, 2013.

[35] P. R Dormitzer. Rapid production of synthetic influenza vaccines. In *Influenza Pathogenesis and Control-Volume II*, pages 237–273. Springer, 2014.

[36] E. M. Plummer and M. Manchester. Viral nanoparticles and virus-like particles: platforms for contemporary vaccine design. *Wires Nanomed. Nanobiotech.*, 3(2):174–196, 2011.

[37] F. Pitoiset, T. Vazquez, and B. Bellier. Enveloped virus-like particle platforms: vaccines of the future? *Expert Rev. Vaccines*, 14(7):913–915, 2015.

[38] Q. J. Zhao, S. W. Li, H. Yu, N. S. Xia, and Y. Modis. Virus-like particle-based human vaccines: quality assessment based on structural and functional properties. *Trends Biotechnol.*, 31(11):654–663, 2013.

[39] F. Krammer. Novel universal influenza virus vaccine approaches. *Curr. Opin. Virol.*, 17:95–103, 2016.

[40] S.-M. Kang, J.-M. Song, F.-S. Quan, and R. W. Compans. Influenza vaccines based on virus-like particles. *Virus Res.*, 143(2):140–146, 2009.

[41] Y. V. Liu, M. J. Massare, M. B. Pearce, X. Sun, J. A. Belser, T. R. Maines, H. M. Creager, G. M. Glenn, P. Pushko, G. E. Smith, and T. M. Tumpey. Recombinant virus-like particles elicit protective immunity against avian influenza a (h7n9) virus infection in ferrets. *Vaccine*, 33(18):2152–2158, 2015.

[42] F.-S. Quan, Y.-T. Lee, K.-H. Kim, M.-C. Kim, and S.-M. Kang. Progress in developing virus-like particle influenza vaccines. *Expert Rev. Vaccines*, 15(10):1281–1293, 2016.

[43] C. L. Effio and J. Hubbuch. Next generation vaccines and vectors: Designing downstream processes for recombinant protein-based virus-like particles. *Biotechnol. J.*, 10(5):715–727, 2015.

[44] M. G Mateu. Virus engineering: functionalization and stabilization. *Protein Eng. Des. Sel.*, 24(1-2):53–63, 2010.

[45] S. J. Kaczmarczyk, K. Sitaraman, H. A. Young, S. H. Hughes, and D. K. Chatterjee. Protein delivery using engineered virus-like particles. *Proc. Natl. Acad. Sci. USA*, 108(41):16998–17003, 2011.

[46] W. Wu, S. C. Hsiao, Z. M. Carrico, and M. B. Francis. Genome-free viral capsids as multivalent carriers for taxol delivery. *Angew. Chem. Int. Ed.*, 48(50):9493–9497, 2009.

[47] S. G. Tarasov, V. Gaponenko, O. M. Z. Howard, Y. H. Chen, J. J. Oppenheim, M. A. Dyba, S. Subramaniam, Y. Lee, C. Michejda, and N. I. Tarasova. Structural plasticity of a transmembrane peptide allows self-assembly into biologically active nanoparticles. *Proc. Natl. Acad. Sci. USA*, 108(24):9798–9803, 2011.

[48] FLUAD Seqirus Inc. Us package insert. 2018.

[49] A. Doroshenko and S. A. Halperin. Trivalent mdck cell culture-derived influenza vaccine optaflu®(novartis vaccines). *Expert Rev. Vaccines*, 8(6):679–688, 2009.

[50] I. Manini, A. Domnich, D. Amicizia, S. Rossi, T. Pozzi, R. Gasparini, D. Panatto, and E. Montomoli. Flucelvax (optaflu) for seasonal influenza. *Expert Rev. Vaccines*, 14(6):789–804, 2015.

[51] M. M. J. Cox and Y. Hashimoto. A fast track influenza virus vaccine produced in insect cells. *J. Invertebr. Pathol.*, 107:S31–S41, 2011.

[52] R. Morenweiser. Downstream processing of viral vectors and vaccines. *Gene Ther.*, 12(S1):S103–S110, 2005.

[53] D. P. Sequeira, R. Correia, M. J. T. Carrondo, A. Roldão, A. P. Teixeira, and P. M. Alves. Combining stable insect cell lines with baculovirus-mediated expression for multi-ha influenza vlp production. *Vaccine*, 36(22):3112–3123, 2018.

[54] S. B. Carvalho, J. M. Freire, M. G. Moleirinho, F. Monteiro, D. Gaspar, M. A. R. B. Castanho, M. J. T. Carrondo, P. M. Alves, G. J. L. Bernardes, and C. Peixoto. Bioorthogonal strategy for bioprocessing of specific-site-functionalized enveloped influenza-virus-like particles. *Bioconjug. Chem.*, 27(10):2386–2399, 2016.

[55] S. B. Carvalho, M. G. Moleirinho, D. Wheatley, J. Welsh, R. Gantier, P. M. Alves, C. Peixoto, and M. J. T. Carrondo. Universal label-free in-process quantification of influenza virus-like particles. *Biotechnol. J.*, 12(8):1700031, 2017.

[56] S. B. Carvalho, A. R. Fortuna, M. W. Wolff, C. Peixoto, P. M. Alves, U. Reichl, and M. J. T. Carrondo. Purification of influenza virus-like particles using sulfated cellulose membrane adsorbers. *J. Chem. Technol. Biot.*, 93:1988–1996, 2018.

[57] S. B. Carvalho, R. Silva, A. S. Moreira, B. Cunha, J. J. Clemente, P. M. Alves, M. J. T. Carrondo, A. Xenopoulos, and C. Peixoto. Efficient filtration strategies for the clarification of influenza virus-like particles derived from insect cells. *Submitted*.

[58] S. B. Carvalho, R. Silva, M. G. Moleirinho, B. Cunha, A. S. Moreira, P. M. Alves, M. J. T. Carrondo, A. Xenopoulos, and C. Peixoto. Membrane-based approach for the downstream processing of influenza virus-like particles. *Submitted*.

[59] C. M. Thompson, E. Petiot, A. Mullick, M. G. Aucoin, O. Henry, and A. A. Kamen. Critical assessment of influenza vlp production in sf9 and hek293 expression systems. *BMC Biotechnol.*, 15(1):31, 2015.

[60] Y. Ho, H.-R. Lo, T.-C. Lee, C. P. Y. Wu, and Y.-C. Chao. Enhancement of correct protein folding in vivo by a non-lytic baculovirus. *Biochem. J.*, 382(2):695–702, 2004.

[61] L. Besnard, V. Fabre, M. Fettig, E. Gousseinov, Y. Kawakami, N. Laroudie, C. Scanlan, and P. Pattnaik. Clarification of vaccines: An overview of filter based technology trends and best practices. *Biotechnol. Adv.*, 34(1):1–13, 2016.

[62] M. W. Wolff and U. Reichl. Downstream processing of cell culture-derived virus particles. *Expert Rev. Vaccines*, 10(10):1451–1475, 2011.

[63] FDA Briefing Document. Cell lines derived from human tumors for vaccine manufacture. *Vaccines and Related Biological Products Advisory Committee Meeting*, 2012.

[64] P. Nestola, C. Peixoto, R. R. J. S. Silva, P. M. Alves, J. P. B. Mota, and M. J. T. Carrondo. Improved virus purification processes for vaccines and gene therapy. *Biotechnol. Bioeng.*, 112(5):843–857, 2015.

[65] T. Kröber, M. W. Wolff, B. Hundt, A. Seidel-Morgenstern, and U. Reichl. Continuous purification of influenza virus using simulated moving bed chromatography. *J. Chromatogr. A*, 1307:99–110, 2013.

[66] B. Michen and T. Graule. Isoelectric points of viruses. *J. Appl. Microbiol.*, 109(2):388–397, 2010.

[67] A. Wang, R. Lewus, and A. S. Rathore. Comparison of different options for harvest of a therapeutic protein product from high cell density yeast fermentation broth. *Biotechnol. Bioeng.*, 94(1):91–104, 2006.

[68] N. Singh, K. Pizzelli, J. K. Romero, J. Chrostowski, G. Evangelist, J. Hamzik, N. Soice, and K. S. Cheng. Clarification of recombinant proteins from high cell density mammalian cell culture systems using new improved depth filters. *Biotechnol. Bioeng.*, 110(7):1964–1972, 2013.

[69] B. Kalbfuss, Y. Genzel, M. Wolff, A. Zimmermann, R. Morenweiser, and U. Reichl. Harvesting and concentration of human influenza a virus produced in serum-free mammalian cell culture for the production of vaccines. *Biotechnol. Bioeng.*, 97(1):73–85, 2007.

[70] K. Hughes, A. Zachertowska, S. Wan, L. Li, D. Klimaszewski, M. Euloth, and T. F. Hatchette. Yield increases in intact influenza vaccine virus from chicken allantoic fluid through isolation from insoluble allantoic debris. *Vaccine*, 25(22):4456–4463, 2007.

[71] M. Felo, B. Christensen, and J. Higgins. Process cost and facility considerations in the selection of primary cell culture clarification technology. *Biotechnol. Progr.*, 29(5):1239–1245, 2013.

[72] M. W. Wolff and U. Reichl. Downstream processing: from egg to cell culture-derived influenza virus particles. *Chem. Eng. Technol.*, 31(6):846–857, 2008.

[73] P. Kramberger, L. Urbas, and A. Štrancar. Downstream processing and chromatography based analytical methods for production of vaccines, gene therapy vectors, and bacteriophages. *Hum. Vacc. Immunother.*, 11(4):1010–1021, 2015.

[74] T. J. Hahn, M. Hamer, M. Masoud, J. Wong, K. Taylor, J. Hatch, E. Shane, M. Nathan, H. Jiang, Z. Wei, J. Higgins, K.-H. Roh, J. Burd, M. Malou-Williams, D. P. Baskind, and G. E. Smith. Rapid manufacture and release of a gmp batch of avian influenza a(h7n9) virus-like particle vaccine made using recombinant baculovirus-sf9 insect cell culture technology. *BioProcess. J.*, 12:4–17, 2013.

[75] Y.-F. Tseng, T.-C. Weng, C.-C. Lai, P.-L. Chen, M.-S. Lee, and A. Y.-C. Hu. A fast and efficient purification platform for cell-based influenza viruses by flow-through chromatography. *Vaccine*, 36(22):3146–3152, 2018.

[76] D. P. Nayak, S. Lehmann, and U. Reichl. Downstream processing of mdck cell-derived equine influenza virus. *J. Chromatogr. B*, 823(2):75–81, 2005.

[77] S. R. Wickramasinghe, B. Kalbfuss, A. Zimmermann, V. Thom, and U. Reichl. Tangential flow microfiltration and ultrafiltration for human influenza a virus concentration and purification. *Biotechnol. Bioeng.*, 92(2):199–208, 2005.

[78] N. N. Asanzhanova, Sh. Zh. Ryskeldinova, O. V. Chervyakova, B. M. Khairullin, M. M. Kasenov, and K. K. Tabynov. Comparison of different methods of purification and concentration in production of influenza vaccine. *B. Exp. Biol. Med.*, 164(2):229–232, 2017.

[79] C. Teepakorn, K. Fiaty, and C. Charcosset. Comparison of membrane chromatography and monolith chromatography for lactoferrin and bovine serum albumin separation. *Processes*, 4(3):31, 2016.

[80] K. Benčina, M. Benčina, A. Podgornik, and A. Štrancar. Influence of the methacrylate monolith structure on genomic dna mechanical degradation, enzymes activity and clogging. *J. Chromatogr. A*, 1160(1-2):176–183, 2007.

[81] J. H. Vogel, H. Nguyen, R. Giovannini, J. Ignowski, S. Garger, A. Salgotra, and J. Tom. A new large-scale manufacturing platform for complex biopharmaceuticals. *Biotechnol. Bioeng.*, 109(12):3049–3058, 2012.

[82] B. Kalbfuss, M. Wolff, L. Geisler, A. Tappe, R. Wickramasinghe, V. Thom, and U. Reichl. Direct capture of influenza a virus from cell culture supernatant with sartobind anion-exchange membrane adsorbers. *J. Membrane Sci.*, 299:251–260, 2007.

[83] B. Kalbfuss, M. Wolff, R. Morenweiser, and U. Reichl. Purification of cell culture-derived human influenza a virus by size-exclusion and anion-exchange chromatography. *Biotechnol. Bioeng.*, 96(5):932–944, 2007.

[84] M. Banjac, E. Roethl, F. Gelhart, P. Kramberger, B. L. Jarc, M. Jarc, A. Štrancar, T. Muster, and M. Peterka. Purification of vero cell derived live replication deficient influenza a and b virus by ion exchange monolith chromatography. *Vaccine*, 32(21):2487–2492, 2014.

[85] M. Zhao, M. Vandersluis, J. Stout, U. Haupts, M. Sanders, and R. Jacquemart. Affinity chromatography for vaccines manufacturing: Finally ready for prime time? *Vaccine*, 2018.

[86] L. Opitz, J. Salaklang, H. Büttner, U. Reichl, and M. W. Wolff. Lectin-affinity chromatography for downstream processing of mdck cell culture derived human influenza a viruses. *Vaccine*, 25(5):939–947, 2007.

[87] L. Opitz, S. Lehmann, U. Reichl, and M. W. Wolff. Sulfated membrane adsorbers for economic pseudo-affinity capture of influenza virus particles. *Biotechnol. Bioeng.*, 103(6):1144–1154, 2009.

[88] L. Opitz, S. Lehmann, U. Reichl, and M. W. Wolff. Sulfated membrane adsorbers for economic pseudo-affinity capture of influenza virus particles. *Biotechnol. Bioeng.*, 103(6):1144–1154, 2009.

[89] T. Oka, K. Ohkuma, T. Kawahara, and M. Sakoh. Method for purification of influenza virus, February 9 1988. US Patent 4,724,210.

[90] Y. Sakoda, M. Okamatsu, N. Isoda, N. Yamamoto, K. Ozaki, Y. Umeda, S. Aoyama, and H. Kida. Purification of human and avian influenza viruses using cellulose sulfate ester (cellufine sulfate) in the process of vaccine production. *Microbiol. Immunol.*, 56(7):490–495, 2012.

[91] L. Opitz, S. Lehmann, A. Zimmermann, U. Reichl, and M. W. Wolff. Impact of adsorbents selection on capture efficiency of cell culture derived human influenza viruses. *J. Biotechnol.*, 131(3):309–317, 2007.

[92] T. Weigel, T. Solomaier, S. Wehmeyer, A. Peuker, M. W. Wolff, and U. Reichl. A membrane-based purification process for cell culture-derived influenza a virus. *J. Biotechnol.*, 220:12–20, 2016.

[93] M. Wolff, U. Reichl, and L. Opitz. Method for the preparation of sulfated cellulose membranes and sulfated cellulose membranes, 2012. US Patent 8,173,021.

[94] L. Villain, H.-H. Hörl, and C. Brumm. Sulfated cellulose hydrate membrane, method for producing same, and use of the membrane as an adsorption membrane for a virus purification process, September 8 2016. US Patent App. 15/029,203.

[95] A. R. Fortuna, F. Taft, L. Villain, M. W. Wolff, and U. Reichl. Optimization of cell culture-derived influenza a virus particles purification using sulfated cellulose membrane adsorbers. *Eng. Life Sci.*, 18(1):29–39, 2018.

[96] C. M. Thompson, E. Petiot, A. Lennaertz, O. Henry, and A. A. Kamen. Analytical technologies for influenza virus-like particle candidate vaccines: challenges and emerging approaches. *Virol. J.*, 10(1):141, 2013.

[97] F. Monteiro, N. Carinhas, M. J. T. Carrondo, V. Bernal, and P. M. Alves. Toward system-level understanding of baculovirus–host cell interactions: from molecular fundamental studies to large-scale proteomics approaches. *Front. Microbiol.*, 3:391, 2012.

[98] L. Opitz, A. Zimmermann, S. Lehmann, Y. Genzel, H. Lübben, U. Reichl, and M. W. Wolff. Capture of cell culture-derived influenza virus by lectins: Strain independent, but host cell dependent. *J. Virol. Methods*, 154(1-2):61–68, 2008.

[99] M. W. Wolff, C. Siewert, S. P. Hansen, R. Faber, and U. Reichl. Purification of cell culture-derived modified vaccinia ankara virus by pseudo-affinity membrane adsorbers and hydrophobic interaction chromatography. *Biotechnol. Bioeng.*, 107(2):312–320, 2010.

[100] P. Gagnon. Chromatographic purification of virus particles. In *Encyclopedia of Industrial Biotechnology: Bioprocess, Bioseparation, and Cell Technology*, pages 1–21. Wiley Online Library, 2009.

[101] G. Iyer, S. Ramaswamy, K.-S. Cheng, N. Sisowath, U. Mehta, A. Leahy, F. Chung, and D. Asher. Flow-through purification of viruses-a novel approach to vaccine purification. *Procedia Vaccinol.*, 6:106–112, 2012.

[102] Y. Kurosawa, M. Saito, D. Yoshikawa, and M. Snyder. Mammalian virus purification using ceramic hydroxyapatite. *BIO-RAD Tech Note*, Bulletin 6549, 2014.

[103] T. Weigel, T. Solomaier, A. Peuker, T. Pathapati, M. W. Wolff, and U. Reichl. A flow-through chromatography process for influenza a and b virus purification. *J. Virol. Methods*, 207:45–53, 2014.

[104] European Pharmacopoeia. Influenza vaccine (whole virion, inactivated, prepared in cell cultures). *Eur. Dir. Qual. Med.*, 2012.

[105] P. Marichal-Gallardo, M. M. Pieler, M. W. Wolff, and U. Reichl. Steric exclusion chromatography for purification of cell culture-derived influenza a virus using regenerated cellulose membranes and polyethylene glycol. *J. Chromatogr. A*, 1483:110–119, 2017.

[106] P. Nestola, R. J. S. Silva, C. Peixoto, P. M. Alves, M. J. T. Carrondo, and J. P. B. Mota. Adenovirus purification by two-column, size-exclusion, simulated countercurrent chromatography. *J. Chromatogr. A*, 1347:111–121, 2014.

[107] L. M. Fischer, M. W. Wolff, and U. Reichl. Purification of cell culture-derived influenza a virus via continuous anion exchange chromatography on monoliths. *Vaccine*, 36(22):3153–3160, 2018.

[108] A. Rajendran, G. Paredes, and M. Mazzotti. Simulated moving bed chromatography for the separation of enantiomers. *J. Chromatogr. A*, 1216(4):709–738, 2009.

[109] R. Godawat, K. Brower, S. Jain, K. Konstantinov, F. Riske, and V. Warikoo. Periodic counter-current chromatography–design and operational considerations for integrated and continuous purification of proteins. *Biotechnol. J.*, 7(12):1496–1508, 2012.

[110] S. N. Politis, P. Colombo, G. Colombo, and D. M. Rekkas. Design of experiments (doe) in pharmaceutical development. *Drug Dev. Ind. Pharm.*, 43(6):889–901, 2017.

[111] D. B. Hibbert. Experimental design in chromatography: a tutorial review. *J. Chromatogr. B*, 910:2–13, 2012.

[112] S. Muthukumar and A. S. Rathore. High throughput process development (htpd) platform for membrane chromatography. *J. Membrane Sci.*, 442:245–253, 2013.

[113] Y. Ji, Y. Tian, M. Ahnfelt, and L. Sui. Design and optimization of a chromatographic purification process for streptococcus pneumoniae serotype 23f capsular polysaccharide by a design of experiments approach. *J. Chromatogr. A*, 1348:137–149, 2014.

[114] A. Afonso, P. Pereira, J. A. Queiroz, Â. Sousa, and F. Sousa. Purification of pre-mir-29 by a new o-phospho-l-tyrosine affinity chromatographic strategy optimized using design of experiments. *J. Chromatogr. A*, 1343:119–127, 2014.

[115] A. M. Almeida, J. A. Queiroz, F. Sousa, and A. Sousa. Optimization of supercoiled hpv-16 e6/e7 plasmid dna purification with arginine monolith using design of experiments. *J. Chromatogr. B*, 978:145–150, 2015.

[116] P. Nestola, C. Peixoto, L. Villain, P. M. Alves, M. J. T. Carrondo, and J. Mota. Rational development of two flowthrough purification strategies for adenovirus type 5 and retro virus-like particles. *J. Chromatogr. A*, 1426:91–101, 2015.

[117] A. F. Rodrigues, M. J. T. Carrondo, P. M. Alves, and A. S. Coroadinha. Cellular targets for improved manufacturing of virus-based biopharmaceuticals in animal cells. *Trends Biotechnol.*, 32(12):602–607, 2014.

[118] A. F. Rodrigues, H. R. Soares, M. R. Guerreiro, P. M. Alves, and A. S. Coroadinha. Viral vaccines and their manufacturing cell substrates: New trends and designs in modern vaccinology. *Biotechnol. J.*, 10(9):1329–1344, 2015.

[119] C. Sheridan. Gene therapy finds its niche. *Nat. Biotechnol.*, page 121–128, 2011.

[120] M. C. Milone and U. O'Doherty. Clinical use of lentiviral vectors. *Leukemia*, page 1, 2018.

[121] J. O. Josefsberg and B. Buckland. Vaccine process technology. *Biotechnol. Bioeng.*, 109(6):1443–1460, 2012.

[122] J. Smith, M. Lipsitch, and J. W. Almond. Vaccine production, distribution, access, and uptake. *The Lancet*, 378(9789):428–438, 2011.

[123] P. Pushko, M. B. Pearce, A. Ahmad, I. Tretyakova, G. Smith, J. A. Belser, and T. M. Tumpey. Influenza virus-like particle can accommodate multiple subtypes of hemagglutinin and protect from multiple influenza types and subtypes. *Vaccine*, 29(35):5911–5918, 2011.

[124] W. J. Marks Jr., J. L. Ostrem, L. Verhagen, P. A. Starr, P. S. Larson, R. A. E. Bakay, R. Taylor, D. A. Cahn-Weiner, A. J. Stoessl, C. W. Olanow, and R. T. Bartus. Safety and tolerability of intraputaminal delivery of cere-120 (adeno-associated virus serotype 2–neurturin) to patients with idiopathic parkinson's disease: an open-label, phase i trial. *Lancet Neurol.*, 7(5):400–408, 2008.

[125] L. Zhou, M. Miranda-Saksena, and N. K. Saksena. Viruses and neurodegeneration. *Virol. J.*, 10(1):172, 2013.

[126] EMEA. Specifications: Test procedures and acceptance criteria for biotechnological / biological products. 1999.

[127] ECH. Viral safety evaluation of biotechnology products derived from cell lines of human or animal origin. ich q5a(r1). 1999.

[128] ECH. Evaluation and recommendation of pharmacopoeial texts for use in the ich regions. ich q4b. 2007.

[129] G. Jagschies, E. Lindskog, K. Lacki, and P. M. Galliher. *Biopharmaceutical Processing: Development, Design, and Implementation of Manufacturing Processes*. Elsevier, 2018.

[130] A. P. Manceur and A. A. Kamen. Critical review of current and emerging quantification methods for the development of influenza vaccine candidates. *Vaccine*, 33(44):5913–5919, 2015.

[131] A. M. Hashem, C. Gravel, A. Farnsworth, W. Zou, M. Lemieux, K. Xu, C. Li, J. Wang, M.-F. Goneau, M. Merziotis, R. He, M. Gilbert, and X. Li. A novel synthetic receptor-based immunoassay for influenza vaccine quantification. *PLoS One*, 8(2):e55428, 2013.

[132] M. S. Williams. Single-radial-immunodiffusion as an in vitro potency assay for human inactivated viral vaccines. *Vet. Microbiol.*, 37(3-4):253–262, 1993.

[133] L. R. Kuck, S. Saye, S. Loob, S. Roth-Eichhorn, R. Byrne-Nash, and K. L. Rowlen. Vaxarray assessment of influenza split vaccine potency and stability. *Vaccine*, 35(15):1918–1925, 2017.

[134] P. Minor. Assaying the potency of influenza vaccines. *Vaccines*, 3(1):90–104, 2015.

[135] F. Schmeisser, G. M. Vodeiko, V. Y. Lugovtsev, R. R. Stout, and J. P. Weir. An alternative method for preparation of pandemic influenza strain-specific antibody for vaccine potency determination. *Vaccine*, 28(12):2442–2449, 2010.

[136] M. L. Killian. Hemagglutination assay for influenza virus. In *Animal Influenza Virus*, pages 3–9. Springer, 2014.

[137] X.-C. Tang, H.-R. Lu, and T. M. Ross. Hemagglutinin displayed baculovirus protects against highly pathogenic influenza. *Vaccine*, 28(42):6821–6831, 2010.

[138] R. C. Buxton, B. Edwards, R. R. Juo, J. C. Voyta, M. Tisdale, and R. C. Bethell. Development of a sensitive chemiluminescent neuraminidase assay for the determination of influenza virus susceptibility to zanamivir. *Anal. Biohem.*, 280(2):291–300, 2000.

[139] D. P. Nayak and U. Reichl. Neuraminidase activity assays for monitoring mdck cell culture derived influenza virus. *J. Virol. Methods*, 122(1):9–15, 2004.

[140] K. Xu, C. Li, C. Gravel, Z. Jiang, B. Jaentschke, G. Domselaar, X. Li, and J. Wang. Universal type/subtype-specific antibodies for quantitative analyses of neuraminidase in trivalent influenza vaccines. *Sci. Rep.-UK*, 8(1):1067, 2018.

[141] I. Legastelois, M. Chevalier, M.-C. Bernard, A. de Montfort, M. Fouque, A. Pilloud, C. Serraille, N. Devard, O. Engel, R. Sodoyer, and C. Moste. Avian glycan-specific igm monoclonal antibodies for the detection and quantitation of type a and b haemagglutinins in egg-derived influenza vaccines. *J. Virol. Methods*, 178(1-2):129–136, 2011.

[142] L. R. Kuck, M. Sorensen, E. Matthews, I. Srivastava, M. M. J. Cox, and K. L. Rowlen. Titer on chip: new analytical tool for influenza vaccine potency determination. *PloS one*, 9(10):e109616, 2014.

[143] J. C. Kapteyn, A. M. Porre, E. J. P. De Rond, W. B. Hessels, M. A. Tijms, H. Kessen, A. M. E. Slotboom, M. A. Oerlemans, D. Smit, J. van der Linden, P. Schoen, and J. L. G. Thus. Hplc-based quantification of haemagglutinin in the production of egg-and mdck cell-derived influenza virus seasonal and pandemic vaccines. *Vaccine*, 27(9):1468–1477, 2009.

[144] J. C. Kapteyn, M. D. Saidi, R. Dijkstra, C. Kars, J. C. M. S.-K. Tjon, G. J. Weverling, M. L. de Vocht, R. Kompier, B. A. van Montfort, J.-Y. Guichoux, J. Goudsmit, and F. M. Lagerwerf. Haemagglutinin quantification and identification of influenza a&b strains propagated in per. c6® cells: a novel rp-hplc method. *Vaccine*, 24(16):3137–3144, 2006.

[145] Y. Wen, L. Han, G. Palladino, A. Ferrari, Y. Xie, A. Carfi, P. R. Dormitzer, and E. C. Settembre. Conformationally selective biophysical assay for influenza vaccine potency determination. *Vaccine*, 33(41):5342–5349, 2015.

[146] B. Lorbetskie, J. Wang, C. Gravel, C. Allen, M. Walsh, A. Rinfret, X. Li, and M. Girard. Optimization and qualification of a quantitative reversed-phase hplc method for hemagglutinin in influenza preparations and its comparative evaluation with biochemical assays. *Vaccine*, 29(18):3377–3389, 2011.

[147] J. Transfiguracion, A. P. Manceur, E. Petiot, C. M Thompson, and A. A. Kamen. Particle quantification of influenza viruses by high performance liquid chromatography. *Vaccine*, 33(1):78–84, 2015.

[148] C. E. Nilsson, S. Abbas, M. Bennemo, A. Larsson, M. D. Hämäläinen, and Å. Frostell-Karlsson. A novel assay for influenza virus quantification using surface plasmon resonance. *Vaccine*, 28(3):759–766, 2010.

[149] X. Xiong, S. R. Martin, L. F. Haire, S. A. Wharton, R. S. Daniels, M. S. Bennett, J. W. McCauley, P. J. Collins, P. A. Walker, J. J. Skehel, and S. J. Gamblin. Receptor binding by an h7n9 influenza virus from humans. *Nature*, 499(7459):496–499, 2013.

[150] S. Khurana, L. R. King, J. Manischewitz, E. M. Coyle, and H. Golding. Novel antibody-independent receptor-binding spr-based assay for rapid measurement of influenza vaccine potency. *Vaccine*, 32(19):2188–2197, 2014.

[151] C. L. Pierce, T. L. Williams, H. Moura, J. L. Pirkle, N. J. Cox, J. Stevens, R. O. Donis, and J. R. Barr. Quantification of immunoreactive viral influenza proteins by immunoaffinity capture and isotope-dilution liquid chromatography–tandem mass spectrometry. *Anal. Chem.*, 83(12):4729–4737, 2011.

[152] T. L. Williams, J. L. Pirkle, and J. R. Barr. Simultaneous quantification of hemagglutinin and neuraminidase of influenza virus using isotope dilution mass spectrometry. *Vaccine*, 30(14):2475–2482, 2012.

[153] World Health Organization. *Influenza (Seasonal) Fact Sheet No. 211.* 2014.

[154] A. Iwasaki and P. S. Pillai. Innate immunity to influenza virus infection. *Nat. Rev. Immunol.*, 14(5):315–328, 2014.

[155] J. Stevens, O. Blixt, J. C. Paulson, and I. A. Wilson. Glycan microarray technologies: tools to survey host specificity of influenza viruses. *Nat. Rev. Microbiol.*, 4(11):857–864, 2006.

[156] E. Suenaga, H. Mizuno, and K. K. R. Penmetcha. Monitoring influenza hemagglutinin and glycan interactions using surface plasmon resonance. *Biosens. Bioelectron.*, 32(1):195–201, 2012.

[157] F. Krammer. Emerging influenza viruses and the prospect of a universal influenza virus vaccine. *Biotechnol. J.*, 10(5):690–701, 2015.

[158] J. A. Mena, O. T. Ramírez, and L. A. Palomares. Titration of non-occluded baculovirus using a cell viability assay. *Biotechniques*, 34(2):260–264, 2003.

[159] A. Roldão, R. Oliveira, M. J. T. Carrondo, and P. M. Alves. Error assessment in recombinant baculovirus titration: evaluation of different methods. *J. Virol. Methods*, 159(1):69–80, 2009.

[160] E. Montomoli, B. Capecchi, and K. Hoschler. Correlates of protection against influenza. In *Influenza vaccines for the future*, pages 199–222. Springer, 2011.

[161] S. G. Vachieri, X. Xiong, P. J. Collins, P. A. Walker, S. R. Martin, L. F. Haire, Y. Zhang, J. W. McCauley, S. J. Gamblin, and J. J. Skehel. Receptor binding by h10 influenza viruses. *Nature*, 511(7510):475, 2014.

[162] J. Bodle, E. E. Verity, C. Ong, K. Vandenberg, R. Shaw, I. G. Barr, and S. Rockman. Development of an enzyme-linked immunoassay for the quantitation of influenza haemagglutinin: an alternative method to single radial immunodiffusion. *Influenza Other Resp.*, 7(2):191–200, 2013.

[163] I. Margine, L. Martinez-Gil, Y.-Y. Chou, and F. Krammer. Residual baculovirus in insect cell-derived influenza virus-like particle preparations enhances immunogenicity. *PloS one*, 7(12):e51559, 2012.

[164] F. Fernandes, A. P. Teixeira, N. Carinhas, M. J. T. Carrondo, and P. M. Alves. Insect cells as a production platform of complex virus-like particles. *Expert Rev. Vaccines*, 12(2):225–236, 2013.

[165] L. H. L. Lua, N. K. Connors, F. Sainsbury, Y. P. Chuan, N. Wibowo, and A. P. J. Middelberg. Bioengineering virus-like particles as vaccines. *Biotechnol. Bioeng.*, 111(3):425–440, 2014.

[166] P. S. Banerjee, P. Ostapchuk, P. Hearing, and I. S. Carrico. Unnatural amino acid incorporation onto adenoviral (ad) coat proteins facilitates chemoselective modification and retargeting of ad type 5 vectors. *J. Virol.*, 85(15):7546–7554, 2011.

[167] A. M. ElSohly, C. Netirojjanakul, I. L. Aanei, A. Jager, S. C. Bendall, M. E. Farkas, G. P. Nolan, and M. B. Francis. Synthetically modified viral capsids as versatile carriers for use in antibody-based cell targeting. *Bioconjug. Chem.*, 26(8):1590–1596, 2015.

[168] E. V. L. Grgacic and D. A. Anderson. Virus-like particles: passport to immune recognition. *Methods*, 40(1):60–65, 2006.

[169] K. Madalinski, S. P. E. Sylvan, U. Hellström, J. Mikolajewicz, E. Zembrzuska-Sadkowska, and E. Piontek. Antibody responses to pres components after immunization of children with low doses of biohepb. *Vaccine*, 20(1-2):92–97, 2001.

[170] C. Ludwig and R. Wagner. Virus-like particles-universal molecular toolboxes. *Curr. Opin. Biotecnol.*, 18(6):537–545, 2007.

[171] J. C. M. van Hest, K. L. Kiick, and D. A. Tirrell. Efficient incorporation of unsaturated methionine analogues into proteins in vivo. *J. Am. Chem. Soc.*, 122(7):1282–1288, 2000.

[172] K. L. Kiick, E. Saxon, D. A. Tirrell, and C. R. Bertozzi. Incorporation of azides into recombinant proteins for chemoselective modification by the staudinger ligation. *Proc. Natl. Acad. Sci. USA*, 99(1):19–24, 2002.

[173] N. J. Agard, J. A. Prescher, and C. R. Bertozzi. A strain-promoted [3+2] azide- alkyne cycloaddition for covalent modification of biomolecules in living systems. *J. Am. Chem. Soc.*, 126(46):15046–15047, 2004.

[174] T. A. Kost, J. P. Condreay, and D. L. Jarvis. Baculovirus as versatile vectors for protein expression in insect and mammalian cells. *Nat. Biotechnol.*, 23(5):567–575, 2005.

[175] E. Strable, D. E. Prasuhn Jr., A. K. Udit, S. Brown, A. J. Link, J. T. Ngo, G. Lander, J. Quispe, C. S. Potter, D. A. Carragher, B.and Tirrell, and M. G. Finn. Unnatural amino acid incorporation into virus-like particles. *Bioconjug. Chem.*, 19(4):866–875, 2008.

[176] S. tom Dieck, L. Kochen, C. Hanus, M. Heumüller, I. Bartnik, B. Nassim-Assir, K. Merk, T. Mosler, S. Garg, S. Bunse, D. A. Tirrell, and E. M. Schuman. Direct visualization of newly synthesized target proteins in situ. *Nat. Meth.*, 12(5):411–414, 2015.

[177] M. H. Nielsen, H. Beck-Nielsen, M. N. Andersen, and A. Handberg. A flow cytometric method for characterization of circulating cell-derived microparticles in plasma. *J. Extracell. Vesicles*, 3(1):20795, 2014.

[178] E. J. van der Vlist, E. N. Nolte-'t, W. Stoorvogel, G. J. Arkesteijn, and M. H. Wauben. Fluorescent labeling of nano-sized vesicles released by cells

and subsequent quantitative and qualitative analysis by high-resolution flow cytometry. *Nat. Protoc.*, 7(7):1311–1326, 2012.

[179] C. Undey, D. Low, J. C. Menezes, and M. Koch. *On-line and at-line process analyzers are inserted in one of the major categories of process analytical technology (pat) tools, having important applications in the biopharmaceutical industry.* CRC Press, 2011.

[180] C. Peixoto, M. F. Q. Sousa, A. C. Silva, M. J. T. Carrondo, and P. M. Alves. Downstream processing of triple layered rotavirus like particles. *J. Biotechnol.*, 127(3):452–461, 2007.

[181] N. K. Sauter, J. E. Hanson, G. D. Glick, J. H. Brown, R. L. Crowther, S. J. Park, J. J. Skehel, and D. C. Wiley. Binding of influenza virus hemagglutinin to analogs of its cell-surface receptor, sialic acid: analysis by proton nuclear magnetic resonance spectroscopy and x-ray crystallography. *Biochemistry*, 31(40):9609–9621, 1992.

[182] A. J. Eisfeld, G. Neumann, and Y. Kawaoka. Influenza a virus isolation, culture and identification. *Nat. Protoc.*, 9(11):2663–2681, 2014.

[183] T. Noda. Native morphology of influenza virions. *Front. Microbiol.*, 2:269, 2012.

[184] J. Fontana, G. Cardone, J. B. Heymann, D. C. Winkler, and A. C. Steven. Structural changes in influenza virus at low ph characterized by cryo-electron tomography. *J. Virol.*, 86:2919–2929, 2012.

[185] T. W. Kwang, X. Zeng, and S. Wang. Manufacturing of AcMNPV baculovirus vectors to enable gene therapy trials. *Mol. Ther. Methods Clin. Dev.*, 3:15050, 2016.

[186] T.-C. Li, P. D. Scotti, T. Miyamura, and N. Takeda. Latent infection of a new alphanodavirus in an insect cell line. *J. Virol.*, 81(20):10890–10896, 2007.

[187] O. W. Merten. Attention with virus contaminated cell lines. *Cytotechnology*, 55(1):1–2, 2007.

[188] S. D. McClenahan, C. Uhlenhaut, and P. R. Krause. Evaluation of cells and biological reagents for adventitious agents using degenerate primer PCR and massively parallel sequencing. *Vaccine*, 32(52):7115–7121, 2014.

[189] G. K. Hirst. The agglutination of red cells by allantoic fluid of chick embryos infected with influenza virus. *Science*, 94(2427):22–23, 1941.

[190] T. Vicente, C. Peixoto, M. J. T. Carrondo, and P. M. Alves. Purification of recombinant baculoviruses for gene therapy using membrane processes. *Gene Ther.*, 16(6):766, 2009.

[191] World Health Organization. *Influenza (Seasonal) Fact Sheet No. 211.* 2016.

[192] J. C. Cook, J. G. Joyce, H. A. George, L. D. Schultz, W. M. Hurni, K. U. Jansen, R. W. Hepler, C. Ip, R. S. Lowe, P. M. Keller, and E. D. Lehman. Purification of virus-like particles of recombinant human papillomavirus type 11 major capsid protein l1 from saccharomyces cerevisiae. *Protein Expres. Purif.*, 17(3):477–484, 1999.

[193] A. Negrete, A. Pai, and J. Shiloach. Use of hollow fiber tangential flow filtration for the recovery and concentration of hiv virus-like particles produced in insect cells. *J. Virol. Methods*, 195:240–246, 2014.

[194] Z. Jiang, G. Tong, B. Cai, Y. Xu, and J. Lou. Purification and immunogenicity study of human papillomavirus 58 virus-like particles expressed in pichia pastoris. *Protein Expres. Purif.*, 80(2):203–210, 2011.

[195] F. S. Quan, D. Steinhauer, C. Huang, T. M. Ross, R. W. Compans, and S.-M. Kang. A bivalent influenza vlp vaccine confers complete inhibition of virus replication in lungs. *Vaccine*, 26(26):3352–3361, 2008.

[196] I. Tretyakova, M. B. Pearce, R. Florese, T. M. Tumpey, and P. Pushko. Intranasal vaccination with h5, h7 and h9 hemagglutinins co-localized in a virus-like particle protects ferrets from multiple avian influenza viruses. *Virology*, 442(1):67–73, 2013.

[197] I. Tretyakova, R. Hidajat, G. Hamilton, N. Horn, B. Nickols, R. O. Prather, T. M. Tumpey, and P. Pushko. Preparation of quadri-subtype influenza virus-like particles using bovine immunodeficiency virus gag protein. *Virology*, 487:163–171, 2016.

[198] E. I. Trilisky and A. M. Lenhoff. Sorption processes in ion-exchange chromatography of viruses. *J. Chromatogr. A*, 1142(1):2–12, 2007.

[199] S. M. Cramer and M. A. Holstein. Downstream bioprocessing: recent advances and future promise. *Curr. Opin. Chem. Eng.*, 1(1):27–37, 2011.

[200] J. O. Konz, R. C. Livingood, A. J. Bett, A. R. Goerke, M. E. Laska, and S. L. Sagar. Serotype specificity of adenovirus purification using anion-exchange chromatography. *Hum. Gene Ther.*, 16(11):1346–1353, 2005.

[201] H. Ruppach. Log10 reduction factors in viral clearance studies. *BioProcessing*, 2014, 2013.

[202] H. Lutz. *Ultrafiltration for bioprocessing.* Elsevier, 2015.

[203] H. T. Groves, J. U. McDonald, P. Langat, E. Kinnear, P. Kellam, J. McCauley, J. Ellis, C. Thompson, R. Elderfield, L. Parker, W. Barclay, and J. S. Tregoning. Mouse models of influenza infection with circulating strains to test seasonal vaccine efficacy. *Front. Immunol.*, 9:126, 2018.

[204] J. M. Galarza, T. Latham, and A. Cupo. Virus-like particle (vlp) vaccine conferred complete protection against a lethal influenza virus challenge. *Viral Immunol.*, 18(1):244–251, 2005.

[205] G. E. Smith, X. Sun, Y. Bai, Y. V. Liu, M. J. Massare, M. B. Pearce, J. A. Belser, T. R. Maines, H. M. Creager, G. M. Glenn, D. Flyer, P. Pushko, M. Z. Levine, and T.M. Tumpey. Neuraminidase-based recombinant virus-like particles protect against lethal avian influenza a (h5n1) virus infection in ferrets. *Virology*, 509:90–97, 2017.

[206] V. Orr, L. Zhong, M. Moo-Young, and C. P. Chou. Recent advances in bioprocessing application of membrane chromatography. *Biotechnol. Adv.*, 31(4):450–465, 2013.

[207] R. Ghosh. Protein separation using membrane chromatography: opportunities and challenges. *J. Chromatogr. A*, 952(1-2):13–27, 2002.

[208] V. Lohr, Y. Genzel, I. Behrendt, K. Scharfenberg, and U. Reichl. A new mdck suspension line cultivated in a fully defined medium in stirred-tank and wave bioreactor. *Vaccine*, 28(38):6256–6264, 2010.

[209] AB: MU, MODDE 11 - User Guide, Malmö, Sweden, 2015.

[210] L E, Design of experiments : principles and applications, in Umetrics Academy - training in multivariate technology, in Umetrics AB, Umea Stockholm, 2000.

[211] B. Kalbfuss, A. Knöchlein, T. Kröber, and U. Reichl. Monitoring influenza virus content in vaccine production: precise assays for the quantitation of hemagglutination and neuraminidase activity. *Biologicals*, 36(3):145–161, 2008.

[212] S. Zhang, T. Iskra, W. Daniels, J. Salm, C. Gallo, R. Godavarti, and G. Carta. Structural and performance characteristics of representative anion exchange resins used for weak partitioning chromatography. *Biotechnol. Progr.*, 33(2):425–434, 2017.

[213] G. Carta and A. Jungbauer. *Downstream processing of biotechnology products, in Protein Chromatography: Process Development and Scale-Up*. Wiley-VCH, Weinheim, Germany, 2010.

[214] M. A. Skidmore, A. Kajaste-Rudnitski, N. M. Wells, S. E. Guimond, T. R. Rudd, E. A. Yates, and E. Vicenzi. Inhibition of influenza h5n1 invasion by modified heparin derivatives. *MedChemComm*, 6(4):640–646, 2015.

[215] G. P. Pijlman, J. C. F. M. Dortmans, A. M. G. Vermeesch, K. Yang, D. E. Martens, R. W. Goldbach, and J. M. Vlak. Pivotal role of the non-hr origin of dna replication in the genesis of defective interfering baculoviruses. *J. Virol.*, 76(11):5605–5611, 2002.

[216] P. C. Soema, R. Kompier, J.-P. Amorij, and G. F. A. Kersten. Current and next generation influenza vaccines: formulation and production strategies. *Eur. J. Pharm. Biopharm.*, 94:251–263, 2015.

[217] P. Steppert, D. Burgstaller, M. Klausberger, E. Berger, P. P. Aguilar, T. A. Schneider, P. Kramberger, A. Tover, K. Nöbauer, E. Razzazi-Fazeli, and A. Jungbauer. Purification of hiv-1 gag virus-like particles and separation of other extracellular particles. *J. Chromatogr. A*, 1455:93–101, 2016.

[218] P. Steppert, D. Burgstaller, M. Klausberger, P. Kramberger, A. Tover, E. Berger, K. Nöbauer, E. Razzazi-Fazeli, and A. Jungbauer. Separation of hiv-1 gag virus-like particles from vesicular particles impurities by hydroxyl-functionalized monoliths. *J. Sep. Sci.*, 40(4):979–990, 2017.

[219] M. Marek, M. M. van Oers, F. F. Devaraj, J. M. Vlak, and O.-W. Merten. Engineering of baculovirus vectors for the manufacture of virion-free biopharmaceuticals. *Biotechnol. Bioeng.*, 108(5):1056–1067, 2011.

[220] S. Welsch, B. Müller, and H.-G. Kräusslich. More than one door–budding of enveloped viruses through cellular membranes. *Febs Lett.*, 581(11):2089–2097, 2007.

[221] G. Raposo and W. Stoorvogel. Extracellular vesicles: exosomes, microvesicles, and friends. *J. Cell Biol.*, 200(4):373–383, 2013.

[222] F. Krammer, A. García-Sastre, and P. Palese. Is it possible to develop a "universal" influenza virus vaccine? potential target antigens and critical aspects for a universal influenza vaccine. *CSH Perspect. Biol.*, 10(7):a028845, 2018.

[223] C. Fee. 3d-printed porous bed structures. *Curr. Opin. Chem. Eng.*, 18:10–15, 2017.

Apoio financeiro da FCT, bolsa n° SFRH/BD/52302/2013

ITQB-UNL | Av. da República, 2780-157 Oeiras, Portugal
Tel (+351) 214 469 100 | Fax (+351) 214 411 277

www.itqb.unl.pt